

**CARBON SEQUESTRATION AND TURNOVER BY  
VETIVER (*CHRYSOPOGON* SPP.)**

**Piyanut Khanema**

**A Thesis Submitted in Partial Fulfillment of the Requirements for the**

**Degree of Doctor of Philosophy in Environmental Biology**

**Suranaree University of Technology**

**Academic Year 2009**

# การกักเก็บและการหมุนเวียนคาร์บอนโดยแฝก (*CHRYSOPOGON* SPP.)

นางสาวปิยนุช คณะณมา

วิทยานิพนธ์นี้เป็นส่วนหนึ่งของการศึกษาตามหลักสูตรปริญญาวิทยาศาสตรดุษฎีบัณฑิต  
สาขาวิชาชีววิทยาสังแวดล้อม  
มหาวิทยาลัยเทคโนโลยีสุรนารี  
ปีการศึกษา 2552

# **CARBON SEQUESTRATION AND TURNOVER BY VETIVER**

**(*CHRYSOPOGON SPP.*)**

Suranaree University of Technology has approved this thesis submitted in partial fulfillment of the requirements for the Degree of Doctor of Philosophy.

Thesis Examining Committee

---

(Asst. Prof. Dr. Yupaporn Chaiseha)

Chairperson

---

(Assoc. Prof. Dr. Sompong Thammathaworn)

Member (Thesis Advisor)

---

(Assoc. Prof. Dr. Charlie Navanugraha)

Member

---

(Assoc. Prof. Dr. Sura Pattanakiat)

Member

---

(Asst. Prof. Dr. Nathawut Thanee)

Member

---

(Prof. Dr. Sukit Limpijumnong)

Vice Rector for Academic Affairs

---

(Assoc. Prof. Dr. Prapun Manyum)

Dean of Institute of Science

ปิยนุช คะณเฑาะ : การกักเก็บและการหมุนเวียนคาร์บอนโดยแฝก (*CHRYSOPOGON SPP.*)

(CARBON SEQUESTRATION AND TURNOVER BY VETIVER (*CHRYSOPOGON SPP.*))

อาจารย์ที่ปรึกษา : รองศาสตราจารย์ ดร.สมพงษ์ ธรรมถาวร, 270 หน้า.

แฝก (*Chrysopogon nemoralis* (Balan.) Holtt. Camus และ *C. zizanioides* (L.) Roberty) มีชื่อเสียงในเรื่องลดการพังทลายของดิน โดยอาศัยระบบรากลึกและหนา ปัจจุบันแฝกถูกทำทนายในเรื่องการกักเก็บคาร์บอน การศึกษานี้มีวัตถุประสงค์เพื่ออธิบายศักยภาพการกักเก็บคาร์บอนของแฝก 11 พันธุ์ คือ กำแพงเพชร 1 เลข นครสวรรค์ ประจวบคีรีขันธ์ ราชบุรี ร้อยเอ็ด กำแพงเพชร 2 พระราชทาน สงขลา 3 ศรีลังกา และสุราษฎร์ธานี โดยสำรวจโครงสร้างภายในใบ ไฟโตลิท และองค์ประกอบเคมีในซากพืช รวมถึงประเมินความสัมพันธ์ระหว่างมวลจุลินทรีย์ วัสดุสลายง่าย และสมบัติดิน ต่อการหายใจของดิน สารประกอบคาร์บอนในดิน และระยะเวลาการหมุนเวียนคาร์บอน

ผลการศึกษาพบว่า ภายในใบแฝกพบช่องว่างขนาดใหญ่คล้ายฟิซัน้ำ คาดว่าเกี่ยวข้องกับการหมุนเวียนอากาศที่ราก ใบยังพบโครงสร้างครานซ์แบบพีชชีส์ แสดงถึงความสามารถในการสังเคราะห์แสงสูง นอกจากนี้ บันเดิลแคปของใบพันธุ์เลขประกอบด้วยเซลล์สเกลอเรนจิมจำนวนมาก คาดว่ามีสองหน้าที่ คือ ความแข็งแรงและลำเลียงน้ำ ไฟโตลิทจำนวนมากที่พบในใบแฝกพันธุ์ราชบุรี สงขลา 3 และสุราษฎร์ธานี มีนัยสำคัญต่อศักยภาพการดูดน้ำและคาร์บอนที่ข่อยสลายยาก โครงสร้างไฟโตลิท เช่น ไคซีตรอนของพันธุ์กำแพงเพชร 2 และโครงสร้างหนาของพันธุ์สุราษฎร์ธานี คาดว่าช่วยกระจายความร้อนในช่วงมิดอินฟราเรดเช่นเดียวกับไฟโตนิคคริสตัล ตัวแปรที่สำคัญ เช่น มวลชีวภาพใต้ดิน และองค์ประกอบเคมีในซากพืช ระบุว่า แฝกพันธุ์เลขมีศักยภาพในการกักเก็บคาร์บอน การศึกษาความสัมพันธ์ของการหายใจของดินต่อมวลจุลินทรีย์ วัสดุสลายง่าย และสมบัติดิน พบว่า ดินเหนียวเป็นปัจจัยสำคัญในการสะสมคาร์บอน ผลการศึกษาด้วย  $1D^1H$  NMR พบว่า ลิกนินเริ่มถูกย่อยสลายตั้งแต่วางแรกและต่อเนื่องถึงปีที่ 7 ของการปลูกแฝก อินทรีย์คาร์บอนที่ข่อยสลายง่าย เช่น โพลีแซคคาไรด์ เปปไทด์ หรือสารประกอบโปรตีนไม่ถูกย่อยสลาย คาดว่าเนื่องจากกลไกปกป้องทางกายภาพจากการศึกษาแบบลำดับต่อเนื่อง ปริมาณคาร์บอนในดินลึก 1.2 เมตร เพิ่มขึ้น 10 เท่า จากการปลูกแฝกเป็นระยะเวลา 7 ปี (จาก 24 เพิ่มเป็น 229 ตันคาร์บอนต่อเฮกแตร์) และระยะเวลาการหมุนเวียนคาร์บอนข่อยสลายง่ายเร็วที่สุด คือ 18 วัน และช้าที่สุด คือ 108 วัน

โดยสรุปแล้ว แฝก สามารถใช้ในการกักเก็บคาร์บอน โดยเฉพาะพันธุ์เลข

PIYANUT KHANEMA : CARBON SEQUESTRATION AND TURNOVER BY  
VETIVER (*CHRYSOPOGON* SPP.). THESIS ADVISOR : ASSOC. PROF.  
SOMPONG THAMMATHAWORN, Ph.D. 270 PP.

#### INTERNAL LEAF STRUCTURE/PHYTOLITH/LITTER/MICROBIAL BIOMASS

Vetiver (*Chrysopogon nemoralis* (Balan.) Holtt. Camus and *C. zizanioides* (L.) Roberty) is well known in soil erosion reduction by directly deep and dense root system, and as for now it is challenged in C sequestration. The aim of this study was to elucidate the potentially C sequestration of 11 vetiver provenances, Kamphaeng Phet 1 (KP1), Loei (LI), Nakhon Sawan (NS), Prachuabkhirikhan (PK), Ratchaburi (RB), Roi Et (RE), Kamphaeng Phet 2 (KP2), Phraratchathan (PT), Songkhla 3 (SK), Sri Lanka (SL) and Surat Thani (ST), through the investigation of internal leaf structures, phytoliths and chemical components in plant residues. Also, the estimation of interaction among microbial biomass, substrate availability and soil properties to soil respiration, soil C functional groups and C turnover time was included in the study.

The results showed that vetiver leaves presented large lysigenous intercellular spaces like water plants, assuming related gas circulation at roots. Also, the leaves presented Kranz structure like C4 plants, demonstrating high photosynthetic capacity. Moreover, bundle caps of LI laminas consisted of more sclerenchyma cells, anticipating played a dual function of mechanic and hydraulic. More abundance of phytoliths in RB, SK and ST leaves was significant to the potentially water absorption and recalcitrant C. Likewise a photonic crystal, phytoliths such dihedron structure of KP2 provenance and thick shape of ST provenance, suggesting enable thermal emission in the mid-infrared. Significant variables such as belowground biomass and chemical components in plant residues indicted LI provenance had an efficiency in C sequestration. Study on

relationships of soil respiration to microbial biomass, substrate availability and soil properties found that clay was a key role in C storage in soils. Results of 1D  $^1\text{H}$  NMR study demonstrated that lignin was initially degraded since an early stage and substantially extended to the 7 year vetiver plantation. Labile organic C such as polysaccharide, peptide or protein compounds were selectively preserved in vetiver soils, anticipating caused by physically protective mechanisms. From a chronosequence study, the mean C storages in soil at 1.2 m depth increased about 10 times within 7 years of vetiver plantation (from 24 to 229 tC ha $^{-1}$ ), and the labile organic C turnover time was the fastest at 18 days and the slowest at 108 days.

In conclusion, vetiver could be used in C sequestration, especially LI provenance.

School of Biology

Student's Signature\_\_\_\_\_

Academic Year 2009

Advisor's Signature\_\_\_\_\_

## ACKNOWLEDGEMENTS

This thesis could not be completed without the generous support and advice of many persons. I, therefore, would like to thank:

**Assoc. Prof. Dr. Sompong Thammathaworn**, my thesis advisor, who gave me the golden opportunity to have experiences in all of my thesis. Without his suggestion and never-ending support, this work would have not been possible.

**Assoc. Prof. Dr. Charlie Navanugraha** and **Assoc. Prof. Dr. Sura Pattanakiat**, my thesis committees, who gave me very kindly helps and valuable suggestions in my thesis.

**Asst. Prof. Dr. Nathawut Thanee**, my thesis committee, and **Dr. Pongthap Suwanwaree**, my proposal committee, for their generous and kind support.

I thank the Thai Tapioca Development Institute (TTDI), especially Mr. Precha and all staffs at there, the Regional Office 3, Land Development Department (LDD), the LDD at Pak Chong District, the Iam Seng factory, Mr. Thawatchai, Mr. Sawang Kodpakdee, Mr. Thongdat Phraidiphanao, and Mr. Yuang Praeng-Di, all for their kind helps, encouragements and allowing for plant and soil samplings.

My thanks also go to Mahasarakham University (MSU) and Suranaree University of Technology (SUT) for financial support and laboratory facilities.

Finally, thanks to all of my family, my dad, my mom, my two elder sisters and Mana Sathian family for their love and support.

Piyanut Khanema

# CONTENTS

	<b>Page</b>
ABSTRACT IN THAI.....	I
ABSTRACT IN ENGLISH.....	II
ACKNOWLEDFEMENTS.....	IV
CONTENTS.....	V
LIST OF TABLES.....	XIV
LIST OF FIGURES.....	XVI
LIST OF ABBREVIATIONS.....	XXV
<b>CHAPTER</b>	
<b>I INTRODUCTION.....</b>	<b>1</b>
1.1 Introduction.....	1
1.1.1 Situation of atmospheric CO <sub>2</sub> .....	1
1.1.2 C sequestration: significant in global warming reduction.....	2
1.1.3 Vertiver: challenge in C sequestration.....	3
1.1.4 Outline of the experiments.....	4
1.2 Research objectives.....	4
1.3 Scope and limitation of the study.....	5
1.4 Benefices of the study.....	5
1.5 References.....	6
<b>II LITERATURE REVIEWS.....</b>	<b>7</b>
2.1 Vetiver species.....	7
2.2 Photosynthetic pathways of C <sub>3</sub> , C <sub>4</sub> and CAM plants.....	10
2.3 Internal leaf structure.....	13

## CONTENTS (Continued)

	<b>Page</b>
2.4 Plant chemical composition and decomposition.....	14
2.4.1 Cytoplasm and storage components.....	14
2.4.2 Hemicellulose, pectin and cellulose.....	15
2.4.3 Lignin.....	16
2.4.4 Main groups of bacteria and fungi in plant component decomposition.....	19
2.4.5 Microbial biomass.....	20
2.4.6 Turnover of soil inputs.....	21
2.5 Formation of soil organic matter.....	23
2.6 Recently C sequestration study.....	24
2.7 Some mechanisms of SOC protection.....	27
2.7.1 SOC protection by soil aggregate.....	27
2.7.2 SOC protection by clay.....	28
2.8 Phytoliths.....	29
2.8.1 Composition and characteristics.....	29
2.8.2 Phytolithic classification.....	30
2.8.3 Phytoliths and C sequestration.....	32
2.9 References.....	34
<b>III GENERAL MATERIALS AND METHODS.....</b>	<b>41</b>
3.1 Dichromate oxidation method.....	41
3.2 Kjeldahl method.....	42
3.3 Ammonium acetate-extractable element method.....	43
3.4 Hydrometer method.....	46

## CONTENTS (Continued)

	<b>Page</b>
3.5 Bulk density.....	48
3.6 High combustion method.....	49
3.7 Chloroform fumigation extraction method.....	49
3.8 Chloroform fumigation incubation method.....	51
3.9 Liquid state 1D <sup>1</sup> H NMR technique.....	52
3.10 References.....	64
<b>IV INTERNAL LEAF STRUCTURES OF VETIVER.....</b>	<b>66</b>
4.1 Abstract.....	66
4.2 Introduction.....	67
4.3 Objectives of this chapter.....	68
4.4 Materials and methods.....	68
4.4.1 Plant description.....	68
4.4.2 Leaf cross section.....	69
4.5 Results.....	69
4.5.1 Internal leaf structure of Kamphaeng Phet 1.....	69
4.5.2 Internal leaf structure of Loei.....	70
4.5.3 Internal leaf structure of Nakhon Sawan.....	71
4.5.4 Internal leaf structure of Prachuabkhirikhan.....	73
4.5.5 Internal leaf structure of Ratchaburi.....	74
4.5.6 Internal leaf structure of Roi Et.....	75
4.5.7 Internal leaf structure of Kamphaeng Phet 2.....	77
4.5.8 Internal leaf structure of Phraratchathan.....	78

## CONTENTS (Continued)

	<b>Page</b>
4.5.9 Internal leaf structure of Songkhla 3.....	79
4.5.10 Internal leaf structure of Sri Lanka.....	80
4.5.11 Internal leaf structure of Surat Thani.....	82
4.6 Discussion.....	95
4.6.1 Comparing angle of leaf wings among 11 provenances.....	95
4.6.2 Leaf anatomy comparison of vetiver to other grasses.....	95
4.6.3 Fibers and hydraulics within leaves.....	98
4.6.4 Lysigenous intercellular spaces and aeration system.....	100
4.7 Conclusions.....	106
4.8 References.....	107
<b>V VETIVER PHYTOLITHS: SUSTAINABLE VETIVER CLASSIFICATION AND LEAF THERMAL EMISSION.....</b>	<b>109</b>
5.1 Abstract.....	109
5.2 Introduction.....	110
5.3 Objectives of this chapter.....	111
5.4 Materials and methods.....	111
5.4.1 Plant description.....	111
5.4.2 Phytolithic preparation.....	112
5.5 Results.....	112
5.5.1 Morphological classification of vetiver phytoliths.....	112
5.5.2 Phytoliths and vetiver identification.....	114
5.6 Discussion.....	115

## CONTENTS (Continued)

	<b>Page</b>
5.6.1 Variation of phytolithic shapes.....	115
5.6.2 Phytoliths in water absorption and classification of vetiver group.....	116
5.6.3 Phytoliths functioning in thermal protective mechanism.....	119
5.7 Conclusions.....	122
5.8 References.....	123
<b>VI CHEMICAL COMPONENTS IN VETIVER RESIDUES.....</b>	<b>127</b>
6.1 Abstract.....	127
6.2 Introduction.....	128
6.3 Objectives of this chapter.....	129
6.4 Materials and methods.....	130
6.4.1 Plant and site description.....	130
6.4.2 Method of plant biomass measurement.....	130
6.4.3 Method of total C, total N and C/N ratio measurement.....	131
6.4.4 Methods of cellulose and lignin determination.....	131
6.4.5 Method of total phenolic measurement.....	132
6.4.6 Method of soluble carbohydrate measurement.....	132
6.4.7 Statistical analysis.....	133
6.5 Results.....	133
6.5.1 Plant biomass.....	133
6.5.2 Total C, total N and C/N ratio of plant residues.....	134
6.5.3 Fibrous C, total phenolics and soluble carbohydrate of plant residues...135	135
6.6 Discussion.....	139

## **CONTENTS (Continued)**

	<b>Page</b>
6.6.1 Lignin: a controller of litter decomposition.....	139
6.6.2 Quality of plant residues and the supply of nitrogen.....	143
6.6.3 Polyphenolic compounds on either humification or N leaching.....	143
6.6.4 Residue quality and soil aggregation.....	144
6.7 Conclusions.....	145
6.8 References.....	148
<b>VII RELATIONSHIPS OF SOIL RESPIRATION TO MICROBIAL BIOMASS</b>	
<b>AND SUBSTRATE AVAILABILITY IN DIFFERENT VETIVER SOILS.....</b>	<b>155</b>
7.1 Abstract.....	155
7.2 Introduction.....	156
7.3 Objectives of this chapter.....	157
7.4 Materials and methods.....	157
7.4.1 Site description.....	157
7.4.2 Climate description.....	159
7.4.3 Method of soil sampling.....	160
7.4.4 Methods of soil physical and chemical property measurement.....	160
7.4.5 Method of microbial biomass measurement.....	160
7.4.6 Carbon availability index.....	161
7.4.7 Flush of CO <sub>2</sub> following rewetting of dried soils.....	161
7.4.8 Statistical analysis.....	162
7.5 Results.....	162
7.5.1 Pool sizes and CO <sub>2</sub> evolution rates.....	162

## CONTENTS (Continued)

	Page
7.5.2 Interactive effects of microbial biomass, substrate supply and other soil properties to soil respiration.....	164
7.6 Discussion.....	166
7.6.1 Clay interactions with C storage.....	166
7.6.2 Bulk density on total C accumulation.....	169
7.7 Conclusions.....	169
7.8 References.....	169
<b>VIII CARBON FUNCTIONAL GROUPS IN SOILS BY 1D <sup>1</sup>H NMR STUDY.....</b>	<b>182</b>
8.1 Abstract.....	182
8.2 Introduction.....	183
8.3 Objectives of this chapter.....	184
8.4 Materials and methods.....	184
8.4.1 Soil property measurement.....	184
8.4.2 Soil preparation for NMR measurement.....	187
8.4.3 Conditions for <sup>1</sup> H NMR study.....	187
8.4.4 1D <sup>1</sup> H NMR analysis.....	188
8.4.5 <sup>1</sup> H NMR information.....	193
8.5 Results.....	194
8.5.1 Spectra lower than δ 2.5 ppm.....	194
8.5.2 Spectra δ 3.0 - 5.5 ppm.....	195
8.5.3 Spectra δ ~8.3 ppm.....	195
8.5.4 Effects of soil profiles and soil types.....	195

## CONTENTS (Continued)

	<b>Page</b>
8.6 Discussion.....	203
8.6.1 Spectra $\delta$ 3.8 ppm: the evidence of lignin existence.....	203
8.6.2 Physically protected biodegradation.....	204
8.6.3 Alkyl: referring humification process.....	206
8.7 Conclusions.....	207
8.8 References.....	207
 <b>IX SOIL LABILE ORGANIC CARBON AND CARBON TURNOVER</b>	
<b>TIMES</b> .....	211
9.1 Abstract.....	211
9.2 Introduction.....	212
9.3 Objectives of this chapter.....	213
9.4 Materials and methods.....	213
9.4.1 Site description.....	213
9.4.2 Soil sampling.....	213
9.4.3 Physical and chemical properties of soils.....	214
9.4.4 Soil microbial biomass C.....	214
9.4.5 Soil labile organic C.....	215
9.4.6 Statistical analysis.....	216
9.5 Results.....	216
9.5.1 Soil organic C and nitrogen.....	216
9.5.2 Soil microbial biomass C and soil labile organic C.....	222
9.6 Discussion.....	225

**CONTENTS (Continued)**

	<b>Page</b>
9.7 Conclusions.....	226
9.8 References.....	227
<b>X CONCLUSIONS.....</b>	<b>230</b>
APPENDICES	
APPENDIX A CLIMATE DATA OF NAKHON RATHASIMA DURING 2000 - 2008.....	233
APPENDIX B PHYTOLITHIC DISTRIBUTION.....	237
APPENDIX C SOIL PROPERTIES AND SOIL C FRACTIONS.....	242
APPENDIX D RESONANT SIGNALS FROM 1D <sup>1</sup> H NMR STUDY.....	261
CURRICULUM VITAE.....	270

## LIST OF TABLES

Table		Page
2.1	Common vetiver provenances in Thailand.....	7
2.2	Comparison of two vetiver species.....	8
2.3	Characteristics of plants with different photosynthetic pathways.....	11
2.4	Some general properties of the main groups of bacteria and fungi.....	19
2.5	Decomposition rates and turnover of various plant and microbial soil inputs..	22
2.6	The area, stocks of C, net primary production (NPP) and C turnover of various biomes.....	25
2.7	Comparing C sequestration among ecosystems and land uses.....	26
2.8	Interactions of organic molecules and clay minerals in soil organic C (SOC) sequestration.....	28
3.1	<sup>1</sup> H Substituent parameters ( $\Delta\delta_x$ , ppm) for substituents on tetrahedral carbons.....	55
3.2	<sup>1</sup> H Chemical shifts of unsubstituted cycloalkanes.....	57
3.3	Substituent parameters ( $\Delta\delta_x$ , ppm) for vinyl hydrogen chemical shift.....	58
3.4	Aromatic substituent parameters ( $\Delta\delta_x$ , ppm).....	62
4.1	Classification of vetiver provenance based on angle of leaf wings.....	95
4.2	Vascular bundle arrangement of some C4 grasses.....	96
5.1	Distribution of types of phytoliths.....	115
5.2	Classification for “Faek Don” and “Faek Lum” group.....	117
5.3	Suggestion for provenance rearrangement in “Faek Don” and “Faek Lum”..	118
6.1	Properties of plant residues of 11 vetiver provenances.....	152
6.2	Conclusion of the potentially C sequestration of 11 vetiver provenances.....	147

## LIST OF TABLES (Continued)

<b>Table</b>	<b>Page</b>
7.1	Soil properties.....174
7.2	Substrate availability index, MBC and CO <sub>2</sub> production.....176
7.3	Correlation matrix ( <i>r</i> values) for physical, chemical and microbiological characteristics in different vetiver soils (0 - 120 cm depth).....178
7.4	Correlation matrix for physical, chemical and microbiological characteristics in different vetiver soils (0 - 10 cm depth).....179
7.5	Correlation matrix for physical, chemical and microbiological characteristics in different vetiver soils (10 - 60 cm depth).....180
7.6	Correlation matrix for physical, chemical and microbiological characteristics in different vetiver soils (60 - 120 cm depth).....181
8.1	Some physical and chemical properties of soils collecting from the study sites in Nakhon Ratchasima.....185
8.2	<sup>1</sup> H Substituent parameters ( $\Delta\delta_x$ , ppm) for substituents on tetrahedral carbons.....189
8.3	Substituent parameters ( $\Delta\delta_x$ , ppm) for vinyl hydrogen chemical shift.....190
8.4	Aromatic substituent parameters ( $\Delta\delta_x$ , ppm).....192
9.1	Selected characteristic of the study soils from the sites at TTDI, Nakhon Ratchasima, Thailand.....219
9.2	Soil microbial biomass carbon and pool sizes of soil labile organic carbon...224
10.1	Conclusion of the potentially C sequestration of 11 vetiver provenances.....231

## LIST OF FIGURES

Figure		Page
1.1	Carbon fluxes (1 Giga ton = $10^9$ g = $10^6$ kg).....	1
1.2	The situation of atmospheric CO <sub>2</sub> .....	2
2.1	The standard leaf has three tissue regions: the epidermis, the mesophyll and the vascular bundles or veins (Rand, 2001).....	13
2.2	<i>Eleusine coracana</i> (Poaceae), transverse section of leaf with Kranz structure. bc = bulliform cell, is = inner bundle sheath, os = outer bundle sheath, ph = phloem, rc = radiate chlorenchyma, sg = sclerenchyma girder, x = xylem (Versiteit Nijmegen, 2010).....	13
2.3	Part of the cellulose fiber is attacked by an endo-1, 4-β-glucanase (endo-1, 4-β-glucanase) breaking the chains and splitting off oligosaccharides in a random manner, including soluble shorter chains with, for example, 3 to 5 glucose units. An exo-1, 4-β-glucanase (exocellulase) splits off cellobiose units from the non-reducing end of the carbohydrate chains. G Glucose unit (Berg and McClaugherty, 2008).....	16
2.4	Schematic representation of hypothetical lignin resulting from the ectopic signification incorporating coniferyl-ferulate or sinapyl-ferulate conjugates and normal monolignols (coniferyl or/and sinapyl alcohols). The hypothetical lignin has several readily cleavable ester bonds (demarked by arrows) resulting from the copolymerization of coniferyl alcohol and the ferulate conjugates that would permit rapid solubilization of the cell wall under alkaline reaction conditions (Grabber et al., 2009).....	18

## LIST OF FIGURES (Continued)

Figure		Page
2.5	Internationally defined morphological phytolith shapes from the International Code for Phytolith Nomenclature 1.0 (Madella et al., 2005).....	31
2.6	Illustrate the percentages of resistant decomposed phytoliths comparing to ther organic matter fraction (Parr and Sullivan, 2005).....	32
2.7	Forming humic macromolecule complexes from silicic acid.....	33
3.1	LECO Analyzer (CNS 2000).....	49
3.2	NMR spectroscopy and a NMR tube.....	52
3.3	Effect of diamagnetic shielding. The dotted ellipses represent motion of electrons in their orbital under the influence of $B_0$ (Macomber, 1998).....	53
3.4	Structures and $^1\text{H}$ chemical shifts of vinyl groups.....	60
3.5	Anisotropic-induced magnetic field (dotted lines) in the proximity of an aromatic ring. The ellipses above and below the ring represent the ring current of $\pi$ electrons.....	61
3.6	Structures and $^1\text{H}$ chemical shifts of hydrogens attached to oxygen groups...	63
3.7	Structures and $^1\text{H}$ chemical shifts of hydrogens attached to nitrogen groups..	63
4.1	TS of Kamphaeng Phet 1 leaves showing a steep angle of leaf wings ( $\sim 45^\circ$ ) with curve wings at the ends (large arrow), and large intercellular spaces.....	84
4.2	Focus on a large vascular bundle of a mature leaf.....	84
4.3	TS of a developing leaf showing lysigenous intercellular spaces and a lysis of parenchyma cells.....	84
4.4	TS of Loei leaf showing a steep angle of leaf wings ( $\sim 45^\circ$ ) with curve (from middle to end), and lysigenous intercellular spaces (ls).....	85
4.5	TS of a large vascular bundle.....	85

## LIST OF FIGURES (Continued)

<b>Figure</b>		<b>Page</b>
4.6	TS of medium and small vascular bundles.....	85
4.7	TS of a mature leaf showing bundle caps attach at adaxial and abaxial surfaces.....	85
4.8	TS of a developing leaf showing an early stage of parenchyma lysis.....	85
4.9	TS of Nakhon Sawan leaf showing two leaf wings like a U - shape upside down (∩) and lysigenous intercellular spaces.....	86
4.10	TS of a large vascular bundle in a developing leaf.....	86
4.11	TS of a developing leaf showing parenchyma lysis.....	86
4.12	TS of a mature leaf showing different vascular bundles and large lysigenous intercellular spaces.....	86
4.13	TS of Prachuabkhirikhan leaf showing a steep angle of leaf wings (~45°) with curve (from middle to end), and lysigenous intercellular spaces (ls).....	87
4.14	Two sizes of vascular bundles, medium and small.....	87
4.15	Focus on a large vascular bundle.....	87
4.16	Two sizes of vascular bundles, large and small.....	87
4.17	TS of Ratchaburi leaf showing a steep angle of leaf wings (~45°) without curve, and lysigenous intercellular spaces (ls).....	88
4.18	TS of a developing leaf showing an early stage of parenchyma lysis.....	88
4.19	TS of a mature leaf.....	88
4.20	TS of a mature leaf comparing three sizes of vascular bundles, large, medium and small.....	88

## LIST OF FIGURES (Continued)

Figure		Page
4.21	TS of Roi Et leaf showing a wide angle of leaf wings ( $\sim 60^\circ$ ) with curve wings (from middle to end).....	89
4.22	Focus on a large vascular bundle.....	89
4.23	TS of a developing leaf.....	89
4.24	TS of a mature leaf showing the three sizes of vascular bundles.....	89
4.25	TS of Kamphaeng Phet 2 showing a wide angle of leaf wings ( $\sim 60^\circ$ ) without curve wings, and lysigenous intercellular spaces (ls).....	90
4.26	Focus on a large vascular bundle.....	90
4.27	TS of a mature leaf showing parenchyma lysis.....	90
4.28	TS of Phraratchathan leaf showing a steep angle of leaf wings ( $\sim 45^\circ$ ) without curve wings, and lysigenous intercellular spaces (ls).....	91
4.29	Focus on a large vascular bundle in a developing leaf.....	91
4.30	TS of a developing leaf showing an early stage of parenchyma lysis.....	91
4.31	TS of Songkhla 3 leaf showing a wide angle of leaf wings ( $> 90^\circ$ ), and lysigenous intercellular spaces (ls).....	92
4.32	Focus on small vascular bundles.....	92
4.33	Focus on a large vascular bundle.....	92
4.34	TS of a developing leaf showing an early stage of parenchyma lysis.....	92
4.35	TS of Sri Lanka leaves showing a steep angle of leaf wings ( $\sim 45^\circ$ ) with curve wings (at the ends), and lysigenous intercellular spaces (ls).....	93
4.36	TS of a mature leaf showing large lysigenous intercellular spaces and three sizes of vascular bundles, large, medium and small.....	93
4.37	Focus on a large vascular bundle.....	93

## LIST OF FIGURES (Continued)

Figure		Page
4.38	Focus on small vascular bundles.....	93
4.39	TS of Surat Thani leaf showing a very steep angle of leaf wings (< 45°), and lysigenous intercellular spaces (ls).....	94
4.40	Focus on a large vascular bundle.....	94
4.41	TS of a developing leaf showing an early stage of parenchyma lysis.....	94
4.42	TS of a mature leaf showing large lysigenous intercellular spaces and three sizes of vascular bundles, large, medium and small.....	94
4.43	TS of Leaves of (a) paragrass, (b) lemongrass, (c) maize, (d) cogongrass, (e) sugarcane, (f) goose grass and (g) guinea grass.....	97
4.44	Schemes of CO <sub>2</sub> and H <sub>2</sub> O distribution to photosynthetic sites of LI leaf: (a) at Kranz of the large vascular bundle; and (b) at Kranz of the small vascular bundles.....	99
4.45	Mature fully expanded lamina of <i>Gnetum gnemon</i> . (Left) TS of Lamina immature but intercellular space system of mesophyll fully established, fibers (F) thin-walled and highly vacuolated and therefore obscure. (Right) An SEM transverse view of leaf tissue with mature fibers (F). Scale bar = 100 μm. (Tomlinson and Fisher, 2005).....	99
4.46	Leaves of two species of conifer and cycad, <i>Podocarpus dispersmis</i> and <i>Sciadopitys verticillata</i> show hydraulic flow path (from the midrib (V) to the stomata (black asterisks) facilitate by water-conducting sclereids (Brodribb et al., 2007).....	100

## LIST OF FIGURES (Continued)

Figure		Page
4.47	Leaf TS of (a) typha ( <i>Typha angustifolia</i> ), (b) banana ( <i>Musa sapientum</i> Linn.), and (c) Phai ruak ( <i>Thyrsostachys siamensis</i> Gamble.).....	102
4.48	TS of vetiver root from LI provenance.....	102
4.49	Signal chain that leads to programmed cell death (PCD) upon aerenchyma formation, including environmental factors that control it (Drew et al., 2000).....	104
4.50	<i>Phragmites</i> : humidity-induced convection. The difference in humidity between the sub-stomatal gas-space of the plant and the drier atmosphere favours the inward diffusion of O <sub>2</sub> and N <sub>2</sub> through leaf sheath and nodal stomata. A pressurised flow of gases is induced through the rhizome because of stomatal resistance to backflow. The throughflow results in increased diffusion of O <sub>2</sub> into root and rhizosphere (Armstrong et al., 1996).....	105
4.51	<i>Phragmites</i> : Venturi-induced convection. A suction pressure, $\Delta P$ (Pa) is created by the wind such that $\Delta P = \left(\frac{1}{2}\right)\rho V^2$ , where $\rho$ is the density of air (approx. 1.2 - 1.25 kg m <sup>-3</sup> ) and V, the wind velocity (ms <sup>-1</sup> ). The convective flow through the rhizome results in an increased diffusion of oxygen to root and rhizosphere (Armstrong et al., 1996).....	106
5.1	Classification of vetiver phytoliths. All phytoliths were oriented as they occur in the epidermal cells with the long axis of the leaf horizontal....	114
5.2	Phytolithic distribution of ST provenance, the example of high potentially water absorption.....	118

## LIST OF FIGURES (Continued)

Figure		Page
5.3	(a) Type B1 phytolith <i>in situ</i> in epidermal leaves of KP2 provenance and (b) the scheme of emissivity of dihedron structure. “ $\epsilon_i$ ” is the spectral emissivity and “ $T_i$ ” is temperature of the material.....	120
5.4	(a) The scheme of birefringence represents by Type F4 phytolith: $R(\lambda)$ , Reflectance; $\epsilon(\lambda)$ , emissivity; $\Gamma(\lambda)$ , Transmittance. (b) Vetiver leaves positioning a steep angle. (c) No transit radiant when an incident angle equals a critical angle ( $\theta_i = \theta_c$ ). (d) Total internal reflection when an incident angle is over than a critical angle ( $\theta_i > \theta_c$ ).....	121
6.1	Belowground biomass of 11 vetiver provenances (mean $\pm$ S.D., n = 3).....	133
6.2	(a) total C, (b) total N and (c) C/N ratio of plant residues of 11 vetiver provenances (mean $\pm$ S.D., n = 3).....	135
6.3	Chemical components in plant residues of 11 vetiver provenances: (a) cellulose; (b) lignin; (c) proportion of cellulose and lignin in fibrous C; (d) total phenolics; and (e) soluble carbohydrate (mean $\pm$ S.D., n = 3).....	137
6.4	Model for chemical changes and rate-regulating factors during decomposition (Berg and Matzner, 1997).....	140
7.1	Location of study sites in Nakhon Ratchasima, Thailand.....	159
7.2	Relationship between substrate availability index, total C and MBC.....	164
8.1	The procedure of soil sample preparation for NMR analysis.....	187
8.2	$^1\text{H}$ NMR chemical shift information.....	193
8.3	1D $^1\text{H}$ NMR spectra of continuous vetiver for 3 year soils, samplings from TTDI. Spectra arranged across soil profiles.....	197

## LIST OF FIGURES (Continued)

Figure	Page
	from TTDI. Spectra arranged across soil profiles.....197
8.4	1D <sup>1</sup> H NMR spectra of continuous vetiver for 5 year soils, samplings from TTDI. Spectra arranged across soil profiles.....198
8.5	1D <sup>1</sup> H NMR spectra of continuous vetiver for 7 year soils, samplings from TTDI. Spectra arranged across soil profiles.....199
8.6	1D <sup>1</sup> H NMR spectra of surface soils of continuous vetiver for 3, 5 and 7 years, samplings from soil 7/1, 1/1 and 6/1 at TTDI, respectively.....200
8.7	1D <sup>1</sup> H NMR spectra of surface soils of continuous vetiver for 2 years, samplings from soil 15/1 and 16/1.....201
8.8	1D <sup>1</sup> H NMR spectra of surface soils of continuous vetiver for 3 years, samplings from soil 1/1, 10/1, 11/1, 17/1 and 18/1.....202
8.9	Schematic illustration of the structure of an algaenan-containing algae cell wall (above) and proteinaceous organic matter encapsulated within degraded algal cell wall material (below). By capsulation instinctically labile proteins and peptides might be physically protected from biodegradation (Knicker and Hatcher, 2001).....206
9.1	Levels of (a) SOC and (b) organic N in a chronosequence of soils under continuous vetiver grass. Error bars indicate standard deviation (n = 3).....217
9.2	Changes in the mean carbon storage in soil at 120 cm depth under continuous vetiver grass (the equation excluded the 5 year site by data validation).....218

## LIST OF FIGURES (Continued)

<b>Figure</b>		<b>Page</b>
9.3	Effect of continuous vetiver grass on (a) soil microbial biomass carbon and (b) soil labile organic carbon. Error bars indicate standard deviation (n = 3).....	222
10.1	Schematic of quantity of C storage through vetiver plantation, representing by LI provenance (* = the value did not notice to specific provenance).....	232

## LIST OF ABBREVIATIONS

a.s.l.	=	above sea level
b	=	bulliform cell
bc	=	bundle cap
bs	=	bundle sheet cell
C	=	carbon
c	=	cuticle
ck	=	cork
C <sub>labile</sub>	=	labile organic carbon
C <sub>microbial</sub>	=	microbial biomass carbon
co	=	collenchyma
ct	=	cortex
en	=	endodermis
ep	=	epidermis
hy	=	hypodermis
is	=	inner bundle sheath
k	=	potential turnover rate
KP1	=	Kamphaeng Phet 1
KP2	=	Kamphaeng Phet 2
le	=	lower epidermis
LI	=	Loei
ls	=	lysigenous intercellular space
MBC	=	microbial biomass carbon
mgC g <sup>-1</sup> soil	=	milli-gram carbon per gram soil

**LIST OF ABBREVIATIONS (Continued)**

NS	=	Nakhon Sawan
os	=	outer bundle sheath
pa	=	palisade mesophyll
ph	=	phloem
PK	=	Prachuabkhirikhan
pm	=	parenchyma mesophyll
PT	=	Phraratchathan
RB	=	Ratchaburi
rc	=	radiate chlorenchyma
RE	=	Roi Et
SK	=	Songkhla 3
SL	=	Sri Lanka
SOC	=	soil organic carbon
SOM	=	soil organic matter
sp	=	spongy mesophyll
ST	=	Surat Thani
TC	=	total carbon
TN	=	total nitrogen
TS	=	transverse section
ue	=	upper epidermis
VB	=	vascular bundle
x	=	xylem

# CHAPTER I

## INTRODUCTION

### 1.1 Introduction

#### 1.1.1 Situation of atmospheric CO<sub>2</sub>

Rapidly increasing the atmospheric CO<sub>2</sub> concentration is a serious problem for now. Currently, the atmosphere holds about 775 Gt of C as gaseous CO<sub>2</sub> (Figure 1.1) and this has increased by some 20 - 30 Gt since the mid-nineteenth century (Lawlor, 2001). The future emissions of CO<sub>2</sub> are projected from 29 to 44 GtCO<sub>2</sub> year<sup>-1</sup> in the year 2020, and from 23 to 84 GtCO<sub>2</sub> year<sup>-1</sup> in the year 2050 (Figure 1.2), which it is expected that the number of CO<sub>2</sub> emission sources from the electric power and industrial sectors will increase significantly until 2050, mainly in South and East Asia (Marland and Boden, 2001). The increase in atmospheric CO<sub>2</sub> is indisputable, but sinks for this C are not well understood.

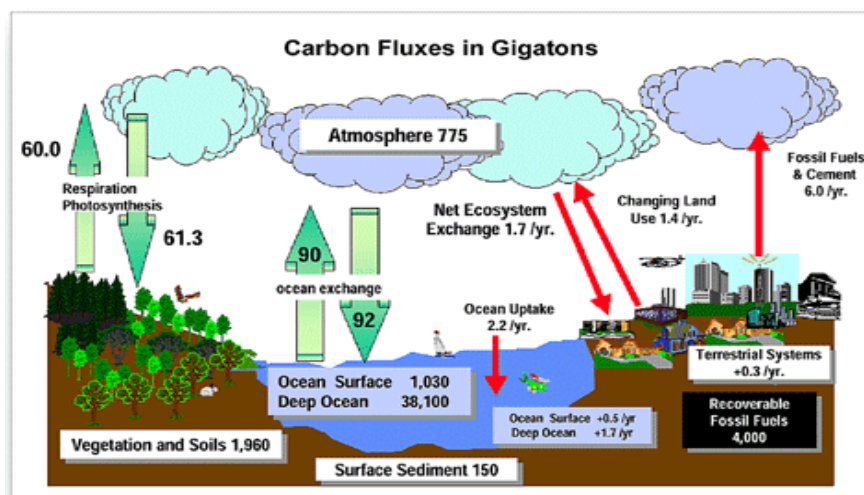
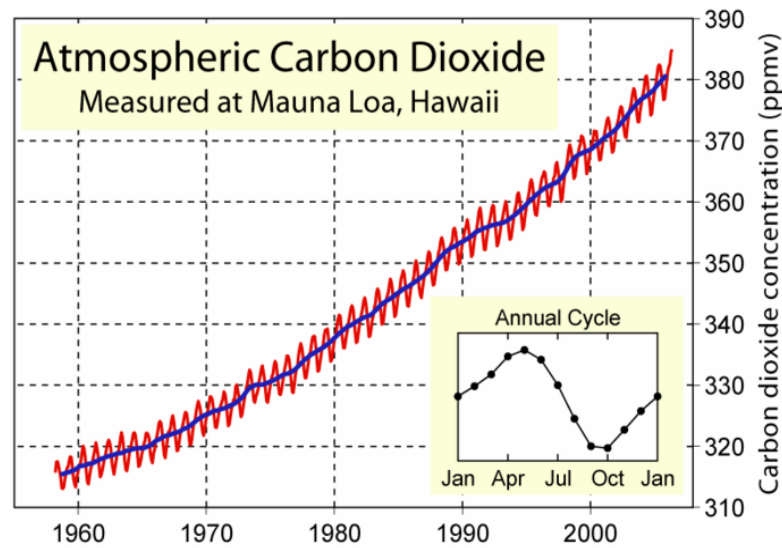


Figure 1.1 Carbon fluxes (1 Giga ton = 10<sup>9</sup> g = 10<sup>6</sup> kg) (CDIACa, 2009).



**Figure 1.2** The situation of atmospheric CO<sub>2</sub> (CDIACb, 2008).

### 1.1.2 C Sequestration: significant in global warming reduction

Carbon sequestration is the result of a series of processes through which CO<sub>2</sub> in the atmosphere is removed from biogeochemical circulation and accumulated in soil and biomass. The present article emphasizes the soil-dependent factors that have bearing on the effectiveness of C sequestration regardless of the general climatic constraints.

In a first stage, atmospheric C is incorporated by photosynthetic plants, which synthesize complex biomacromolecules. When organic remains in addition to microbial bodies decay in soil, a portion of the C stabilizes into the soil (soil C sequestration or humification), and the remainder being released mainly as CO<sub>2</sub> and H<sub>2</sub>O (mineralization). In environmental situations where the above balance shifts to humification, a progressive increase in soil C concentration will be produced through time. This contributes to alleviating the greenhouse effect, global warming and hence climatic change (Batjes, 1998).

Rough estimations point to the fact that the principal C reservoir in the Earth's surface is not terrestrial or marine biomass, but soil organic matter (SOM), the latter

amounting about 1,500 to 2,000 Pg soil organic C (Batjes, 1996). Assuming that SOM pool represents more than twice the C in living vegetation (around 560 Pg) or in the atmosphere (775 Pg) (Eswaran et al., 1995). SOC was estimated about 7 - 10 tC ha<sup>-1</sup> in the tropics, 7 - 13 tC ha<sup>-1</sup> in the subtropics, 11 - 13 tC ha<sup>-1</sup> in temperate regions, and 21 - 24 tC ha<sup>-1</sup> in boreal, polar and alpine areas (Batjes, 1999). It is clear that changes in soil C sequestration rates in local sinks could have a noticeable bearing on the global C balance.

Plant acts as a mediator of C sequestration from atmosphere to soil via photosynthetic process. Primary production therefore sets the upper limit on the amount of C that can be stored in soil. The biomass produced by net primary production will ultimately be available for decomposition and incorporation into the soil either directly as dead plant material or as organic matter that has passed through the animal food chain. Therefore, to promote C sequestration in soils the plant needs to have more potential in C assimilation, belowground biomass accumulation and enable grown in varieties of environments such as soil textures, soil moisture, soil nutrients, and climate; which all characters are difficult present in general plants.

### **1.1.3 Vetiver: challenge in C sequestration**

Vetiver is a miracle grass with more sticky culms, more root biomass and vertically deep root penetration, which is not normally for general plants. His Majesty the King had been suggested in applying vetiver in soil erosion reduction and in mitigating nutrient loss in topsoils. Moreover, vetiver can act in many routs such as decreasing rate of water flow, increasing soil humidity, preventing soil sedimentation in distributing canals, reservoirs, and rivers, protecting the slope of road side, and preventing water and soil contamination. However, there was very few documents influencing C sequestration via vetiver as far as I have known.

### **1.1.4 Outline of the experiments**

Due to C could be sequestered in forms of plant parts and soils, so this research carried out six experiments (chapter IV to IX) which decided to reveal the potentially C sequestration of vetiver as shown below:

Experiment 1: Investigation of internal leaf structures of vetiver (Chapter IV)

Experiment 2: Vetiver phytoliths: Sustainable provenance classification and leaf thermal emission (Chapter V)

Experiment 3: Chemical components in vetiver residues (Chapter VI)

Experiment 4: Relationships of soil respiration to microbial biomass and substrate availability in different vetiver soils (Chapter VII)

Experiment 5: Carbon functional groups in vetiver soils by 1D <sup>1</sup>H NMR study (Chapter VIII)

Experiment 6: Soil labile organic C and C turnover times (Chapter IX)

## **1.2 Research objectives**

1.2.1 To investigate internal leaf structures supporting the potentially C sequestration of vetiver by comparing among 11 provenances

1.2.2 To investigate phytolithic structures among 11 provenances which the abundance is significant in C sequestration

1.2.3 To measure biomass and chemical components in plant residues by comparing among 11 provenances

1.2.4 To investigate relationship among microbial biomass, substrate availability and soil properties to soil respiration

1.2.5 To characterize C functional groups in different vetiver soils

1.2.6 To determine C turnover times of vetiver soils

### **1.3 Scope and limitation of the study**

1.3.1 The comparisons of internal leaf structures, phytoliths, and chemical components in plant residues were carried out 11 provenances of two vetiver species, *Chrysopogon nemoralis* and *C. zizanioides*. *C. nemoralis* consists of 6 provenances: Kamphaeng Phet 1, Loei, Nakhon Sawan, Prachuabkhirikhan, Ratchaburi and Roi Et; whereas *C. zizanioides* has 5 provenances: Kamphaeng Phet 2, Phraratchathan, Songkhla 3, Sri Lanka and Surat Thani. All plants were grown on loamy sand on November 2004 - 2007 at the experimental plots of the Regional Office 3, Land Development Department, Muang District, Nakhon Ratchasima, Thailand.

1.3.2 The comparisons of soil C chemicals, their relationship and the C turnover times were conducted on the study sites distributing in Nakhon Ratchasima.

1.3.3 “Vetiver soil”, in this study, means soil that has vetiver grown.

### **1.4 Benefices of the study**

1.4.1 After the study, we will know which provenance of vetiver has the great powerful in C sequestration, how large of C sequestration through vetiver plantation and how long of labile organic C turnover to the atmosphere.

1.4.2 The results of this study hopefully use to guarantee the potentially C sequestration of vetiver and attribute vetiver as a global warming redactor.

1.4.3 Equations deriving from the interaction among microbial biomass, substrate availability and soil properties to soil respiration can be used to estimate amounts of CO<sub>2</sub> emission from vetiver soils and perhaps modify to other grasses.

1.4.4 Internal leaf structure and phytolithic study can be benefit in vetiver classification.

1.4.5 Due to composed of more silica, vetiver phytoliths can be applied in synthesizing photonic crystals or semi-conductors.

## 1.5 References

- Batjes, N.H. (1996). Total carbon and nitrogen in the soils of the world. **European Journal of Soil Science** 47: 151-163.
- Batjes, N.H. (1998). Mitigation of atmospheric CO<sub>2</sub> concentrations by increased carbon sequestration in the soil. **Biology and Fertility of Soils** 27: 230-235.
- Batjes, N.H. (1999). **Management Option for Reducing CO<sub>2</sub> - Concentrations in the Atmosphere by Increasing Carbon Sequestration in the Soil**. Wageningen, the Netherlands: International Soil Reference and Information Center.
- Carbon Dioxide Information Analysis Center (CDIACa). (2009). **Global carbon project** [On-line]. Available: <http://www.CDIAC.ornl.gov/>
- Carbon Dioxide Information Analysis Center (CDIACb). (2008). **The situation of atmospheric CO<sub>2</sub>** [On-line]. Available: <http://www.CDIAC.ornl.gov/>
- Eswaran, H., Berg, V.P., Reich, P. and Kimble, J. (1995). Global soil carbon resources. In R. Lal, J.M. Kimble, E. Levine and B.A. Stewart (eds.). **Soils and Global Change** (pp. 25-43). Boca Raton, FL: CRC/Lewis Publishers.
- Lawlor, D.W. (2001). **Photosynthesis** (3rd ed.). Oxford: Bios Scientific.
- Marland, G. and Boden, T. (2001). **The increasing concentration of atmospheric CO<sub>2</sub>: How much, when, and why?** [On-line]. Available: <http://www.cdiac.ornl.gov/>

## CHAPTER II

### LITERATURE REVIEWS

#### 2.1 Vetiver species

Vetiver, or faek, has many species, but there are two common species in Thailand, *Chrysopogon nemoralis* (Balan.) Holtt. Camus and *C. zizanioides* (L.) Roberty. Twenty nine provenances, 17 of *C. nemoralis* and 12 of *C. zizanioides*, had been studied and compared the differences (Table 2.1 and 2.2). However, this study focuses on 11 provenances, 6 of *C. nemoralis* and 5 of *C. zizanioides*: there are Kamphaeng Phet 1 (KP1), Loei (LI), Nakhon Sawan (NS), Prachuabkhirikhan (PK), Ratchaburi (RB), Roi Et (RE), Kamphaeng Phet 2 (KP2), Phraratchathan (PT), Songkhla 3 (SK), Sri Lanka (SL) and Surat Thani (ST).

**Table 2.1** Common vetiver provenances in Thailand.

Species	Provenance
<i>C. nemoralis</i>	Chaiyaphum, Chanthaburi, Huai Kha Khaeng, Kamphaeng Phet 1, Kanchanaburi, Loei, Nakhon Phanom 1, Nakhon Phanom 2, Nakhon Sawan, Phitsanulok, Prachuabkhirikhan, Ratchaburi, Roi Et, Saraburi 1, Saraburi 2, Udon Thani 1 and Udon Thani 2
<i>C. zizanioides</i>	Chiang Mai, Chiang Rai, Kamphaeng Phet 2, Mae Hong Son, Songkhla 1, Songkhla 2, Songkhla 3, Sri Lanka, Surat Thani, Trang 1, Trang 2 and Phraratchathan

Data from Chaipattana (2010).

**Table 2.2** Comparison of two vetiver species.

Variable	<i>C. nemoralis</i>	<i>C. zizanioides</i>
1. Soil type suggestion		
1.1 Sandy soil	NS, KP1, RE and RB	KP2 and SK
1.2 Clay loam soil	LI, NS, RB, KP1 and PK	ST and SK
1.3 Leterite soil	PK and LI	KP2, SK, ST and SL
2. Region suggestion		
2.1 North	NS and KP1	SL
2.2 Northeast	RE	SK
2.3 Central and east region	RB and KP1	KP2, SK and ST
2.4 South	-	SK and ST
3. Origin		
	Southeast Asia: Thailand, Laos, Cambodia and Vietnam	In the central part of the Asia Continent, presumably India
4. Distribution		
	Wildly multiplied in natural conditions, and not cultivated for multiplication purpose	Generally planted for multiplication
5. General morphology		
5.1 Leaf arrangement	Tufted with leaves bending down like lemongrass	Clumpy with long, erect leaves
5.2 Aboveground height	100 - 150 cm high	150 - 200 cm high

**Table 2.2** (Continued).

Variable	<i>C. nemoralis</i>	<i>C. zizanioides</i>
5.3 Method of cultivation	Normally incapable of ratooning and aerial branching	Capable of ratooning and aerial branching
6. Leaf		
6.1 Length	35 - 80 cm long and 0.4 - 0.8 cm broad	45 - 100 cm long and 0.6 - 1.2 cm broad
6.2 Color	Pale green, upper surface flapped with a triangular ridge, lower surface paler than upper surface, septum not clearly seen when held against sunlight	Dark green, curved upper surface, white lower surface with a septum, texture clearly seen when held against sunlight
6.3 Texture	Coarse texture, with little wax coating, unwaxy appearance	Smooth texture, with wax coating giving soft and waxy appearance
7. Inflorescence and Spikelet		
7.1 Length	100 - 150 cm long	150 - 250 cm long inflorescence
7.2 Color	Color varies from creamy white to purple	Mostly purple colour
7.3 Florets	Florets with awn	Most florets without awn

**Table 2.2** (Continued).

Variable	<i>C. nemoralis</i>	<i>C. zizanioides</i>
8. Seed	Relatively smaller	Relatively larger
9. Roots		
9.1 Fragrance	Have no fragrance	Have mild fragrance with volatile oils of 1.4 - 1.6% dry weight
9.2 Root penetration	Shorter roots, can anchor as deep as 80 - 100 cm	Can anchor as deep as 100 - 300 cm
10. Uses	In Thailand, leaves are used for roof thatching, but not popular	Roots are used to extract volatile oils to make perfume, soaps, and other products like handbags, fan, clothes-hangers, and also used as herbal medicine and closet insect repellents

Data from Chaipattana (2010); ORDPB (2000); TVNI (2010).

## 2.2 Photosynthetic pathways of C3, C4 and CAM plants

Due to an identification of plant metabolisms (C3, C4 or CAM) can indicate to the efficiency of CO<sub>2</sub> assimilation and photosynthetic yields, but it is unclear for vetiver provenances. Recently, many documents show increasing atmospheric CO<sub>2</sub> lead to higher photosynthetic rates, but little corroborate evidences to suggest plants are C limited. Plant

water use efficiency will increase for plant species that rely on the photosynthetic enzyme Ribulose biphosphate carboxylase to produce a 3C (C3) sugar during photosynthesis. C3 plants can loose up to 50% of fixed C to photorespiration and would benefit greatly under higher partial pressures of CO<sub>2</sub> that reduce transpired water loss during photosynthesis. In comparison, plants fixing CO<sub>2</sub> to 4C sugar (C4) or those using Crassulacean acid metabolism (CAM) are more efficient at fixing CO<sub>2</sub> and show little if any change under elevated CO<sub>2</sub>. So, different photosynthetic pathways among C3, C4 and CAM plants have been concluded in Table 2.3.

**Table 2.3** Characteristics of plants with different photosynthetic pathways.

Characteristics	C3	C4	CAM
Leaf structure	Laminar	Mesophyll	Cells with have
chloroplasts	mesophyll,	arranged radially	large vacuoles
bundle sheath	parenchymatic	around bundle	
	chlorenchymatic	sheaths (“Kranz” - type-anatomy) <sup>c</sup>	
Chloroplasts	Granal <sup>a</sup>	Mesophyll: granal; bundle-sheath cells	Granal or agranal <sup>b</sup>
Chlorophyll a/b	ca. 3	ca. 3	≤ 3
Primary CO <sub>2</sub> acceptor	RuBP (substrate: CO <sub>2</sub> )	PEP (substrate: HCO <sub>3</sub> <sup>-</sup> )	In light: RuBP In dark: PEP
First product of photosynthesis	C3 acids (PGA)	C4 acids (oxaloacetate, malate, aspartate)	In light: PGA In dark: malate

**Table 2.3** (Continued).

Characteristics	C3	C4	CAM
C isotope ratio in photosynthates ( $\delta^{13}\text{C}$ )	ca. -20 to -40%	ca. -10 to -20%	ca. -10 to -35%
Photosynthesis depression by $\text{O}_2$	yes	no	yes
$\text{CO}_2$ release in light (apparent photorespiration)	yes	no	no
$\text{CO}_2$ compensation concentration at optimal temperature	30 - 50 $\mu\text{l l}^{-1}$	< 10 $\mu\text{l l}^{-1}$	In light: 0 - 200 $\mu\text{l l}^{-1}$ In dark: < 5 $\mu\text{l l}^{-1}$
Ratio of mesophyll resistance to minimal stomatal resistance	4 - 5	0.5 - 1	
Net photosynthetic capacity	Slight to high	High to very high	In light: slight In dark: medium
Light saturation of photosynthesis	At intermediate intensities	No saturation, even at highest intensities	At intermediate to high intensities
Redistribution of assimilation products	Slow	Rapid	Variable
Dry matter production	Medium	High	Low

<sup>a</sup>Thylakoids stacked; <sup>b</sup>thylakoid lamellar, <sup>c</sup>not in aquatic plant.

Data from Fitter and Hay (2002), Lacher (2001), Nobel and Jordan (1983).

## 2.3 Internal leaf structure

Influence photosynthetic pathways and environment, some plants have been modified internal leaf structures different from the standard (Figure 2.1 and 2.2). For instance, Kranz structure refers high photosynthetic capacity which present in some C<sub>4</sub> plants but does not in C<sub>3</sub> plants, or bulliform cell and sclerenchyma girder indict xerophytes.

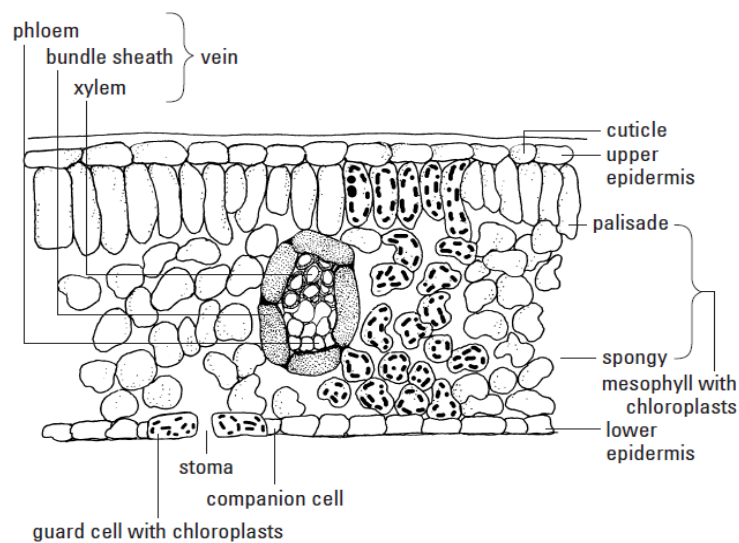


**Figure 2.1** The standard leaf has three tissue regions: the epidermis, the mesophyll and the vascular bundles or veins (Rand, 2001).

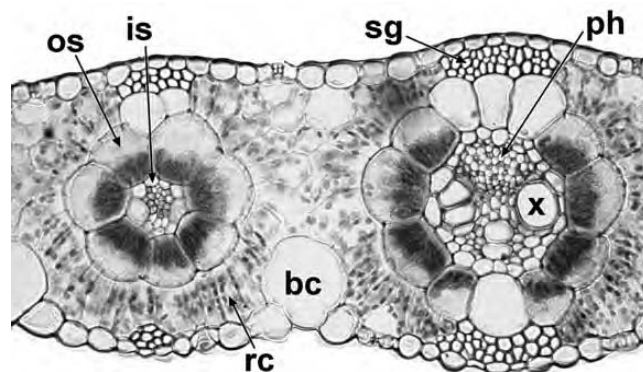


**Figure 2.2** *Eleusine coracana* (Poaceae), transverse section of leaf with Kranz structure. bc = bulliform cell, is = inner bundle sheath, os = outer bundle sheath, ph = phloem, rc = radiate chlorenchyma, sg = sclerenchyma girder, x = xylem (Versiteit Nijmegen, 2010).

## **2.4 Plant chemical composition and decomposition**

The biological fixation of CO<sub>2</sub> or photosynthesis to produce organic compounds is termed gross primary production (GPP). Following losses to respiration, growth and maintenance the newly formed biomass is termed net primary production (NPP). Net secondary production (NSP) occurs when consumers such as herbivores or decomposers of NPP produce new biomass (Chesworth, 2008). The quantity and quality of NPP and subsequent NSP determines the outcome of decomposition processes and regulates the accumulation of SOM.

### **2.4.1 Cytoplasm and storage components**

Lipids range from simple fatty acids to complex sterols, phospholipids, chlorophyll, waxes and resins (cutins and suberins). As a class of compounds, the decomposability of lipids depends on their chemical complexity. Long chain aliphatic fatty acids and phospholipids, components of membranes, are degraded relatively quickly depending on the degree of saturation or double bond content. More complex waxes and resins are resistant to decomposition and form some of the most resistant substances in soil. The hydrophobic character of these substances allows them to sorb into hydrophobic domains of SOM, shielding them from enzymatic attack.

Starch is a polymer of glucose synthesized and stored in plastids, such as amyloplasts of roots and tubers. Starch consists of two glucose polymers, amylose and amylopectin. Amylose contains long unbranched chains of  $\alpha(1-4)$ -glucose units. For most plants, amylose can account for up to 30% of the total starch. Amylopectin has a similar structure linked every 20 to 30 glucose residues by  $\alpha(1-6)$ -glucose bonds. A class of enzymes known as amylases readily degrades starch into glucose. Starch represents a

significant energy source but requires a supply of exogenous nutrients to complete microbial growth and other NSP (Joshi and Mansfield, 2007).

#### **2.4.2 Hemicellulose, pectin and cellulose**

The majority of plant carbohydrates are found as the polysaccharides, cellulose hemicellulose and pectin in the secondary cell wall. Hemicelluloses contain xylans (xylose polymer), an uronic acids (i.e., sugar acid), and arabinose (another 5C sugar). Pectin is composed of three main polysaccharide types: polygalacturonan (repeating galacturonic acid monosaccharide subunits), rhamnogalacturonan I (alternating rhamnose and galacturonic acid subunits) and rhamnogalacturonan II (highly branched polysaccharide). Because of their sugar content, hemicellulose and pectin are a rich energy source for microbes, but require an extensive suite of enzymes to complete its decomposition (Mansfield, 2009).

Cellulose consists of glucose units linked by  $\beta(1-4)$  bonds to form long glucose chains. The chains are cross-linked by hydrogen bonds to form paracrystalline assemblages called microfibrils. The cellulose microfibrils are cross-linked into a network or scaffold with hemicellulose. Cellulose microfibrils are decomposed by the enzyme system cellulase composed of endoglucanase, exoglucanase and  $\beta$ -glucosidase (also known as cellobiases). Cellulose degradation begins with the disruption of the crystalline structure of the microfibrils followed by the depolymerization into short glucose chains (Joshi and Mansfield, 2007). A wide range of organisms degrade the energy rich cellulose, but only a few have demonstrated the complete depolymerization (Figure 2.3).

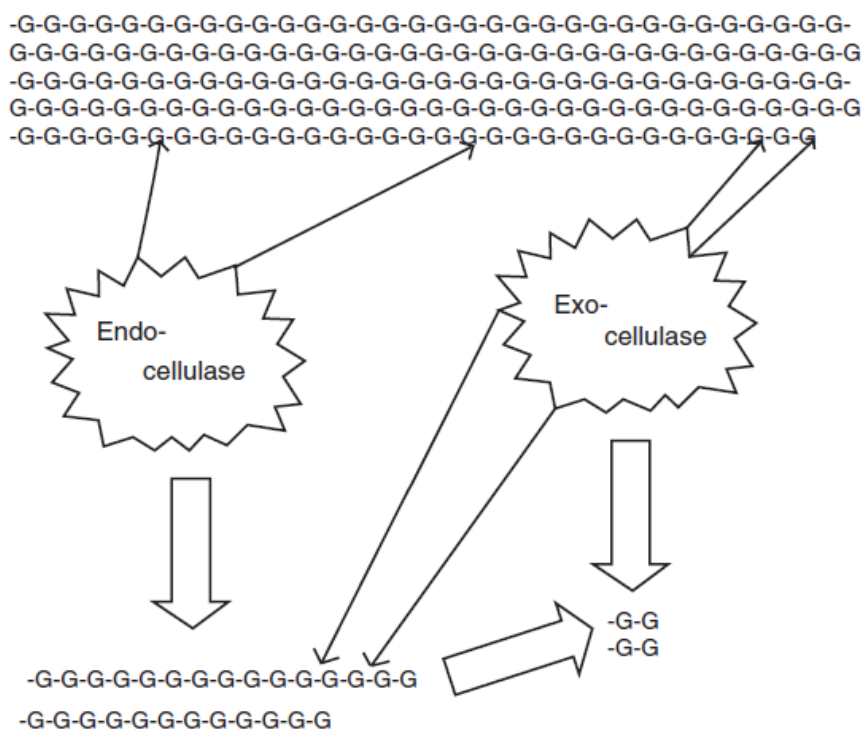


**Figure 2.3** Part of the cellulose fiber is attacked by an endo-1, 4- $\beta$ -glucanase (endocellulase) breaking the chains and splitting off oligosaccharides in a random manner, including soluble shorter chains with, for example, 3 to 5 glucose units. An exo-1, 4- $\beta$ -glucanase (exocellulase) splits off cellobiose units from the non-reducing end of the carbohydrate chains. *G* Glucose unit (Berg and McClaugherty, 2008).

### 2.4.3 Lignin

Lignin is a complex and dense amorphous secondary cell wall polymer typically found in the trachea elements and sclerenchyma of terrestrial plants. The dense hydrophobic nature of lignin makes it difficult for enzymes to penetrate. The precursors of lignin come from the shikimic and phenylpropanoid pathway that converts the amino acids phenylalanine and tyrosine to hydroxycinnamyl alcohol and then to monolignols -p-coumaryl, coniferyl and synapyl alcohols. The monolignols are assembled randomly on a protein template. The lignin polymer provides structural rigidity and a mechanical barrier

against pest and pathogens. Lignin is accounted about 30% of the over  $1.4 \times 10^{12}$  kg of C sequestered each year (Boerjan et al., 2003).

The decomposition of lignin is primarily attributed to fungi, actinomycetes, and bacteria under aerobic conditions. Fungi are the most efficient lignin degraders in nature and for this reason play a key role in C cycling. Fungal species that degrade lignin are often grouped into soft rot, brown rot and white rot fungi based on the color of the decayed substrate. White rot fungi are the most active lignin degraders. The interaction of cellulose and lignin to form lignocellulose produces a difficult to degrade structure compared to its individual components (Battle et al., 2000). Figure 2.4 shows a scheme of lignin degradation.

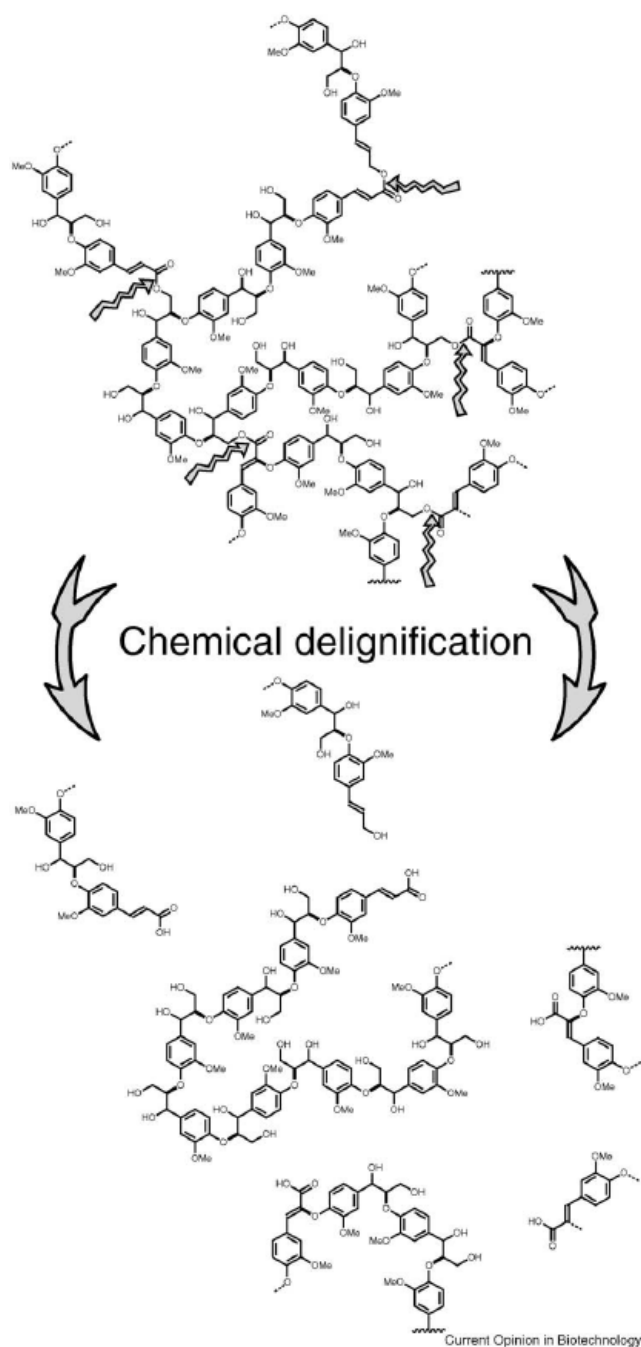


**Figure 2.4** Schematic representation of hypothetical lignin resulting from the ectopic lignification incorporating coniferyl-ferulate or sinapyl-ferulate conjugates and normal monolignols (coniferyl or/and sinapyl alcohols). The hypothetical lignin has several readily cleavable ester bonds (demarked by arrows) resulting from the copolymerization of coniferyl alcohol and the ferulate conjugates that would permit rapid solubilization of the cell wall under alkaline reaction conditions (Grabber et al., 2009).

#### 2.4.4 Main groups of bacteria and fungi in plant component decomposition

The bacteria include both aerobic and anaerobic organisms, which distinguishes them from the exclusively aerobic fungi. Both groups have organisms able to degrade all the main polymers such as lignin, cellulose, and the hemicelluloses. For many bacteria, the diameters range largely from 0.1 to 2  $\mu\text{m}$  and for filamentous fungi from ca. 1 to less than 20  $\mu\text{m}$ . Bacteria may be either immobile, or mobile, with one or more flagella, a whip-like structure. Fungal mycelia demonstrate mobility in another way, in that they simply grow in one direction and thus move their protoplasm, leaving an empty cell-wall structure behind (Berg and McClaugherty, 2008). Some of the general properties of main groups of bacteria and fungi are collected in Table 2.4.

**Table 2.4** Some general properties of the main groups of bacteria and fungi.

Property	Bacteria	Fungi
Mobility	+	+
Spore -forming ability	+	+
Can degrade cellulose /hemicellulose	+	+
Can degrade lignin completely	+	+
Can degrade lignin anaerobically <sup>a</sup>	+	-
Can degrade intact fiber walls	+	+
Species with N repression of the ligninase system	? <sup>b</sup>	+
Species without N repression of the ligninase system	? <sup>b</sup>	+

<sup>a</sup>Incomplete degradation to be compared to the brown-rot type.

<sup>b</sup>Not known.

Data from Berg and McClaugherty (2008).

#### **2.4.5 Microbial biomass**

Microbial biomass represents NSP derived from photosynthetically fixed C. Net secondary production may be recycled to produce more generations of microbial decomposer biomass. The turnover of the soil microbial biomass represents a significant source of labile and resistant C and potential substrate for SOM formation. Bacteria have many C compounds that are similar to plants. Protein makes up 55% of the cell dry weight of common bacteria. Fungi have less protein than bacteria, concentrating their metabolic constituents at the tips of growing hyphae. For this reason, bacteria have narrow C to N ratios that range from 5 to 8 while fungi often have C to N ratios in excess of 8. Differences in C to N ratio and cell wall components are often related to the decomposability of soil organisms, as was mentioned earlier for plant residues (Giri et al., 2005; Lipson et al., 2005).

The complexity of the microbial cell walls makes them resistant to decay, similar to that of plants, but the building blocks are vastly different. Microbial cell walls contain constituents such as amino sugars and the D-form of certain amino acids that are resistant to decay. Most amino sugars in soil are of microbial origin, especially of fungi (Guggenberger et al., 2001) Bacterial cell walls are composed of a rigid layer of N-acetylglucosamine and N-acetylmuramic acid chains. They are linked into a rigid layer called peptidoglycan by peptide bonds. The cross-linked peptidoglycan called murein is composed repeating units of L-alanine, D-alanine, D-glutamic acid, and either lysine or diaminopimelic acid. Bacterial cell walls contain anywhere from 10 to 90% peptidoglycan with grampositive bacteria containing the most. A major component of the fungal cell wall is chitin, which is composed of repeating units of N-acetylglucosamine. Fungi also contain dark-colored pigments called melanins that are resistant to decay and are thought to contribute directly to SOM formation.

#### 2.4.6 Turnover of soil inputs

The turnover of C inputs to soil is often substrate dependent and therefore follows first order reaction kinetics (Horwath, 2008). Proteins and sugars are degraded rapidly and exhibit high turnover rates. The turnover of polymers such as cellulose, lignin and peptidoglycan that require extensive enzyme suites and microbial succession have longer turnover rates. The rate of turnover of a soil C input or substrate ( $A$ ) with time ( $t$ ) is defined in Eq. (2.1).

$$\frac{dA}{dt} = -kA \quad (2.1)$$

where the product of the decomposition rate constant  $k$  and  $A$  describes the change in  $A$  with time. The time required transforming or turnover substrate  $A$  is in Eq. (2.2).

$$\text{turnover time} = \frac{1}{k} \quad (2.2)$$

The turnover time is often referred to as the mean residence time (MRT). Upon integration Eq. (2.3) becomes

$$A_t = Ae^{-kt} \quad (2.3)$$

where  $A_t$  is the substrate remaining at any time during the decomposition processes. The decomposition rate constant  $k$  is expressed as per unit of time (e.g.,  $\text{min}^{-1}$ ,  $\text{h}^{-1}$ ,  $\text{d}^{-1}$ ,  $\text{yr}^{-1}$ , etc.). The time required to turnover one half of substrate  $A$  is expressed as the logarithmic function (Eq. (2.4))

$$\ln \left[ \frac{A - \frac{1}{2}}{A} \right] = -kt_{1/2} \quad (2.4)$$

where  $t_{1/2}$  is the time required to turn over one half of substrate  $A$  (half life). Eq (2.5) is integrated to

$$t_{1/2} = \frac{0.693}{k} \quad (2.5)$$

Table 2.5 shows typical turnover times of various plant and microbial inputs to soil. The turnover times reflects the decomposability of the soil inputs. Catechol, a simple phenol, composes of cellulose and lignin, has a two compartment, one labile and one more stable which impacts on decomposability. Catechol is transformed into two groups of soil C with different degradability, one (17%) is relatively labile to degradation with a half-life of 27.8 days, and another (83%) is relatively recalcitrant with a half-life of 4.75 years (Vinken et al., 2005).

**Table 2.5** Decomposition rates and turnover of various plant and microbial soil inputs.

Soil input	Decomposition rate constant (day <sup>-1</sup> )	Half life (days)	Turnover (days)
Sugar, amino acid	0.2	3.5	5.0
Cellulose	0.08	8.7	12.5
Lignin	0.01	69.0	100.0
Fungal cell wall	0.02	34.7	50.0

## 2.5 Formation of soil organic matter

Soil decomposers act as the “Waste Management” crew of an ecosystem. The decomposition of plant and microbial inputs to soil plays an important role in maintaining the global C budget by cycling most of the CO<sub>2</sub> fixed through NPP back to the atmosphere. The C fixed as NPP and converted to NSP is decomposed at a rate very similar to the amount produced on an annual basis. A small fraction of NPP and NSP is persevered as stable soil C in the form of SOM through a process called humus formation (IPCC, 2000).

Humus formation is an essential process that determines NPP and NSP by controlling the availability of essential nutrients. The most efficient procedure to remove humic substances from soil is an alkali extraction. The extraction yields fulvic and humic acids. Fulvic acids are characterized as having low molecular weight (1,000 to 30,000), soluble in water and are commonly found in soil solution and aquatic environments. Humic acids have higher molecular weight (10,000 to 100,000 and more), are insoluble in water and generally are the larger fraction of the two acids. Humic structure includes aromatic and aliphatic (O-alkyl and alkyl) domains and oxygen-containing functional groups in surface with different derivatives. The higher molecular weight of humic acids is presumably due to the condensation of smaller compounds. The alkali unextractable portion of SOM is termed humin and represents up to 30 to 50% of total SOM. Humin is thought to be strongly attached to soil minerals and according to <sup>14</sup>C-dating studies are often 1,000 or more years in age (Hiradate et al., 2006).

During the formation of SOM, nutrients such as N, P and S are incorporated into its structure. The structure of SOM consists of approximately 50 - 55% C, 5% H, 33% O, 4.5% N, and 1% S and P. In addition, other metals and micronutrients, such as Ca, Zn and Cu are present in much smaller amounts. The association of SOM with secondary minerals such as clay and amorphous oxides create soil structure through the formation of

aggregates. Aggregate formation enhances soil physical structure by ordering soil mineral grains, promoting aeration and water infiltration and storage (Kögel-Knabner, 2000).

## **2.6 Recently C sequestration study**

Different biomes contain different amount of SOM which regulate nutrient cycling and impacting physical properties plays a major role in sustaining ecosystem productivity (Table 2.6). The quantity of SOM is dependent on the balance between NPP and the rate of decomposition and also the presence of silt and clay and low temperature and low oxygen concentration generally preserve more C in soils. However, human activities also determine SOC accumulation in each ecosystem or lands (Table 2.7).

**Table 2.6** The area, stocks of C, net primary production (NPP) and C turnover of various biomes<sup>a</sup>.

Biome	Area (10 <sup>9</sup> ha)	Global C stock (Gg C ha <sup>-1</sup> )			NPP (Pg C yr <sup>-1</sup> )	Turnover (years) <sup>b</sup>
		Plant	Soil	Total		
		Tropical forests	1.76	340		
Temperate forests	1.04	139	153	292	7.3	29
Boreal forests	1.37	57	338	395	2.9	91
Tropical savannas and grasslands	2.51	79	247	326	16.3	10
Temperate grasslands and shrublands	1.52	23	176	199	6.15	61
Deserts and semi deserts	3.66	10	159	169	2.45	37
Tundra	0.76	2	115	117	0.75	490
Croplands	1.48	4	165	169	5.45	21
Wetlands	0.35	15	225	240	4.3	520
Total	15.0	669	1791	2460	63.4	

<sup>a</sup>Adapted from Houghton et al. (2001).

<sup>b</sup>Adapted from Raich and Schelsinger (1992) and Paul and Clark (1996).

**Table 2.7** Comparison of C sequestration among ecosystems and land uses.

Location	Depth (cm)	Ecosystem/ Land use/	SOC		Reference
			(tC ha <sup>-1</sup> )	(gC kg <sup>-1</sup> )	
Queensland, AU	0 - 20	CT + SR + N0*	78.8	-	Wang and Dalal (2006)
		CT + SR + NF	79.6	-	
		NT + SR + N0	78.5	-	
		NT + SR + NF	84	-	
Cheyenne, WY	0 - 5	Light grazing	13.8	-	Ganjegunte et al. (2005)
		Heavy grazing	10.9	-	
		Non-grazed exclosure	10.8	-	
Viterbo, IT	5 - 35	CT	-	28	Marinari et al. (2007)
		NF	-	26.8	
Quenland, AU	0 - 10	Natural forest	-	79.6	Chen et al. (2004)
		First hoop pine rotation	-	63.8	
		Second hoop pine rotation	-	64	
Sakaerat, Nakhon Ratchasima, TL	0 - 100	Dry evergreen	210.9	-	Janmahasatien et al. (2005)
Maeklong, Kanchanaburi, TL	0 - 100	Mixed deciduous forest	223.9	-	

**Table 2.7** (Continued).

Location	Depth (cm)	Ecosystem/ Land use/	SOC		Reference
			(tC ha <sup>-1</sup> )	(gC kg <sup>-1</sup> )	
Fang, Chiang	0 - 50	<i>Acacia confusa</i>	-	123.9	Poolsiri (2005)
Mai, TL		<i>Liquidambar</i>	-	136.6	
		<i>formosana</i>			
		<i>Cinnamomum</i>	-	157.5	
		<i>camphora</i>			
		<i>Cunning hamia</i>	-	100	
		<i>lanceolata</i>			
		<i>Fraxinus griffithii</i>	-	150.6	
Sakaerat,	0 - 50	Dry evergreen forest	118	-	Chidthaisong and
Nakhon		Reforest ( <i>Acacia</i>	66	-	Lichaikul (2005)
Ratchasima,		<i>mangium</i> )			
TL		Agricultural (maize)	60	-	
		soils			

\*CT: conventional tillage; NT: no-till; SR: stubble remained; N0: no N fertilizer application; NF: N fertilizer applied.

## 2.7 Some mechanisms of SOC protection

### 2.7.1 SOC protection by soil aggregate

Soil aggregate is a one mechanism to protection of light fraction (LF) organic matter by reducing its decomposition rate by half or more. Grandy et al. (2006) found that within 60 days of incubation, the proportion of total LF protected within 2000 to 8000  $\mu\text{m}$  aggregates decreased from 28 to 16%. Releasing LF and other substrates from physical

protection, coupled with increased soil temperature and other environmental changes, increased SOM mineralization. This increased soil  $\text{NO}_3^-$  concentrations to more than  $15 \mu\text{g N g}^{-1}$  and greatly accelerated mean annual  $\text{CO}_2$  emissions over 3 years by 28 to 65% ( $1.0 - 1.9 \text{ gC m}^{-2} \text{ d}^{-1}$ ) and  $\text{N}_2\text{O}$  emissions by 200 to 700% (Grandy and Robertson, 2006).

### 2.7.2 SOC protection by clay

Because of clay minerals, clay surface and interlayer materials (such as Al or Fe making a porous structure), clay is one factor in organic C security as shown in conclusions in Table 2.8.

**Table 2.8** Interactions of organic molecules and clay minerals in soil organic C (SOC) sequestration.

Location	Soil	Interactions	Reference
Canada	Silty clay loam and clay loam	C-enriched humic and fulvic acids are found in coarse clay, whereas aliphatics are in clays and noncrystalline minerals.	Schnitzer and Kodama (1992)
Canada	Silty clay loam and clay loam	Organic C is positively correlated with extractable Al and chloritized vermiculite but negatively with total clay content.	Monreal and Kodama (1997)
New Zealand	Clay	Surface area and electrical charge of clay minerals rather than total clay content control the protection of SOC from microbial decay.	Saggar et al. (1996)

**Table 2.8** (Continued).

<b>Location</b>	<b>Soil</b>	<b>Interactions</b>	<b>Reference</b>
Aberdeen	Clay	Ability of clay correlates with adsorbing amounts of polysaccharide, but not amino groups.	Cheshire et al. (2000)
Waseca, MI	Clay loam	Dense humic compounds associate with coarse and medium clay particles, whereas diffuse humic compounds interact with fine clay minerals.	Laird et al. (2001)
Germany	Fine sand	Organic C is bound to the clay matrix in interaction with hydrous Al and Fe minerals particularly in subsurface horizons.	Kaiser et al. (2002)
Ames, IA	Silt loam	Clay mineralogy controls the formation and stabilization of C-enriched humic compounds, which are primarily concentrated on fine smectite clay surfaces.	Gonzalez and Laird (2003)

## 2.8 Phytoliths

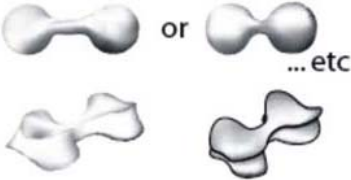
### 2.8.1 Composition and characteristics

Phytoliths are largely composed of amorphous (noncrystalline) silicon dioxide (SiO<sub>2</sub>) and about 4 to 9% water (Rowlett and Pearsall, 1993). Phytoliths can also contain significant amounts of occluded, chemisorbed or solid solution impurities such Al, Fe, Ti, Mn, P, Cu, N and C. Carbon presents within phytoliths is the result of the trapping of plant cellular material during phytolith formation within living cells. In addition, it has been demonstrated that more than 50% of this encapsulated C is protected from oxidation, and thus provides another source of paleoenvironmental and paleoclimatic information (Kelly

et al., 1991). The development of accelerator mass spectrometry (AMS) radiocarbon techniques using very small samples allows for the dating of phytolith C (Mulholland and Prior, 1993). Moreover, C isotope analysis can also be used to provide additional information about the photosynthetic pathway of plants. For example, knowledge as to whether C<sub>3</sub> and C<sub>4</sub> grasses dominated a given environment is an indication of climate at the time those plants were growing (Smith and Anderson, 2001; Smith and White, 2004).

### **2.8.2 Phytolithic classification**

Over the last few decades a number of attempts have been made to develop a universally accepted standard phytolith classification scheme (Rapp and Mullholland, 1992; Bowdery et al., 2001). However, it was not until the 3<sup>rd</sup> International Meeting on Phytolith Research (IMPR) in Bruxelles, in August, 2000. This group has now reported with the “International Code for Phytolith Nomenclature 1.0 (Madella et al., 2005)”. Some approved terms are illustrated in Figure 2.5.

Schematic drawings*	ICPN names	Former nicknames
	Bilobate short cell	Dumbbell or bilobate
	Trapeziform short cell	Square or rectangle
	Cylindrical polylobate	Polylobate
	Trapeziform polylobate	Polylobate
	Trapeziform sinuate	
	Elongate echinate long cell	Elongate spiny or elongate sinuous
	Cuneiform bulliform cell	Bulliform or fan-shaped
	Parallelepipedal bulliform cell	Bulliform
	Acicular hair cell	Point-shaped
	Unciform hair cell	Point-shaped
	Globular granulate	Spherical rugose
	Globular echinate	Spherical crenate
	Cylindric sulcate tracheid	Tracheid

\*Several drawings are made after Fredlund and Tieszen (1994).

**Figure 2.5** Internationally defined morphological phytolith shapes from the International Code for Phytolith Nomenclature 1.0 (Madella et al., 2005).

### 2.8.3 Phytoliths and C sequestration

Well-preserved by silica suggests phytoliths retain longer C occluded over than thousand years, while other organic C already decomposed (Figure 2.6). Some high phytolithic plants which were recommended by Sullivan and Parr (2008): there were *Bambusa forbesii* (Ridl) Holttum, *Brachiaria brizantha* (Hoscht. ExA.Rich) Stap f., *Imperata cylindrical* P. Beauv., *I. exaltata* (Roxb.) Brogn., and *Saccharum officinaruni* (L.).

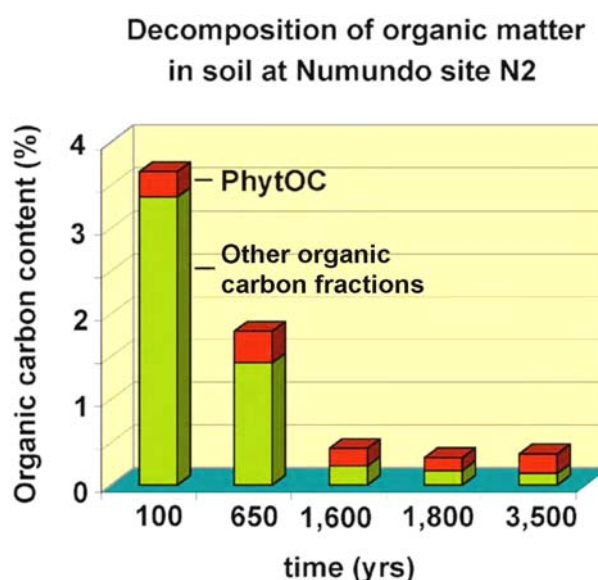


**Figure 2.6** Illustrate the percentages of resistant decomposed phytoliths comparing to other organic matter fraction (Parr and Sullivan, 2005).

C4 grass phytoliths mainly contained silicon and oxygen; whereas of woods composed of many element aggregations such as aluminum, iron, or potassium and of conifers had Si/Al co-deposit (Carnelli et al., 2002; Krull et al., 2003; Tsartsidou et al., 2007). As a result, organic C within C4 grass phytoliths were well-preserved by highly purify silicon from fungal decomposition or burning process, while siliceous aggregate of wood phytoliths did not resist burning but oxidized to calcitric ash, and if not good preservation it would convert subsequently into various more insoluble phosphate minerals

(Tsartsidou et al., 2007). Grass roots found high potential in aluminum blocking at endodermis and selecting out of germanium during germanium and silicon uptake and translocation to phytolith sites (Blecker et al., 2007); while pine and fir such as *Pinus sylvestris*, *Fagus sylvatica*, *Calluna vulgaris*, *Abies alba*, and *Festuca sylvatica* allowed aluminum and silicon transfer to needles and deposit mostly on phytolith surface rather than that of whole phytoliths, causing lower solubility (Carnelli et al., 2002). Major organic C reserved within phytoliths composed of simple carbohydrate, but the minor was lipid materials (Krull et al., 2003).

More silicic acid ( $H_4SiO_4$ ), the transporting form of silica, assuming attribute a formation of humic macromolecules after plant decomposition (Figure 2.7). Silicic acid could promote oxidative polymerization and ring cleavage of catechol resulted darkening and forming humic macromolecule complexes, but the reaction must be under acidic condition (Ghabbour and Davies, 2000). In particular, more than 50% carboxyl groups of catechol would deprotonate at pH 5.0 and attracted anion of silicic acid forming a hexacoordinated complex of silicon with catechol. This complicated structure suggesting was more recalcitrant C.

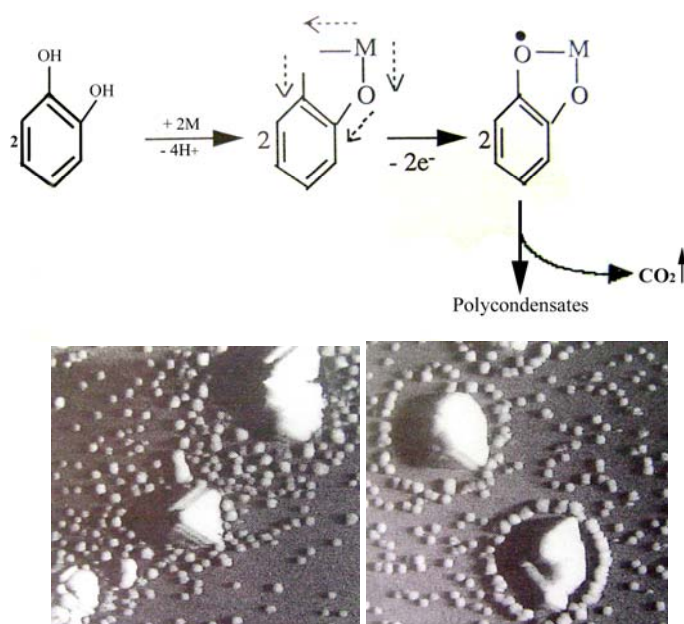


**Figure 2.7** Forming humic macromolecule complexes from silicic acid.

## 2.9 References

- Battle, M., Bender, M.L., Tans, P.P., White, J.W.C., Ellis, J.T., Conway, T. and Francey, R.J. (2000). Global carbon sinks and their variability inferred from atmospheric O<sub>2</sub> and δ<sup>13</sup>C. **Science** 287: 2467-2470.
- Berg, B. and McClaugherty, C. (2008). **Plant Litter: Decomposition, Hummus Formation, Carbon Sequestration** (2nd ed.). Verlag: Springer.
- Blecker, S.W., King, S.L., Derry, L.A., Chadwick, O.A., Ippolito, J.A. and Kelly, E.F. (2007). The ratio of germanium to silicon in plant phytoliths: Quantification of biological discrimination under controlled experimental conditions. **Biogeochemistry** 86(2): 189-199.
- Boerjan, W., Ralph, J. and Baucher, M. (2003). Lignin biosynthesis. **Annual Reviews of Plant Biology** 54: 519-549.
- Bowdery, D., Hart, D.M., Lentfer, C. and Wallis, L.A. (2001). A universal phytolith key. In J.D. Meunier and F. Colin (eds.). **Phytolith: Applications in Earth Sciences and Human History** (pp 267-278). Balkema.
- Carnelli, A.L., Adella, M.M., Theurillat, J.P. and Ammann, B. (2002). Aluminum in the opal silica reticule of phytoliths: A new tool in palaeoecological studies. **American Journal of Botany** 89(2): 346-351.
- Chaipattana. (2010). **Vetiver** [On-line]. Available: <http://www.chaipat.or.th>
- Chen, C.R., XU, Z.H. and Mathers, N.J. (2004). Soil carbon pools in adjacent natural and plantation forests of subtropical Australia. **Soil Science Society of America Journal** 68: 282-291.
- Cheshire, M.V., Dumat, C., Fraser, A.R., Hillier, S. and Staunton, S. (2000). The interaction between soil organic matter and soil clay minerals by selective removal and controlled addition of organic matter. **European Journal of Soil Science** 51: 497-509.

- Chesworth, W. (ed.). (2008). **Encyclopedia of Soil Science**. Dordrecht: Springer.
- Chidthaisong, A. and Lichaikul, N. (2005). Carbon stock and emission in dry evergreen forest, reforestation and agricultural soils. In **Proceeding of the Climatic Forestation “Potential of Forest in Supporting Kyoto Protocol”**.
- Fitter, A.H. and Hay, R.K.M. (2002). **Environmental Physiology of Plants** (3rd ed.). San Diego: Academic Press.
- Ganjugunte, G.K., Vance, G.F., Preston, C.M., Schuman, G.E., Ingram, L.J., Stahl, P.D. and Welker, J.M. (2005). Soil organic carbon composition in a northern mixed-grass prairie effects of grazing. **Soil Science Society of America Journal** 69: 1746-1756.
- Ghabbour, E.A. and Davies, G. (eds.). (2000). **Humic Substances: Versatile Components of Plants, Soils and Water**. The Royal Society of Chemistry.
- Giri, B., Giang, P.H., Kumari, R., Prasad, R. and Varma, A. (2005). Microbial diversity in soils. In F. Buscot and A. Varma (eds.). **Microorganisms in Soils: Roles in Genesis and Functions**. Verlag: Springer.
- Gonzalez, J.M. and Laird, D.A. (2003). Carbon sequestration in clay mineral fractions from C-14-labeled plant residues. **Soil Science Society of America Journal** 67: 1715-1720.
- Grabber, J.H., Hatfield, R.D., Lu, F. and Ralph, J. (2009). Coniferyl ferulate incorporation into lignin enhances the alkaline delignification and enzymatic degradation of maize cell walls. **Biomacromolecules** 9: 2510-2516.
- Grandy, A.S. and Robertson, G.P. (2006). Cultivation of a temperate region soil at maximum carbon equilibrium immediately accelerates aggregate turnover and CO<sub>2</sub> and N<sub>2</sub>O emissions. **Global Change Biology** 12: 1507-1520.

- Grandy, A.S., Robertson, G.P. and Thelen, K.D. (2006). Do productivity and environmental trade-offs justify periodically cultivating no-till cropping system? **Agronomy Journal** 98: 1377-1383.
- Guggenberger, S.G., Paustian, K., Haumaier, L., Elliott, E.T. and Zech, W. (2001). Sources and composition of soil organic matter fractions between and within soil aggregates. **European Journal of Soil Science** 52: 607-618.
- Hiradate, S., Yonezawa, T. and Takesako, H. (2006). Isolation and purification of hydrophilic fulvic acids by precipitation. **Geoderma** 132: 196-205.
- Horwath, W.R. (2008). Carbon cycling and formation of soil organic matter. In W. Chesworth (ed.). **Encyclopedia of Soil Science**. Dordrecht: Springer.
- Houghton, J.T., Ding, Y., Griggs, D.J., Noguier, M., van der Linden, P.J., Dai, X., Maskell, K. and Johnson, C.A. (eds.). (2001). **Climate Change 2001: The Scientific Basis**. New York: Cambridge University Press. Intergovernmental Panel on Climate Change.
- IPCC. (2000). **Land Use, Land Use Change and Forestry**. A special report of the IPCC. Cambridge, UK: Cambridge University Press.
- Janmahasatien, S., Phooinit, S. and Wichienopparat, W. (2005). Soil carbon in the Sakaerat dry evergreen and the Maeklong mixed deciduous forest. In **Proceeding of the Climatic Forestation “Potential of Forest in Supporting Kyoto Protocol”**.
- Joshi, C.P. and Mansfield, S.D. (2007). The cellulose paradox-simple molecule, complex biosynthesis. **Current Opinion of Plant Biology** 10: 220-226.
- Kaiser, K., Eusterhues, K., Rumpel, C., Guggenberger, G. and Kogel-Knabner, I. (2002). Stabilization of organic matter by soil minerals-investigations of density and particle-size fractions from two acid forest soils. **Journal of Plant Nutrition and Soil Science** 165: 451-459.

- Kelly, E.F., Amundson, R.G., Marino, B.D. and Deniro, M.J. (1991). Stable isotope ratios of carbon in phytoliths as a quantitative method of monitoring vegetation and climate change. **Quaternary Research** 35: 222-233.
- Kögel-Knabner, I. (2000). Analytical approaches for characterizing soil organic matter. **Organic Geochemistry** 31: 609-625.
- Krull, E.S., Skjemstad, J.O., Graetz, D., Grice, K., Dunning, W., Cook, G. and Parr, J.F. (2003). <sup>13</sup>C-depleted charcoal from C<sub>4</sub> grasses and the role of occluded carbon in phytoliths. **Organic Geochemistry** 34: 1337-1352.
- Laird, D.A., Martens, D.A. and Kingery, W.L. (2001). Nature of clay-humic complexes in an agricultural soil: I. Chemical, Biochemical, and Spectroscopic Analyses. **Soil Science Society of America Journal** 65: 1413-1418.
- Larcher, W. (2001). **Physiological Plant Ecology** (4th ed.). Berlin: Springer.
- Lipson, D.A., Wilson, R.F. and Oechel, W.C. (2005). Effects of elevated atmospheric CO<sub>2</sub> on soil microbial biomass, activity, and diversity in a chaparral ecosystem. **Applied and Environmental Microbiology** 71(12): 8573-8580.
- Madella, M., Alexandre, A. and Ball, T. (2005). International code for phytolith nomenclature 1.0. **Annals of Botany** 96: 253-260.
- Mansfield, S.D. (2009). Solutions for dissolution-engineering cell walls for deconstruction. **Current Opinion in Biotechnology** 20: 286-294.
- Marinari, S., Liburdi, K., Masciandaro, G., Ceccanti, B. and Grego, S. (2007). Humification-mineralization pyrolytic indices and carbon fractions of soil under organic and conventional management in central Italy. **Soil and Tillage Research** 92: 10-17.
- Monreal, C.M. and Kodama, H. (1997). Influence of aggregate architecture and minerals on living habitats and soil organic matter. **Canadian Journal of Soil Science** 77: 367-377.

- Mulholland, S.C., C.A. and Prior, C.A. (1993). AMS radiocarbon dating of phytoliths. In D.M. Pearsall and D.R. Piperno (eds.). **Current Research in Phytolith Analysis: Applications in Archaeology and Paleoecology** (pp 21-23). MASCA Research Papers in Science and Archaeology.
- Nobel, P.S. and Jordan, P.W. (1983). Transpiration stream of desert species: Resistances and capacitances for a C<sub>3</sub>, a C<sub>4</sub>, and a CAM plant. **Journal of Experimental Botany** 34(147): 1379-1391.
- ORDPB. (2000). **Factual Tips about Vetiver Grass**. Office of the Royal Development Projects Board, Bangkok, Thailand.
- Parr, J.F. and Sullivan, L.A. (2005). Soil carbon sequestration in phytoliths. **Soil Biology and Biochemistry** 37: 117-124.
- Paul, E.A. and Clark, F.E. (1996). **Soil Microbiology and Biochemistry** (2nd ed.). New York: Wiley.
- Poolsiri, R. (2005). Soil carbon and nitrogen in plantations of exotic tree species on highland soils in northern Thailand. In **Proceeding of the Climatic Forestation "Potential of Forest in Supporting Kyoto Protocol"**.
- Raich, J.W. and Scheslinger, W.H. (1992). The global carbon dioxide in soil respiration and its relationship to vegetation and climate. **Tellus** 44B: 81-99.
- Rand, P.J. (2001). **Plant Biology**. Foster City, CA: Worldwide.
- Rapp, G.Jr. and Mulholland, S.C. (1992). **Phytolith Systematics, Emerging Issues**. New York: Plenum Press.
- Rowlett, R.M. and Pearsall, D.M. (1993). Archaeological age determinations derived from opal phytoliths in thermoluminescence. In D.M. Pearsall and D.R. Piperno (eds.). **Current Research in Phytolith Analysis: Applications in Archaeology and Paleoecology** (pp 1-25). MASCA Research Papers in Science and Archaeology.

- Saggar, S., Parshotam, A., Sparling, G.P., Feltham, C.W. and Hart, P.B.S. (1996).  $^{14}\text{C}$ -labelled ryegrass turnover and residence times in soils varying in clay content and mineralogy. **Soil Biology and Biochemistry** 28: 1677-1686.
- Schnitzer, M. and Kodama, H. (1992). Interactions between organic and inorganic components in particle-size fractions separated from four soils. **Soil Science Society of America Journal** 56: 1099-1105.
- Smith, F.A. and Anderson, K.B. (2001). Characterization of organic compounds in phytoliths: improving the resolving power of phytolith  $\delta^{13}\text{C}$  as a tool for paleoecological reconstruction of C3 and C4 grasses. In J.D. Meunier and F. Colin (eds.). **Phytoliths: Applications in Earth Science and Human History** (pp 317-341). Lisse, Netherlands: A.A. Balkema Publishers.
- Smith, F.A. and White, J.W.C. (2004). Modern calibration of phytolith carbon signatures for C3/C4 paleograssland reconstruction. **Palaeogeography, Palaeoclimatology, Palaeoecology** 207: 277-304.
- Sullivan, L.A. and Parr, J.F. (2008). Systems and methods for determining carbon credits [114 paragraphs]. **Patent Application Publication** [On-line serial], Available: US2008/0131974A1.
- Tsartsidou, G., Lev-Yadun, S., Albert, R.M., Miller-Rosen, A., Efstratiou, N. and Weiner, S. (2007). The phytolith archaeological record: strengths and weaknesses evaluated based on a quantitative modern reference collection from Greece. **Journal of Archaeological Science** 34: 1262-1275.
- TVNI. (2010). **Vetiver** [On-line]. Available: <http://www.vetiver.org>
- Versiteit Nijmegen. (2010). **Bundle sheath and kranz anatomy** [On-line]. Available: <http://www.vcbio.science.ru.nl>
- Vinken, R., Schäffer, A. and Ji, R. (2005). Abiotic association of soilborne monomeric phenols with humic substances. **Organic Geochemistry** 36: 583-593.

Wang, W.J. and Dalal, R.C. (2006). Carbon inventory for a cereal cropping system under contrasting tillage, nitrogen fertilization and stubble management practices. **Soil and Tillage Research** 91: 68-74.

# CHAPTER III

## GENERAL MATERIALS AND METHODS

This chapter will give a general description of major materials and methods used in the work presented in this thesis. More details pertinent to each study are given in each chapter.

### 3.1 Dichromate oxidation method

This method is for organic C measurement following to Walkley and Black (1934).

#### 3.1.1 Apparatus

3.1.1.1 Apparatus for titration

3.1.1.2 Hood

#### 3.1.2 Reagents

3.1.2.1 1 N  $K_2Cr_2O_7$ : Dry 98 g  $K_2Cr_2O_7$  at 105°C, dilute and adjust volume to 2 L

3.1.2.2 0.5 N  $Fe(NH_4)_2(SO_4)_2 \cdot 6H_2O$ : Dilute 400 g  $Fe(NH_4)_2(SO_4)_2 \cdot 6H_2O$ , add 50 mL  $H_2SO_4$  and adjust volume to 2 L

3.1.2.3 0.025 M O-phenanthroline indicator: Dilute 0.7 g  $FeSO_4 \cdot 7H_2O$  and 1.48 g O-phenanthroline, and adjust volume to 100 mL

3.1.2.4 Concentrated  $H_2SO_4$

#### 3.1.3 Procedure

3.1.3.1 Weight 1 g of air dry soil in Erlenmeyer flask and add 10 mL 1 N  $K_2Cr_2O_7$

3.1.3.2 Add 15 mL conc.  $H_2SO_4$  and slightly shake 1 - 2 min and incubate 30 min

3.1.3.3 Add 50 mL distilled water

3.1.3.4 After cool, add 5 drops O-phenanthroline indicator and titrate with 0.5 N  $\text{Fe}(\text{NH}_4)_2(\text{SO}_4)_2 \cdot 6\text{H}_2\text{O}$  to the end point

3.1.3.5 Calculate the organic C concentration following Eq. (3.1):

$$\text{Organic C (\%)} = \left[ \frac{(B-T)N}{B} \times \frac{3}{77} \times \frac{100}{1000} \times \frac{10}{w} \right] \times 100 \quad (3.1)$$

where  $B$  is the  $\text{Fe}(\text{NH}_4)_2(\text{SO}_4)_2 \cdot 6\text{H}_2\text{O}$  volume titrating with blank (mL),  $T$  is the  $\text{Fe}(\text{NH}_4)_2(\text{SO}_4)_2 \cdot 6\text{H}_2\text{O}$  volume titrating with sample (mL),  $N$  is normality of  $\text{K}_2\text{Cr}_2\text{O}_7$  (N), and  $w$  is weight of soil sample (g).

## 3.2 Kjeldahl method

This method is for organic N measurement following Bremner and Mulvaney (1982).

### 3.2.1 Apparatus

3.2.1.1 250 mL Kjeldahl flask

3.2.1.2 Apparatus for titration

3.2.1.3 Digestion block

3.2.1.4 Nitrogen distillator

3.2.1.5 Hood

### 3.2.2 Reagents

3.2.2.1 Catalyst mixture (1:10 of  $\text{K}_2\text{SO}_4$  and  $\text{CuSO}_4$ )

3.2.2.2 Mixed indicator: Dilute 0.1 g methyl red and 0.1 g bromocresol green with 96% EtOH and adjust volume to 100 mL

3.2.2.3 32% NaOH: Dilute 320 g NaOH and adjust volume to 1 L

3.2.2.4 0.025 M HCl: Dilute 8.3 mL and adjust volume to 1 L

3.2.2.5 Concentrated  $\text{H}_2\text{SO}_4$

3.2.2.6 4% H<sub>3</sub>BO<sub>3</sub>: Dilute 40 g H<sub>3</sub>BO<sub>3</sub> and adjust volume to 1 L

### 3.2.3 Procedure

3.2.3.1 Weight 0.5 - 1 g of air dry soil in 250 mL Kjeldahl flask, 0.2 g catalyst mixture and 10 mL conc. H<sub>2</sub>SO<sub>4</sub>

3.2.3.2 Digest the sample in a digestion block at 380°C for 3 h or until the precipitate turning to white color

3.2.3.3 After cool, distill the sample in a nitrogen distillator. Before distilling, add 3 - 4 drops of mixed indicator, 50 mL distilled water and 25 mL 32% NaOH

3.2.3.4 Pipette 25 mL 4% H<sub>3</sub>BO<sub>3</sub> in 250 mL Erlenmeyer flask to capture gaseous NH<sub>3</sub> resulting from distillation

3.2.3.5 Titrate H<sub>3</sub>BO<sub>3</sub> solution with 0.025 M HCl to the end point

3.2.3.6 Calculate the concentration of organic N following Eq. (3.2):

$$\text{Total organic N (\%)} = \left[ \frac{N \times (V - B) \times 0.014 \times mf}{w} \right] \times 100 \quad (3.2)$$

where  $N$  is the concentration of HCl (M),  $V$  is the HCl volume titrating with sample (mL),  $B$  is the HCl volume titrating with blank (mL),  $w$  is weight of soil sample (g), and  $mf$  is moisture factor.

## 3.3 Ammonium acetate-extractable element method

This method is for cation exchangeable capacity (CEC) and base saturation (BS) measurement following to Chapman (1965). The 1 N ammonium acetate (NH<sub>4</sub>OAc) extraction method is the most widely used procedure to extract the water-soluble and rapidly exchangeable fraction. This method is used to assess the amount of K, Mg, Ca, Na, Li, Ba and Sr. Soils are tested for Na to diagnose sodic and sodic-saline problems.

### 3.3.1 Apparatus

3.3.1.1 125 mL Erlenmeyer flasks

3.3.1.2 Repiprocating shaker

3.3.1.3 Apparatus for filtration

3.3.1.4 Atomic absorption spectrophotometer

3.3.1.5 Apparatus for distillation and titration

### 3.3.2 Reagents

3.3.2.1 1 N  $\text{NH}_4\text{OAc}$ : Dilute 77.1 g of  $\text{NH}_4\text{OAc}$  to 1 L in a volumetric flask with distilled water. Adjust pH to 7.0 with  $\text{NH}_4\text{OH}$  or acetic acid as required.

3.3.2.2 10%  $(\text{NH}_4)_2\text{C}_2\text{O}_4\text{H}_2\text{O}$ : Dilute 10 g of  $(\text{NH}_4)_2\text{C}_2\text{O}_4$  and adjust volume to 100 mL

3.3.2.3 50% $\text{NH}_4\text{OH}$ : Dilute 50 g of  $\text{NaOH}$  and adjust volume to 100 mL

3.3.2.4 1N  $\text{NH}_4\text{Cl}$ : Dilute 53.5 g  $\text{NH}_4\text{Cl}$ , adjust volume to 1 L and adjust pH 7 by  $\text{NaOH}$

3.3.2.5 0.25 N  $\text{NH}_4\text{Cl}$ : Dilute 13.38 g  $\text{NH}_4\text{Cl}$ , adjust volume to 1 L and adjust pH 7 by  $\text{NaOH}$

3.3.2.6 0.1 N  $\text{AgNO}_3$ : Dilute 16.99 g  $\text{AgNO}_3$  and adjust volume to 1 L

3.3.2.7 Standard Ca, Mg, K and Na: the concentrations following the AAS requirement

3.3.2.8 Chemicals for distillation and titration of  $\text{NH}_4^+$  following Kjeldahl method

### 3.3.3 Procedure

3.3.3.1 Weight 5 - 10 g air dry soils in Erlenmeyer flasks and add 60 mL of 1N  $\text{NH}_4\text{OAc}$

3.3.3.2 Shake 12 h and filter

3.3.3.3 Wash the samples with 1N  $\text{NH}_4\text{OAc}$  until certainly all  $\text{Ca}^{2+}$  release (testing the solution with 1N  $\text{NH}_4\text{Cl}$ , 10%  $(\text{NH}_4)_2\text{C}_2\text{O}_4\text{H}_2\text{O}$  and 50% $\text{NH}_4\text{OH}$ )

3.3.3.4 Adjust the filtrate volume to 100 mL with distilled water and measure the concentration of Ca, Mg, K and Na by Atomic absorption spectrophotometer (AAS)

3.3.3.5 Calculate the concentration of Ca, Mg, K and Na following Eq. (3.3):

$$\text{Exchangable cations in meq/100g} = \frac{R \times C \times df}{10 \times A \times \text{eq. wt. Cation}} \quad (3.3)$$

where  $A$  is weight of soil sample (g),  $df$  is a dilution factor,  $C$  is the volume of extract (mL), and  $R$  is the cation measured by AAS ( $\text{mg L}^{-1}$ ).

3.3.3.6 Wash the precipitate with 1 N  $\text{NH}_4\text{Cl}$  4 time, 0.25 N  $\text{NH}_4\text{Cl}$  1 time, 150 - 200 mL 95% EtOH until  $\text{Cl}^-$  release (testing with 0.1 N  $\text{AgNO}_3$ )

3.3.3.7 Add 225 mL acidified NaCl for  $\text{Na}^+$  replacing  $\text{NH}_4^+$  and filter

3.3.3.8 Distilled and titrate the filtrates by following the Kjeldahl method

3.3.3.9 Calculate the CEC following Eq. (3.4):

$$\text{CEC} = \frac{(A - B) N \times 100}{w} \quad (3.4)$$

where  $A$  is the HCl volume titrating with the sample (mL),  $B$  is the HCl volume titrating with the standard (mL),  $N$  is normality of HCl (N), and  $w$  is weight of soil samle (g).

3.3.3.10 Calculate base saturation following Eq. (3.5):

$$\text{Base saturation (\%)} = \left[ \frac{\sum \text{Exch. cation}}{\text{CEC}} \right] \times 100 \quad (3.5)$$

where  $\sum \text{Exch. Cation}$  is the summary of exch.  $\text{Ca}^{2+}$  + exch.  $\text{Mg}^{2+}$  + exch.  $\text{Na}^{+}$  + exch.  $\text{K}^{+}$ ,  $\text{CEC}$  is cation exchangeable capacity (by  $\text{NH}_4\text{OAc}$  extraction, pH 7.0  $\text{cmol kg}^{-1}$ ).

### 3.4 Hydrometer method

This method is for soil texture classification following Bouyoucos (1962).

#### 3.4.1 Apparatus

3.4.1.1 Mechanical stirrer

3.4.1.2 Soil dispersion cup

3.4.1.3 Bouyoucos jar

3.4.1.4 Standard hydrometer

#### 3.4.2 Reagents

3.4.2.1 50% Hydrogen peroxide ( $\text{H}_2\text{O}_2$ )

3.4.2.2 Sodiumhexametaphosphate

3.4.2.3 Sodium carbonate

#### 3.4.3 Procedure

3.4.3.1 Weight 50 g dry soil (after sieving through 2 mm) in beaker

3.4.3.2 Add 100 mL distilled water and mix

3.4.3.3 Slightly add 5 - 10 mL 30%  $\text{H}_2\text{O}_2$  until bubble gone

3.4.3.4 Add 100 mL calgon and 100 mL distilled water and set for at least 10 min

3.4.3.5 Stir with a mechanical stirrer for 5 min

3.4.3.6 Transfer the mixture to a bouyoucos jar

3.4.3.7 Place hydrometer into a bouyoucos jar and fill water to 1,130 mL

3.4.3.8 Stir the mixture 20 - 25 times

3.4.3.9 At 40 sec and 2 h, read hydrometer and temperature of the colloid

3.4.3.10 For control, add 100 mL 5% calgon in another bouyoucos jar, add 100 - 200 mL distilled water and do the same manner of the sample.

3.4.3.11 Calculate a hydrometer reading of calgon solution at T°C ( $R_c$ ) following Eq. (3.6):

$$R_c = A - 0.5(T - B) \quad (3.6)$$

where  $R_c$  is a hydrometer reading of calgon solution at T°C ( $\text{g L}^{-1}$ ),  $A$  is a hydrometer reading of calgon solution,  $T$  is temperature reading from soil solution (°C),  $B$  is is temperature reading from calgon (°C).

3.4.3.12 Calibrate the hydrometer reading of sample ( $R'_s$ ) by minus with  $R_c$

3.4.3.13 Adjust  $R'_s$  to an accurate soil particle at std. temperature (20°C) following Eq. (3.7):

$$R_s = R'_s + 0.36(T - L) \quad (3.7)$$

where  $R_s$  is the correct gram soil particle ( $\text{g L}^{-1}$ ),  $R'_s$  is the gram soil particle measuring by hydrometer ( $\text{g L}^{-1}$ ),  $L$  is temperature at hydrometer (20°C).

3.4.3.14 Calculate %Sand, Silt and Clay following Eq. (3.8) to (3.11):

$$\% (\text{Silt} + \text{Clay}) = \left[ \frac{R_s \text{ at } 40s}{\text{soil weight}} \right] \times 100 \quad (3.8)$$

$$\% \text{ Clay} = \left[ \frac{R_s \text{ at } 2h}{\text{soil weight}} \right] \times 100 \quad (3.9)$$

$$\% \text{ Sand} = 100 - (\text{Silt} + \text{Clay}) \quad (3.10)$$

$$\% \text{ Silt} = \% (\text{Silt} + \text{Clay}) - \% \text{ Clay} \quad (3.11)$$

### 3.5 Bulk density

Bulk density is defined as the mass (weight) of a unit volume of dry soil. Bulk density is expressed as a ratio of grams per cubic centimeter ( $\text{g cm}^{-3}$ ). The method follows Blake (1965).

3.5.1 For each horizon in soil profile, push a can into the side of horizon and dig around the can to remove it using a shovel.

3.5.2 Trim the soil from the top and around the edges of the can so the volume of the soil is the same as the volume of the can.

3.5.3 Cover the labeled can with its lid

3.5.4 Repeat this procedure so that it has three bulk density samples for each horizon

3.5.5 Weight after drying

3.5.6 Sieve and collect weight of rock present and collect volume of rock and root present

3.5.7 Calculate bulk density following Eq. (3.12):

$$\text{Bulk density} = \frac{\text{dried soil weight} - \text{rock weight}}{\text{soil volume} - \text{rock volume}} \quad (3.12)$$

### 3.6 High combustion method

This method is for total C and total N measurement. Total C and N in dried soils and plants were determined by LECO analyzer (CNS 2000) as shown in Figure 3.1. The 0.2 g air-dried and finely ground sample is weighed into a tared ceramic boat and loaded into the autoloader where it combusts in a furnace at 1350°C. Approximately 1 g of combustion catalyst is added to each sample to ensure complete combustion of the sample in the furnace. Combustion gases are collected in a 4.5 L ballast tank and then flow to the detectors. C and S (as CO<sub>2</sub> and SO<sub>2</sub>) are detected by infra-red absorption measurement and N<sub>2</sub> by thermal conductivity detection.



**Figure 3.1** LECO Analyzer (CNS 2000).

### 3.7 Chloroform fumigation extraction method

This method is for microbial biomass measurement in chapter VII (CFE-MBC). Microbial biomass of soil is defined as the part of the organic matter in the soil that constitutes living microorganisms smaller than the 5 - 10  $\mu\text{m}^3$ . It is generally expressed in the milligrams of C per gram of dry weigh of soil. Typical biomass C ranges from 1 to 5% of soil organic matter. The soil is fumigated with chloroform to kill the microbial

population. After the microbes are killed by fumigation, cytoplasm is released into the soil environment. The soil biomass C is extracted with potassium sulfate on both fumigated and unfumigated soil. The C content of the extract is tested and the biomass is calculated based on the difference between the C content of fumigated vs. the unfumigated soil. The C is measured by dichromate oxidation. The step of CFE-MBC calculation is shown in Eq. (3.13) to (3.17) (Voroney et al., 1993):

### 3.7.1 Soil Water Content (WS)

$$WS(\%) = \left[ \frac{\text{Soil wet weight (g)} - \text{Soil oven dry weight (g)}}{\text{Soil oven dry weight (g)}} \right] \times 100 \quad (3.13)$$

### 3.7.2 Microbial Biomass Measurement (MS)

$$MS(\text{g}) = \frac{\text{Soil wet weight (g)} \times 100}{(100 + WS(\%))} \quad (3.14)$$

### 3.7.3 Total Volume of Solution (mL) in the Extract Soil (VS)

$$VS(\text{mL}) = \text{Soil wet weight (g)} - \text{Soil oven dry weight (g)} + \text{Extract volume (mL)} \quad (3.15)$$

### 3.7.4 Total Weight of Extractable C and N in the Fumigated ( $O_F$ ) and Unfumigated ( $O_{UF}$ ) Soil Samples

$$OC_{F, OC_{UF}} (\mu\text{g g}^{-1}\text{soil}) = \frac{\text{Extractable C } (\mu\text{g mL}) \times VS (\text{mL})}{MS(\text{g})} \quad (3.16)$$

### 3.7.5 Soil Microbial Biomass C

$$\text{CFE} - \text{MBC} (\mu\text{g g}^{-1}\text{soil}) = \frac{\text{OC}_F - \text{OC}_{UF}}{k_{EC}} \quad (3.17)$$

where  $k_{EC} = 0.45$ .

## 3.8 Chloroform fumigation incubation method

This method is for microbial biomass measurement in chapter VII (CFI-MBC) following Jenkinson and Powlson (1976).

3.8.1 Weight two 30 g subsamples of soil and place in 100 mL containers.

3.8.2 One subsample was fumigated with free alcohol  $\text{CHCl}_3$  in the dark for 24 h, while the other subsample was kept in the dark at  $4^\circ\text{C}$  for 24 h.

3.8.3 Add 0.5 - 1 mL supernatant of 1% inoculate field-moist soil to the two subsamples

3.8.4 Incubated both fumigated and unfumigated soils at  $25^\circ\text{C}$  for 10 days.

3.8.5 Absorb the  $\text{CO}_2$  evolved from the two subsamples in 1 M NaOH and determine titrimetrically with 1 M HCl using phenolphthalein as an indicator.

3.8.6 Calculate CFI-MBC following Eq. (3.18):

$$\text{CFI} - \text{MBC} (\text{mgC g}^{-1}\text{soil}) = \frac{\text{CO}_{2(F)} - \text{CO}_{2(UF)}}{0.45} \quad (3.18)$$

where  $\text{CO}_{2(F)}$  is  $\text{CO}_2$  evolved during the 10 days in fumigated sample,  $\text{CO}_{2(UF)}$  is  $\text{CO}_2$  evolved during the 10 days in unfumigated sample.

### 3.9 Liquid state 1D $^1\text{H}$ NMR technique

This technique is for C functional group characterization, carrying out in chapter VIII. Nuclear magnetic resonance (NMR) is a physical phenomenon based upon the quantum mechanical magnetic properties of an atom's nucleus (Figure 3.2). All nuclei that contain odd numbers of protons and/or neutrons have an intrinsic magnetic moment and angular momentum, in other words a spin  $> 0$ . The most commonly measured nuclei are  $^1\text{H}$  (the most NMR-sensitive isotope after unstable  $^3\text{H}$ ) and  $^{13}\text{C}$  are used in NMR spectroscopy as well. NMR resonant frequencies for a particular substance are directly proportional to the strength of the applied magnetic field, in accordance with the equation for the Larmor precession frequency.



**Figure 3.2** NMR spectroscopy and a NMR tube.

The relationship between the chemical shift of a given  $^1\text{H}$  nucleus and its molecular environment can be used to preliminary characterize chemical structures. Basically, a perfect reference of nucleus  $^1\text{H}$  is tetramethylsilane (TMS) hydrogens represents at  $\delta$  0.00 ppm. The  $^1\text{H}$  scale shows frequency increases from right to left in a typical spectrum. Therefore, the TMS hydrogens process slowest, while the ring hydrogens ( $\delta$  7.23 ppm) process fastest at a given field strength. Figure 3.3 show an electric current moving through

a wire generates a magnetic field. In an analog way, the *external magnetic field* ( $B_0$ ) causes each electron pair surrounding the nucleus to circulate through its orbital in such a way as to generate an *induced magnetic field* ( $B_i$ ) opposed to the external field.

$$B_{\text{eff}} = B_0 - B_i$$

$$B_{\text{eff}} = \sigma B_0$$

$$B_{\text{eff}} = (1 - \sigma) B_0$$

$$V_{\text{precession}} = \frac{\gamma(1 - \sigma)B_0}{2\pi}$$

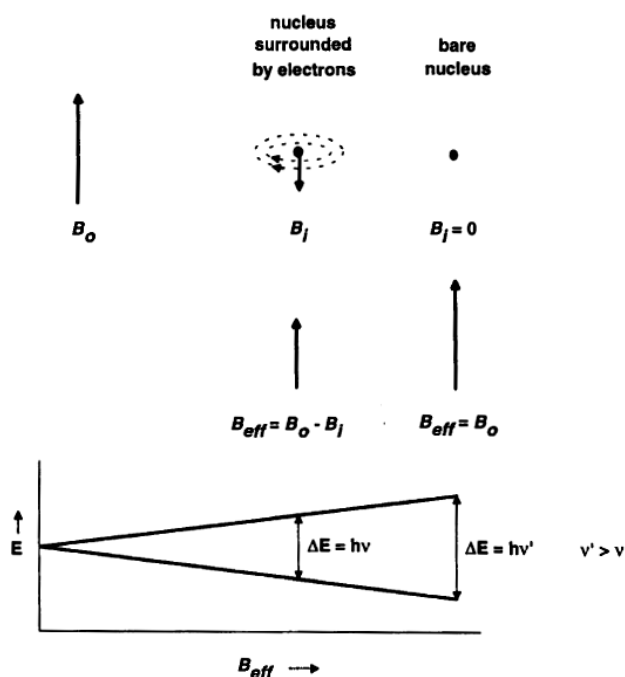


**Figure 3.3** Effect of diamagnetic shielding. The dotted ellipses represent motion of electrons in their orbital under the influence of  $B_0$  (Macomber, 1998).

### 3.9.1 Chemical shifts of hydrogen attached to tetrahedral C

#### 3.9.1.1 Methyl hydrogens

A C atom that is singly bonded to four other atoms is called tetrahedral. The simplest molecule containing a tetrahedral C is methane ( $\text{CH}_4$ ). If one of hydrogen in methane is substituted by a different atom or group (X), the result molecule,  $\text{CH}_3\text{X}$ , is still

tetrahedral at C and consist of a methyl group attached to X. Sequential substitution of two more hydrogens leads first to  $XCH_2Y$  (a methylene group with two substituents) and then to  $XCH(Y)Z$  (a methine group with three substituents), both still tetrahedral at C. One way to begin to organize data, at least the methyl group, is to regard each of these compounds as a derivative ( $CH_3X$ ) of methane whose  $^1H$  signal occurs at 0.23 ppm. Therefore, the calculation for a chemical shift position of a substituent (X) is Eq. (3.19):

$$\delta_{\text{cal}} = \text{base value} + \Sigma(\Delta\delta_x) \quad (3.19)$$

where the base value is the chemical shift of the appropriate unsubstituted molecule (e.g.  $\delta$  0.23 for methane) and  $\Sigma(\Delta\delta_x)$  is the sum of  $\Delta\delta_x$  values for all contributing substituents (Table 3.1). In Table 3.1, the values labeled  $\Delta\delta_{\alpha-X}$  are to be used when X is directly attached to the methyl group, while the value labeled  $\Delta\delta_{\beta-X}$  are used when a methylene group separated the methyl from the X ( $CH_3CH_2X$ ). When using one or more  $\Delta\delta_{\beta-X}$  values in a calculation, be sure to add 0.62 for the deshielding effect of the intervening  $CH_2$  group.

**Table 3.1**  $^1\text{H}$  Substituent parameters ( $\Delta\delta_x$ , ppm) for substituents on tetrahedral carbons<sup>a</sup>.

Group X <sup>b</sup>	$\Delta\delta_{\alpha-x}$	$\Delta\delta_{\beta-x}$ <sup>c</sup>	Group X <sup>b</sup>	$\Delta\delta_{\alpha-x}$	$\Delta\delta_{\beta-x}$ <sup>c</sup>
-R	0.62	0.01	-SPh	2.27	
-CF <sub>3</sub>	1.20		-S(=O) <sub>1,2</sub> R	2.37	
-CH=C(R/H) <sub>2</sub>	1.37	0.15	-Br	2.47	0.95
-C≡C(R/H)	1.50	0.35	-SC≡N	2.47	
-C(=O)OR	1.77	0.33	-N=CR <sub>2</sub>	2.67	
-C(=O)N(R/H) <sub>2</sub>	1.77	0.25	-N <sup>+</sup> (R/H) <sub>3</sub>	2.72	0.55
-C(=O)OH	1.87	0.33	-NHC(=O)R	2.72	0.25
-S(R/H)	1.87	0.43	-SO <sub>3</sub> (R/H)	2.77	
-C(=O)R	1.87	0.20	-Cl	2.80	0.70
-C≡N	1.92	0.43	-O(R/H)	2.97	0.35
-I	1.94	0.90	-P <sup>+</sup> Cl <sub>3</sub>	3.07	
-C(=O)H	1.97	0.25	-N=C=S	3.17	
-NR <sub>2</sub>	2.00	0.20	-OC(=O)(R/H)	3.40	0.45
-Ph	2.00	0.33	-OSO <sub>2</sub> R	3.47	
PR <sub>2</sub> , -P(=O)R <sub>2</sub>	2.00		-OPh	3.60	0.45
-C(=O)Ph	2.17	0.33	-OC(=O)Ph	3.60	0.80
-SSR	2.17		-NO <sub>2</sub>	3.82	0.75
-NH <sub>2</sub>	2.27		-F	4.00	0.70

<sup>a</sup>Compiled from Silverstein, Bassler and Morrill (1991 quoted in Macomber, 1998). All numeric data in ppm. When calculating the chemical shift of a methylene group (X-CH<sub>2</sub>-Y), decrease by 10% the value calculated from Eq. (3.19) [See Eq. (3.20)].

<sup>b</sup>R represents any alkyl group; R/H represents either alkyl or hydrogen; Ph represent phenyl

<sup>c</sup>When using these values to calculate the methyl chemical shift of CH<sub>3</sub>CH<sub>2</sub>X, be sure to add 0.62 ppm for the effect of the CH<sub>2</sub> group.

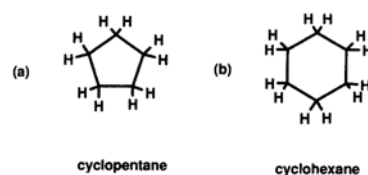
### 3.9.1.2 Acyclic methylene and methine hydrogens

Suppose a methylene group were connected to two of the substituent groups from Table 3.1. If the two substituents (X and Y) exert their (de)shielding effects independently, then the chemical shift of the methylene group could be calculated by adding the substituent parameters of both substituents to the chemical shift of methane (Eq. (3.20)):

$$\Delta\delta(\text{XCH}_2\text{Y}) = 0.23 + \Delta\delta_{\alpha\text{-X}} + \Delta\delta_{\alpha\text{-Y}} \quad (3.20)$$

### 3.9.1.3 Methylene and methine groups that are part of rings

Many chemical compounds contain rings formed by the cyclic connection of three or more atoms. When calculating the chemical shift, the rings must be assumed as a planar and the base value should be used from Table 3.2.

**Table 3.2**  $^1\text{H}$  Chemical shifts of unsubstituted cycloalkanes<sup>a</sup>.

Name	Ring size	$\delta$ (ppm)
Cyclopropane	3	0.22
Cyclobutane	4	1.96
Cyclopentane	5	1.51
Cyclohexane	6	1.43
Cycloheptane	7	1.53
Cyclooctane	8	1.57
Cyclodecane	10	1.51

<sup>a</sup>Data from Silverstein, Bassler and Morrill (1991) and Pouchert (1983) (Both quoted in Macomber, 1998).

### 3.9.1.4 Index of unsaturation

The index of unsaturation (IOU) is a trick to calculate how many rings plus  $\pi$  bonds there must be in any legitimate isomer with that molecule formula  $C_cH_hN_nO_oX_x$  (where X represents halogen: F, Cl, Br, or I) (Eq. (3.21)).

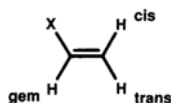
$$\text{IOU} = \frac{1}{2}[2c + 2 + n - (h + x)] \quad (3.21)$$

where  $c$ ,  $h$ ,  $n$ ,  $o$  and  $x$  are numbers of C, H, N, O, and halogen.

### 3.9.2 Vinyl and formyl hydrogen chemical shifts

Two C connected by a double bond are called “Vinyl C” and hydrogens attached directly to vinyl C are called “Vinyl hydrogens.” Vinyl hydrogens have less electron density around them than do hydrogens attached to tetrahedral C. As a result, vinyl hydrogens are deshielded, and their signals appear downfield of hydrogens attached to tetrahedral C. Vinyl hydrogens typically appear in the  $\delta$  4.5 - 7.0 ppm region of the  $^1\text{H}$  spectrum. In a calculation of vinyl hydrogen chemical shifts, the base value is used  $\delta$  5.28 (the simplest alkene, ethylene) as the base value in Eq. 3.19, and the substituted compounds can be checked a list in Table 3.3.

**Table 3.3** Substituent parameters ( $\Delta\delta_x$ , ppm) for vinyl hydrogen chemical shift<sup>a</sup>.



-X	$\Delta\delta_{\text{gem}}$	$\Delta\delta_{\text{cis}}$	$\Delta\delta_{\text{tran}}$
-C $\equiv$ N	0.23	0.78	0.58
-R(alkyl)	0.44	-0.26	-0.29
-C $\equiv$ CR	0.50	0.35	0.10
-CH <sub>2</sub> SR	0.53	-0.15	-0.15
-CH <sub>2</sub> NR <sub>2</sub>	0.66	-0.05	-0.23
-CH <sub>2</sub> OR	0.67	-0.02	-0.07
-CH <sub>2</sub> I	0.67	-0.02	-0.07
-NR <sub>2</sub>	0.69(2.30)	-1.19(-0.73)	-1.31(-0.81)
-Cycloalkenyl <sup>b</sup>	0.71	-0.33	-0.30
-CH <sub>2</sub> Cl	0.72	0.12	0.07

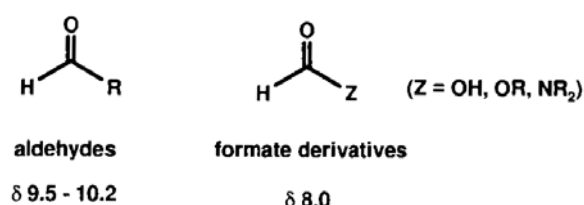
**Table 3.3** (Continued).

-X	$\Delta\delta_{\text{gem}}$	$\Delta\delta_{\text{cis}}$	$\Delta\delta_{\text{tran}}$
-CH <sub>2</sub> Br	0.72	0.12	0.07
-C(=O)OR	0.84(0.68)	1.15(1.02)	0.56(0.33)
-CH=CH <sub>2</sub>	0.98(1.26)	-0.04(0.08)	-0.21(-0.01)
-C(=O)OH	1.00(0.69)	1.35(0.97)	0.74(0.39)
-Cl	1.00	0.19	0.03
-SR	1.00	-0.24	-0.04
-C(=O)H	1.03	0.97	1.21
-Br	1.04	0.40	0.55
-C(=O)R	1.10(1.06)	1.13(1.01)	0.81(0.95)
-C(=O)Cl	1.10	1.41	0.99
-OR	1.18(1.14)	-1.06(-0.65)	-1.28(-1.05)
-Ph	1.35	0.37	-0.10
-C(=O)NR <sub>2</sub>	1.37	0.93	0.35
-SO <sub>2</sub> R	1.58	1.15	0.95
-OC(=O)R	2.09	-0.40	-0.67

<sup>a</sup>Data (in ppm) from Silverstein et al. (1991 quoted in Macomber, 1998). Recall that a negative value of  $\Delta\delta$  corresponds to an upfield shift. The data in parentheses are to be used if either the X group or the C=C is further conjugated.

<sup>b</sup>The double bond is endocyclic to a ring.

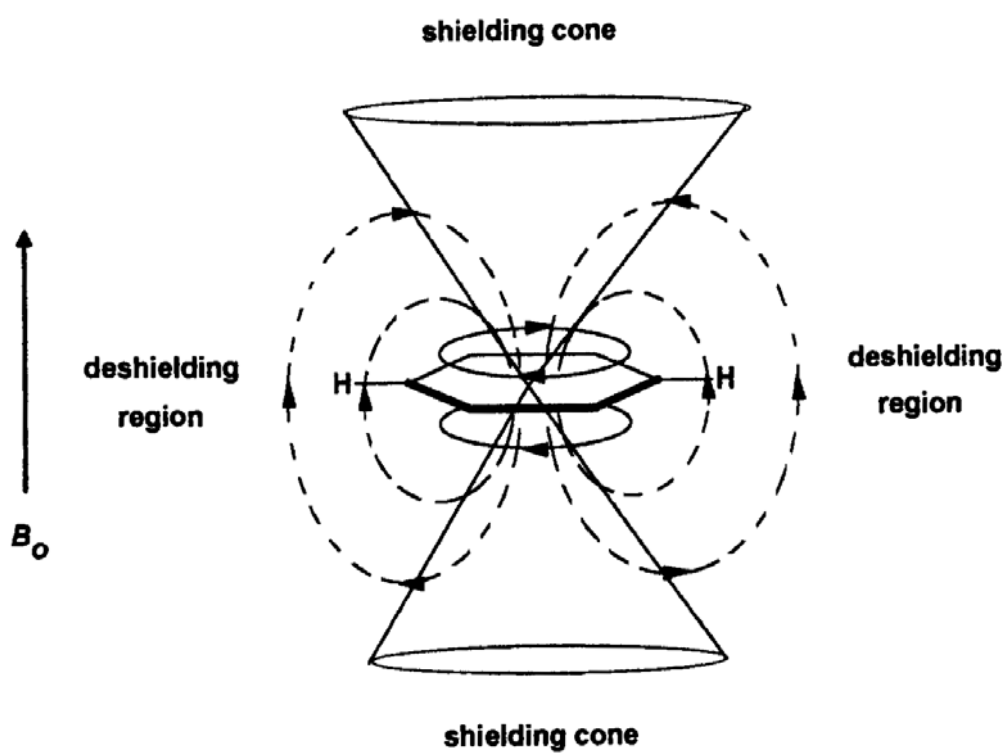
There is another type of hydrogen that appears quite similar to a vinyl hydrogen. It is called a formyl (or aldehydic) hydrogen and is directly bonded to a carbonyl (i.e., C=O) C (Figure 3.4):



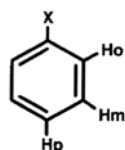
**Figure 3.4** Structures and <sup>1</sup>H chemical shifts of vinyl groups.

### 3.9.3 Aromatic hydrogen chemical shift correlations

Aromatic hydrogens are deshielded compared to their vinyl cousins is a direct consequence of magnetic anisotropy of the aromatic  $\pi$  system. When immersed in an external magnetic field, these  $\pi$  electrons begin to circulate just as the electron in a triple bond. This circulation, called a ring current in the context of aromatic molecules, generates an analogous induced field whose lines of magnetic flux are shown by the dashed lines in Figure 3.5. Above and below the center of the ring, the induced field is opposed to the external field, given rise to a shielding effect on nuclei located in that region. However, in the donut-shaped region outside the periphery of the ring where aromatic hydrogens are located, the induced field is aligned with the external field, causing deshielding of nuclei in that region. Thus, aromatic hydrogens experience a deshielding effect due to the ring current of the aromatic  $\pi$  electrons. Aromatic hydrogens typically occur in the  $\delta$  6.5 - 8.0 chemical shift range. Table 3.4 is a list of substituent parameters have been developed for aromatic substituents and benzene chemical shift is used as a base value,  $\delta$  7.27.



**Figure 3.5** Anisotropic-induced magnetic field (dotted lines) in the proximity of an aromatic ring. The ellipses above and below the ring represent the ring current of  $\pi$  electrons.

**Table 3.4** Aromatic substituent parameters ( $\Delta\delta_x$ , ppm)<sup>a</sup>.

X	H <sub>ortho</sub>	H <sub>meta</sub>	H <sub>para</sub>	X	H <sub>ortho</sub>	H <sub>meta</sub>	H <sub>para</sub>
-CH <sub>3</sub>	-0.17	-0.09	-0.18	-I	0.40	-0.26	-0.03
-CH <sub>2</sub> CH <sub>3</sub>	-0.15	-0.06	-0.18	-OH	-0.50	-0.14	-0.4
-CH(CH <sub>3</sub> ) <sub>2</sub>	-0.14	-0.09	-0.18	-OR	-0.27	-0.08	-0.27
-C(CH <sub>3</sub> ) <sub>3</sub>	0.01	-0.10	-0.24	-OC(=O)R	-0.22	0	0
-CH=CH <sub>2</sub>	0	0	0	-OSO <sub>2</sub> Ar	-0.26	-0.05	0
-C≡CH	0.20	0	0	-C(=O)H	0.58	0.21	0.27
-Ph	0.18	0	0.08	-C(=O)R	0.64	0.09	0.3
-CF <sub>3</sub>	0.25	0.25	0.25	-C(=O)OH	0.80	0.14	0.20
-CH <sub>2</sub> Cl	0	0.01	0	-C(=O)OR	0.74	0.07	0.20
-CHCl <sub>2</sub>	0.10	0.06	0.10	-C(=O)Cl	0.83	0.16	0.30
-CCl <sub>3</sub>	0.80	0.20	0.20	-C≡N	0.27	0.11	0.30
-CH <sub>2</sub> OH	-0.10	-0.10	-0.10	-NH <sub>2</sub>	-0.75	-0.24	-0.63
-CH <sub>2</sub> OR	0	0	0	-NR <sub>2</sub>	-0.60	-0.10	-0.62
-CH <sub>2</sub> NH <sub>2</sub>	0.0	0.0	0.0	-NHC(=O)R	0.23		
-SR	-0.03	0	0	-N <sup>+</sup> H <sub>3</sub>	0.63	0.25	0.25
-F	-0.30	-0.02	-0.22	-NO <sub>2</sub>	0.95	0.17	0.33
-Cl	0.02	-0.06	-0.04	-N=C=O	-0.20	-0.20	-0.20
-Br	0.22	-0.13	-0.03				

<sup>a</sup>Data abstracted from Gunther (1973) and Silverstein et al. (1991) (both are quoted in Macomber, 1998).

### 3.9.4 Hydrogen attached to elements other than C

#### 3.9.4.1 Hydrogen attached to oxygen

Substituent groups which have a hydroxyl group in a part (Figure 3.6) have specific  $^1\text{H}$  chemical shift regions: alcohol ( $\delta$  1 - 4); phenols ( $\delta$  4.0 - 7.5); enols ( $\delta$  6 - 7 for enols of cyclic  $\alpha$ -diketones,  $\delta$  14.5 - 16.5 for enols of  $\beta$ -dicarbonyls); carboxylic acids ( $\delta$  10 - 14). It must be aware because O-H signals are subjected by hydrogen bonding and exchange effects.

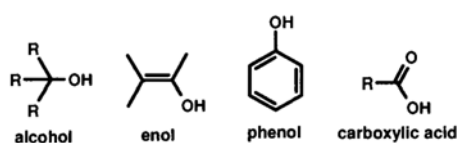


**Figure 3.6** Structures and  $^1\text{H}$  chemical shifts of hydrogens attached to oxygen groups.

#### 3.9.4.2 Hydrogens attached to nitrogen

Hydrogens can directly bonded to nitrogen occurs in several classes of compounds, as shown in Figure 3.7. Because N-H hydrogen signals tend to be less deshielded and appear at higher field (lower frequency) than their O-H counterparts. The normal chemical shifts are amines (0.5 - 3.0), aryl amines (3 - 5), amides (4 - 7), ammonium salts (6.0 - 8.5), imines (5 - 11). As a case of O-H hydrogens, N-H signals are also affected by hydrogen bonding and exchange and are therefore also dependent on temperature, concentration and solvent. N-H hydrogen signals in  $^1\text{H}$  spectra are exceptionally broad, so broad, and sometimes difficult to differentiate from baseline noise.

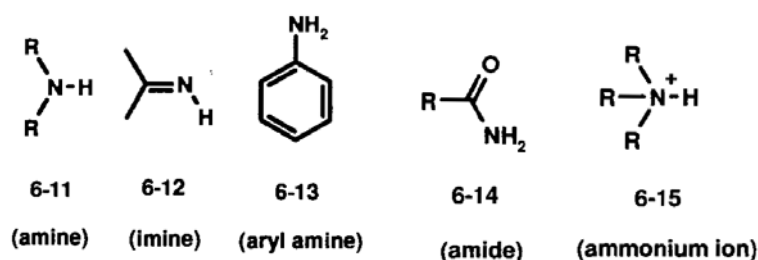


**Figure 3.7** Structures and  $^1\text{H}$  chemical shifts of hydrogens attached to nitrogen groups.

### 3.10 References

- Blake, G.R. (1965). Bulk Density. In American Society of Agronomy. **Methods of Soil Analysis** (ed. C.A.Black) (pp 374-390). Wisconsin.
- Bouyoucos, G.J. (1962). Hydrometer method improved for making particle size analyses of soils. **Agronomy Journal** 54: 464-465.
- Bremner, J.M. and Mulvaney, C.S. (1982). Nitrogen-Total. In A.L. Page. (ed.). **Methods of Soil Analysis, Part 2 Chemical and Microbiological Properties**. SSSA Book series No. 9. (pp 595-622). Madison.
- Chapman, H.D. (1965). **Cation Exchange Capacity by Ammonium Saturation Method**. **Methods of Soil Analysis** (Part 2, 57: pp 891-899). Madison, Wisconsin, USA: American Society of Agronomy.
- Gunther, H. (1973). **NMR Spectroscopy, an Introduction**. New York: Wiley. Quoted in R.S. Macomber. (1998). **A Complete Introduction to Modern NMR Spectroscopy**. New York: Wiley.
- Jenkinson, D.S. and Powlson, D.S. (1976). The effects of biocidal treatments on metabolism in soil. V: A method for measuring soil biomass. **Soil Biology and Biochemistry** 8: 209-213.
- Macomber, R.S. (1998). **A Complete Introduction to Modern NMR Spectroscopy**. New York: Wiley.
- Pourchert, C.J. (1983). **The Aldrich Library of NMR Spectra** (2nd ed.). Milwaukee: Aldrich Chemical Company. Quoted in R.S. Macomber, (1998). **A Complete Introduction to Modern NMR Spectroscopy**. New York: Wiley.
- Silverstein, R.M., Bassler, G.C. and Morrill, T.C. (1991). **Spectrometric Identification of Organic Compounds** (5th ed). New York: Wiley. Quoted in Macomber, R.S. (1998). **A Complete Introduction to Modern NMR Spectroscopy**. New York: Wiley.

Voroney, R.P., Winter, J.P. and Beyaert, R.P. (1993). Soil microbial biomass C and N. In M.R. Carter (ed.). **Soil Sampling and Methods of Analysis**. Boca Raton: Lewis Publishers.

Walkley, A. and Black, A.I. (1934). An examination of the different method for determining soil organic matter, and proposed modification of the chromic acid titration method. **Soil Science** 37: 29-38.

## **CHAPTER IV**

### **INTERNAL LEAF STRUCTURES OF VETIVER**

#### **4.1 Abstract**

Investigation of internal leaf structures can give a primary explanation of the potentially C sequestration of the plant. This chapter aimed to describe internal leaf structures of 11 vetiver provenances and observe some relative structures. The results found that all 11 provenances had a similar pattern of vascular bundle arrangement with the ratio of 1:3:1:3:1 for large:small:medium:small:large and Kranz structure which is similar C<sub>4</sub> plants. Like aquatic plants, large lysigenous intercellular spaces in vetiver leaves strongly related aeration system. Evident of aerenchyma at cortex layer could confirm gas circulation from leaves to roots and encouraged deeply root penetration of vetiver by avoiding hypoxia condition. Moreover, “Humidity-induced convection” and “Venturi-induced convection” were assumed as a strategy to gain more gas circulation of vetiver. Especially, sclerenchyma (fiber) in bundle caps of Loei provenance extended from abaxial to adaxial surface believed playing a dual function of mechanic and hydraulic (a short cut of water pathways) which could retain stomata open and longer gas exchange. Angle of leaf wings reflected an adaptive high radiation and was useful for provenance classification.

In conclusion, the internal leaf structures attributed all 11 vetiver provenances to sequester more C and especially Loei provenance.

**Keywords:** Kranz, lysigenous intercellular space, aerenchyma, vascular bundle.

## 4.2 Introduction

Investigating internal leaf structures can predict efficiency of C assimilation, photosynthetic mechanisms, environment during the plant grown and subsequently potentially C sequestration. Leaves present palisade and spongy mesophyll normally indicate to C<sub>3</sub> plants, which the photosynthetic capacity is lower than C<sub>4</sub> plants (Larcher, 2001). C<sub>4</sub> plants, a few groups of both dicots and monocots, display a modified leaf anatomy that is termed Kranz structure. It is characterized by elongated mesophyll cells that radiate from a single layer of large parenchymatous bundle-sheath cells containing starch and enlarged chloroplasts (Gunning and Steer, 1996). This normally forms a second bundle sheath layer, though in some grasses the primary vascular bundle sheath is itself recruited for this purpose. Taxonomic character in Poaceae, as double sheaths often occur in festucoid grasses and single sheaths in panicoid grasses, though there are exceptions (Lu and Liu, 2003; Twiss et al., 1969). In particular, internal leaf structures can change toward environmental variation. For example, sun leaves usually are smaller and thicker with more and better defined palisade cells, and more chloroplasts. They frequently have more hairs as well. Sun leaves rarely have chloroplasts in their epidermal cells, but chloroplasts are common in the epidermises of shade leaves (Rand, 2001). Leaves with thick cuticle, multiple epidermis or depressed stomata often found in xerophytes, whereas large intercellular spaces normally present hydrophytes or long term flooding-tolerant plants (Schulze et al., 2002). High laticifers, crystals or tannins serve in high grazing plants (Tomlinson and Fisher, 2005).

Therefore, this chapter aimed to investigate and describe internal leaf structures of 11 vetiver provenances, which the results tentatively induced to the prediction on the potentially C sequestration.

### **4.3 Objectives of this chapter**

4.3.1 To describe internal leaf structures of 11 vetiver provenances.

4.3.2 To investigate some relative structures promoting vetiver in C sequestration.

### **4.4 Materials and methods**

#### **4.4.1 Plant description**

This study conducted on eleven provenances of two vetiver species, *Chrysopogon nemoralis* and *C. zizanioides*. *C. nemoralis* consists of 6 provenances: Kamphaeng Phet 1 (KP1), Loei (LI), Nakhon Sawan (NS), Prachuabkhirikhan (PK), Ratchaburi (RB) and Roi Et (RE); whereas *C. zizanioides* has 5 provenances: Kamphaeng Phet 2 (KP2), Phraratchathan (PT), Songkhla 3 (SK), Sri Lanka (SL) and Surat Thani (ST). All plants were grown on loamy sand on November 2004 at the experimental plots of the Regional Office 3, Land Development Department, Muang District, Nakhon Ratchasima, Thailand (15°05'N, 102°13'E, 167 m a.s.l.) Each plot was of 2 x 10 m. Plants were given manures in an early stage and allowed naturally grown continually for 3 years. During November 2004 to 2007, the mean annual temperature ranged between 23.1 and 33.3°C with the average annual precipitation about 94.38 mm per month and the average annual evaporation about 4.84 mm per day (Nakhon Ratchasima Meteorology Station; Appendix A).

#### **4.4.2 Leaf cross section**

Fresh leaves were free-handed section and stained with safranin solution to provide transverse section slides. The leaves were observed internal structures through a light microscope.

## **4.5 Results**

### **4.5.1 Internal leaf structure of Kamphaeng Phet 1**

Transverse sections of internal leaf structures were shown in Plate 1 (Figure 4.1, 4.2 and 4.3).

#### **4.5.1.1 Angle of leaf wings**

Angle of leaf wings was steeply about 45° with curve wings (at the ends).

#### **4.5.1.2 Epidermis**

Both upper and lower epidermis were single layer with thick cuticle, by the outer walls were thicker than the inner. Stomata were greater in the lower epidermis by setting bellow the spaces between the small vascular bundles.

#### **4.5.1.3 Mesophyll**

Large lysigenous intercellular spaces were found in the mesophyll of mature leaves by positioning upper the small vascular bundles, but the spaces were not prominently in developing leaves.

#### **4.5.1.4 Vascular bundle arrangement**

Three sizes of vascular bundles could be classified, large (L), medium (M) and small (S), and arranged as a single row across lamina by attaching with abaxial surface. The vascular bundles arranged by alternating by sizes with the ratio of 1:3:1:3:1 for L:S:M:S:L.

#### **4.5.1.5 Xylem**

Xylem composes of 4 vessels paralleled with lamina by 1 on the left, 1 on the right, and 2 on the top (nearby a small intercellular space).

#### **4.5.1.6 Phloem**

Sieve tubes and companion cells located lower xylems.

#### **4.5.1.7 Bundle sheath**

Two layers of parenchyma surrounded phloems and xylems: (i) the inner was large cells of fibers containing chloroplasts; (ii) and the outer was chlorenchyma cells radiating from the inner (Kranz structure).

#### **4.5.1.8 Bundle cap**

All vascular bundles, except the middle of the small size, had well developed bundle caps, which composed of small and thick phloem fibers. By the bundle caps extended to lower epidermis. The thickness of bundle caps from phloem to lower epidermis was about 9 - 10, 8, and 2 fiber cell layers which were for the large, medium and small vascular bundle.

### **4.5.2 Internal leaf structure of Loei**

Transverse sections of internal leaf structures were shown in Plate 2 (Figure 4.4, 4.5, 4.6, 4.7 and 4.8).

#### **4.5.2.1 Angle of leaf wings**

Angle of leaf wings was steeply about  $45^\circ$  with curve wings (from middle to end).

#### **4.5.2.2 Epidermis**

Both upper and lower epidermis were single layer with thick cuticle, by the outer walls were thicker than the inner. Stomata were greater in the lower epidermis by setting bellow the spaces between the small vascular bundles.

#### **4.5.2.3 Mesophyll**

Large lysigenous intercellular spaces were found in the mesophyll of mature leaves by positioning upper the small vascular bundles, but the spaces were not prominently in developing leaves.

#### **4.5.2.4 Vascular bundle arrangement**

Three sizes of vascular bundles could be classified, large, medium and small, and arranged as a single row across lamina by attaching with abaxial surface. The vascular bundles arranged by alternating by sizes with the ratio of 1:3:1:3:1 for L:S:M:S:L.

#### **4.5.2.5 Xylem**

Xylem composes of 4 - 5 vessels paralleled with lamina by 1 - 2 on the left, 1 - 2 on the right, and 1 - 2 on the top (nearby a small intercellular space).

#### **4.5.2.6 Phloem**

Sieve tubes and companion cells located lower xylems.

#### **4.5.2.7 Bundle sheath**

Two layers of parenchyma surrounded phloems and xylems: (i) the inner was large cells of fibers containing chloroplasts; and (ii) the outer was chlorenchyma cells radiating from the inner (Kranz structure).

#### **4.5.2.8 Bundle cap**

All vascular bundles, except the middle of the small size, had well developed bundle caps, which composed of small and thick phloem fibers. By the bundle caps extended from the large and medium vascular bundles towards both epidermises. The thickness of bundle caps from phloem to lower epidermis was about 6 - 7, 6 - 7 and 2 - 3 fiber cell layers which were for the large, medium and small vascular bundle; and the thickness of bundle caps from xylem to upper epidermis was about 3 - 4 fiber cell layers.

### **4.5.3 Internal leaf structure of Nakhon Sawan**

Transverse sections of internal leaf structures were shown in Plate 3 (Figure 4.9, 4.10, 4.11 and 4.12).

#### **4.5.3.1 Angle of leaf wings**

Leaf wings attached together like a U - shape upside down (∩).

#### **4.5.3.2 Epidermis**

Both upper and lower epidermis were single layer with thick cuticle, by the outer walls were thicker than the inner. Stomata were greater in the lower epidermis by setting bellow the spaces between the small vascular bundles.

#### **4.5.3.3 Mesophyll**

Large lysigenous intercellular spaces were found in the mesophyll of mature leaves by positioning upper the small vascular bundles, but the spaces were not prominently in developing leaves.

#### **4.5.3.4 Vascular bundle arrangement**

Three sizes of vascular bundles could be classified, large, medium and small, and arranged as a single row across lamina by attaching with abaxial surface. The vascular bundles arranged by alternating by sizes with the ratio of 1:3:1:3:1 for L:S:M:S:L.

#### **4.5.3.5 Xylem**

Xylem composes of 3 vessels paralleled with lamina by 1 on the left, 1 on the right, and 1 on the top (nearby a small intercellular space).

#### **4.5.3.6 Phloem**

Sieve tubes and companion cells located lower xylems.

#### **4.5.3.7 Bundle sheath**

Two layers of parenchyma surrounded phloems and xylems: (i) the inner was large cells of fibers containing chloroplasts; and (ii) the outer was chlorenchyma cells radiating from the inner (Kranz structure).

#### **4.5.3.8 Bundle cap**

All vascular bundles, except the middle of the small size, had well developed bundle caps, which composed of small and thick phloem fibers. By the bundle caps extended to lower epidermis. The thickness of bundle caps from phloem to lower epidermis

was about 5 - 6, 4 - 5, and 1 - 2 fiber cell layers which were for the large, medium and small vascular bundle.

#### **4.5.4 Internal leaf structure of Prachuabkhirikhan**

Transverse sections of internal leaf structures were shown in Plate 4 (Figure 4.13, 4.14, 4.15 and 4.16).

##### **4.5.4.1 Angle of leaf wings**

Angle of leaf wings was steeply about 45° with curve wings (from middle to end).

##### **4.5.4.2 Epidermis**

Both upper and lower epidermis were single layer with thick cuticle, by the outer walls were thicker than the inner. Stomata were greater in the lower epidermis by setting bellow the spaces between the small vascular bundles.

##### **4.5.4.3 Mesophyll**

Large lysigenous intercellular spaces were found in the mesophyll of mature leaves by positioning upper the small vascular bundles, but the spaces were not prominently in developing leaves.

##### **4.5.4.4 Vascular bundle arrangement**

Three sizes of vascular bundles could be classified, large, medium and small, and arranged as a single row across lamina by attaching with abaxial surface. The vascular bundles arranged by alternating by sizes with the ratio of 1:3:1:3:1 for L:S:M:S:L.

##### **4.5.4.5 Xylem**

Xylem composes of 4 vessels paralleled with lamina by 2 (or 1) on the left, 1 on the right, and 1 (or 2) on the top (nearby a small intercellular space).

##### **4.5.4.6 Phloem**

Sieve tubes and companion cells located lower xylems.

#### **4.5.4.7 Bundle sheath**

Two layers of parenchyma surrounded phloems and xylems: (i) the inner was large cells of fibers containing chloroplasts; and (ii) the outer was chlorenchyma cells radiating from the inner (Kranz structure).

#### **4.5.4.8 Bundle cap**

All vascular bundles, except the middle of the small size, had well developed bundle caps, which composed of small and thick phloem fibers. By the bundle caps extended to lower epidermis. The thickness of bundle caps from phloem to lower epidermis was about 10 - 11, 9 - 10 and 6 - 7 fiber cell layers which were for the large, medium and small vascular bundle.

### **4.5.5 Internal leaf structure of Ratchaburi**

Transverse sections of internal leaf structures were shown in Plate 5 (Figure 4.17, 4.18, 4.19 and 4.20).

#### **4.5.5.1 Angle of leaf wings**

Angle of leaf wings was steeply about 45°.

#### **4.5.5.2 Epidermis**

Both upper and lower epidermis were single layer with thick cuticle, by the outer walls were thicker than the inner. Stomata were greater in the lower epidermis by setting bellow the spaces between the small vascular bundles.

#### **4.5.5.3 Mesophyll**

Large lysigenous intercellular spaces were found in the mesophyll of mature leaves by positioning upper the small vascular bundles, but the spaces were not prominently in developing leaves.

#### **4.5.5.4 Vascular bundle arrangement**

Three sizes of vascular bundles could be classified, large, medium and small, and arranged as a single row across lamina by attaching with abaxial surface. The vascular bundles arranged by alternating by sizes with the ratio of 1:3:1:3:1 for L:S:M:S:L.

#### **4.5.5.5 Xylem**

Xylem composes of 5 vessels paralleled with lamina by 1 on the left, 2 on the right, and 2 on the top (nearby a small intercellular space).

#### **4.5.5.6 Phloem**

Sieve tubes and companion cells located lower xylems.

#### **4.5.5.7 Bundle sheath**

Two layers of parenchyma surrounded phloems and xylems: (i) the inner was large cells of fibers containing chloroplasts; and (ii) the outer was chlorenchyma cells radiating from the inner (Kranz structure).

#### **4.5.5.8 Bundle cap**

All vascular bundles, except the middle of the small size, had well developed bundle caps, which composed of small and thick phloem fibers. By the bundle caps extended to lower epidermis. The thickness of bundle caps from phloem to lower epidermis was about 6 - 7, 5 - 6 and 1 - 2 fiber cell layers which were for the large, medium and small vascular bundle.

### **4.5.6 Internal leaf structure of Roi Et**

Transverse sections of internal leaf structures were shown in Plate 6 (Figure 4.21, 4.22, 4.23 and 4.24).

#### **4.5.6.1 Angle of leaf wings**

Angle of leaf wings was about 60° with curve wings (from middle to end).

#### **4.5.6.2 Epidermis**

Both upper and lower epidermis were single layer with thick cuticle, by the outer walls were thicker than the inner. Stomata were greater in the lower epidermis by setting bellow the spaces between the small vascular bundles.

#### **4.5.6.3 Mesophyll**

Large lysigenous intercellular spaces were found in the mesophyll of mature leaves by positioning upper the small vascular bundles, but the spaces were not prominently in developing leaves.

#### **4.5.6.4 Vascular bundle arrangement**

Three sizes of vascular bundles could be classified, large, medium and small, and arranged as a single row across laminas by attaching with abaxial surface. The vascular bundles arranged by alternating by sizes with the ratio of 1:3:1:3:1 for L:S:M:S:L.

#### **4.5.6.5 Xylem**

Xylem composes of 4 vessels paralleled with lamina by 1 on the left, 1 on the right, and 2 on the top (nearby a small intercellular space).

#### **4.5.6.6 Phloem**

Sieve tubes and companion cells located lower xylems.

#### **4.5.6.7 Bundle sheath**

Two layers of parenchyma surrounded phloems and xylems: (i) the inner was large cells of fibers containing chloroplasts; and (ii) the outer was chlorenchyma cells radiating from the inner (Kranz structure).

#### **4.5.6.8 Bundle cap**

All vascular bundles, except the middle of the small size, had well developed bundle caps, which composed of small and thick phloem fibers. By the bundle caps extended to lower epidermis. The thickness of bundle caps from phloem to lower epidermis

was about 6 - 7, 6 - 7 and 2 - 3 fiber cell layers which were for the large, medium and small vascular bundle.

#### **4.5.7 Internal leaf structure of Kamphaeng Phet 2**

Transverse sections of internal leaf structures were shown in Plate 7 (Figure 4.25, 4.26 and 4.27).

##### **4.5.7.1 Angle of leaf wings**

Angle of leaf wings was about 60° without curve wings.

##### **4.5.7.2 Epidermis**

Both upper and lower epidermis were single layer with thick cuticle, by the outer walls were thicker than the inner. Stomata were greater in the lower epidermis by setting bellow the spaces between the small vascular bundles.

##### **4.5.7.3 Mesophyll**

Large lysigenous intercellular spaces were found in the mesophyll of mature leaves by positioning upper the small vascular bundles, but the spaces were not prominently in developing leaves.

##### **4.5.7.4 Vascular bundle arrangement**

Three sizes of vascular bundles could be classified, large, medium and small, and arranged as a single row across lamina by attaching with abaxial surface. The vascular bundles arranged by alternating by sizes with the ratio of 1:3:1:3:1 for L:S:M:S:L.

##### **4.5.7.5 Xylem**

Xylem composes of 4 vessels paralleled with lamina by 1 on the left, 1 on the right, and 2 on the top (nearby a small intercellular space).

##### **4.5.7.6 Phloem**

Sieve tubes and companion cells located lower xylems.

#### **4.5.7.7 Bundle sheath**

Two layers of parenchyma surrounded phloems and xylems: (i) the inner was large cells of fibers containing chloroplasts; and (ii) the outer was chlorenchyma cells radiating from the inner (Kranz structure).

#### **4.5.7.8 Bundle cap**

All vascular bundles, except the middle of the small size, had well developed bundle caps, which composed of small and thick phloem fibers. By the bundle caps extended to lower epidermis. The thickness of bundle caps from phloem to lower epidermis was about 8 - 9, 5 - 6 and 2 - 3 fiber cell layers which were for the large, medium and small vascular bundle.

### **4.5.8 Internal leaf structure of Phraratchathan**

Transverse sections of internal leaf structures were shown in Plate 8 (Figure 4.28, 4.29 and 4.30).

#### **4.5.8.1 Angle of leaf wings**

Angle of leaf wings was steeply about  $45^\circ$  without curve wings.

#### **4.5.8.2 Epidermis**

Both upper and lower epidermis were single layer with thick cuticle, by the outer walls were thicker than the inner. Stomata were greater in the lower epidermis by setting bellow the spaces between the small vascular bundles.

#### **4.5.8.3 Mesophyll**

Large lysigenous intercellular spaces were found in the mesophyll of mature leaves by positioning upper the small vascular bundles, but the spaces were not prominently in developing leaves.

#### **4.5.8.4 Vascular bundle arrangement**

Three sizes of vascular bundles could be classified, large, medium and small, and arranged as a single row across lamina by attaching with abaxial surface. The vascular bundles arranged by alternating by sizes with the ratio of 1:3:1:3:1 for L:S:M:S:L.

#### **4.5.8.5 Xylem**

Xylem composes of 4 vessels paralleled with lamina by 1 on the left, 1 on the right, and 2 on the top (nearby a small intercellular space).

#### **4.5.8.6 Phloem**

Sieve tubes and companion cells located lower xylems.

#### **4.5.8.7 Bundle sheath**

Two layers of parenchyma surrounded phloems and xylems: (i) the inner was large cells of fibers containing chloroplasts; and (ii) the outer was chlorenchyma cells radiating from the inner (Kranz structure).

#### **4.5.8.8 Bundle cap**

All vascular bundles, except the middle of the small size, had well developed bundle caps, which composed of small and thick phloem fibers. By the bundle caps extended to lower epidermis. The thickness of bundle caps from phloem to lower epidermis was about 7 - 8, 7 - 8 and 1 - 2 fiber cell layers which were for the large, medium and small vascular bundle.

### **4.5.9 Internal leaf structure of Songkhla 3**

Transverse sections of internal leaf structures were shown in Plate 9 (Figure 4.31, 4.32, 4.33 and 4.34).

#### **4.5.9.1 Angle of leaf wings**

Angle of leaf wings was very wide (over than 90°).

#### **4.5.9.2 Epidermis**

Both upper and lower epidermis were single layer with thick cuticle, by the outer walls were thicker than the inner. Stomata were greater in the lower epidermis by setting bellow the spaces between the small vascular bundles.

#### **4.5.9.3 Mesophyll**

Large lysigenous intercellular spaces were found in the mesophyll of mature leaves by positioning upper the small vascular bundles, but the spaces were not prominently in developing leaves.

#### **4.5.9.4 Vascular bundle arrangement**

Three sizes of vascular bundles could be classified, large, medium and small, and arranged as a single row across laminas by attaching with abaxial surface. The vascular bundles arranged by alternating by sizes with the ratio of 1:3:1:3:1 for L:S:M:S:L.

#### **4.5.9.5 Xylem**

Xylem composes of 4 vessels paralleled with lamina by 1 on the left, 1 on the right, and 2 on the top (nearby a small intercellular space).

#### **4.5.9.6 Phloem**

Sieve tubes and companion cells located lower xylems.

#### **4.5.9.7 Bundle sheath**

Two layers of parenchyma surrounded phloems and xylems: (i) the inner was large cells of fibers containing chloroplasts; and (ii) the outer was chlorenchyma cells radiating from the inner (Kranz structure).

#### **4.5.9.8 Bundle cap**

All vascular bundles, except the middle of the small size, had well developed bundle caps, which composed of small and thick phloem fibers. By the bundle caps extended to lower epidermis. The thickness of bundle caps from phloem to lower epidermis

was about 6 - 7, 6 - 7 and 1 - 2 fiber cell layers which were for the large, medium and small vascular bundle.

#### **4.5.10 Internal leaf structure of Sri Lanka**

Transverse sections of internal leaf structures were shown in Plate 10 (Figure 4.35, 4.36, 4.37 and 4.38).

##### **4.5.10.1 Angle of leaf wings**

Angle of leaf wings was steeply about 45° with curve wings (at the ends).

##### **4.5.10.2 Epidermis**

Both upper and lower epidermis were single layer with thick cuticle, by the outer walls were thicker than the inner. Stomata were greater in the lower epidermis by setting bellow the spaces between the small vascular bundles.

##### **4.5.10.3 Mesophyll**

Large lysigenous intercellular spaces were found in the mesophyll of mature leaves by positioning upper the small vascular bundles, but the spaces were not prominently in developing leaves.

##### **4.5.10.4 Vascular bundle arrangement**

Three sizes of vascular bundles could be classified, large, medium and small, and arranged as a single row across lamina by attaching with abaxial surface. The vascular bundles arranged by alternating by sizes with the ratio of 1:3:1:3:1 for L:S:M:S:L.

##### **4.5.10.5 Xylem**

Xylem composes of 4 vessels paralleled with lamina by 1 on the left, 2 on the right, and 1 on the top (nearby a small intercellular space).

##### **4.5.10.6 Phloem**

Sieve tubes and companion cells located lower xylems.

#### **4.5.10.7 Bundle sheath**

Two layers of parenchyma surrounded phloems and xylems: (i) the inner was large cells of fibers containing chloroplasts; and (ii) the outer was chlorenchyma cells radiating from the inner (Kranz structure).

#### **4.5.10.8 Bundle cap**

All vascular bundles, except the middle of the small size, had well developed bundle caps, which composed of small and thick phloem fibers. By the bundle caps extended to lower epidermis. The thickness of bundle caps from phloem to lower epidermis was about 4 - 5, 7 - 8 and 1 - 2 fiber cell layers which were for the large, medium and small vascular bundle.

### **4.5.11 Internal leaf structure of Surat Thani**

Transverse sections of internal leaf structures were shown in Plate 11 (Figure 4.39, 4.40, 4.41 and 4.42).

#### **4.5.11.1 Angle of leaf wings**

Angle of leaf wings was very steep (less than 45°).

#### **4.5.11.2 Epidermis**

Both upper and lower epidermis were single layer with thick cuticle, by the outer walls were thicker than the inner. Stomata were greater in the lower epidermis by setting bellow the spaces between the small vascular bundles.

#### **4.5.11.3 Mesophyll**

Large lysigenous intercellular spaces were found in the mesophyll of mature leaves by positioning upper the small vascular bundles, but the spaces were not prominently in developing leaves.

#### **4.5.11.4 Vascular bundle arrangement**

Three sizes of vascular bundles could be classified, large, medium and small, and arranged as a single row across laminae by attaching with abaxial surface. The vascular bundles arranged by alternating by sizes with the ratio of 1:3:1:3:1 for L:S:M:S:L.

#### **4.5.11.5 Xylem**

Xylem composes of 4 - 5 vessels paralleled with lamina by 1 - 2 on the left, 1 on the right, and 1 - 2 on the top (nearby a small intercellular space).

#### **4.5.11.6 Phloem**

Sieve tubes and companion cells located lower xylems.

#### **4.5.11.7 Bundle sheath**

Two layers of parenchyma surrounded phloems and xylems: (i) the inner was large cells of fibers containing chloroplasts; and (ii) the outer was chlorenchyma cells radiating from the inner (Kranz structure).

#### **4.5.11.8 Bundle cap**

All vascular bundles, except the middle of the small size, had well developed bundle caps, which composed of small and thick phloem fibers. By the bundle caps extended to lower epidermis. The thickness of bundle caps from phloem to lower epidermis was about 5 - 7, 7 - 8 and 1 - 2 fiber cell layers which were for the large, medium and small vascular bundle.

Plate 1 Internal Leaf Structure of Kamphaeng Phet 1

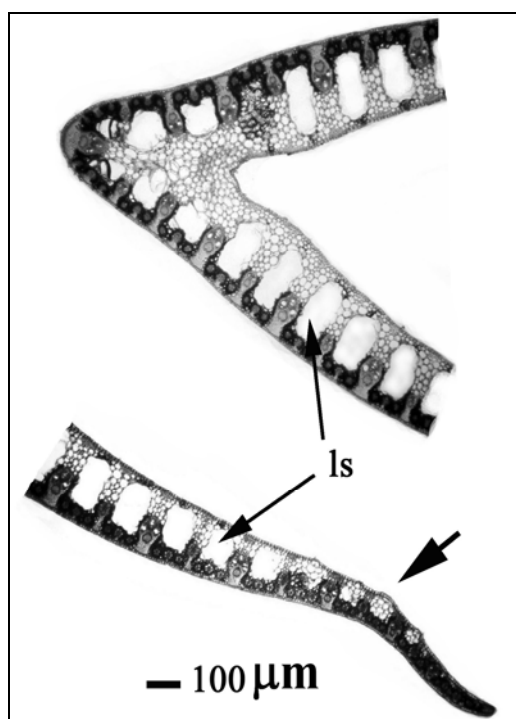


Figure 4.1

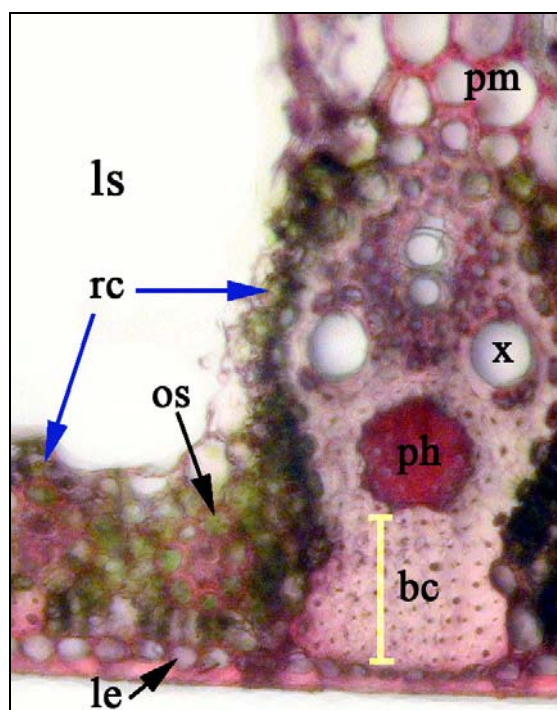


Figure 4.2

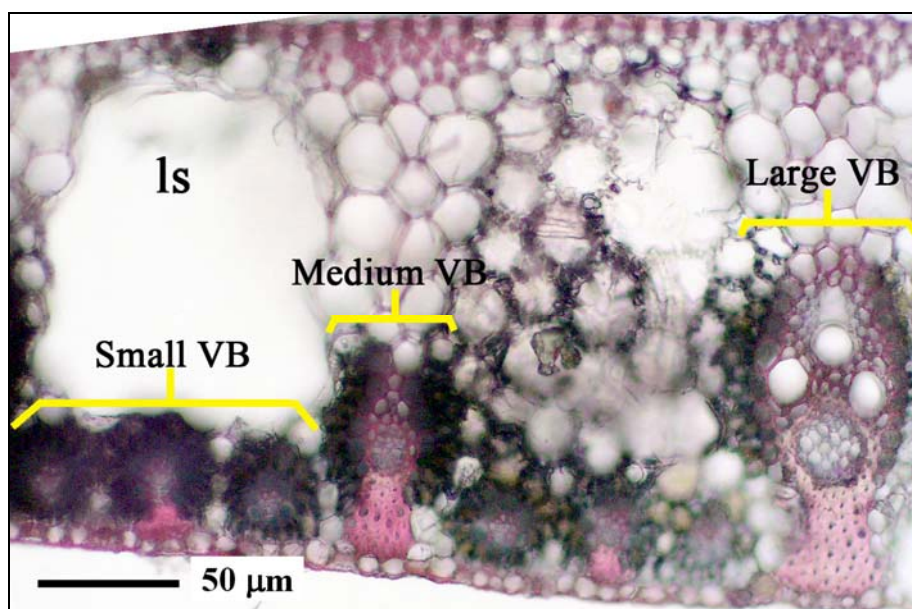


Figure 4.3

**Figure 4.1** TS of Kamphaeng Phet 1 leaves showing a steep angle of leaf wings ( $\sim 45^\circ$ ) with curve wings at the ends (large arrow), and large intercellular spaces (ls).

**Figure 4.2** Focus on a large vascular bundle of a mature leaf.

**Figure 4.3** TS of a developing leaf showing lysigenous intercellular spaces and a lysis of parenchyma cells.

### Plate 2 Internal Leaf Structure of Loei

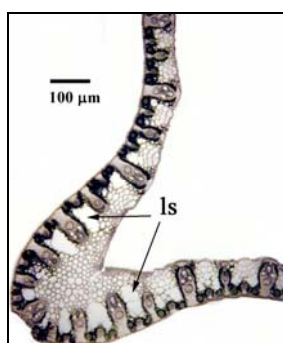


**Figure 4.4**

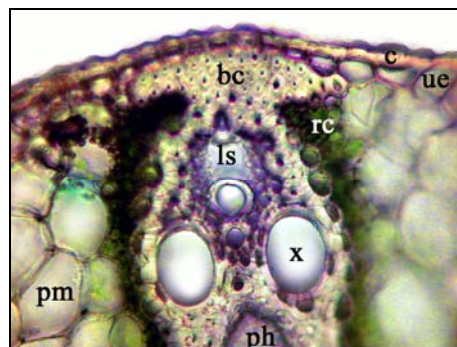


**Figure 4.5**

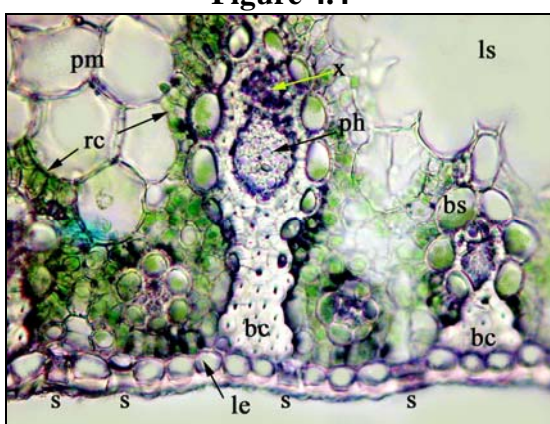


**Figure 4.6**

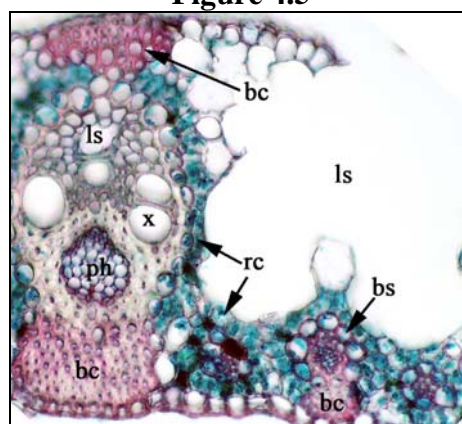


**Figure 4.7**

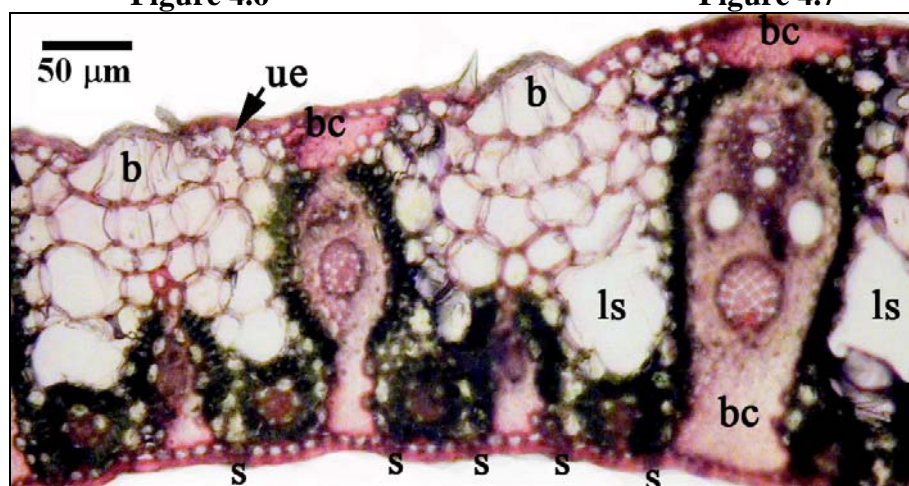


**Figure 4.8**

**Figure 4.4** TS of Loei leaf showing a steep angle of leaf wings ( $\sim 45^\circ$ ) with curve (from middle to end), and lysigenous intercellular spaces (ls).

**Figure 4.5** TS of a large vascular bundle.

**Figure 4.6** TS of medium and small vascular bundles.

**Figure 4.7** TS of a mature leaf showing bundle caps attach at adaxial and abaxial surfaces.

**Figure 4.8** TS of a developing leaf showing an early stage of parenchyma lysis.

**Plate 3 Internal Leaf Structure of Nakhon Sawan**

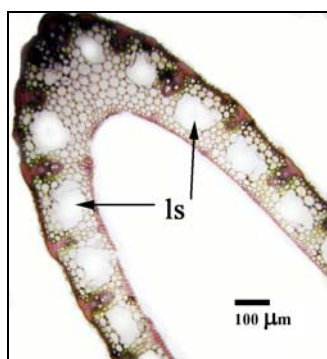


**Figure 4.9**

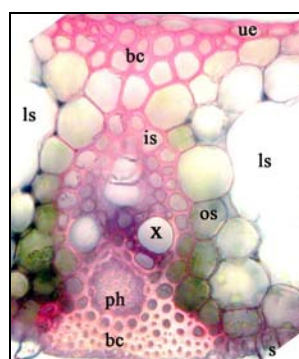


**Figure 4.10**

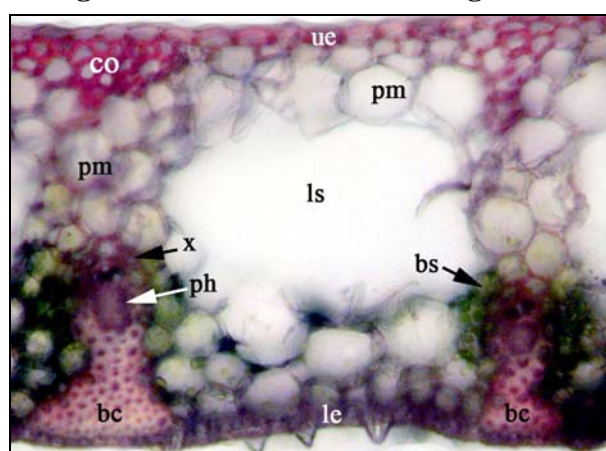


**Figure 4.11**

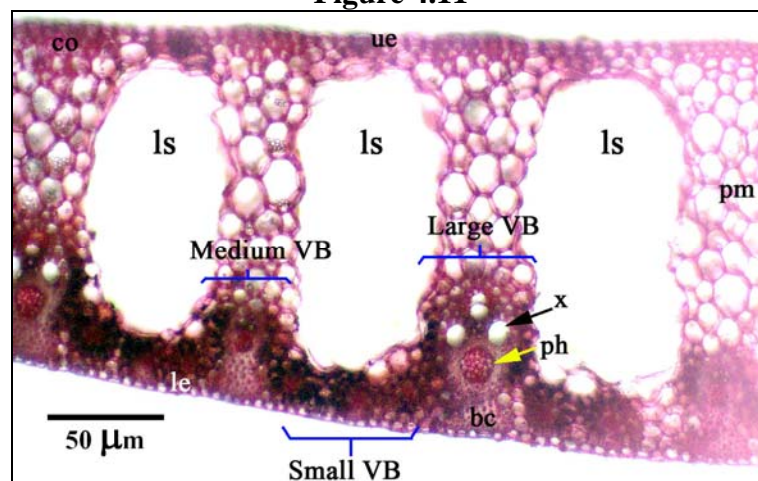


**Figure 4.12**

**Figure 4.9** TS of Nakhon Sawan leaf showing two leaf wings like a U - shape upside down (∩) and lysigenous intercellular spaces (ls).

**Figure 4.10** TS of a large vascular bundle in a developing leaf.

**Figure 4.11** TS of a developing leaf showing parenchyma lysis.

**Figure 4.12** TS of a mature leaf showing different vascular bundles and large lysigenous intercellular spaces.

### Plate 4 Internal Leaf Structure of Prachuabkhirikhan

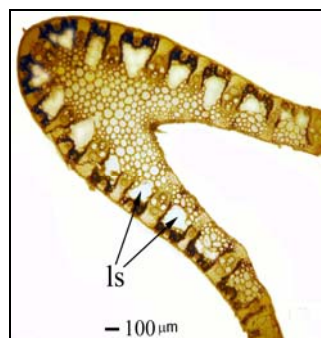


**Figure 4.13**

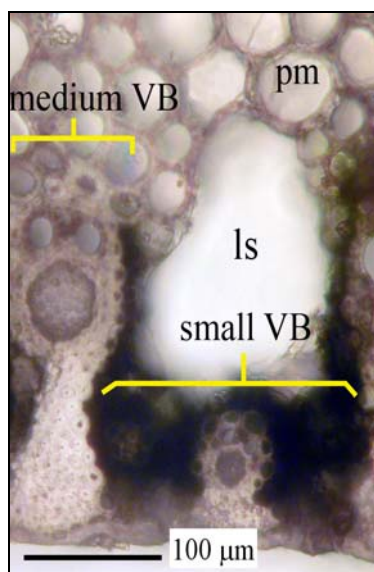


**Figure 4.14**

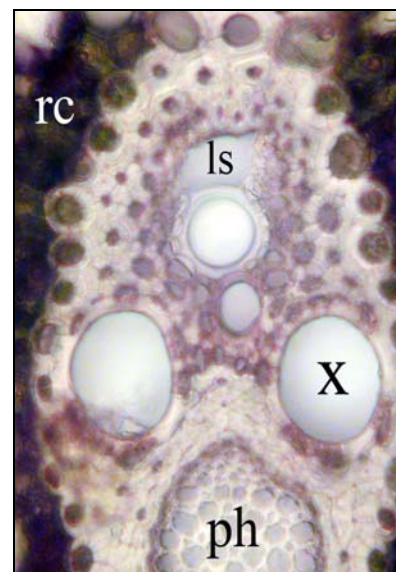


**Figure 4.15**

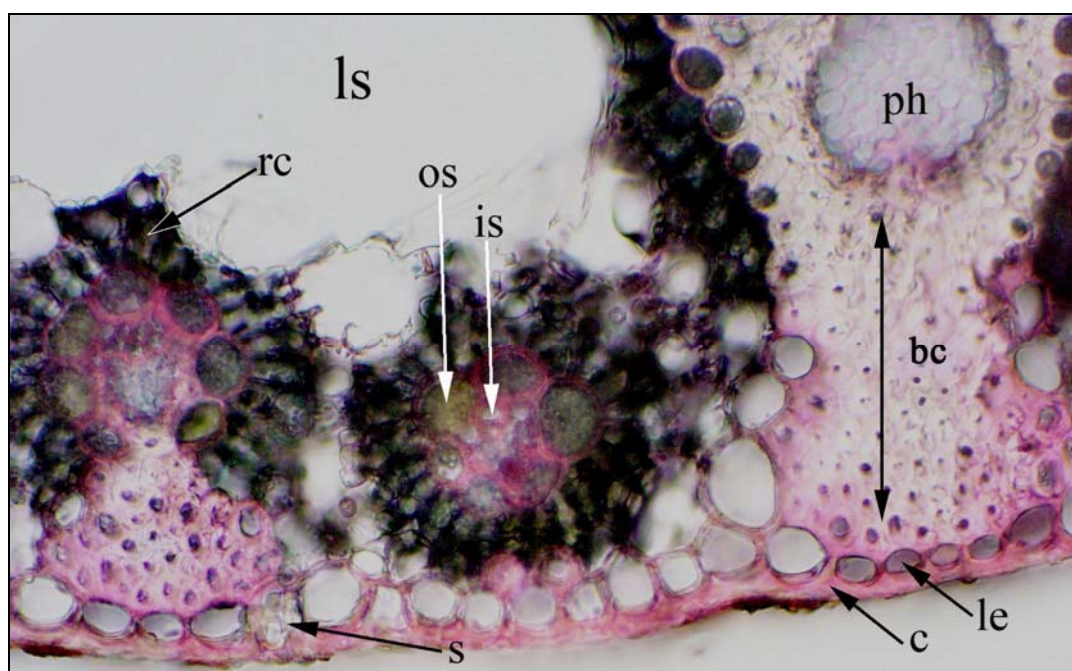


**Figure 4.16**

**Figure 4.13** TS of Prachuabkhirikhan leaf showing a steep angle of leaf wings ( $\sim 45^\circ$ ) with curve (from middle to end), and lysigenous intercellular spaces (ls).

**Figure 4.14** Two sizes of vascular bundles, medium and small.

**Figure 4.15** Focus on a large vascular bundle.

**Figure 4.16** Two sizes of vascular bundles, large and small.

### Plate 5 Internal Leaf Structure of Ratchaburi

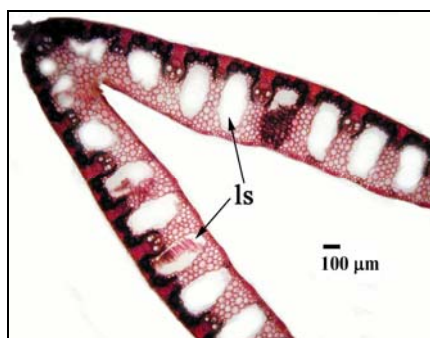


**Figure 4.17**

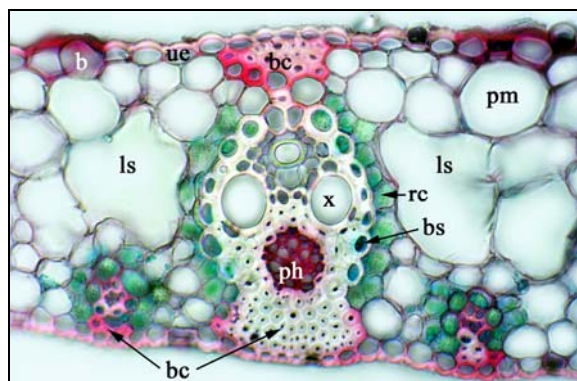


**Figure 4.18**

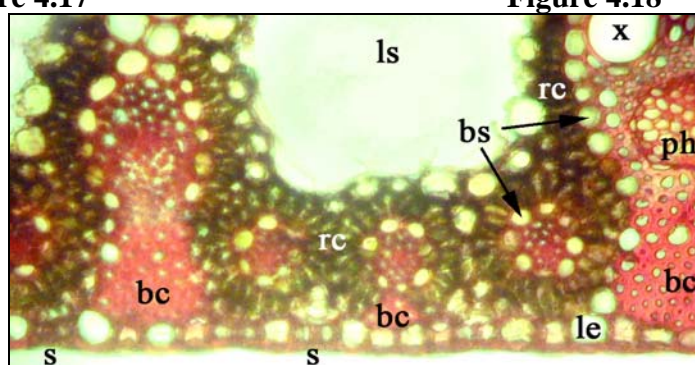


**Figure 4.19**

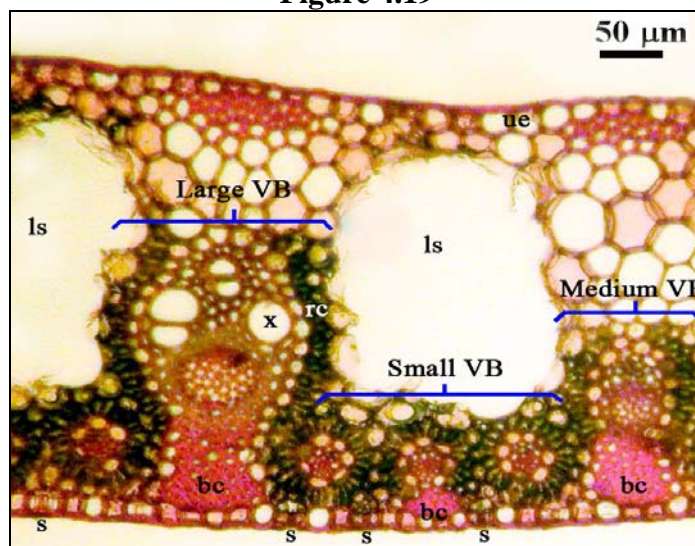


**Figure 4.20**

**Figure 4.17** TS of Ratchaburi leaf showing a steep angle of leaf wings ( $\sim 45^\circ$ ) without curve, and lysigenous intercellular spaces (ls).

**Figure 4.18** TS of a developing leaf showing an early stage of parenchyma lysis.

**Figure 4.19** TS of a mature leaf.

**Figure 4.20** TS of a mature leaf comparing three sizes of vascular bundles, large, medium and small.

**Plate 6 Internal Leaf Structure of Roi Et**

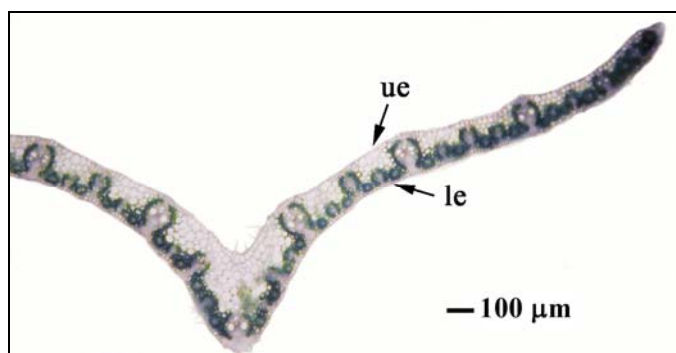


**Figure 4.21**

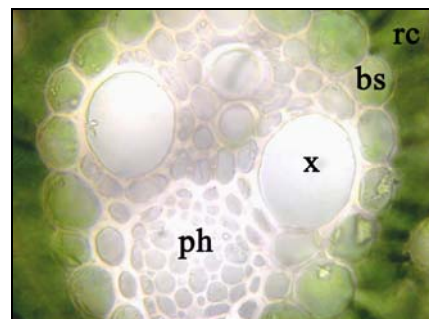


**Figure 4.22**

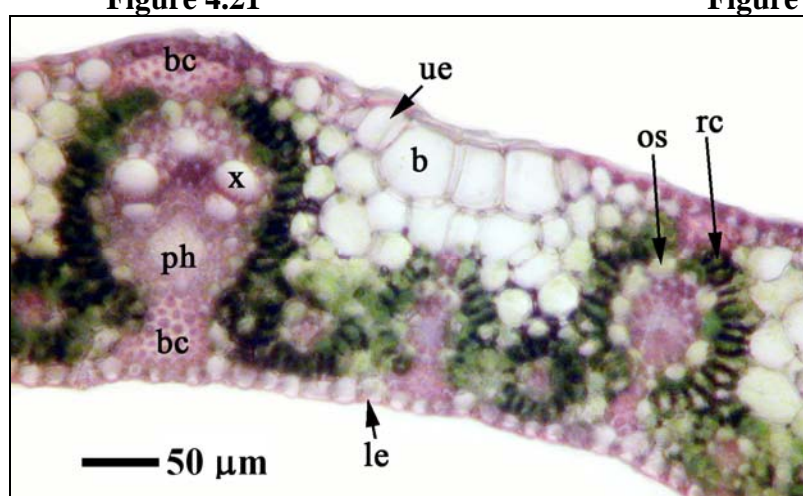


**Figure 4.23**

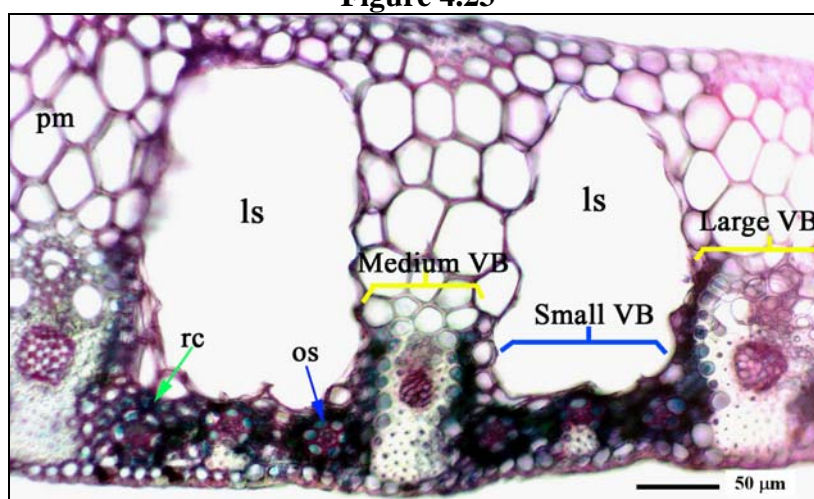


**Figure 4.24**

**Figure 4.21** TS of Roi Et leaf showing a wide angle of leaf wings ( $\sim 60^\circ$ ) with curve wings (from middle to end).

**Figure 4.22** Focus on a large vascular bundle.

**Figure 4.23** TS of a developing leaf.

**Figure 4.24** TS of a mature leaf showing the three sizes of vascular bundles.

**Plate 7 Internal Leaf Structure of Kamphaeng Phet 2**

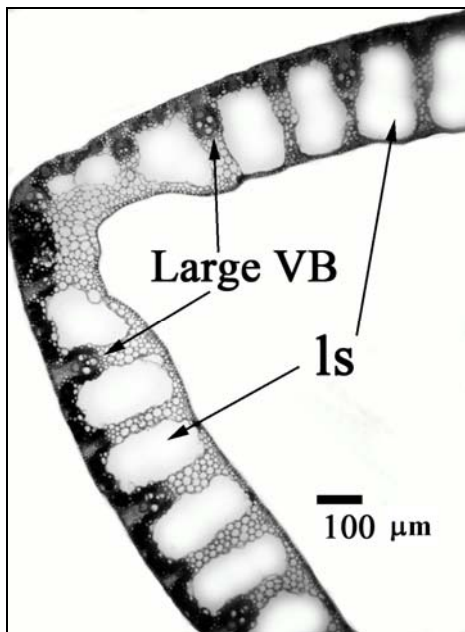


**Figure 4.25**

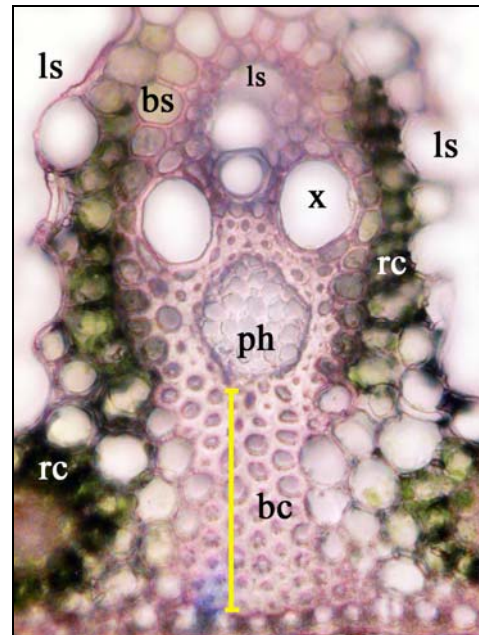


**Figure 4.26**

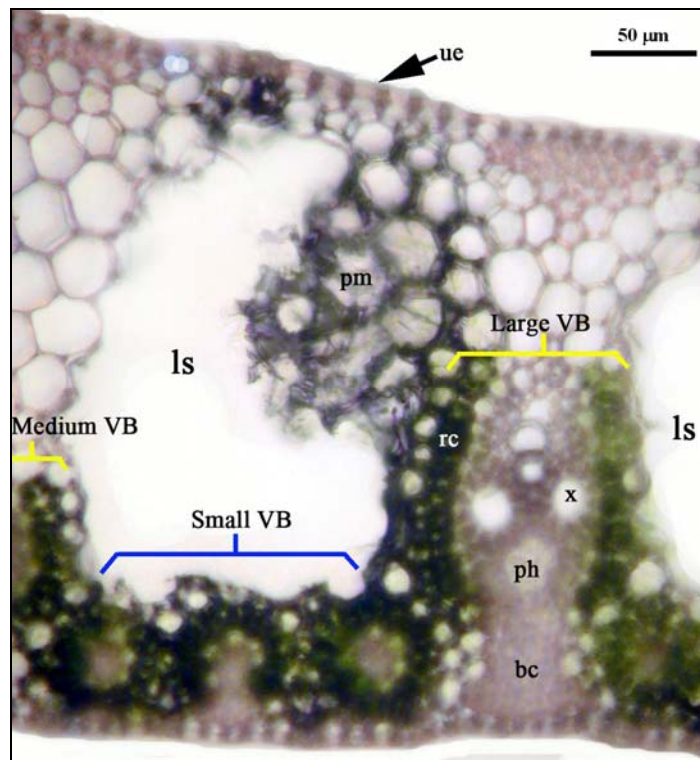


**Figure 4.27**

**Figure 4.25** TS of Kamphaeng Phet 2 showing a wide angle of leaf wings ( $\sim 60^\circ$ ) without curve wings, and lysigenous intercellular spaces (ls).

**Figure 4.26** Focus on a large vascular bundle.

**Figure 4.27** TS of a mature leaf showing parenchyma lysis.

**Plate 8 Internal Leaf Structure of Phraratchathan**

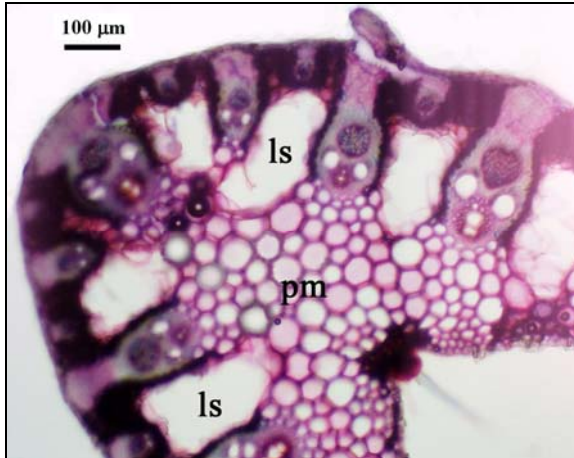


**Figure 4.28**

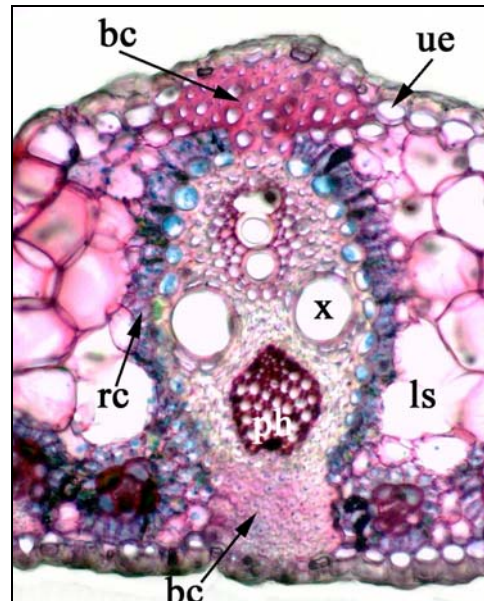


**Figure 4.29**

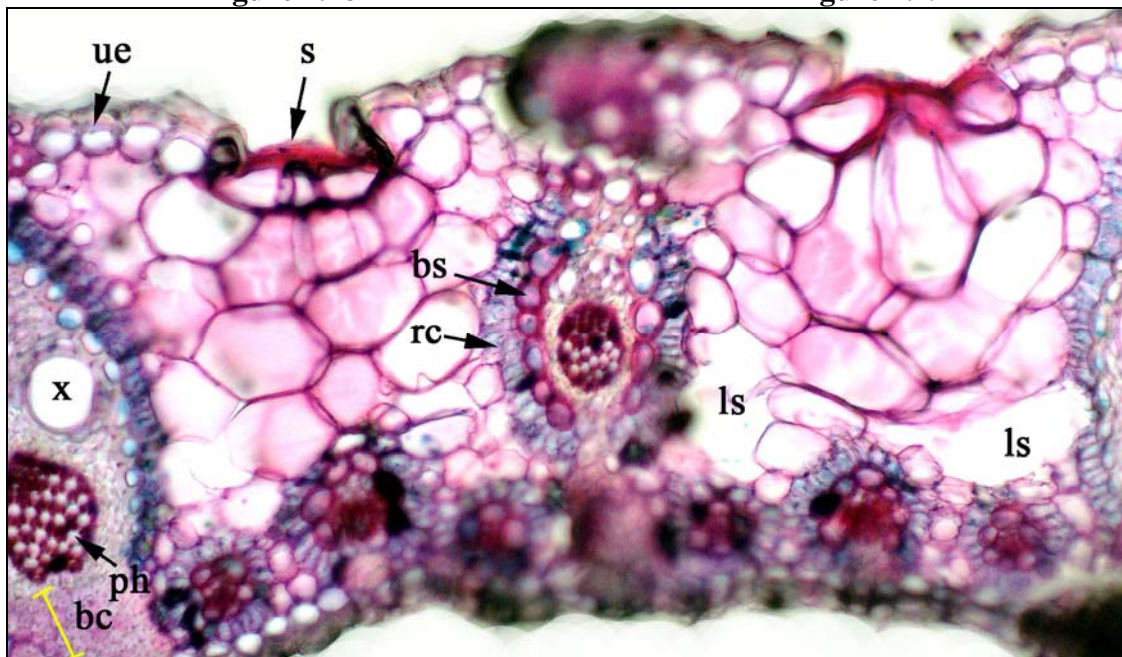


**Figure 4.30**

**Figure 4.28** TS of Phraratchathan leaf showing a steep angle of leaf wings ( $\sim 45^\circ$ ) without curve wings, and lysigenous intercellular spaces (ls).

**Figure 4.29** Focus on a large vascular bundle in a developing leaf.

**Figure 4.30** TS of a developing leaf showing an early stage of parenchyma lysis.

**Plate 9 Internal Leaf Structure of Songkhla 3**

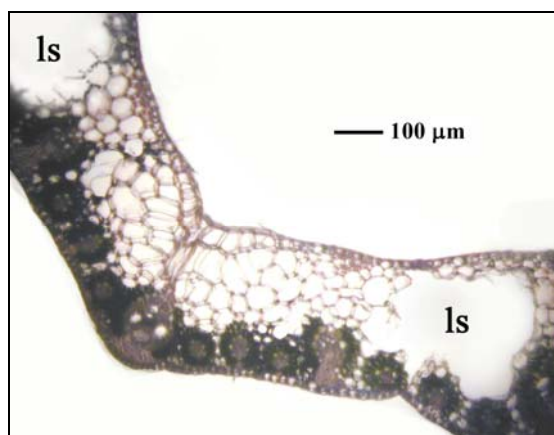


**Figure 4.31**

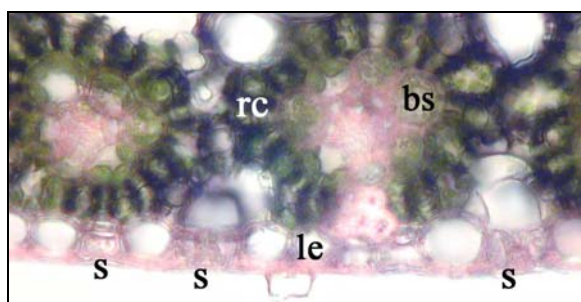


**Figure 4.32**

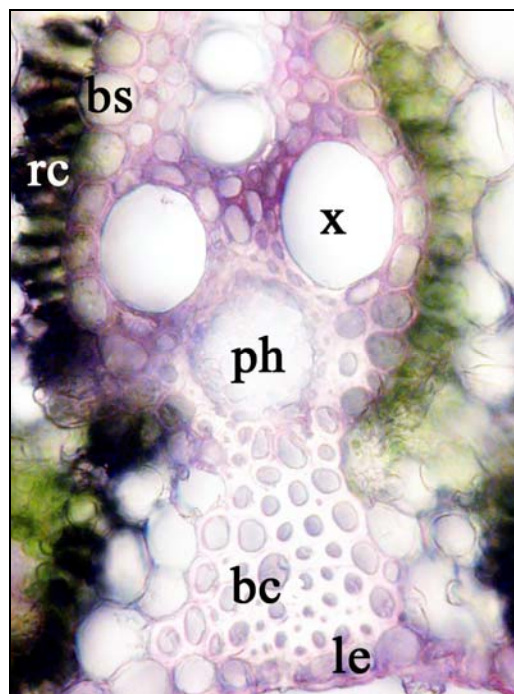


**Figure 4.33**

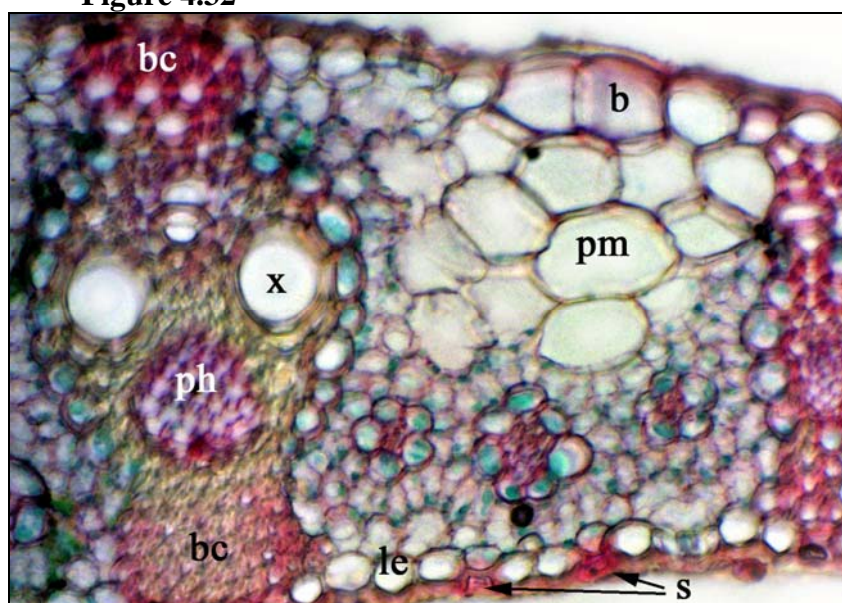


**Figure 4.34**

**Figure 4.31** TS of Songkhla 3 leaf showing a wide angle of leaf wings ( $> 90^\circ$ ), and lysigenous intercellular spaces (ls).

**Figure 4.32** Focus on small vascular bundles.

**Figure 4.33** Focus on a large vascular bundle.

**Figure 4.34** TS of a developing leaf showing an early stage of parenchyma lysis.

Plate 10 Internal Leaf Structure of Sri Lanka

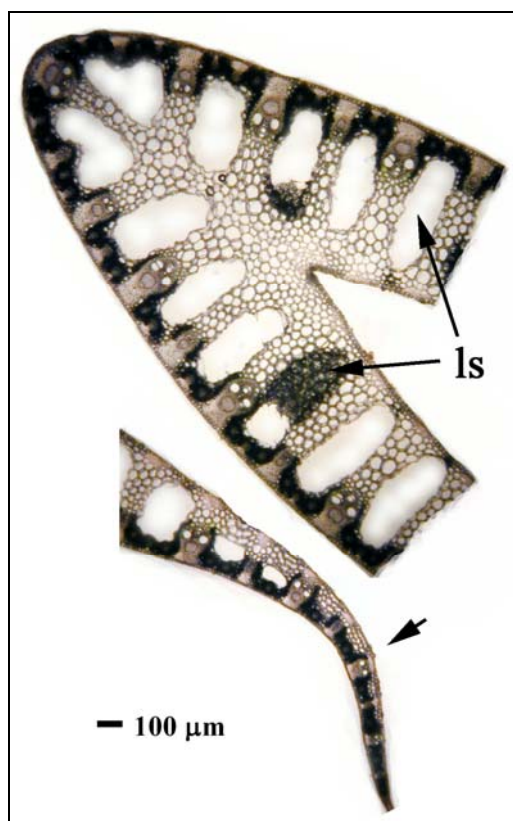


Figure 4.35

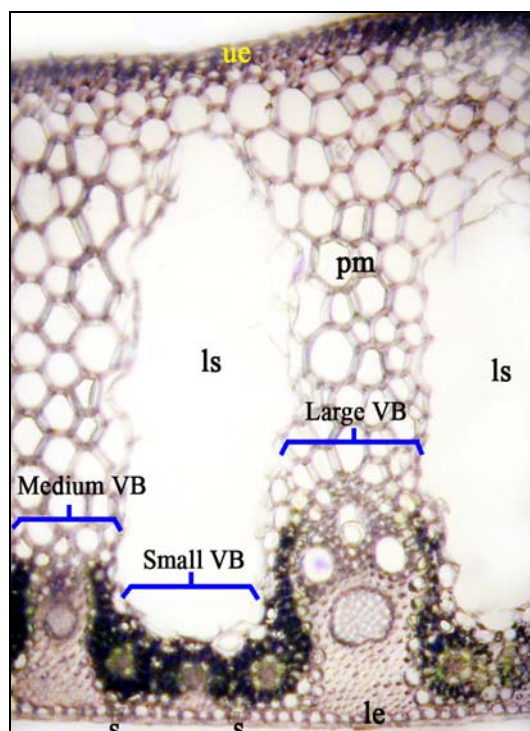


Figure 4.36

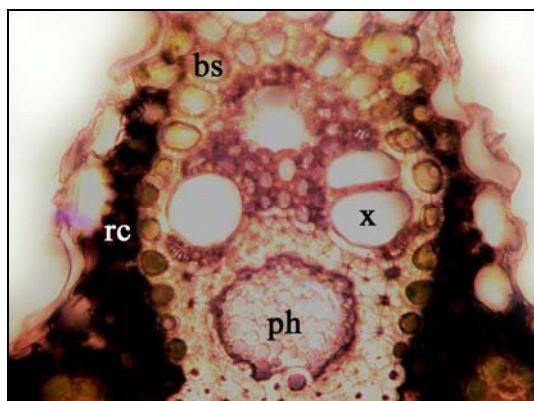


Figure 4.37

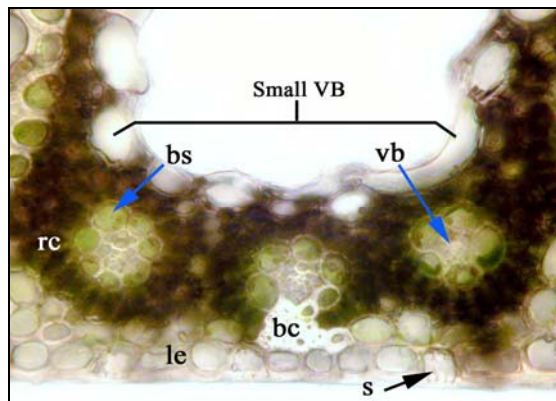


Figure 4.38

**Figure 4.35** TS of Sri Lanka leaves showing a steep angle of leaf wings (~45°) with curve wings (at the ends), and lysigenous intercellular spaces (ls).

**Figure 4.36** TS of a mature leaf showing large lysigenous intercellular spaces and three sizes of vascular bundles, large, medium and small.

**Figure 4.37** Focus on a large vascular bundle.

**Figure 4.38** Focus on small vascular bundles.

**Plate 11 Internal Leaf Structure of Surat Thani**

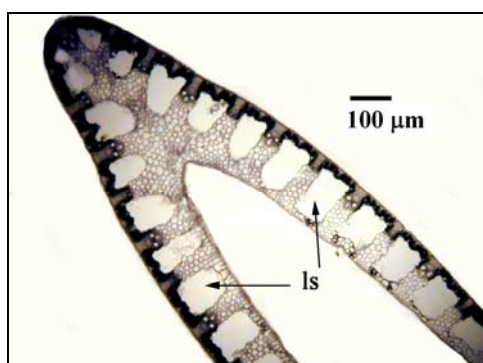


**Figure 4.39**

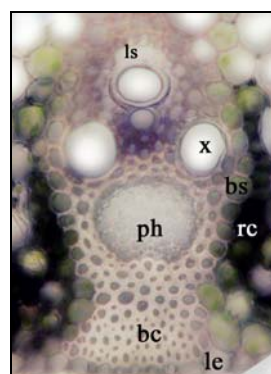


**Figure 4.40**

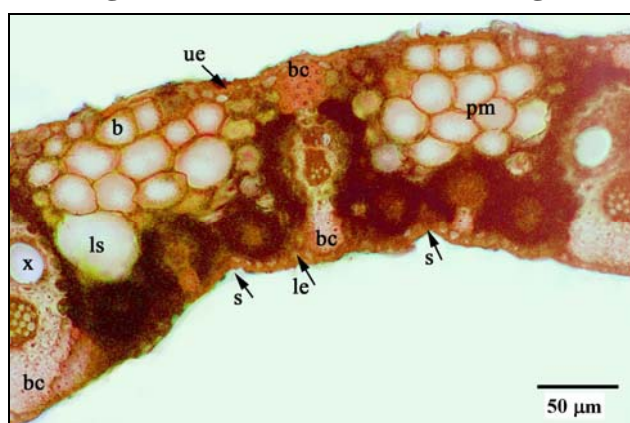


**Figure 4.41**

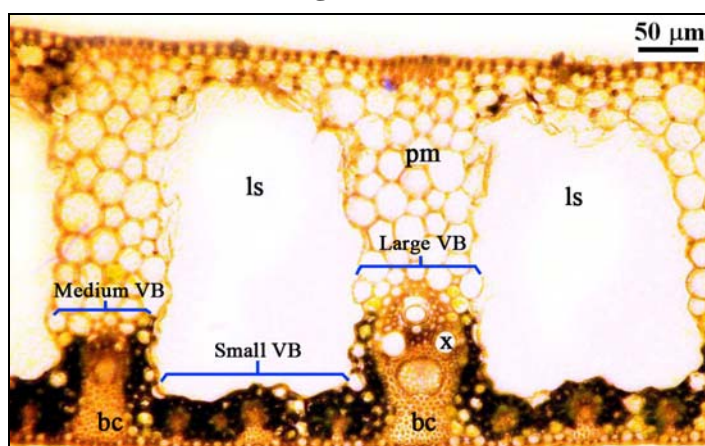


**Figure 4.42**

**Figure 4.39** TS of Surat Thani leaf showing a very steep angle of leaf wings ( $< 45^\circ$ ), and lysigenous intercellular spaces (ls).

**Figure 4.40** Focus on a large vascular bundle.

**Figure 4.41** TS of a developing leaf showing an early stage of parenchyma lysis.

**Figure 4.42** TS of a mature leaf showing large lysigenous intercellular spaces and three sizes of vascular bundles, large, medium and small.

## 4.6 Discussion

### 4.6.1 Comparing angle of leaf wings among 11 provenances

Angle of leaf wings was different among 11 provenances, but it could be benefit in provenance classification as shown in Table 4.1. Steep angle of leaf wings, except SK provenance, indicated an adaptation of vetiver leaves to high radiation such as very steep angle of ST provenance ( $< 45^\circ$ ). However, SK provenance seemed to have high radiant tolerance with wide angle of leaf wings ( $> 90^\circ$ ).

**Table 4.1** Classification of vetiver provenance based on angle of leaf wings.

Angle of leaf wings	Vetiver provenance
$< 45^\circ$	ST
$\sim 45^\circ$ without curve wings	RB and PT
$\sim 45^\circ$ with curve wings (from middle to end)	LI and PK
$\sim 45^\circ$ with curve wings (at the ends)	KP1 and SL
$\sim 60^\circ$ without curve wings	KP 2
$\sim 60^\circ$ with curve wings (from middle to end)	RE
$> 90^\circ$	SK
U - shape upside down ( $\cap$ )	NS

### 4.6.2 Leaf anatomy comparison of vetiver to other grasses

More study, I investigated seven grass species which had leaf characters similar vetiver, by the ratio of vascular bundles and leaf transverse sections were shown in Table 4.2 and Figure 4.43. Comparative arrangement of vascular bundles between vetiver and the selective grasses, it could find that only paragrass and sugarcane which the arrangement

was similar vetiver (the ratio of 1:3:1:3:1 for L:S:M:S:L), but differ in particular. By leaves of sugarcane had more abundant chloroplasts in Kranz structure and lignified cells in bundle caps, and very large bulliform cells; while leaves of paragrass had very large bulliform cells and very less parenchyma cells. Moreover, chloroplast contents, lignified cells and parenchyma cells of vetiver did not prominent, if comparing to selective grasses.

**Table 4.2** Vascular bundle arrangement of some C4 grasses.

Common name	Vascular bundle	
	Arrangement	ratio
Paragrass ( <i>Brachiaria mutica</i> (Forsk.) Stapf)	L:S:M:S:L*	1:3:1:3:1
Lemongrass ( <i>Cymbopogon citratus</i> (DC.) Staph)	L:S:L	1:3:1
Maize ( <i>Zea mays</i> L.)	L:S:L	1:6:1
Cogongrass ( <i>Imperata cylindrical</i> (L.) P. Beauv.)	L:S:M:S:M:S:M:S:M:S:L	1:1:1:1:1:1:1:1:1:1:1
Sugarcane ( <i>Saccharum officinarum</i> L.)	L:S:M:S:L	1:3:1:3:1
Goose grass ( <i>Eleusine indica</i> (L.) Gaertn)	L:S:L	1:4:1
Guinea grass ( <i>Panicum maximum</i> Jacq.)	L:S:L	1:10:1

\*L = large vascular bundle, M = medium vascular bundle, S = small vascular bundle.

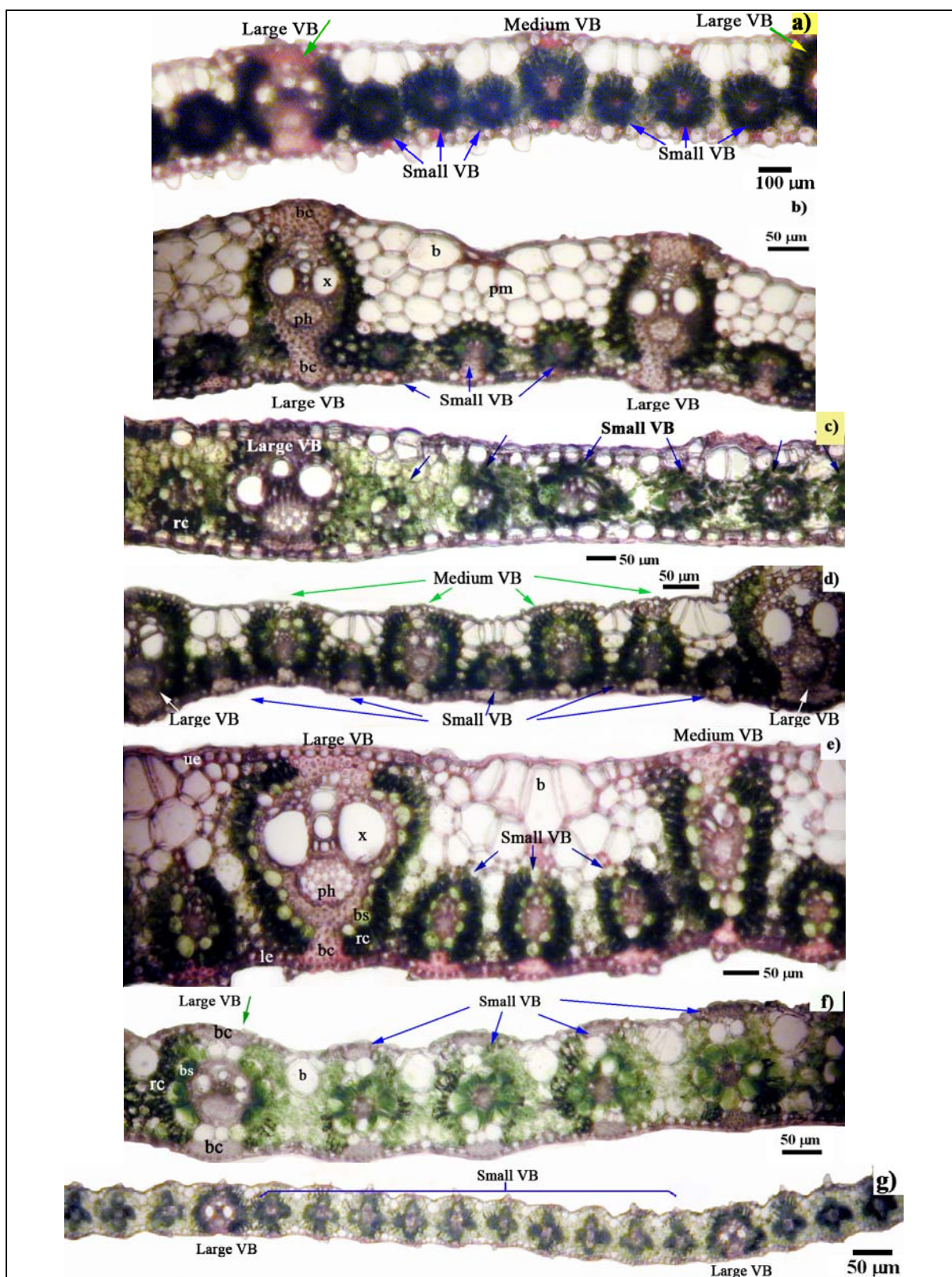


**Figure 4.43** TS of Leaves of (a) paragrass, (b) lemongrass, (c) maize, (d) cogongrass, (e) sugarcane, (f) goose grass and (g) guinea grass.

### 4.6.3 Fibers and hydraulics within leaves

Moreover, I found only LI provenance has bundle caps (sclerenchyma) extend from the large and the medium vascular bundles towards both epidermises. These bundle sheath extensions are termed girders which afford mechanical support to the leaf and are a xeromorphic feature. Moreover, I believe that sclerenchyma acts as a short cut of water pathways resulting sustainable higher photosynthetic rates (Figure 4.44). *Gnetum gnemon*, a forest understory species, also has large lysigenous intercellular spaces and the fibers were proved by fluorescent dyes in an additional function of hydraulics (Tomlinson and Fisher, 2005; Figure 4.45). This apoplastic transport system is responsible for maintaining a high internal humidity and consequently stomata tend to remain open, by promoting more extensive gas exchange. Two species of conifer and cycad, *Podocarpus dispersmis* and *Sciadopitys verticillata* also had sclereids act as a hydraulic short cut through the mesophyll tissues, which exhibited much higher the hydraulic conductance ( $K_{\text{leaf}}$ ) as well as greater net  $\text{CO}_2$  assimilation rate ( $A_{\text{max}}$ ) (Brodribb et al., 2007; Figure 4.46). General plants with no facilitating water-conducting sclereids, the length of hydraulic pathway ( $D_m$ ) (from veins across the mesophyll to where it evaporates from the leaf) exerted a controlling influence over  $K_{\text{leaf}}$  and secondarily  $A_{\text{max}}$ , by the  $D_m$  traversed by the transpiration stream (Brodribb et al., 2007). However, water moves in a continuous path from soil through the roots, stems, and leaves to the atmosphere at rates also determined by gradients in water potential and the resistances to flow. The water potential  $\psi^J$  at any site  $J$  in this pathway is governed by: (1)  $\psi^{\text{soil}}$ ; (2)  $\psi$  of other possible sources of water, such as tissues storage; (3) the resistances to water flow from parts of the plant downstream and to parts upstream; and (4) the rate of water movement (Nobel and Jordan, 1983). Water moves in response not only to evaporation from the leaves but also to the exchange of water between the tissues of a plant and the xylem adjacent to these tissues. The amount and kinetics of this

exchange is determined by the capacitance (water potential to water content) of the storage tissue  $C^J$  and the resistance  $R_s^J$  to flow between such tissues and the xylem (Nobel and Jordan, 1983).

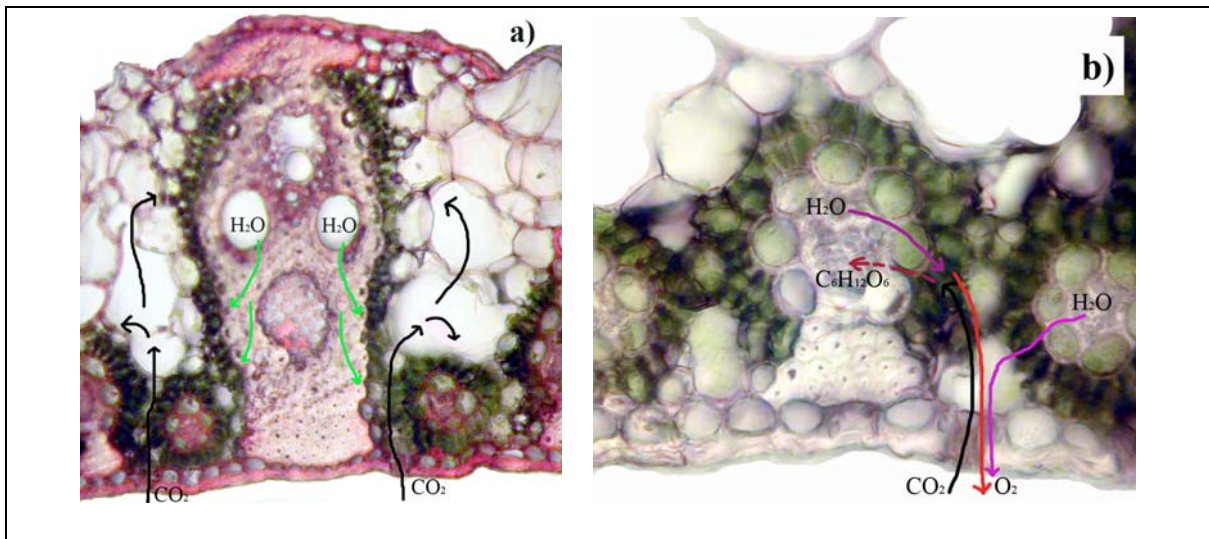


**Figure 4.44** Schemes of  $\text{CO}_2$  and  $\text{H}_2\text{O}$  distribution to photosynthetic sites of LI leaf: (a) at Kranz of the large vascular bundle; and (b) at Kranz of the small vascular bundles.

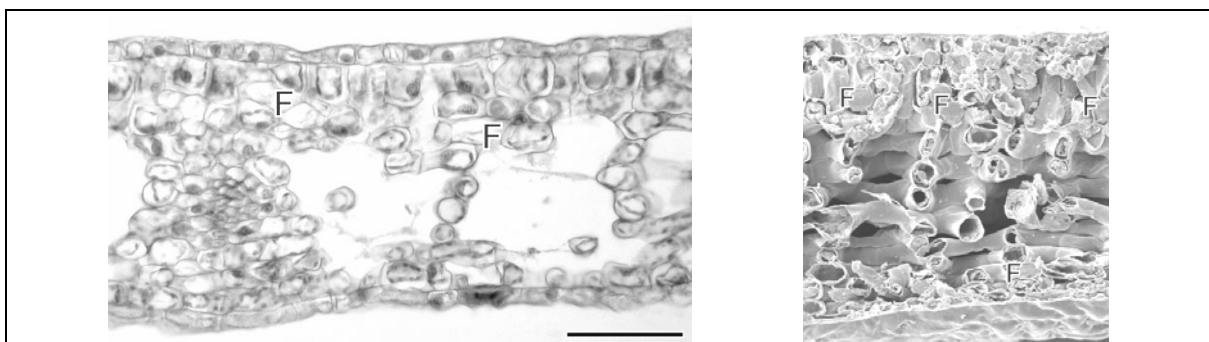


**Figure 4.45** Mature fully expanded lamina of *Gnetum gnemon*. (Left) TS of Lamina immature but intercellular space system of mesophyll fully established, fibers (F) thin-walled and highly vacuolated and therefore obscure. (Right) An SEM transverse view of leaf tissue with mature fibers (F). Scale bar = 100  $\mu\text{m}$ . (Tomlinson and Fisher, 2005).

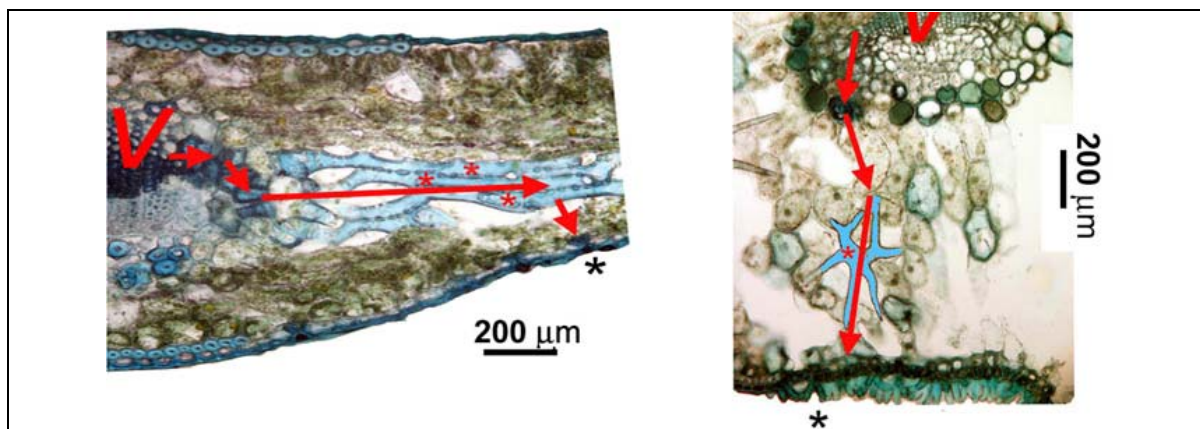


**Figure 4.46** Leaves of two species of conifer and cycad, *Podocarpus dispersmis* and *Sciadopitys verticillata* show hydraulic flow path (from the midrib (V) to the stomata (black asterisks) facilitate by water-conducting sclereids (Brodrribb et al., 2007).

#### 4.6.4 Lysigenous intercellular spaces and aeration system

Leaves of all 11 provenances found large lysigenous intercellular spaces being upper the small vascular bundles, which were similarly water plants, typha, banana or even bamboo leaves (Figure 4.47). The lysigenous intercellular spaces appeared even developing leaves but with a small size and the size developed larger in mature leaves, which was opposite to bulliform cells. I guessed that vetiver used bulliform cells functioning for water and/or gas accumulation before the lysigenous intercellular space development. In principal, large lysigenous intercellular spaces within leaves of water plants provide to eliminate hypoxia/anoxia effects at roots by promoting oxygen from leaves to roots. Aerenchyma at cortex layer of roots is another evidence for sustaining oxygen to roots, which was found in vetiver roots, also. I extended study on vetiver roots and found the parenchyma cells at cortex layer were lysed to aerenchyma and the parenchyma cells at the inner vascular cylinder were lysed to intercellular spaces, as shown an example of LI provenance in Figure 4.48. Large lysigenous intercellular spaces at leaves

and aerenchyma at roots could be evident to confirm a great aeration system of vetiver as well as a potential of deeply root penetration. Similar prolonged flooding, oxygen concentrations at deep soils are very low but vice versa for ethylene concentrations, which does not support for general plant grown, except some plants such as vetiver. Under hypoxia conditions, ethylene formation increases, and it accumulates in and around roots and submerged shoots because of its low solubility in water. Ethylene concentrations of 0.1 - 0.5 ppm are sufficient to induce formation of intercellular space-rich tissues by programmed cell death (PCD) or apoptosis. PCD does not take place in differentiated older cells, rather an aerenchyma is initiated already at the end of the elongation zone of the organ. Formation of aerenchyma is lytic, e.g. in maize, *Luronium*, and *Nymphoides*, but usually schizogenous in petioles, e.g. of *Caltha*, *Rumex*, or *Filipendula*. Formation of aerenchyma is not restricted to helophytes and submerged plants; even terrestrial plants, such as maize and sunflower, may develop aerenchyma in roots and the basal part of the shoot. In many helophytes (such as rice and arrowhead), the formation of aerenchyma is genetically fixed (constitutive), and the induction of PCD is not dependent on oxygen deficiency or ethylene accumulation. Aerenchyma formation caused by hypoxia commonly results in irregular air spaces, whereas those constitutively developed show regular patterns of air channels. Aerenchyma allows air circulation in tissues, additionally supported by pressure ventilation.

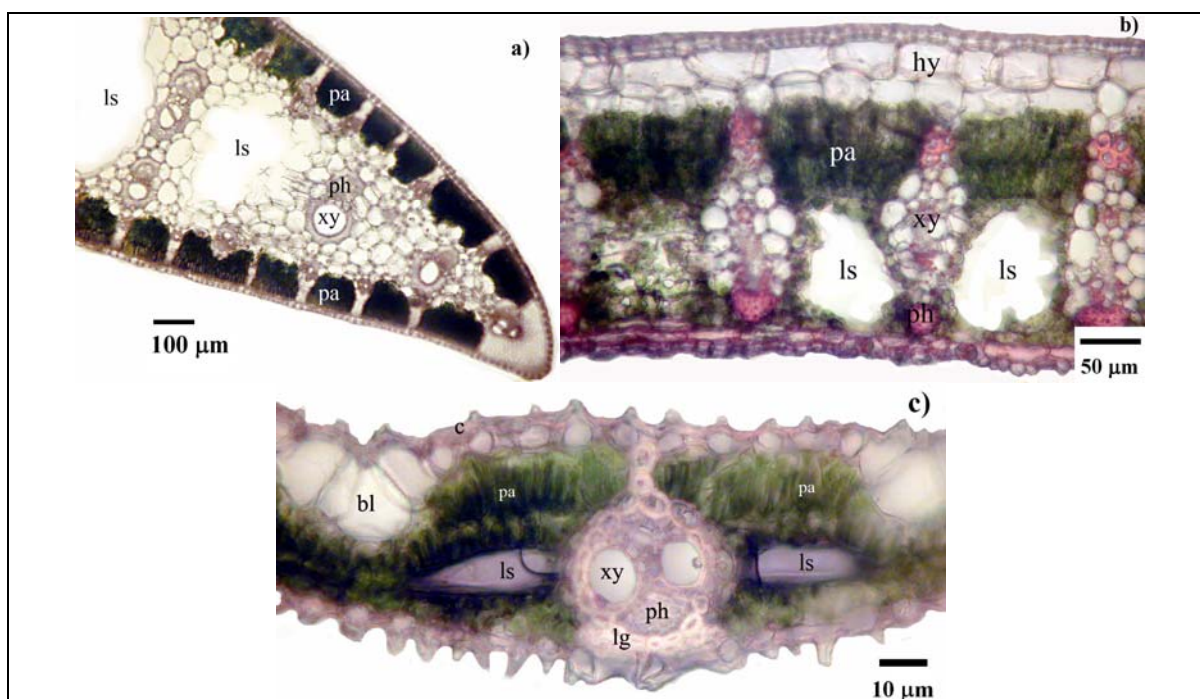


**Figure 4.47** Leaf TS of (a) typha (*Typha angustifolia*), (b) banana (*Musa sapientum* Linn.) and (c) Phai ruak (*Thyrsostachys siamensis* Gamble.).

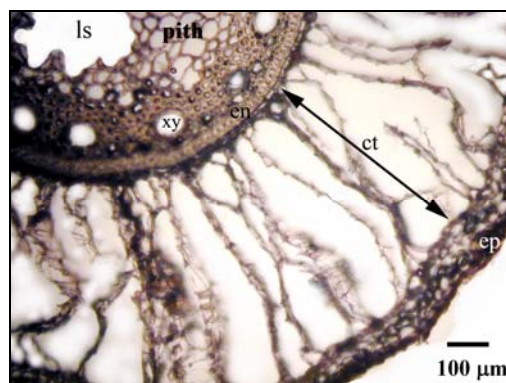


**Figure 4.48** TS of vetiver root from LI provenance.

Primary roots of terrestrial plants usually cannot tolerate hypoxia and die. Hypoxia-resistant plants (e.g. maize, ash, willow, *Forsythia*, *Rumex palustris*) are able within a few days to produce adventitious roots with a well-developed aerenchyma from basal shoot parts or the lower nodes. These roots do not penetrate as deeply into the soil as the primary root system into a well-aerated substrate.

The individual cell layers of young adventitious roots are differently supplied with oxygen. The exodermis is the only cell layer which is usually oxygen-free; cell walls of

this layer are often suberised, thus preventing diffusion of oxygen from the interior of the root to the external medium. Formation of aerenchyma not only guarantees the aerenchyma of tissues, but also reduces the number of oxygen-consuming cells in that tissue.

Lytic aerenchyma formation (i.e. from disintegration of cells; Drew et al., 2000) occurs selectively in the cortex of adventitious roots, starting in those parts of the tissues that are least supplied with oxygen. Lysis of cells often requires not more than 24 h. Ethylene induces this process more or less independently of normoxia or hypoxia, but hypoxia stimulates ethylene synthesis. Inhibition of ethylene synthesis, on the other hand, suppresses formation of aerenchyma. The genus *Rumex* comprised hypoxia-sensitive (*R. acetosa*, *acetosella*) as well as hypoxia-tolerant species (*R. palustris*). In the flooding-tolerant *R. palustris* ethylene production is relatively low and almost the same under aerobic and anaerobic conditions. The internal ethylene concentration slightly decreases even long-term submergence. In flooding-intolerant sorrel, however, internal ethylene concentration increases with the duration of submergence. Low concentration of ethylene increases elongation growth, while a long-term increasing ethylene concentration, as in *R. acetosella*, causes premature senescence of the whole organ.

It has been shown that ethylene as a signal induces the protein kinase signal transduction pathway via a G-protein,  $\text{Ca}^{2+}$  and inositol-P, which leads to synthesis of lytic enzymes, e.g. cellulase and hemicellulase (Saab and Sachs, 1996). Calcium activates endonucleases, so that the cell death is caused by a controlled breakdown of nucleic acid (by an endonuclease, activated by caspases) and not through breakdown of cell membranes, as after cell damage. Formation of aerenchyma is promoted by further effectors. For example, mechanical resistance of a heavy soil stimulates ethylene synthesis by the growing root and scarcity of minerals increases the sensitivity of the plant tissue to ethylene. Figure 4.49 shows a model of the biochemical processes that take place in the formation of aerenchyma.

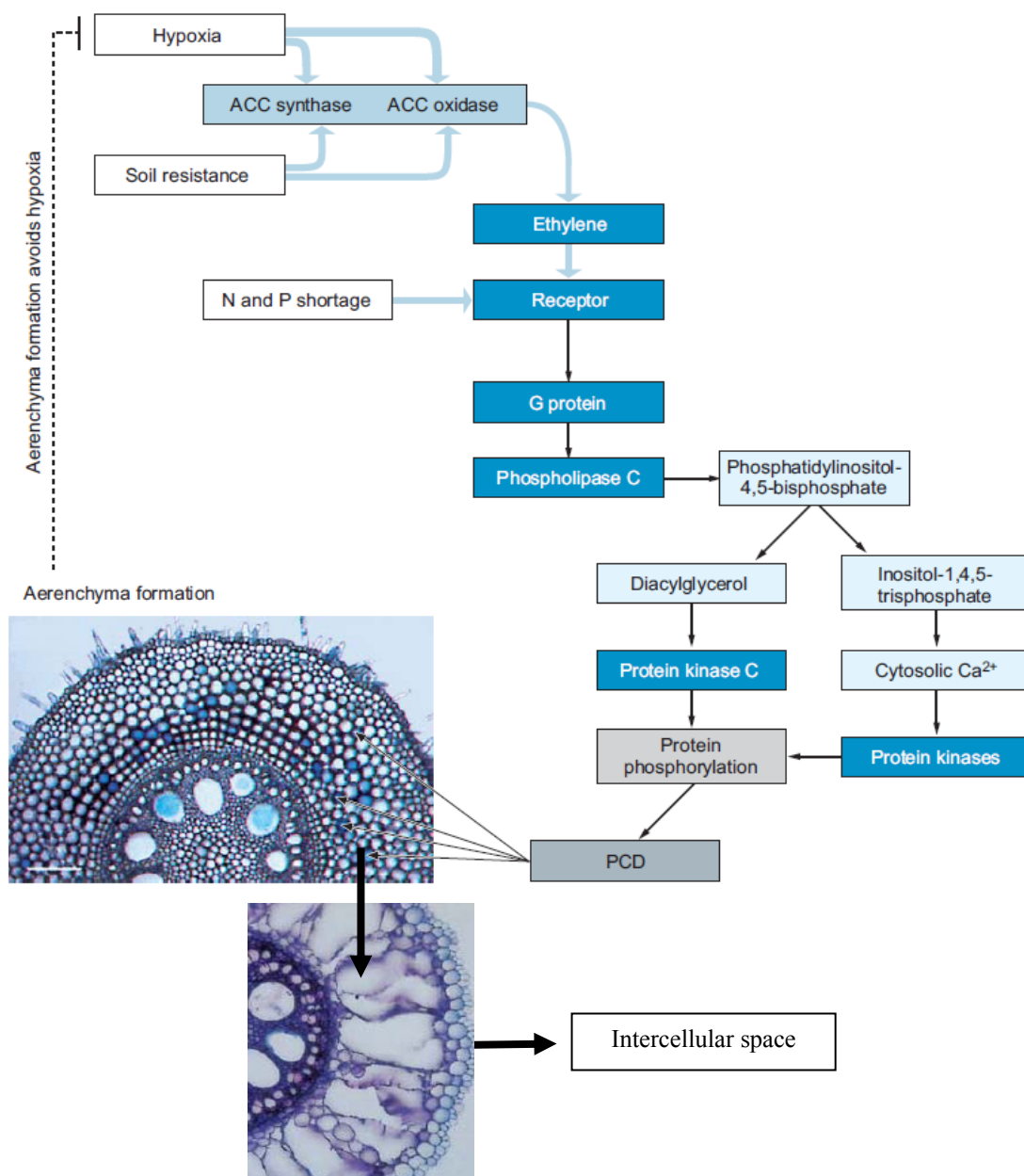


**Figure 4.49** Signal chain that leads to programmed cell death (PCD) upon aerenchyma formation, including environmental factors that control it (Drew et al., 2000).

To promote gas circulation, vetiver was suggested maintaining oxygen to roots via aeration systems called “Humidity-induced convection (HIC)” and “Venturi-induced convection (VIC)”, by the evidence was a pith cavity at culms. Such *Phragmites australis*, an aquatic macrophyte, can maintain aeration system through both HIC and VIC mechanism (Amstrong et al., 1996; Figure 4.50 and Figure 4.51). According to different

humidity, for HIC, gas can ventilate from atmosphere into plant parts via stomata of living culms and exit the plant via broken/die culms, so the gas volumes depend on drier air and more light. VIC implicates wind speeds and different pressures between inside and outside the plant, by both influx and efflux of gas stream are via broken/die culms. Aeration system of vetiver was assumed to strongly influencing with HIC and VIC mechanism because of anatomy supporting. Even large intercellular spaces can encourage aeration system within vetiver and rhizosphere, however, it must trade-off with parenchyma loss.

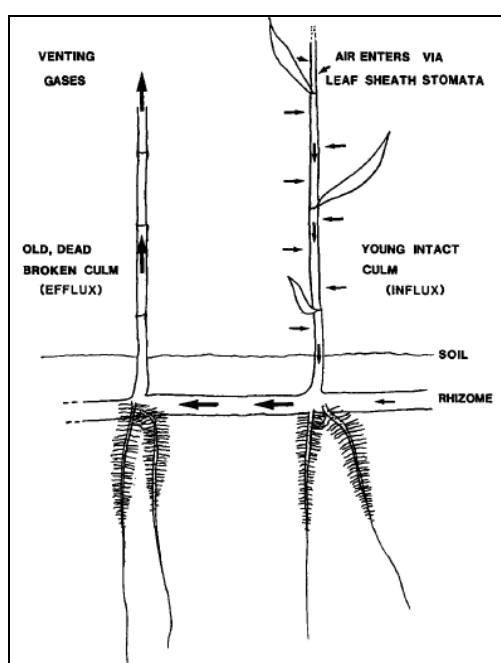


**Figure 4.50** *Phragmites*: humidity-induced convection. The difference in humidity between the sub-stomatal gas-space of the plant and the drier atmosphere favours the inward diffusion of  $O_2$  and  $N_2$  through leaf sheath and nodal stomata. A pressurised flow of gases is induced through the rhizome because of stomatal resistance to backflow. The throughflow results in increased diffusion of  $O_2$  into root and rhizosphere (Armstrong et al., 1996).

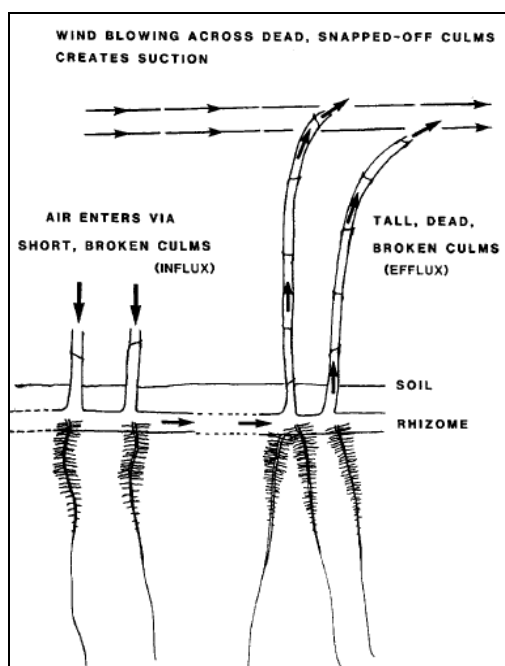


**Figure 4.51** *Phragmites*: Venturi-induced convection. A suction pressure,  $\Delta P$  (Pa) is

created by the wind such that  $\Delta P = \left(\frac{1}{2}\right)\rho V^2$ , where  $\rho$  is the density of air (approx. 1.2- 1.25 kg m<sup>-3</sup>) and V, the wind velocity (ms<sup>-1</sup>). The convective flow through the rhizome results in an increased diffusion of oxygen to root and rhizosphere (Armstrong et al., 1996).

## 4.7 Conclusions

4.7.1 Internal leaf structures of 11 vetiver provenances were different in particularly such as angles of leaf wings, bundle cap present/thickness, and vessel numbers, which could be benefit in provenance classification.

4.7.2 This study found all 11 provenances had uniformly and regularly vascular bundle arrangement with the ratio of 1:3:1:3:1 for Large:Small:Medium:Small:Large.

4.7.3 Like C4 plants, all 11 provenances had Kranz structure surrounding vascular bundles which confirmed high efficient photosynthetic rates.

4.7.4 LI provenance has great bundle caps extend to abaxial and adaxial surfaces, which believed that sclerenchyma acts as a short cut of water pathways and strength.

4.7.5 Large lysigenous intercellular spaces were found in mature leaves, but very small sizes in developing leaves, which suggested relative gas circulation in roots and encouraged deeply root penetration. Consistently, I found that aerenchyma at root cortex and air cavity at pith were strong evidences of aeration system from leaves to roots. To avoid hypoxia/anoxia, large lysigenous intercellular spaces at laminas were a character of aquatic plants or long term flooding-tolerant plants by transporting O<sub>2</sub> from leaves to roots. Moreover, I guessed atmospheric O<sub>2</sub> could pass into vetiver via a pith cavity at culms by the theories calling “Humidity-induced convection” and “Venturi-induced convection”.

## 4.8 References

- Armstrong, J., Armstrong, W., Beckett, P.M., Halder, J.E., Lythe, S., Holt, R. and Sinclair, A. (1996). Pathways of aeration and the mechanisms and beneficial effects of humidity- and Venturi-induced convections in *Phragmites australis* (Cav.)Trin. ex Steud. **Aquatic Botany** 54: 177-197.
- Brodribb, T.J., Field, T.S. and Jordan, G.J. (2007). Leaf maximum photosynthetic rate and venation are linked by hydraulics. **Plant Physiology** 144: 1890-1898.
- Drew, M.C., He, Ch.-J. and Morgan, P.W. (2000). Programmed cell death and aerenchyma formation in roots. **Trends in Plant Science** 5: 123-127.
- Gunning, B.E.S. and Steer, M.W. (1996). **Plant Cell Biology: Structure and Function**. Boston: Jones and Bartlett Publishers.
- Larcher, W. (2001). **Physiological plant ecology** (4th ed.). Berlin: Springer.
- Lu, H. and Liu, K.-B. (2003). Morphological variations of lobate phytoliths from grasses in China and the south-eastern United States. **Diversity and Distributions** 9: 73-87.

- Nobel, P.S. and Jordan, P.W. (1983). Transpiration stream of desert species: Resistances and capacitance for a C<sub>3</sub>, a C<sub>4</sub>, and a CAM plant. **Journal of Experimental Botany** 34(147): 1379-1391.
- Rand, P.J. (2001). **Plant Biology**. CA: IDG Books Worldwide, Inc.
- Saab, I.N. and Sachs, M.M. (1996). A flooding-induced xyloglucan-endo-transglycosylase homolog in maize is responsive to ethylene and associated with aerenchyma. **Plant Physiology** 112: 385-391.
- Schulze, E.-D., Beck, E. and Müller-Hohenstein, K. (2002). **Plant Ecology**. Berlin: Springer.
- Tomlinson, P.B. and Fisher, J.B. (2005). Development of nonlignified fibers in leaves of *Gnetum gnemon* (Gnetales). **American Journal of Botany** 92(3): 383-389.
- Twiss, P.C., Suess, E. and Smith, R.M. (1969). Division S-5 - soil genesis, morphology, and classification (morphological classification of grass phytoliths). **Soil Science Society of America Proceedings** 33: 109-115.

## CHAPTER V

# VETIVER PHYTOLITHS: SUSTAINABLE VETIVER CLASSIFICATION AND LEAF THERMAL EMISSION

### 5.1 Abstract

Phytoliths, biogenic silica bodies, expected to classify 11 vetiver provenances from two common species (*Chrysopogon nemoralis* and *C. zizanioides*) and clarify relative the potentially water absorption and leaf thermal protection. As a result, I found 21 distinct shapes and only 8 of all could be identified to 5 provenances; however, it could not be fully said genetic controls for those shapes. There were 7 provenances which I suggested to exchange the groups. Three provenances, Ratchaburi, Songkla 3 and Surat Thani, showed more phytolithic frequency, saying that they are the great potentially water absorption. Like photonic crystal, vetiver phytoliths suggested capable thermal emission in the mid-infrared which thermal increases slowly for this band. Dihedron structure of Kamphaeng Phet 2 provenance gave multiple reflections enhanced thermal emissivity, but the incident angle should not exceed  $60^\circ$ . Strong birefringence of silica supported more emissivity but an incident angle should not be over a critical angle, approximately  $81.9^\circ$ .

In conclusion, vetiver phytoliths could reveal provenance classification and had qualitative functioning in leaf thermal protection.

**Keywords:** phytolith. vetiver. water absorption. emissivity. birefringence

## 5.2 Introduction

Phytolith is a biogenic silica body deposits in stems, leaves, and inflorescences. Phytoliths are often in monocotyledons such as grasses, banana, palms, etc, also in dicotyledons such as Compositae, Cucurbitaceae, Rosaceae, etc., and gymnosperms (Pinaceae); but less in woods (Epstein, 1999; Tsartsidou et al., 2007.). According to Twiss et al. (1969), grass phytoliths classified into four classes, festucoid, chloridoid, panicoid and elongate, but this is wide range for general grasses. High silica contents benefit phytolithic structures preserving pass through thousand years and useful for researches of palaeoecological reconstruction or paleoclimate information. As for now, well-preserved structures of phytoliths played a new role in carbon sequestration and extended to carbon credit calculation (Sullivan and Parr, 2008). Some grasses with more abundance of phytoliths are under considered such as *Bambusa forbesii* (Ridl) Holttum, *Brachiaria brizantha* (Hoscht. ExA.Rich) Stap f., *Imperata cylindrical* P. Beauv., *I. exaltata* (Roxb.) Brogn., and *Saccharum officinarum* (L.).

In Thailand, we know ‘vetiver’ as a miracle grass for soil erosion alleviation. More thickness, directly deep roots and especially fast growing, vetiver roots is termed as a living dam below ground. Vetiver roots could reach 3 cm per day and over 2 m within 6 months and 6 m within 3 years; as a result, it yielded to 100 - 200 t ha<sup>-1</sup> (Lavania and Lavania, 2009). Vetiver improved soil properties maintained more moisture, organic matter, phosphorous, and potassium, and soil pH balance (Pongkarnjhana and Watthanapapat, 2009). Vetiver is more tolerant to extreme climate variation such as prolonged drought, flood, submergence, extreme temperatures, high acidity to high alkalinity (pH between 3 and 11), high salinity, or more heavy metal contaminants (Islam et al., 2008.).

There are two common vetiver species in Thailand, *Chrysopogon nemoralis* and *C. zizanioides*, calling “Faek Don” and “Faek Lum” believed relative low and high humid

habitats, respectively. But, as I have known, it has no strong scientific affirmation for the group classification and no more confirmation on the potentially water absorption of vetiver provenances. Phytoliths of creeping bentgrass (*Agrostis palustis*) was reviewed in leaf cooling by thermal emission in the mid-infrared (Neethirajan et al., 2009), which challenges to vetiver phytoliths also.

Therefore, this study aimed (i) to set a criterion for vetiver provenance classification, (ii) to clarify the provenance arrangement of “Faek Don” and “Faek Lum” group, (iii) to determine the potentially water absorption for vetiver provenances, and (iv) to observe vetiver phytoliths relative leaf thermal emission.

### **5.3 Objectives of this chapter**

5.3.1 To extract phytoliths from laminas of 11 vetiver provenances

5.3.2 To classify phytolithic structures

5.3.3 To observe phytolithic abundance for each provenance

5.3.4 To identify vetiver provenances through phytolithic study

5.3.5 To determine the potentially water absorption of vetiver provenances through phytolithic study

5.3.6 To classify “Faek Don” and “Faek Lum” group through phytolithic study

5.3.7 To observe vetiver phytoliths relative leaf thermal emission

### **5.4 Materials and methods**

#### **5.4.1 Plant description**

This study conducted on eleven provenances of two vetiver species, *Chrysopogon nemoralis* and *C. zizanioides*. *C. nemoralis* consists of 6 provenances: Kamphaeng Phet 1 (KP1), Loei (LI), Nakhon Sawan (NS), Prachuabkhirikhan (PK), Ratchaburi (RB) and Roi

Et (RE); whereas *C. zizanioides* has 5 provenances: Kamphaeng Phet 2 (KP2), Phraratchathan (PT), Songkhla 3 (SK), Sri Lanka (SL) and Surat Thani (ST). All plants were grown on loamy sand on November 2004 at the experimental plots of the Regional Office 3, Land Development Department, Muang District, Nakhon Ratchasima, Thailand (15°05'N, 102°13'E, 167 m.s.l.) Each plot was of 2 x 10 m. Plants were given manures in an early stage and allowed naturally grown continually for 3 years. During November 2004 to 2007, the mean annual temperature ranged between 23.1 and 33.3°C with the average annual precipitation about 94.38 mm per month and the average annual evaporation about 4.84 mm per day (Nakhon Ratchasima Meteorology Station; Appendix A).

#### **5.4.2 Phytolithic preparation**

Mature leaves were individually hand-washed several times in distilled water and soaked in sodium hypochlorite for 24 hrs and after that placed on a warming tray to accelerate the process. Phytoliths were washed by distilled water 2 - 3 times, and after that decanted to a shell vial and placed in a drying oven to remove excess liquid. Phytolithic samples were observed structures via Scanning Electron Microscope.

### **5.5 Results**

#### **5.5.1 Morphological classification of vetiver phytoliths**

In this study, I had set a criterion to classify vetiver phytoliths. The criterion based on phytolithic outline which detailed on lobe present, lobe connection, length of shank, concave/straight edge could be divided into 6 types from type A to F (Figure 5.1). Each type subsequently divided into levels (1 to 5) according to the body thick.

### **Classification of vetiver phytoliths**

#### **Type A: No lobes**

- A1. Rectangular, slightly concave edge
- A2. Rectangular, sinuous edge
- A3. Oblong, sinuous edge
- A4. Circular, thick, smooth edge

#### **Type B: Cross, narrow shank, deep indented or distinct branches**

- B1. Irregular cross (imbalance between upper and lower), folding branches, smooth edges, thin body (~1.5  $\mu\text{m}$ )
- B2. Regular cross, sharply distal end lobes, smooth edges
- B3. Irregular cross (imbalance between left and right), convex branches
- B4. Irregular cross (imbalance between left and right), slightly bending branches
- B5. Regular cross, convex branches

#### **Type C: Cross, wide shank, convex lobes**

- C1. Square cross, wide and short shank, concave ends
- C2. Rectangular cross, wide and long shank
- C3. Rectangular cross, wide and short shank, concave ends

#### **Type D: Elliptical, lobe connection at the top and at the below**

- D1. Elliptical, wide and short shank, straight or concave ends
- D2. Elliptical, short shank or none, straight ends

#### **Type E: Dumbbell, lobe connection at the sides, wide shank**

- E1. Irregular dumbbell, concave ends, wide and short shank,
- E2. Regular dumbbell, straight ends, wide and long shank
- E3. Irregular dumbbell, straight ends, wide and long shank

#### **Type F: Dumbbell, lobe connection at the sides, homogenous lobes and shank**

- F1. Irregular dumbbell (one side hanging), narrow shank

F2. Regular dumbbell, wide and long shank, straight or concave ends

F3. Irregular dumbbell, wide and long shank, straight ends

F4. Irregular dumbbell, wide and short shank, thick body (~10  $\mu\text{m}$ )

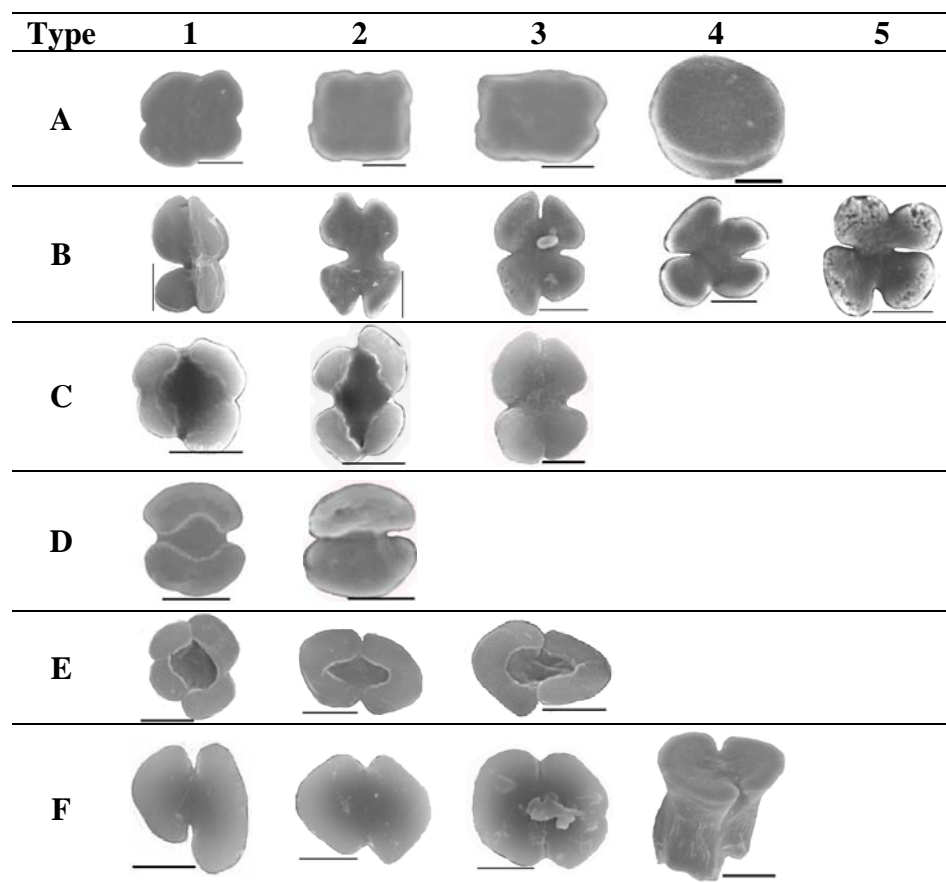


**Figure 5.1** Classification of vetiver phytoliths. All phytoliths were oriented as they occur in the epidermal cells with the long axis of the leaf horizontal. Bar = 5  $\mu\text{m}$ .

### 5.5.2 Phytoliths and vetiver identification

Based on phytolithic frequency, 8 of 21 shapes could be used to identify 5 vetiver provenances (Table 5.1), by type A4 for LI provenance, type B1 for KP2 provenance, type E1 - 3 for RB provenance, type F2 - 3 for SK provenance and type F4 for ST provenance. However, the remains, 13 of 21 shapes, could not be fully said by genetic control, especially type C1 founding in several provenances.

**Table 5.1** Distribution of types of phytoliths.

Provenance	Phytolithic type																Total					
	A				B					C			D		E			F				
	1	2	3	4	1	2	3	4	5	1	2	3	1	2	1	2		3	1	2	3	4
KP1										a	r											2
LI	r			a																r		3
NK													r	r								2
PK										a	c											2
RB										r					c	c	a					4
RE		r	r					c		c												4
KP2					c					a												2
PT						r	r	c	r	r												5
SK																		r	c	a		3
SL											r											1
ST																					a	1
Total	1	1	1	1	1	1	1	2	1	6	2	1	1	1	1	1	1	2	1	1	1	

\*a = abundant, c = common, r = rare, and no designation = none observed (adapted from Twiss, Suess and Smith, 1969). Replication, n = 10.

## 5.6 Discussion

### 5.6.1 Variation of phytolithic shapes

Even phytoliths could be classified distinct shapes; however, variation should be reminded. Some importance such as climate, plant age and physical and chemical attributing soils could distort phytolithic outlines. Metcalfe (1960 quoted in Twiss et al., 1969) mentioned three levels of phytolithic variation: (i) minor anatomical variations occur within a single leaf blade; (ii) structural variations occur among leaves from different layers in an individual plant; and (iii) leaves from plants of a single species can also vary among habitats. However, Wang and Lu (1993 quoted in Lu and Liu, 2003) found the

phytolithic shape of the same species was stable but sizes changed slightly when cultivated grasses in different environmental conditions in China. They guessed that the active control in the short cells was mainly by genetic over than environment. Chaudhary et al. (2001) gave few details in cross-shaped of *C. zizanioides*, while my study found both cross- and dumbbell-shape in both *C. zizanioides* and *C. nemoralis*. Cross- and dumbbell-shape in Panicoid class almost found in ‘tall grasses of true prairie venation’ such as *Panicum virgatum* L., *Andropogon gerardi* Vitman, *A. scoparius* Michx and *Sorghastrum nutans* (L.) Nash (Twiss et al., 1969). Moreover, Twiss (1992) indicated that cross- and dumbbell-shape could refer to “C4 tall grass prairies”, but Lu and Liu (2003) noted that both shapes could be found in several C3 grasses also such as *Zizania caduciflora*, *Oryza sativa*, *Leersia hexandra*, *L. oryzoides* and *Zizaniopsis miliacea*. Lu and Liu (2003) recommended that these shapes relative to moist soils or marshy environment by referring to the distributions of C3 grasses of Oryzoideae and Panicoideae subfamilies. Honaine et al., (2006) suggested that dumbbell-shape did not character to only C4 species but C3 species also. By dumbbell-shapes with short shank and concave/straight-ended found in C3 species such as *Melica brasiliensis* (Pooideae), *Danthonia montevidensis* (Arundinoideae), *Stipa* spp. and *Piptochaetium* spp. (Stipoideae).

### 5.6.2 Phytoliths in water absorption and classification of vetiver group

Phytolithic frequency could be remarkable the potentially water absorption under arid conditions. As silica quantity influenced directly with water volumes passive plants (Kolek and Kozinka, 1991; Sangster and Parry, 1970). Shahack-Gross et al., (1996) mentioned the quantity of silica precipitation was closely to the transpiration stream. Webb and Longstaffe (2006) found that *Calamovilfa longifolia*, a C4 grass, grown in arid sites had the  $\delta^{18}\text{O}_{\text{leaf phytoliths}}$  values over than that of in humid sites, and concluded that phytolithic formation signified by the leaf and stem water, relative humidity and

temperature. They suggested that phytolith formation could be used to determine relative humidity and temperature during the time period of the plant growth. Consistently, a greater rate of silicon entry into plants was found under very low humidity rather than water transpiration (Barber and Shone, 1966).

As above discussion, my hypothesis was phytolith frequency of “Faek Don” (relative low humid habitats) should be prominently over than that of “Faek Lum” (relative high humid habitats). A criterion for “Faek Don” and “Faek Lum” classification and suggestion for provenance rearrangement were set in Table 5.2 and 5.3, respectively. ST provenance, the example of the high potentially water absorption was illustrated in Figure 5.2. As a result, there were 7 provenances recommended to exchange the group: KP1, NK and RE remove from “Faek Don” to “Faek Lum”; while KP2, SK, SL and ST remove from “Faek Lum” to “Faek Don” (Table 5.3). However, this recommendation should be confirmed by more valid experiments.

**Table 5.2** Classification for “Faek Don” and “Faek Lum” group.

Criterion	Potential of water absorption	Provenance group
High phytolith frequency*	High water absorption	Faek Don
Medium phytolith frequency	Medium water absorption	
Low phytolith frequency	Low water absorption	Faek Lum

\*High = >60% cover, Medium = >30% but <60% cover, Low = <30% cover (adapted from Sullivan and Parr, 2008).

**Table 5.3** Suggestion for provenance rearrangement in “Faek Don” and “Faek Lum”.

Provenance	Phytolithic frequency	Potential of water absorption	Original common name	Suggestion
KP1	Low	Low	Faek Don	Faek Lum*
LI	Medium	Medium	Faek Don	Faek Don
NK	Low	Low	Faek Don	Faek Lum*
PK	Medium	Medium	Faek Don	Faek Don
RB	High	High	Faek Don	Faek Don
RE	Low	Low	Faek Don	Faek Lum*
KP2	Medium	Medium	Faek Lum	Faek Don*
PT	Low	Low	Faek Lum	Faek Lum
SK	High	High	Faek Lum	Faek Don*
SL	Medium	Medium	Faek Lum	Faek Don*
ST	High	High	Faek Lum	Faek Don*

\*the provenance recommended to exchange the group. Replication, n = 10.

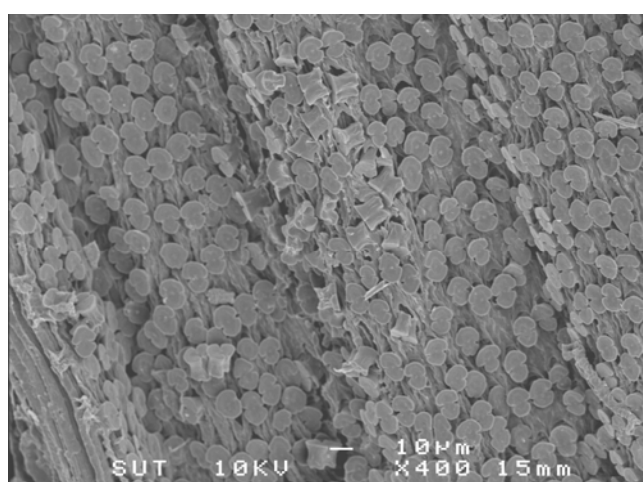


**Figure 5.2** Phytolithic distribution of ST provenance, the example of high potentially water absorption.

However, variation by plant demands and leaf ages on phytolithic frequency should be awarded. Because of the active transport of silica, phytoliths were need for some objectives such as grazing or infecting defensive mechanisms or eliminating metal toxicity (Ma and Yamaji, 2006). In addition, phytoliths could preserve moisture during drought, which related stomata movement and reduce transpiration rate. High phytoliths could promote more light capture and maybe manner like a light piping, and resulted higher photosynthesis (Neethirajan et al., 2009). In addition, for long-lived leaves such as bamboo (*Sasa veitchii*), leaf age could promote phytolithic frequency, which subsequently reduced photosynthetic nitrogen use efficiency (PNUE) and photosynthetic capacity per unit leaf area ( $P_{max}$ ). In the third year, large silica precipitated in chlorenchyma cells and decreased PNUE and  $P_{max}$ , suggesting obstruct  $CO_2$  diffusion from the intercellular spaces to chloroplasts (Motomura et al., 2008).

### 5.6.3 Phytoliths functioning in thermal protective mechanism

As previous mention, phytoliths of creeping bentgrass could mitigate high leaf temperatures by thermal emission in the mid-infrared (Neethirajan et al., 2009), which I hopefully present in vetiver phytoliths. Phytoliths are capable synthesizing biogenic photonic crystals (Wegmuller et al., 2004), which photonic crystals were attractively considered of enhanced thermal emissivity, as compared to black body emission in free spaces (Homeyer et al., 2008). The spectral exitance of a black body, according to Planck's law, is a function of temperature as shown in Eq. (5.1) (Gaussorgues, 1994):

$$\frac{dR(\lambda, T)}{d\lambda} = \frac{2\pi hc^2 \lambda^{-5}}{\exp(hc / \lambda kT) - 1} \quad (5.1)$$

where  $dR(\lambda, T)$  is the spectral exitance, i.e., the power emitted per unit area per unit wavelength,  $h = 6.6256 \times 10^{-34}$  J s (or W s<sup>2</sup>) is Planck's constant,  $k = 1.38054 \times 10^{-23}$  J K<sup>-1</sup>

is Boltzmann's constant,  $c = 2.998 \times 10^8 \text{ ms}^{-1}$  is the speed of light and  $T$  is the absolute temperature of the black body in degree Kelvin (K).

The thermal derivative of the exitance in a spectral band  $\Delta\lambda = \lambda_a - \lambda_b$  especially for  $\Delta\lambda = 8 - 12 \text{ }\mu\text{m}$  (the mid-infrared) increases very slowly when comparing to other bands, by slightly changing from  $1.58 \times 10^{-4} \text{ Wcm}^{-1}\text{K}^{-1}$  at  $T280^\circ\text{K}$  and  $2.17 \times 10^{-4} \text{ Wcm}^{-1}\text{K}^{-1}$  at  $T310^\circ\text{K}$  (Gaussorgues, 1994). Others such as  $\Delta\lambda = 3.5 - 5 \text{ }\mu\text{m}$ , thermal contrast between  $T280^\circ\text{K}$  and  $T310^\circ\text{K}$  is greater,  $1.06 \times 10^{-5}$  and  $2.65 \times 10^{-5} \text{ Wcm}^{-1}\text{K}^{-1}$ , respectively. So, the virtue of thermal emission in the mid-infrared can retard leaf thermal elevation.

Moreover, I found dihedron structure (type B1) of KP2 provenance (Figure 5.3a) which, in theory, dihedron gives multiple reflections (Figure 5.3b) and re-emit to the mid-infrared. In principal, if the angle of energy incident ( $\theta_i$ ) did not exceed  $60^\circ$ , the emissivity is greater, approach to 1.0 (Gaussorgues, 1994). The emissivity of a material depends, on the one hand, on the angle of observation and, on the other, on the polarization of the radiation. As for other phytolith structures, even one plane, but the thermal emissivity of opaque bodies about a few of ten micron were greater than black bodies (Jones et al., 2002), by energy balance explained under "Reflectance  $R(\lambda) +$  Emissivity  $\epsilon(\lambda) = 1$ , Transmittance  $\Gamma(\lambda) = 0$ ".

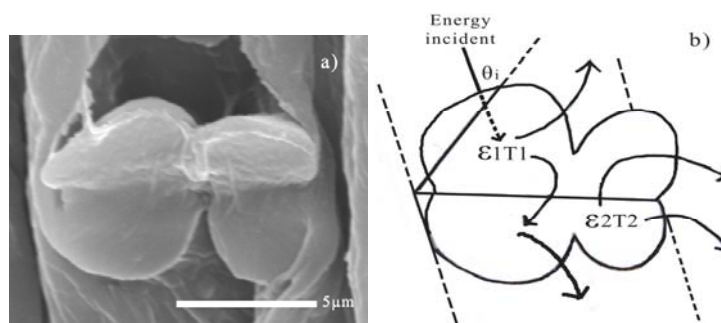


**Figure 5.3** (a) Type B1 phytolith *in situ* in epidermal leaves of KP2 provenance and (b) the scheme of emissivity of dihedron structure. " $\epsilon_i$ " is the spectral emissivity and " $T_i$ " is temperature of the material.

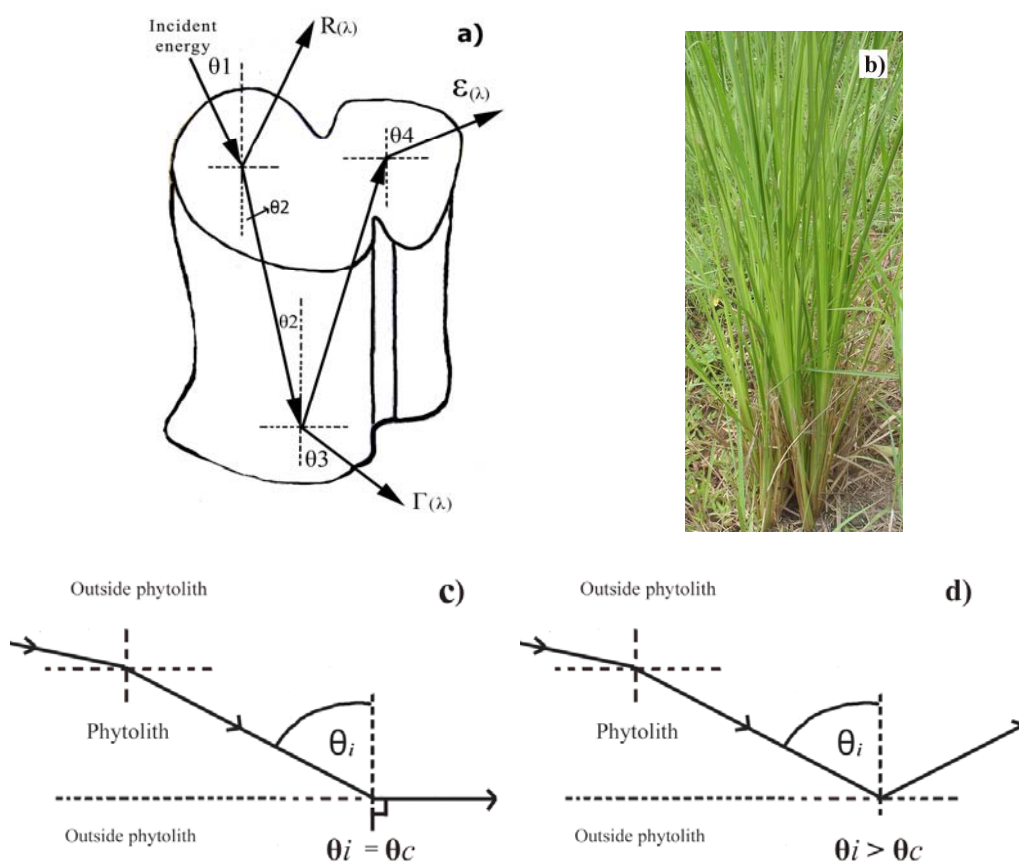


**Figure 5.4** (a) The scheme of birefringence represents by Type F4 phytolith:  $R(\lambda)$ , Reflectance;  $\varepsilon(\lambda)$ , emissivity;  $\Gamma(\lambda)$ , Transmittance. (b) Vetiver leaves positioning a steep angle. (c) No transit radiant when an incident angle equals a critical angle ( $\theta_i = \theta_c$ ). (d) Total internal reflection when an incident angle is over than a critical angle ( $\theta_i > \theta_c$ ).

Because of high refractive index of silica ( $n = 1.41 - 1.47$ ) (Carter, 2007), vetiver phytoliths suggested as great birefringence (Figure 5.4a), depending on the polarization of the light. However, the reflectance depends on a critical angle also. According to Snell's law (Eq. (5.2) and (5.3)), if an incident angle equals a critical angle ( $\theta_i = \theta_c$ ), resulting there is no radiant exitance from a material (Figure 5.4c). And, if an incident angle is over than a critical angle ( $\theta_i > \theta_c$ ), the radiant will be total internal reflection (Figure 5.4d).

$$n_1 \sin \theta_c = n_2 \sin 90^\circ \quad (5.2)$$

$$\theta_c = \sin^{-1}\left(\frac{n_2}{n_1}\right) \quad (5.3)$$

where  $n$  is a refractive index and  $\theta_c$  is a critical angle.

For vetiver, if the refractive index of phytoliths approached the average of silica ( $n_1 = 1.44$ ) and the refractive index of leaf cell walls was approximately the average of cucumber, blackeye pea, tomato, and string bean ( $n_2 = 1.425$ ) (Gausman et al., 1974); therefore, the critical angle was  $81.9^\circ$ . For high efficiency of thermal emissivity of vetiver leaves, the incident angle of the phytoliths should not exceed  $81.9^\circ$ .

Furthermore, to protect leaves, some plants such as soybean (*Glycine max* (L.) Merr.) had the refractive index of the external surface of living leaf hair about 1.48 (Woolley, 1975). And for vetiver, leaves position at a very steep angle to the incoming light for less radiation coming (Figure 5.4b). Dumbbell-shape phytoliths of rice and maize had strong birefringence along with strong polarization-dependent second harmonic generation optical properties (Cheng et al., 2003; Chu et al., 2002). However, silica quenching also depended on dopant ions such as aluminum forming insoluble aluminosilicate which was higher refractive index ( $n = 1.76 - 1.77$ ) than pure silica. But, for monocot leaves there were low aluminosilicate contents because almost were blocked at endodermis (Carnelli et al., 2002).

## 5.7 Conclusions

Phytoliths had efficiency in vetiver provenance identification, the group classification, and provenance determination of the potentially water absorption. Characters similar photonic crystals, dihedron or one plane with a few of ten microns

structures, and birefringence suggested enhanced vetiver phytoliths usefulness for leaf thermal emission.

## 5.8 References

- Barber, D.A. and Shone, M.G.T. (1966). The absorption of silica from aqueous solutions by plants. **Journal of Experimental Botany** 17(3): 569-578.
- Carnelli, A.L., Adella, M.M., Theurillat, J.P. and Ammann, B. (2002). Aluminum in the opal silica reticule of phytoliths: A new tool in palaeoecological studies. **American Journal of Botany** 89(2): 346-351.
- Carter, J.A. (2007). **Ancient climate and environmental history from phytolith-occluded carbon**. Ph.D. Dissertation, Victoria University of Wellington, New Zealand.
- Chaudhary, M.I., Mumtaz, A.S. and Khan, M.A. (2001). Leaf epidermal anatomy of medicinal grasses of Islamabad, Attock and Mirpur (Azad Kashmir). **Pakistan Journal of Biological Science** 4(12): 1466-1469.
- Cheng, P.-c., Sun, C.-K., Cheng, W.Y. and Walden, D.B. (2003). Nonlinear bio-photonic crystal effect of silica deposition in plants. **Microscopy and Microanalysis** 9: 1354-1355.
- Chu, S.-W., Chen, I.-H., Liu, T.-M., Sun, C.-K., Lee, S.-P., Lin, B.-L., Cheng, P.-C., Kuo, M.-X., Lin, D.-J. and Liu, H.-L. (2002). Nonlinear bio-photonic crystal effects revealed with multimodal nonlinear microscopy. **The Journal of Microscopy** 208: 190-200.
- Epstein, E. (1999). Silicon. **Annual Review of Plant Physiology and Plant Molecular Biology** 50: 641-664.
- Gausman, H.W., Allen, W.A. and Escobar, D.E. (1974). Refractive index of plant cell walls. **Applied Optics** 13(1): 109-111.

- Gaussorgues, G. (1994). **Infrared Thermography**. Chapman & Hall.
- Homeyer, E., Houel, J., Checoury, X., Fishman, G., Sauvage, S. and Boucaud, P. (2008). Thermal emission of midinfrared GaAs photonic crystals. **Physical Review** 78: 165305.
- Honaine, M.F., Zucol, A.F. and Osterrieth, M.L. (2006). Phytolith assemblages and systematic associations in grassland species of the south-eastern Pampean Plains, Argentina. **Annals of Botany** 98: 1155-1165.
- Islam, M.P., Bhuiyan, Md.K.H. and Hossain, M.Z. (2008). Vetiver grass a potential source for rural development on bangladesh. **Agricultural Engineering International: the CIGR Ejournal** 5(X): 1-18.
- Jones, R.W., Meglen, R.R., Hames, B.R. and McClelland, J.F. (2002). Chemical analysis of wood chips in motion using thermal-emission mid-infrared spectroscopy with projection to latent structures regression. **Analytical Chemistry** 74(2): 453-457.
- Kolek, J. and Kozinka, V. (eds.). (1991). **Physiology of the Plant Root System**. Kluwer Academic Publishers.
- Lavania, U.C. and Lavania, S. (2009). Sequestration of atmospheric carbon into subsoil horizons through deep-rooted grasses - vetiver grass model. **Current Science** 97(5): 618-619.
- Lu, H. and Liu, K. (2003). Morphological variations of lobate phytoliths from grasses in China and the south-eastern United States. **Diversity and Distributions** 9: 73-87.
- Ma, J.F. and Yamaji, N. (2006). Silicon uptake and accumulation in higher plants. **TRENDS in Plant Science** 11(8): 1-6.
- Metcalf, C.R. (1960). **Anatomy of the Monocotyledons: I. Gramineae**. Oxford Univ. Press. Quoted in P.C. Twiss, E. Suess and R.M. Smith. (1969). Morphological classification of grass phytoliths. **Soil Science Society of America Proceeding** 33(1): 109-115.

- Motomura, H., Hikosaka, K. and Suzuki, M. (2008). Relationships between photosynthetic activity and silica accumulation with ages of leaf in *Sasa veitchii* (Poaceae, Bambusoideae). **Annals of Botany** 101: 463-468.
- Neethirajan, S., Gordon, R. and Wang, L. (2009). Potential of silica bodies (phytoliths) for nanotechnology. **Trends in Biotechnology** 27(8): 461-467.
- Pongkarnjhana, A. and Watthanapapat, K. (2009). Potential of vetiver roots in soil overhaul. **Bhumivarinanurak Pamphlet** 26: 18-24.
- Sangster, A.G. and Parry, D.W. (1970). Silica deposition in the grass leaf in relation to transpiration and the effect of dinitrophenol. **Annals of Botany** 35(3): 667-677.
- Shahack-Gross, R., Shemesh, A., Yakir, D. and Weiner, S. (1996). Oxygen isotopic composition of opaline phytoliths: potential for terrestrial climatic reconstruction. **Geochimica et Cosmochimica Acta** 60: 3949-3953.
- Sullivan, L.A. and Parr, J.F. (2008). Systems and methods for determining carbon credits [114 paragraphs]. **Patent Application Publication** [On-line serial], Available: US2008/0131974A1.
- Tsartsidou, G., Lev-Yadun, S., Albert, R.M., Miller-Rosen, A., Efstratiou, N. and Weiner, S. (2007). The phytolith archaeological record: strengths and weaknesses evaluated based on a quantitative modern reference collection from Greece. **Journal of Archaeological Science** 34: 1262-1275.
- Twiss, P.C. (1992). Predicted world distribution of C3 and C4 grass phytoliths. In G. Rapp and S.C. Mulholland (eds.). **Phytolith Systematics** (pp 113-128). Plenum Press.
- Twiss, P.C., Suess, E. and Smith, R.M. (1969). Division S-5 - soil genesis, morphology, and classification (morphological classification of grass phytoliths). **Soil Science Society of America, Proceedings** 33: 109-115.
- Wang, Y.J. and Lu, H.Y. (1993). **The Study of Phytolith and its Application**. Beijing: China Ocean Press. Quoted in H. Lu and K. Liu. (2003). Morphological

variations of lobate phytoliths from grasses in China and the south-eastern United States. **Diversity and Distributions** 9: 73-87.

Webb, E.A. and Longstaffe, F.J. (2006). Identifying the  $\delta^{18}\text{O}$  signature of precipitation in grass cellulose and phytoliths: Refining the paleoclimate model. **Geochimica et Cosmochimica Acta** 70: 2417-2426.

Wegmuller, M., Legré, M., Gisin, N., Ritari, T., Ludvigsen, H., Folkenberg, J.R. and Hansen, K.P. (2004). Experimental investigation of wavelength and temperature dependence of phase and group birefringence in photonic crystal fibers. **ICTON**: 111-114.

Woolley, J.T. (1975). Refractive index of soybean leaf cell walls. **Plant Physiology** 55: 172-174.

# CHAPTER VI

## CHEMICAL COMPONENTS IN VETIVER RESIDUES

### 6.1 Abstract

This chapter aimed to estimate biomass, total C, total N, C/N ratio, fibrous C (cellulose and lignin), total phenolics and soluble carbohydrate in plant residues of 11 vetiver provenances, by the results expected to indicate the litter quality of provenances which was significant in C sequestration. Methodological methods carried out a high combustion for total C, total N and C/N ratio, acid detergent fiber and acid detergent lignin for fibrous C, Folin-Ciocalteu method for total phenolics and phenol-sulfuric acid method for soluble carbohydrate. The results showed that Loei (LI), and Ratchaburi (RB) yielded the highest and the lowest of belowground biomass (about 535 and 72 kg ha<sup>-1</sup>yr<sup>-1</sup>, respectively). Total C in leaf and stem residues from 3 provenances, Kamphaeng Phet 1 (KP1), LI and Songkhla 3 (SK) remained large amount rather than others. Total N was the greatest in stem residues of KP1 provenance. The C/N ratio asserting to the rate of N release from substrates was the fastest in leaf (KP2) and stem (LI, RB, PT, SK and SL) residues, whereas from root residues the rate was not different among provenances. Amount of cellulose which remained in root residues of KP1, Nakhon Sawan (NS), Ratchaburi (RB), Roi Et (RE) and Kamphaeng Phet 2 (KP2) provenance was larger over than that of others. Lignin remained in root residues rather than in leaf and stems residues, except KP1 and LI provenance which was opposite and PK and KP2 which was not significant different, by only LI provenance which lignin was greater in leaf, stem and root residues. Total phenolics remained in leaf residues rather than in stem and root residues with the large

amount of RB provenance. Almost provenances, except RE and SL, contained large amount of soluble carbohydrate in leaf residues rather than in stem and root residues. In discussion, lignin is more important fibrous C to retard decomposition process, and due to the lignin-to-N ratio SK roots were more resistance to degradation. Polyphenols can be supporting either humification or N leaching from soils, and also polyphenols can function in soil aggregation.

In conclusion, due to belowground biomass and amounts of chemical components in plant residues, LI provenance could be said the highest efficient in C sequestration, while the lowest was NS, PK and KP2 provenance. However, it need more deeply experiment to clarify the specific function of each chemical on organic matter decomposition, humification and C or N mineralization.

**Keywords:** lignin, phenolics, lignin/N ratio, decomposition, litter quality, aggregation

## 6.2 Introduction

The amounts of plant chemicals are the essential controlling factors for organic matter formation and humification processes in soils (Sanger et al., 1997). Plant tissues include intracellular storage materials and structural components in membranes, extracellular or cell walls differ in plant chemical components and the contents are significant to biodegradation (Kögel-Knabner, 2000).

The storage materials of plants such as proteins and soluble carbohydrates are more easily degradable than the structural components and thus are important C and energy sources for microorganisms. Proteins can be decomposed by a multitude of microorganisms and are considered to be very bioavailability (Martin and Haider, 1986). Soluble carbohydrates can be rapidly decomposed by aerobic and anaerobic microorganisms (Martin, 1971). Cellulose, the major structure of cell walls, consists of

85% of a fibrillar structure with crystalline properties, but it is easily degradable by many organisms including fungi and eubacteria, in particular under aerobic conditions (Harborne, 1997). Lignin in Gramineae consists of three different alcohols from C<sub>6</sub> - C<sub>3</sub> pool, coumaryl, coniferyl, and sinapyl alcohol, and small amount of cinnamic acid embedding in a three-dimensional network by polymerization of free radicals, which is the result disordered molecular structure of lignin and completely breaking down by specialized organisms i. e. white rot fungi (Haider 1992). During decomposition of lignin intramolecular bonds between phenylpropanoid components of the lignin are severed and oxidized, and phenolic derivatives are released (Haider, 1992). The fraction derived from lignin in soils becomes increasingly acidic (carboxylic) as biodegradation progresses and the acid-to-aldehyde ratio of phenolic moieties can be used to estimate the extent of lignin biotransformation (Kogel-Knabner, 1993).

Therefore, this chapter aimed to analyze chemical components in plant residues from leaves, stems and roots by comparing among 11 vetiver provenances; there were total C, total N, C/N ratio, cellulose, lignin, total phenolics and soluble carbohydrate. Also, plant biomass was collected at the same time.

### **6.3 Objectives of this chapter**

6.3.1 To measure belowground biomass of 11 vetiver provenances

6.3.2 To compare total C, total N and C/N/ ratio of plant residues among 11 vetiver provenances

6.3.3 To compare cellulose of plant residues among 11 vetiver provenances

6.3.4 To compare lignin of plant residues among 11 vetiver provenances

6.3.5 To compare total phenolics of plant residues among 11 vetiver provenances

6.3.6 To compare soluble carbohydrate of plant residues among 11 vetiver provenances

6.3.7 To indict the vetiver provenances significant to C sequestration

## 6.4 Materials and methods

### 6.4.1 Plant and site description

This study conducted on eleven provenances of two vetiver species, *Chrysopogon nemoralis* and *C. zizanioides*. *C. nemoralis* consists of 6 provenances: Kamphaeng Phet 1 (KP1), Loei (LI), Nakhon Sawan (NS), Prachuabkhirikhan (PK), Ratchaburi (RB) and Roi Et (RE); whereas *C. zizanioides* has 5 provenances: Kamphaeng Phet 2 (KP2), Phraratchathan (PT), Songkhla 3 (SK), Sri Lanka (SL) and Surat Thani (ST). All plants were grown on loamy sand on November 2004 at the experimental plots of the Regional Office 3, Land Development Department, Muang District, Nakhon Ratchasima, Thailand (15°05'N, 102°13'E, 167 m a.s.l.). Each plot was of 2 x 10 m. Plants were given manures in an early stage and allowed naturally grown continually for 3 years. During November 2004 to 2007, the mean annual temperature ranged between 23.1 and 33.3°C with the average annual precipitation about 94.38 mm per month and the average annual evaporation about 4.84 mm per day (Nakhon Ratchasima Meteorology Station; Appendix A).

### 6.4.2 Method of plant biomass measurement

Only belowground biomass was collected, accounting from 1 inch of culm above ground to all fine roots belowground. Flesh mass was weighted and dried at 60°C. Belowground biomass was calculated as following Eq. (6.1).

$$\text{Belowground biomass} = \frac{(\text{Weight of fresh mass}) \times 100}{(\% \text{ Moisture} + 100)} \quad (6.1)$$

### 6.4.3 Method of total C, total N and C/N ratio measurement

Dried and fined plant residues were measured total C and N contents using LECO analyzer (CNS 2000). The C/N ratio derived from the proportion of total C and total N of the plant sample.

### 6.4.4 Methods of cellulose and lignin determination

Cellulose and lignin content were determined from a method of acid detergent fiber (ADF) and acid detergent lignin (ADL) (Van Soest, 1963). Cellulose was derived from the difference between ADF and ADL, whereas lignin was ADL content directly.

Briefly, 1 - 2 g of dried and fined plant residues was weighted in a fritted glass crucible and digested with an acid detergent solution (concentrated H<sub>2</sub>SO<sub>4</sub> and cetyl trimethyl ammonium bromide (CTAB)) in a hot digester for 1 h. After washing, the residues were dried and collected the oven dried weight for ADF calculation (Eq. (6.2)).

$$\% \text{ ADF} = \left[ \frac{(A_1 - B_1)}{C} \right] \times 100 \quad (6.2)$$

where  $A_1$  is the weight of residues including a fritted glass crucible after oven drying,  $B_1$  is the weight of fritted glass crucible, and  $C$  is the initial weight of plant residues.

The ADF was further digested by 72% H<sub>2</sub>SO<sub>4</sub> for 3 h. After washing, the residues were dried and burned at 550°C for 3 h. The ADL was determined following to Eq. (6.3).

$$\% \text{ ADL} = \left[ \frac{(A_2 - B_2)}{C} \right] \times 100 \quad (6.3)$$

where  $A_2$  is the weight of residues including a fritted glass crucible before burning,  $B_2$  is the weight of residues including a fritted glass crucible after burning, and  $C$  is the initial weight of plant residues.

#### **6.4.5 Method of total phenolic measurement**

Total phenolic content followed to Folin-Ciocalteu method (Waterman and Mole, 1994). Briefly, 1 - 2 g of dried and fined plant residues was extract with 50% methanol and heavily shaken for 15 min at the room temperature. After centrifugation (3,000 rpm, 5 min), the supernatant was filtered on filter paper. The pellet was then re-extracted 2 times and all supernatants were pooled together. Next, mixed 150  $\mu\text{L}$  of supernatant with 700  $\mu\text{L}$  distilled water and 150  $\mu\text{L}$  Folin - Ciocalteu solution and settle for 6 min. After that, mixed with 2 mL of 2%  $\text{NaCO}_3$  and settle for 45 min and finally measured the absorbance at 760 nm. The standards were 0, 2.5, 5, 7.5, 10, 15, 20, 25, 30, 35, 40 and 45  $\mu\text{g mL}^{-1}$  of gallic acid.

#### **6.4.6 Method of soluble carbohydrate measurement**

Soluble carbohydrate content followed to phenol-sulfuric acid method (Dubois et al., 1956). Briefly, 1 - 2 g of dried and fined plant residues was extract with 50% methanol and heavily shaken for 15 min at the room temperature. After centrifugation (3,000 rpm, 5 min), the supernatant was filtered on filter paper. The pellet was then re-extracted 2 times and all supernatants were pooled together. Next, mixed 600  $\mu\text{L}$  of supernatant with 1.2 mL distilled water, 600  $\mu\text{L}$  of 5% phenol solution and 3 mL concentrated  $\text{H}_2\text{SO}_4$ . The mixture

was settle for 30 min and measured the absorbance at 490 nm. The standards were 0, 25, 50, 75, 100, 125, 150, 200, 300, 400 and 500  $\mu\text{g mL}^{-1}$  of glucose.

#### 6.4.7 Statistical analysis

Statistical analysis of the data was carried out on the replicates by two-way ANOVA. If the main effects were significant at  $p < 0.05$ , a post hoc separation of means was done by univariate least significant difference (LSD) test. Statistical analysis was conducted with SPSS and Microsoft Excel for Window 2000.

### 6.5 Results

#### 6.5.1 Plant biomass

Because plant biomass was not done in an accurately accumulation method, so only belowground biomasses of 11 vetiver provenances were collected (Figure 6.1 and Table 6.1). After 3 years grown on loamy sand, LI provenance could produce the highest belowground biomass ( $535 \text{ kg ha}^{-1}\text{yr}^{-1}$ ), while RB provenance yielded the lowest ( $72 \text{ kg ha}^{-1}\text{yr}^{-1}$ ). Statistical analysis also showed LI was only one provenance yielding the highest belowground biomass, whereas provenances such KP1, PK, RB, KP2 and PT yielded significantly the lowest ( $p < 0.05$ ).

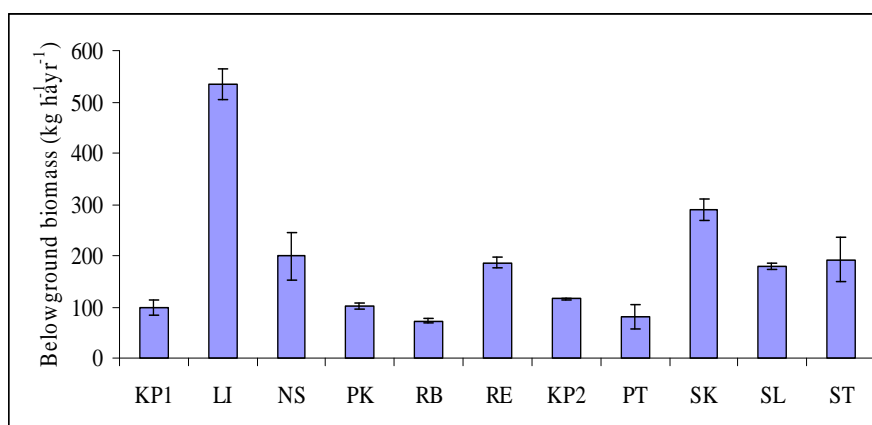


**Figure 6.1** Belowground biomass of 11 vetiver provenances (mean  $\pm$  S.D.,  $n = 3$ ).

### 6.5.2 Total C, total N and C/N ratio of plant residues

Amounts of total C, total N and C/N ratio presented in Figure 6.2 and Table 6.1.

Across plant residues (leaves, stems and roots, same below), total C contents ranged from 18.77 to 35.51%DM, 34.22 to 39.91%DM, and 31.9 to 36.69%DM, averaging 29.4, 37.9 and 34.6%DM, respectively. Only root residues which the total C was not significant difference among provenances, while leaf and stem residues contained larger amounts of total C ( $p < 0.05$ ; Figure 6.2a). Only 3 provenances, KP1, LI and SK, which both leaf and stem residues contained high total C.

Across plant residues, total N contents ranged from 10.92 to 19.03%DM, 17.24 to 20.84%DM, and 14.89 to 18.44%DM, averaging 16.7, 19 and 17.3%DM, respectively (Figure 6.2b). Statistical analysis showed total N was significant difference across provenances and plant residues ( $p < 0.05$ ). Almost provenances contained total N in stem residues, by the highest was of KP1 provenance.

Across plant residues, C/N ratio ranged from 1.03 to 2.56, 1.89 to 2.08, and 1.93 to 2.14, averaging 1.79, 2 and 2%DM, respectively (Figure 6.2c). Only root residue, the C/N ratio was not significant difference among provenances ( $p < 0.05$ ). Provenances such LI, RB, PT, SK and SL contained large amounts of C/N ratio in stems, whereas only KP2 provenances, was the greater in leaf residues.

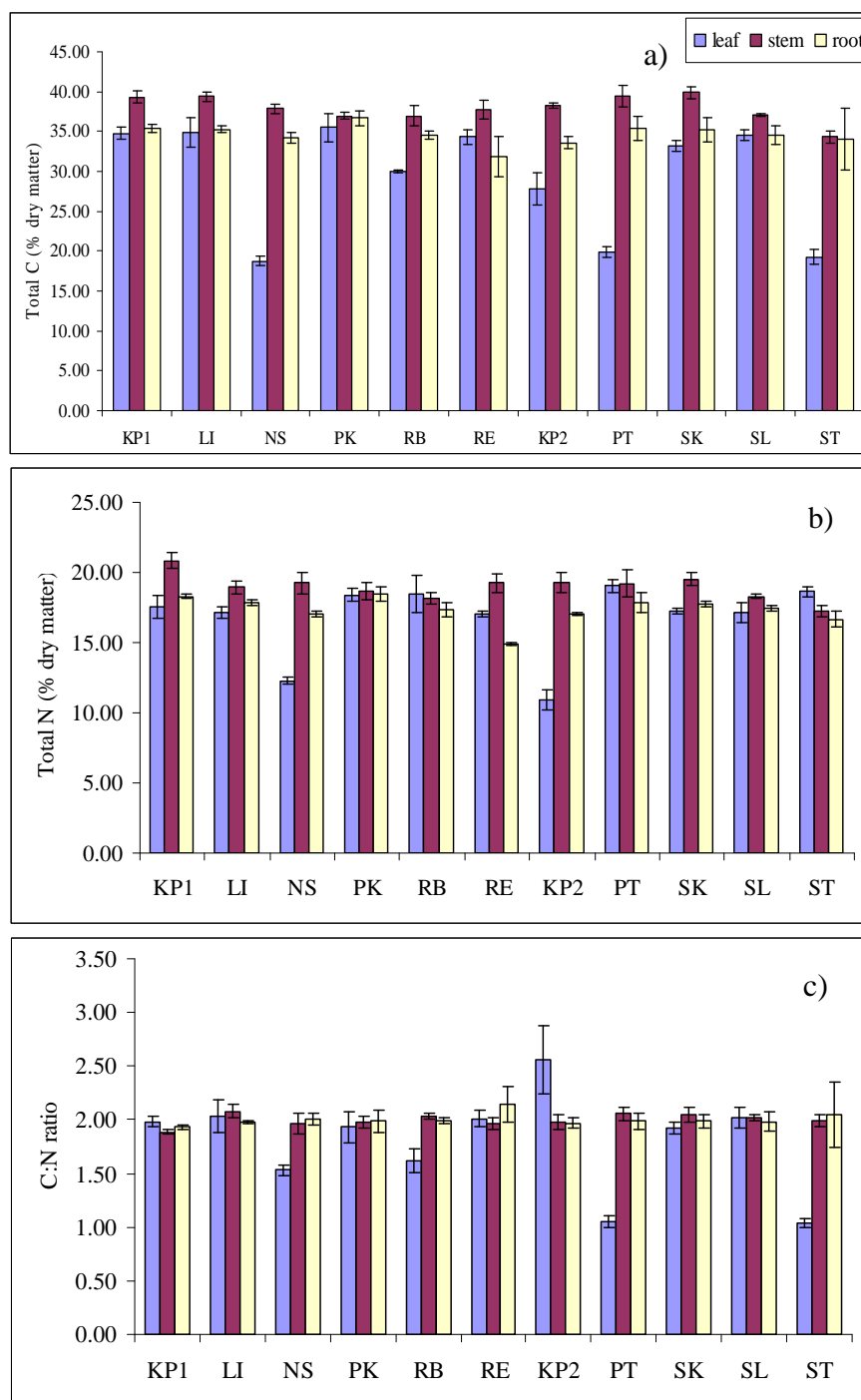


**Figure 6.2** (a) total C, (b) total N and (c) C/N ratio of plant residues of 11 vetiver provenances (mean  $\pm$  S.D., n = 3).

### 6.5.3 Fibrous C, total phenolics and soluble carbohydrate of plant residues

Figure 6.3 and Table 6.1 showed statistical analyses of fibrous C (cellulose and lignin), total phenolics and soluble carbohydrate contents. The amount of fibrous C and total phenolic content of organic residues had been suggested to control the rate of organic

matter decomposition, whereas soluble carbohydrate content supplied in microbial population (Neely et al., 1991).

Across plant residues, cellulose contents ranged from 36 to 45.1%DM, 22.3 to 40.2 %DM, and 33.8 to 54.6 %DM, averaging 39.3, 34.2 and 43.5%DM, respectively (Figure 6.3a). Statistical analysis showed only root cellulose was significant difference among provenances, while leaf and stem residues were not ( $p < 0.05$ ). The provenances contained large cellulose in root residues were KP1, NS, RB, RE, KP2 and SK.

Across plant residues, lignin contents ranged from 7.2 to 12.1%DM, 13.2 to 29.2%DM, and 11.5 to 22.6 %DM, averaging 9.1, 18 and 17.2%DM, respectively (Figure 6.3b). Statistical analysis showed lignin content was significant difference among provenances and plant residues ( $p < 0.05$ ). By there were 7 provenances, LI, NS, RE, RB, PT, SL and ST, contained large amounts of root lignin rather than others.

Comparing a proportion of cellulose and lignin in fibrous C, KP2 provenance contained more cellulose proportion, while LI composed of more lignin proportion (Figure 6.3c).

Across plant residues, total phenolics ranged from 0.64 to 1.76%DM, 0.42 to 0.82%DM, and 0.19 to 0.61%DM, averaging 1.03, 0.59 and 0.40%DM, respectively (Figure 6.3d). Total phenolics were significant difference across provenances and plant residues ( $p < 0.05$ ). Large amount of total phenolics contained in leaves rather than in stem and root residues, by RB leaf residues were significantly the highest.

Across plant residues, soluble carbohydrate ranged from 1.55 to 5.43%DM, 0.97 to 9.21%DM, and 1.35 to 6.07%DM, averaging 4.3, 4.7 and 3%DM, respectively (Figure 6.3e). Soluble carbohydrate contents were significant difference across provenances and plant residues ( $p < 0.05$ ). Provenances such KP1, LI, PK, RB, PT, SK and ST contained large amount of soluble carbohydrate in leaf residues, while two provenances such KP2

and NS contained large soluble carbohydrate in leaf and either stem or root residues, respectively.

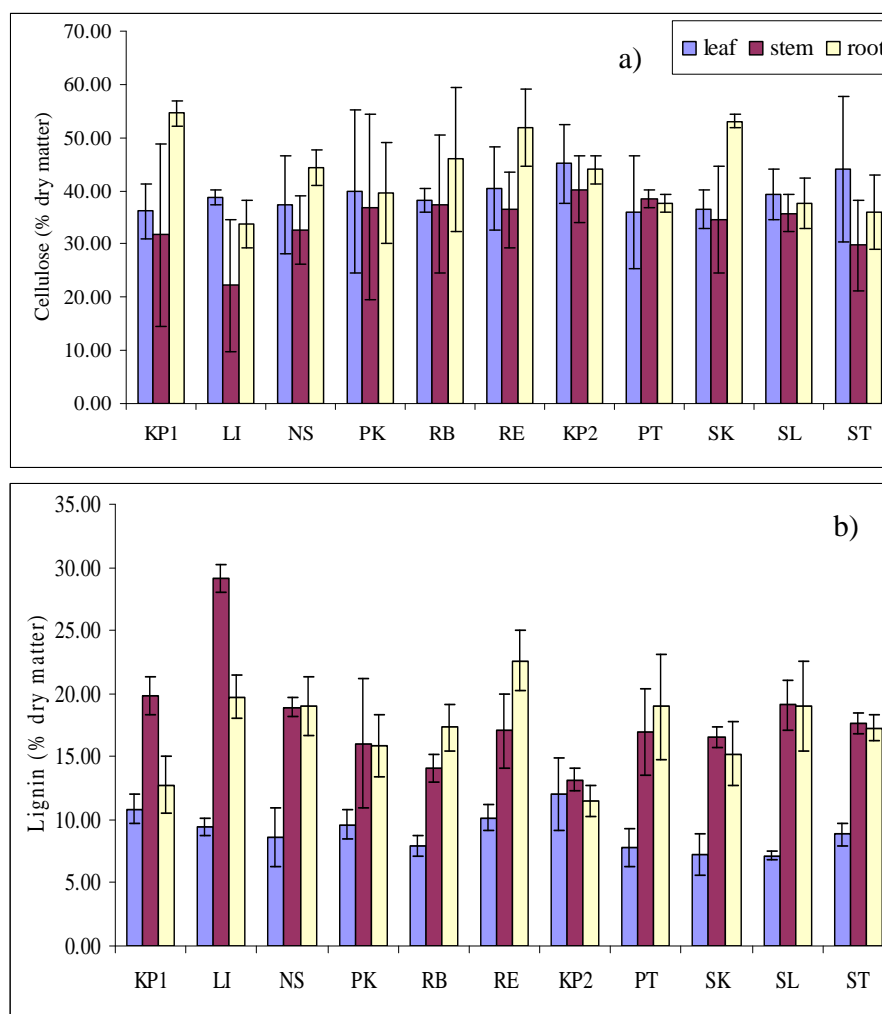


**Figure 6.3** Chemical components in plant residues of 11 vetiver provenances: (a) cellulose; (b) lignin; (c) proportion of cellulose and lignin in fibrous C; (d) total phenolics; and (e) soluble carbohydrate (mean  $\pm$  S.D., n = 3).

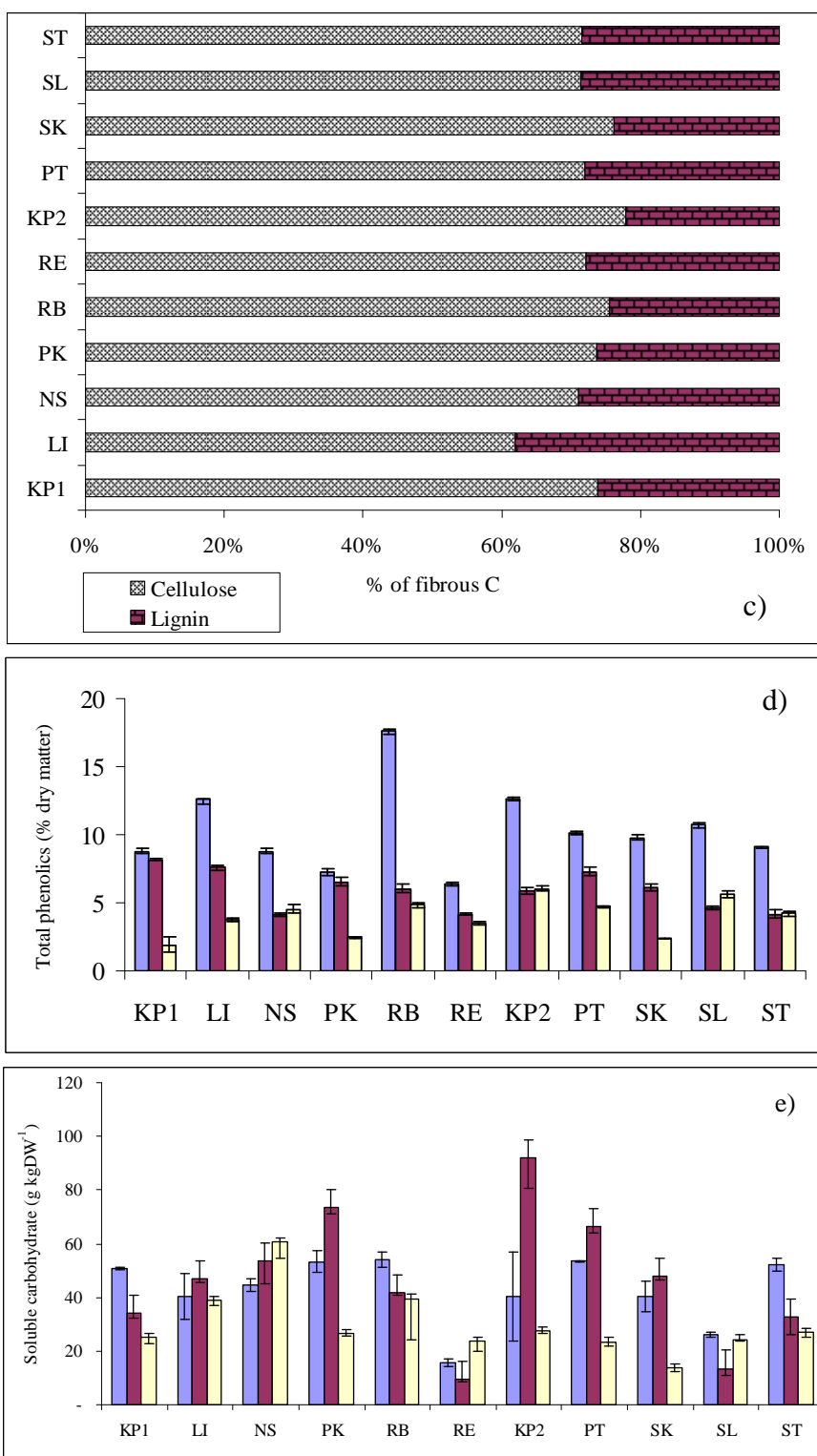


Figure 6.3 (Continued).

## **6.6 Discussion**

### **6.6.1 Lignin: a controller of litter decomposition**

Many theories try to evaluate decay processes from litter quality and find dramatic changes during the decay which cause mainly by litter chemical components. Different plant litter types have different chemical compositions which are active in different stage of litter decomposition.

Below (Figure 6.4) is a newly model of Berg and Matzner (1997) which schemes decomposition model of needle litter of different pine species and appropriates for different types of foliar litter and also grasses and herbs. In the initial stage, the decomposition rate is linearly related to concentration of total N, P and S which an accumulated mass loss of between 26 and 36%. All unshielded holocellulose is decomposed, and only lignin encrusted holocellulose and lignin remain. In the late stage (phase 2), the degradation of lignin controls the litter decomposition rate. Nitrogen hampers the degradation of lignin, and higher N concentrations suppress decomposition, whereas Mn appears to have a stimulating effect on lignin degradation. Mn is a cofactor in lignin-degrading enzymes such as Mn-dependent peroxidase (Perez and Jeffries 1992). Finally, in the humus-near stage (phase 3), the lignin level is nearly constant, often at values of 50 - 55%, the litter decomposition rate is close to zero, and the accumulated mass loss also reaches its limit value.

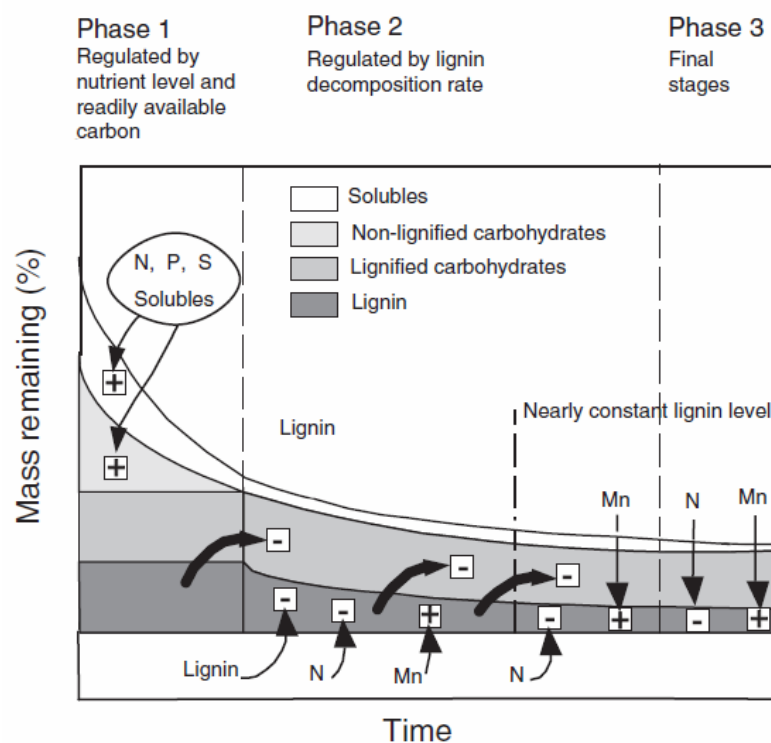


**Figure 6.4** Model for chemical changes and rate-regulating factors during decomposition (Berg and Matzner, 1997).

Consistently, Whitmore and Matus (1996) modeled the effect of resistance to decomposition of a substrate in relation to quality. They assumed that fibrous C (hemicellulose, cellulose and lignin) would impede the action of microorganisms or enzymes in decomposing the rest of the plant residues. As the easily decomposable parts of the residues break down, the fibrous parts became more concentrated in the remainder and retard decomposition to a greater and greater extent.

Likewise, a fraction  $f_R$  in Eq. (6.4) that calculated in a manner analogous proposing by Parton et al. (1987 quoted in Paustain et al., 1997), which decomposition rate of plant residues reduced with a larger amount of a fraction of fibrous C.

$$f_R = \exp\left(\frac{-k_R F C_0}{C_t}\right) \quad (6.4)$$

where  $k_R$  is a constant,  $F$  is the fraction of fibrous C in plant residues (hemicellulose plus cellulose plus lignin),  $C_0$  is the initial C content of the plant residues, and  $C_t$  is the C remaining undecomposed at the time  $t$ .

Under this study, regardless plant residues, large amount of fibrous C was greater in RE provenance, while the proportion composed of lignin was highly in LI provenance (Figure 6.3c).

Another index is the lignin-to-N (lignin/N) ratio (Melillo et al., 1982). This ratio was based on the hypothesis that N and lignin had opposite effects on the decomposition rate, whereby N is a rate-stimulating, and lignin is a rate-retarding factor. The ratio is generally a good predictor of mass loss during initial stage of decay. The correlation between the lignin/N ratio and first-year mass loss may be significant even if the correlation between either lignin or N taken individually with first-year mass loss is not significant. For late stages, this index is of little value, since N for the late stages has a rate-retarding effect. The value of this index as a predictor of decay rate thus decreases as the decay process develops.

Also, the value of the lignin/N ratio benefits in distinguishing plant residues that are difficult to degrade (structural-C with a wide lignin/N ratio) from those that are more easily degraded (metabolic-C with a narrow lignin/N ratio) (Berg and McClaugherty, 2008). In the sample under this study, SK provenance, which by the lignin content the root residues was not highly significant, but by the lignin/N ratio the value was the highest (1.54) which the residues referred to hardly degraded. Regardless provenances, leaf residues were easily degraded (0.54), and later were stem (0.95) and root residues (0.99), respectively. Also,

study of Amelung et al. (1999) confirmed the value of the lignin/N ratio was more sensitive to degree of SOM degradation rather than only considering lignin or C/N ratio. Their results sensitively reflected the lignin/N ratio decreased with the increasing stage of decomposition from coarse- to fine- sand sized SOM (from 15.9 to 0.29). By they concluded that the coarse-sand sized SOM was decomposed more quickly than the fine-sand sized SOM structures that had already been altered by microbes

In particular, lignin degradation depends on its various phenolic subunits. Cinnamyl units decompose faster than syringyl units, while vanillyl units are slowest (Marschner et al., 2008). Bahri et al. (2006) found that after 9 years of maize cultivation on a eutric cambisol, more than 60% of cinnamyl phenols in the soil were maize-derived, but less than 30% was vanillyl units. They proposed various explanations for this observation including a higher degree of cross-linking between vanillyl-type monomers. Consequently, variations in degradation rates between different types of lignin could be attributed to differences in recalcitrance between lignin macromolecules. In study of Rasse et al. (2006) found lignin composed of a two compartment model which was an unprotected lignin pool and a stabilized pool. By the former contained about 92% of the lignin which had a turnover time of less than 1 year, while the latter contained only 8% of the lignin pool which had a longer mean residence time in the soil (18 years). Consequently, all lignin detected in soil samples represented this slow pool as lignin in the fast pool turned over too fast to significantly accumulate in the soil.

Moreover, Hofmann et al. (2009) mentioned that C4-lignin degradation was depended on nitrogen fertilization. By the decay of fresh C4-lignin might be enhanced by nitrogen in contrast to no effect on decay of old C4-lignin, C3-lignin and C3-SOC.

### 6.6.2 Quality of plant residues and the supply of nitrogen

The C/N ratio has long been asserted to be of great relevance to the speed with which N is released in soil, but it is important to realize that this is not the same thing as decomposition. In general, the smaller or narrower the C/N the faster is N released from plant residues (Vanlauwe et al., 1999). Where residues are uniformly decomposable, the following Eq. (6.5) (Whitmore and Handayanto, 1997):

$$N = C_0 \left\{ \frac{1}{Z} - \frac{E}{Y} \right\} \quad (6.5)$$

In this equation,  $N$  is the amount of N mineralized once decomposition is complete or almost so,  $Z$  is the C/N of the substrate,  $E$  is a microbiological efficiency factor that can vary for several seasons but can be taken as about 0.4, and  $Y$  is the C/N of the end product of the decomposition process. Microbes are assumed to have a demand for N in order to decompose plant residues. They and their products must maintain a certain C/N ratio. This value is almost always narrower than the residues themselves but because microbes are not 100% efficient the critical C/N ratio,  $z_c$ , where mineralization switches to immobilization, is often wider than in the residues. Residues that are highly heterogeneous in terms of quality may deviate from what is predicted by Eq. (6.5).

However, quality affects the way different plant residues decompose or release N at low temperatures. For example, at 28°C the decomposition of glucose was 4.6 times faster than holocellulose while at 5°C it was 17.6 times faster (Nicolardot et al., 1994).

### 6.6.3 Polyphenolic compounds on either humification or N leaching

Polyphenolics of plant residues can enhance either humification of SOM or N leaching from soils. Many understand that polyphenolic compounds in plant residues reduce both the extent of decomposition and release of nutrients from plant residues.

However, Kuiters (1990) argued that polyphenols could divert decomposing substrate to humus meanwhile were themselves consumed and leaching from soils. The active polyphenols restrict in the proteins binding capacity ( $P_{BC}$ ) should be additionally considered because some polyphenols reacted with amino compounds much more readily than others. Consequently,  $P_{BC}$  was more correlated with the rate of decomposition and N mineralization. In addition, most active are also soluble in water, they readily bind organic matter throughout soil and make them subject to leaching and removal from soils. Nitrogen is bonded at the same time as C in this enhanced humification process and the C/N ratio of the polyphenol pool is assumed to be the same as that of the residues. Nitrogen is lost too, when polyphenols leach from soils (Whitmore and Matus, 1996).

#### **6.6.4 Residue quality and soil aggregation**

Polyphenols in plant residues can distribute the different mean weight diameter (MWD) in soil aggregates. A size-distribution comparison of soil aggregates resulting from the decomposition of plant residues which different chemicals containing divert different sizes of MWD. Such soils with corn residues (the highest phenolic acid content) could improve the greatest amount of soil aggregates remaining in the 2 and 4 mm sieve when compared to the soils with canola residues (the lowest phenolic acid content but the highest carbohydrate content) which could slightly improve in the 0.5 and 1.0 mm aggregates size fractions (Martens, 2000). Polyphenols from plant sources or microbial synthesis were important precursors of soil humic substances and the formation of humic substances with incubation of the corn residues and decrease in humic substances with incubation of the canola residues supports the importance of plant polyphenols as precursors of soil humic acid (Martens, 2000).

Carbohydrate in plant residues could also slightly improve MWD, but in transient soil aggregation. As Martens and Frankenberger (1992) suggested that simple

carbohydrates stimulated microbial activity, but not the synthesis of polysaccharide binding agents, by microbial products resulting from the residue decomposition interacting with weekly wet-dry cycle could increase the MWD distribution.

As above, polyphenolic contents of plant residues and microbial activity due to metabolism of carbohydrates appeared to be important in the aggregate stability mechanisms and for maintaining organic C and that determination of the organic residue's phenolic composition may help predict C sequestration potential.

## **6.7 Conclusions**

6.7.1 LI and RB yielded the highest and the lowest of belowground biomass (about 535 and 72 kg ha<sup>-1</sup>yr<sup>-1</sup>, respectively).

6.7.2 Amount of total C in leaf and stem residues was significant difference among 11 provenances but was not in root residues. By leaf and stem residues from 3 provenances, KP1, LI and SK, contained the greater total C rather than others.

6.7.3 Only stem residues which total N was large amount rather than others, especially KP1 provenance.

6.7.4 The rate of N release from leaf and stem residues differed among 11 provenances, anticipating the fastest in leaf residues was of KP2 provenance, whereas in stem residues was of LI, RB, PT, SK and SL provenance.

6.7.5 Only root residues which cellulose contents significantly differed, by 5 provenances, KP1, NS, RB, RE and KP2, had the large amount.

6.7.6 Lignin remained in root residues rather than in leaf and stem residues, except KP1 and LI provenance which was opposite and PK and KP2 which was not significant different. And, only one provenance as LI which the residues contained large amount of lignin in leaves, stems and roots.

6.7.7 Total phenolics remained in leaf residues rather than in stem and root residues with the large amount of RB provenance.

6.7.8 Almost provenances, except RE and SL, contained large amount of soluble carbohydrate in leaf residues rather than in stem and root residues.

6.7.9 Regarding chemical components in plant residues, a pool size of belowground biomass with high total C and N in stem and root residues, and high fibrous C (lignin), LI provenance should be considered in C sequestration rather than other provenances.

6.7.10 Due to the lignin/N ratio which root residues of SK provenance had prolonged degradation rather than others.

6.7.11 As a result, it could be concluded the potentially C sequestration of 11 vetiver provenances in Table 6.2, which LI provenance showed the great potential and the second and the third were KP1 and RE and SK provenance, respectively, while the lowest was NS, PK and KP2 provenance.

**Table 6.2** Conclusion of the potentially C sequestration of 11 vetiver provenances.

Potential	KP1	LI	NS	PK	RB	RE	KP2	PT	SK	SL	ST
1. Belowground biomass		+									
2. Total C	++	++							++		
3. Total N	++	+		+				++	+		+
4. Slow N releasing rate (high C/N ratio)		+			+		+	+	+	+	+
5. Cellulose	+		+		+	+	+		+		
6. Lignin	+	+++	++	+	+	++	+	+		+	++
7. Lignin/fibrous C		+									
8. Fibrous C						+					
9. Total phenolics	+				+		+				
10. Low soluble carbohydrate						++			+	+	
<b>Total</b>	<b>7</b>	<b>9</b>	<b>3</b>	<b>2</b>	<b>4</b>	<b>6</b>	<b>4</b>	<b>4</b>	<b>6</b>	<b>3</b>	<b>4</b>

(+) means positively significant in slow decomposition rate.

## 6.8 References

- Amelung, W., Flach, K.W. and Zech, W. (1999). Lignin in particle-size fractions of native grassland soils as influenced by climate. **Soil Science Society of America Journal** 63: 1222-1228.
- Bahri, H., Dignac, M.F., Rumpel, C., Rasse, D.P., Chenu, C. and Mariotti, A. (2006). Lignin turnover kinetics in an agricultural soil is monomer specific. **Soil Biology and Biochemistry** 38: 1977-1988.
- Berg, B. and McClaugherty, C. (2008). **Plant Litter: Decomposition, Hummus Formation, Carbon Sequestration** (2nd ed.). Verlag: Springer.
- Berg, B. and Matzner, E. (1997). The effect of N deposition on the mineralization of C from plant litter and humus. **Environmental Reviews** 5: 1-25.
- Dubois, M., Gilles, K.A., Hamilton, J.K., Rebers, P.A. and Smith, F. (1956). Colorimetric method for determination of sugars and related substances. **Analytical Chemistry** 28: 350-356.
- Haider, K. (1992). Problems related to the humification processes in soils of the temperate climate. In J.-M. Bollag and G. Stotzky (eds.). **Soil Biochemistry**, Vol 7 (pp 55-94). New York: Marcel Dekker.
- Harborne, J.B. (1997). Role of phenolic secondary metabolites in plants and their degradation in nature. In G. Cadisch and K.E. Giller (eds.). **Driven by Nature: Plant Litter Quality and Decomposition** (pp 67-74). Wallingford: CAB International.
- Hofmann, A., Heim, A., Gioacchini, P., Miltner, A., Gehre, M. and Schmidt, M.W.I. (2009). Nitrogen fertilization did not affect decay of old lignin and SOC in a <sup>13</sup>C-labeled arable soil over 36 years. **Biogeosciences Discussions** 6: 1657-1675.

- Kogel-Knabner, I. (1993). Biodegradation and humification processes in forest soils. **Soil Biochemistry** 8: 101-135.
- Kögel-Knabner, I. (2000). Analytical approaches for characterizing soil organic matter. **Organic Geochemistry** 31: 609-625.
- Kuiters, A.T. (1990). Role of phenolic substances from decomposing forest litter in plant-soil interactions. **Acta Botanica Neerlandica** 39: 329-348.
- Marschner, B., Brodowski, S., Dreves, A., Gleixner, G., Gude, A., Grootes, P.M., Hamer, U., Heim, A., Jand, G., Ji, R., Kaiser, K., Kalbitz, K., Kramer, C., Leinweber, P., Rethemeyer, J., Schäffer, A., Schmidt, M.W.I., Schwark, L. and Wiesenberg, G.L.B. (2008). How relevant is recalcitrance for the stabilization of organic matter in soils? **Journal of Plant Nutrition and Soil Science** 171: 91-110.
- Martens, D. A. (2000). Plant residue biochemistry regulates soil carbon cycling and carbon sequestration. **Soil Biology and Biochemistry** 32: 361-369.
- Martens, D.A. and Frankenberger, Jr.W.T. (1992). Decomposition of bacterial polymers in soil and their influence on soil structure. **Biology and Fertility of Soils** 13: 65-73.
- Martin, J.P. (1971). Decomposition and binding action of polysaccharides in soils. **Soil Biology and Biochemistry** 3: 33-41.
- Martin, J.P. and Haider, K. (1986). Influence of mineral colloids on turnover rates of soil organic carbon. In P.M. Huang and M. Schnitzer (eds.). **Interactions of Soil Minerals with Natural Organics and Microbes**, Vol. 17 (pp 283-304). Madison: Soil Science Society of America.
- Mellilo, J.M., Aber, J.D. and Muratore, J.F. (1982). Nitrogen and lignin control of hardwood leaf litter decomposition dynamics. **Ecology** 63: 621-626.

- Neely, C.L., Beare, M.H., Hargrove, W.L. and Coleman, D.C. (1991). Relationships between fungal and bacterial substrate-induced respiration, biomass and plant residue decomposition. **Soil Biology and Biochemistry** 23: 947-954.
- Nicolardot, B., Fauvet, G. and Cheneby, D. (1994). Carbon and nitrogen cycling through soil microbial biomass at various temperatures. **Soil Biology and Biochemistry** 26: 253-261.
- Parton, W.J., Schimel, D.S., Cole, C.V. and Ojima, D.S. (1987). Analysis of factors controlling soil organic matter levels in great plains grasslands. **Soil Science Society of America Journal** 51: 1173-1179. Quoted in K. Paustain, G.I. Ågren and E. Bosatta. (1997). Modeling litter quality effects on decomposition and soil organic matter dynamics. In G. Cadisch and K.E. Giller (eds.). **Driven by Nature: Plant Litter Quality and Decomposition** (pp 313-336). Cambridge, UK: CAB INTERNATIONAL.
- Perez, J. and Jeffries, T.W. (1992). Roles of manganese and organic acid chelators in regulating lignin degradation and biosynthesis of peroxidases by *Phanerochaete chrysosporium*. **Applied and Environmental Microbiology** 58: 2402-2409.
- Rasse, D.P., Dignac, M.F., Bahri, H., Rumpel, C., Mariotti, A. and Chenu, C. (2006). Lignin turnover in an agricultural field: from plant residues to soil-protected fractions. **European Journal of Soil Science** 57: 530-538.
- Sanger, L.J., Anderson, J.M., Little, D. and Bolger, T. (1997). Phenolic and carbohydrate signatures of organic matter in soils developed under grass and forest plantations following changes in land use. **European Journal of Soil Science** 48: 311-317.
- Van Soest, P.J. (1963). Use of detergents in analysis of fibrous feeds. II. A rapid method for the determination of fibre and lignin. **Association of Official Agricultural Chemists Journal** 46: 829-835.

- Vanlauwe, B., Nwoke, O.C., Sanginga, N. and Merckx, R. (1999). Evaluation of methods for measuring microbial biomass C and N and relationships between microbial biomass and soil organic matter particle size classes in West-Africa soils. **Soil Biology and Biochemistry** 31: 1071-1082.
- Waterman, P.G. and Mole, S. (1994). **Analysis of Phenolic Plant Metabolites. Methods in Ecology**. London: Blackwell Scientific Publications.
- Whitmore, A.P. and Handayanto, E. (1997). Simulating the mineralization of N from crop residues in relation to residue quality. In G. Cadisch and K.E. Giller (eds.). **Driven by Nature: Plant Litter Quality and Decomposition** (pp 337-348). Cambridge, UK: CAB INTERNATIONAL.
- Whitmore, A.P. and Matus, F.J. (1996). The decomposition of wheat and clover residues in soil: Measurements and modeling. **Proceedings of the 8th Nitrogen Workshop on Soils, Ghent** (in press).



**Table 6.1** Properties of plant residues of 11 vetiver provenances\*.

Provenance	Plant part	Belowground Biomass (kg ha <sup>-1</sup> yr <sup>-1</sup> )	Total C	Total N	C/N ratio	Cellulose	Lignin	Total phenolics	Soluble carbohydrate
KP1	leaves	97.56 <sup>D</sup>	34.76 <sup>Ab</sup> (0.80)	17.54 <sup>Bb</sup> (0.84)	1.98 <sup>B</sup> (0.05)	36.12 (5.15)	10.85 <sup>Ab</sup> (1.14)	0.87 <sup>F</sup> (0.01)	5.07 <sup>Aa</sup> (0.06)
	stems		39.35 <sup>Aa</sup> (0.68)	20.84 <sup>Aa</sup> (0.58)	1.89 <sup>B</sup> (0.03)	31.72 (17.15)	19.86 <sup>Ba</sup> (1.47)	0.82 <sup>A</sup> (0.01)	3.40 <sup>Db</sup> (0.15)
	roots		35.35 <sup>b</sup> (0.48)	18.30 <sup>Ab</sup> (0.17)	1.93 (0.03)	54.58 <sup>A</sup> (2.43)	12.74 <sup>Bb</sup> (2.27)	0.19 <sup>F</sup> (0.05)	2.50 <sup>Dc</sup> (0.23)
LI	leaves	535.16 <sup>A</sup>	34.87 <sup>Ab</sup> (1.80)	17.17 <sup>Bb</sup> (0.40)	2.03 <sup>B</sup> (0.15)	38.86 (1.37)	9.44 <sup>Aa</sup> (0.71)	1.26 <sup>B</sup> (0.03)	4.03 <sup>A</sup> (0.85)
	stems		39.36 <sup>Aa</sup> (0.64)	18.94 <sup>Ba</sup> (0.46)	2.08 <sup>A</sup> (0.06)	22.29 (12.40)	29.17 <sup>Aa</sup> (1.08)	0.76 <sup>B</sup> (0.02)	4.69 <sup>C</sup> (0.12)
	roots		35.29 <sup>b</sup> (0.44)	17.86 <sup>Ab</sup> (0.17)	1.98 (0.02)	33.78 <sup>B</sup> (4.55)	19.74 <sup>Ab</sup> (1.68)	0.37 <sup>D</sup> (0.01)	3.87 <sup>C</sup> (0.16)
NS	leaves	198.98 <sup>C</sup>	18.77 <sup>Dc</sup> (0.55)	12.27 <sup>Cc</sup> (0.25)	1.53 <sup>Cb</sup> (0.05)	37.46 (9.21)	8.60 <sup>Ab</sup> (2.34)	0.87 <sup>Fa</sup> (0.01)	4.47 <sup>Ab</sup> (0.25)
	stems		37.85 <sup>Ba</sup> (0.57)	19.28 <sup>Ba</sup> (0.76)	1.97 <sup>Ba</sup> (0.10)	32.70 (6.46)	18.92 <sup>Ba</sup> (0.78)	0.42 <sup>Gb</sup> (0.01)	5.34 <sup>Cb</sup> (0.84)
	roots		34.22 <sup>b</sup> (0.71)	17.05 <sup>Bb</sup> (0.18)	2.01 <sup>a</sup> (0.05)	44.25 <sup>A</sup> (3.35)	18.99 <sup>Aa</sup> (2.31)	0.45 <sup>Cb</sup> (0.03)	6.07 <sup>Aa</sup> (0.59)
PK	leaves	101.41 <sup>D</sup>	35.51 <sup>A</sup> (1.81)	18.42 <sup>B</sup> (0.45)	1.93 <sup>B</sup> (0.14)	39.83 (15.31)	9.64 <sup>A</sup> (1.21)	0.73 <sup>Ga</sup> (0.03)	5.32 <sup>Ab</sup> (0.40)
	stems		36.98 <sup>B</sup> (0.47)	18.68 <sup>B</sup> (0.62)	1.98 <sup>B</sup> (0.05)	36.86 (17.40)	16.02 <sup>B</sup> (5.12)	0.65 <sup>Ca</sup> (0.03)	7.33 <sup>Ba</sup> (0.21)
	roots		36.69 (0.89)	18.44 <sup>A</sup> (0.50)	1.99 (0.10)	39.64 <sup>B</sup> (9.48)	15.89 <sup>B</sup> (2.48)	0.25 <sup>Eb</sup> (0.01)	2.65 <sup>Dc</sup> (0.09)

**Table 6.1** (Continued).

Provenance	Plant part	Belowground Biomass (kg ha <sup>-1</sup> yr <sup>-1</sup> )	Total C	Total N	C/N ratio	(% dry matter)			
						Cellulose	Lignin	Total phenolics	Soluble carbohydrate
RB	leaves	71.93 <sup>D</sup>	29.93 <sup>Bc</sup> (0.16)	18.51 <sup>B</sup> (1.32)	1.62 <sup>Cb</sup> (0.11)	38.27 (2.20)	7.94 <sup>Bc</sup> (0.80)	1.76 <sup>Aa</sup> (0.02)	5.43 <sup>A</sup> (0.28)
	stems		36.95 <sup>Ba</sup> (1.24)	18.16 <sup>B</sup> (0.37)	2.03 <sup>Aa</sup> (0.03)	37.47 (12.92)	14.05 <sup>Cb</sup> (1.11)	0.60 <sup>Db</sup> (0.03)	4.19 <sup>D</sup> (0.13)
	roots		34.58 <sup>b</sup> (0.52)	17.35 <sup>B</sup> (0.51)	1.99 <sup>a</sup> (0.03)	45.91 <sup>A</sup> (13.50)	17.30 <sup>Aa</sup> (1.79)	0.48 <sup>Cc</sup> (0.02)	3.96 <sup>B</sup> (1.53)
RE	leaves	185.50 <sup>C</sup>	34.31 <sup>Ab</sup> (0.98)	17.07 <sup>Bb</sup> (0.22)	2.01 <sup>B</sup> (0.07)	40.43 (7.79)	10.17 <sup>Ac</sup> (1.00)	0.64 <sup>Ha</sup> (0.01)	1.55 <sup>Cb</sup> (0.15)
	stems		37.79 <sup>Ba</sup> (1.14)	19.27 <sup>Ba</sup> (0.67)	1.96 <sup>B</sup> (0.05)	36.43 (7.02)	17.03 <sup>Bb</sup> (2.90)	0.42 <sup>Gb</sup> (0.01)	0.97 <sup>Ec</sup> (0.12)
	roots		31.90 <sup>b</sup> (2.52)	14.89 <sup>Cc</sup> (0.10)	2.14 (0.17)	51.84 <sup>A</sup> (7.27)	22.62 <sup>Aa</sup> (2.39)	0.35 <sup>Dc</sup> (0.01)	2.37 <sup>Da</sup> (0.40)
KP2	leaves	114.97 <sup>D</sup>	27.77 <sup>Cc</sup> (2.03)	10.92 <sup>Dc</sup> (0.73)	2.56 <sup>Aa</sup> (0.32)	45.09 (7.35)	12.07 <sup>A</sup> (2.86)	1.27 <sup>Ba</sup> (0.01)	4.03 <sup>Ab</sup> (1.64)
	stems		38.26 <sup>Aa</sup> (0.37)	19.31 <sup>Ba</sup> (0.71)	1.98 <sup>Bb</sup> (0.07)	40.23 (6.21)	13.17 <sup>C</sup> (0.91)	0.59 <sup>Db</sup> (0.02)	9.21 <sup>Aa</sup> (1.16)
	roots		33.62 <sup>b</sup> (0.77)	17.07 <sup>Bb</sup> (0.12)	1.97 <sup>b</sup> (0.05)	43.93 <sup>A</sup> (2.66)	11.53 <sup>B</sup> (1.24)	0.61 <sup>Ab</sup> (0.02)	2.73 <sup>Db</sup> (0.08)
PT	leaves	80.58 <sup>D</sup>	19.94 <sup>Dc</sup> (0.69)	19.03 <sup>A</sup> (0.50)	1.05 <sup>Db</sup> (0.05)	35.99 (10.70)	7.79 <sup>Bb</sup> (1.51)	1.01 <sup>Da</sup> (0.01)	5.34 <sup>Ab</sup> (0.03)
	stems		39.41 <sup>Aa</sup> (1.40)	19.20 <sup>B</sup> (0.96)	2.05 <sup>Aa</sup> (0.06)	38.36 (1.67)	16.93 <sup>Ba</sup> (3.38)	0.73 <sup>Bb</sup> (0.03)	6.65 <sup>Ba</sup> (0.27)
	roots		35.43 <sup>b</sup> (1.50)	17.85 <sup>A</sup> (0.68)	1.99 <sup>a</sup> (0.07)	37.76 <sup>B</sup> (1.70)	18.97 <sup>Aa</sup> (4.17)	0.47 <sup>Cc</sup> (0.01)	2.34 <sup>Dc</sup> (0.18)

**Table 6.1** (Continued).

Provenance	Plant part	Belowground Biomass (kg ha <sup>-1</sup> yr <sup>-1</sup> )	Total C	Total N	C/N ratio	(% dry matter)			
						Cellulose	Lignin	Total phenolics	Soluble carbohydrate
SK	leaves	290.53 <sup>B</sup>	33.19 <sup>Ab</sup> (0.69)	17.24 <sup>Bb</sup> (0.25)	1.93 <sup>B</sup> (0.06)	36.55 <sup>a</sup> (3.67)	7.23 <sup>Bb</sup> (1.61)	0.98 <sup>Da</sup> (0.01)	4.03 <sup>Ab</sup> (0.58)
	stems		39.91 <sup>Aa</sup> (0.77)	19.52 <sup>Ba</sup> (0.45)	2.05 <sup>A</sup> (0.07)	34.58 <sup>b</sup> (10.17)	16.50 <sup>Ba</sup> (0.80)	0.61 <sup>Db</sup> (0.02)	4.81 <sup>Ca</sup> (0.15)
	roots		35.19 <sup>b</sup> (1.51)	17.71 <sup>Ab</sup> (0.20)	1.99 (0.06)	53.05 <sup>Aa</sup> (1.21)	15.22 <sup>Ba</sup> (2.57)	0.24 <sup>Ec</sup> (0.00)	1.35 <sup>Ec</sup> (0.13)
SL	leaves	178.92 <sup>C</sup>	34.55 <sup>Ab</sup> (0.61)	17.12 <sup>Bb</sup> (0.69)	2.02 <sup>B</sup> (0.10)	39.34 (4.64)	7.17 <sup>Bb</sup> (0.38)	1.07 <sup>Ca</sup> (0.03)	2.61 <sup>Ba</sup> (0.11)
	stems		37.05 <sup>Ba</sup> (0.17)	18.31 <sup>Ba</sup> (0.16)	2.02 <sup>A</sup> (0.02)	35.81 (3.45)	19.08 <sup>Ba</sup> (1.92)	0.46 <sup>Ec</sup> (0.01)	1.35 <sup>Eb</sup> (0.25)
	roots		34.55 <sup>b</sup> (1.16)	17.43 <sup>Bb</sup> (0.20)	1.98 (0.09)	37.63 <sup>B</sup> (4.84)	19.03 <sup>Aa</sup> (3.59)	0.56 <sup>Bb</sup> (0.02)	2.42 <sup>Da</sup> (0.07)
ST	leaves	191.68 <sup>C</sup>	19.24 <sup>Db</sup> (0.92)	18.62 <sup>Aa</sup> (0.33)	1.03 <sup>Db</sup> (0.04)	44.05 (13.72)	8.84 <sup>Ab</sup> (0.85)	0.92 <sup>Ea</sup> (0.02)	5.22 <sup>Aa</sup> (0.24)
	stems		34.32 <sup>Ca</sup> (0.70)	17.24 <sup>Cb</sup> (0.41)	1.99 <sup>Aa</sup> (0.06)	29.72 (8.46)	17.63 <sup>Ba</sup> (0.84)	0.42 <sup>Fb</sup> (0.03)	3.26 <sup>Db</sup> (0.67)
	roots		34.02 <sup>a</sup> (3.90)	16.66 <sup>Bb</sup> (0.57)	2.05 <sup>a</sup> (0.30)	35.93 <sup>B</sup> (6.97)	17.29 <sup>Aa</sup> (1.00)	0.42 <sup>Cb</sup> (0.02)	2.68 <sup>Db</sup> (0.17)

\*Data are means with the standard deviation in parentheses (n = 3). Different higher and lower case letters represent significant differences (p < 0.05) of the treatment among provenances and among treatment within the same provenance, respectively.

# **CHAPTER VII**

## **RELATIONSHIPS OF SOIL RESPIRATION TO MICROBIAL BIOMASS AND SUBSTRATE AVAILABILITY IN DIFFERENT VETIVER SOILS**

### **7.1 Abstract**

Soils are complexity, heterogeneity and diversity of many processes and interactions driven a variation of a size of microbial biomass (MBC). So, this chapter focused on interactions among MBC, C substrate availability and soil properties of vetiver soils to soil respiration. Eighteen vetiver soils from 8 locations in Nakhon Ratchasima were samplings to measure C fractions and soil properties. Several methodologies were conducted in this experiment such as a high combustion for total C, a chloroform fumigation extraction and a chloroform fumigation incubation method for a pool size of microbial biomass (CFE-MBC and CFI-MBC, respectively), a 0.5 M  $K_2SO_4$  extraction for C substrate availability ( $K_2SO_4$ -C), and a  $CO_2$  flush during 10 days for soil respiration ( $CO_2$ -C). Also, sampling soils were measured physical and chemical properties by appropriate methods. Results of multiple regression analyses suggested that soil respiration under favorable temperature and moisture conditions was determined by clay content rather than by total C content, but a pool size of microbial biomass and C substrate availability had no effect on. Clay content limited relative C mineralization rate ( $CO_2$ -C/TC) but attributed microbial biomass (CFI-MBC). SOC preservation by clay was suggested depending on reactions at outer clay surfaces due to the main clay mineral was kaolinite. Soil C storage assumed the preservation strongly by soil ions and by continuous vetiver.

In conclusion, this study suggested that the protective effect of clay on substrate decomposition became significant as the substrate supply and microbial demand approached to an equilibrium state.

**Keywords:** total C, microbial biomass, K<sub>2</sub>SO<sub>4</sub>-C, CO<sub>2</sub> flush, clay, interaction

## 7.2 Introduction

Soils, in definition of scientists, do not define only as the earth surface layer exploited by roots, but deeply mean to a biologically driven process influencing the intervening factors, i.e., the parent material, the relief, the climate, the organisms involved and time (Buscot and Varma, 2005). Soils also point out the complexity and the heterogeneity of the resulting medium. In addition, soils are the diversity resulting from combinations of the interaction of very diverse and complex organism communities on different types of rock material under variable climatic and topographic conditions and over time scales. Soil properties determine soil moisture, soil aeration, water percolation and evaporation and also soil microorganisms themselves, as they influence the balance between oxidative and reductive processes which drive biogeochemical cycles in soils (Kara and Bolat, 2008).

Microbial biomass is an indicator of soil quality, which is faster detective rather than soil organic C (SOC) (e.g. Hargreaves et al., 2003). Microbial biomass plays a role of pollution treatment, driving C cycling and including C sequestration; however, a size of MBC should be caution due to a level of variation of field soils (Broos et al., 2007). Some factors such as quantity and quality of readily substrate, clay content, soil texture, soil depth, elements and so on could affect on a size of MBC. So, study on interaction of soil C fractions and soil properties to soil respiration should present some meanings rather than only on amount of MBC.

Vetiver is well known in deep and dense roots which are capable grown in various soils. As for now, the character of more root biomass conducts to more saying in C sequestration.

As above, this chapter aimed to characterize interactions among MBC, C substrate availability, and soil properties in different vetiver soils to CO<sub>2</sub> production. Results of this chapter hopefully expressed the main factors contributing C sequestration of vetiver soils.

### **7.3 Objectives of this chapter**

7.3.1 To measure physical and chemical soil properties of different vetiver soils

7.3.2 To measure microbial biomass in different vetiver soils

7.3.3 To measure substrate availability index in different vetiver soils

7.3.4 To measure soil respiration in different vetiver soils

7.3.5 To find interaction among MBC, substrate availability index and soil properties of different vetiver soils to soil respiration

### **7.4 Materials and methods**

#### **7.4.1 Site description**

The study sites were conducted in 8 locations, consisting 18 sites, located in Nakhon Ratchasima, northeast Thailand (Figure 7.1; Appendix C).

**Location A:** This location is at the Thai Tapioca Development Institute (TTDI), Huai Bong Subdistrict, Dan Kun Tod District, Nakhon Ratchasima (15°16' N, 101°51' E; 312 m a.s.l.), approximately 320 ha. The land was cultivated tapioca more than 10 years. The organic carbon input into soils was through manure, plant root system, stubble and crop residues remaining on the field. Most soils are loam, sandy loam and sandy clay loam.

Vetiver was cultivated across contours to protect soil erosion. Soils were sampling from 3, 5 and 7 years continuous vetiver, consisting of the sites no. 1 to 7.

**Location B:** This location belongs to Mr. Thawatchai at Ban Nong Kradon, Bueng O Subdistrict, Kham Thale So District, Nakhon Ratchasima (15°04' N, 101°89' E; 210 m a.s.l.), approximately 2.5 ha. Soil textures were sand, loamy sand, sandy clay loam, loamy sand and sandy loam. Soils were sampling from 1, 2 and 3 years continuous vetiver, noting as the sites no. 8 to 10.

**Location C:** This location belongs to Mr. Thongdat Phraidiphanao at Suk Pai Bun Subdistrict, Soeng Sang District, Nakhon Ratchasima (14°52' N, 102°49' E; 236 m a.s.l.). Mainly soil textures were sandy clay and sandy clay loam. Soils were sampling from 3 years continuous vetiver, noting as the sites no. 11 and 12.

**Location D:** This location is at the Iam Seng factory (tapioca mill), Non Sombun Subdistrict, Soeng Sang District, Nakhon (14°43' N, 102°50' E; 229 m a.s.l.). Mainly soil textures were sandy clay and sandy clay loam. Soils were sampling from 2 years, noting as the sites no. 13 and 14.

**Location E:** This location belongs to Mr. Yuang Praeng-Di (14°36' N, 102°43' E; 273 m a.s.l.) at Noon Sumboon Subdistrict, Soeng Sang District, Nakhon. Mainly soil textures were sand and loamy sand. Soils were sampling from 2 years continuous vetiver, noting as the sites no. 15.

**Location F:** This location belongs to Mr. Sawang Kodpakdee at Ban Thai Charoen, Pak Chong District, Nakhon Ratchasima (14°76' N, 101°31' E; 423 m a.s.l.). Mainly soil textures were sandy clay and sandy clay loam. Soils were sampling from 2 years continuous vetiver, noting as the sites no. 16.

**Location G:** This location is at Land Development Department, Pak Chong District, Nakhon Ratchasima (14°67' N, 101°41' E; 312 m a.s.l.) which vetiver had planted

as a line between the experimental plots, approximately 3 years. Mainly soil textures were clay and clay loam, noting as the sites no. 17.

**Location H:** This location is at the experimental plot of the Regional Office 3, Land Development Department, Mueang District, Nakhon Ratchasima (15°05' N, 102°10' E; 167 m a.s.l.) which had cultivated vetiver continually for 3 years. Mainly soil texture was loamy sand, noting as the sites no. 18.

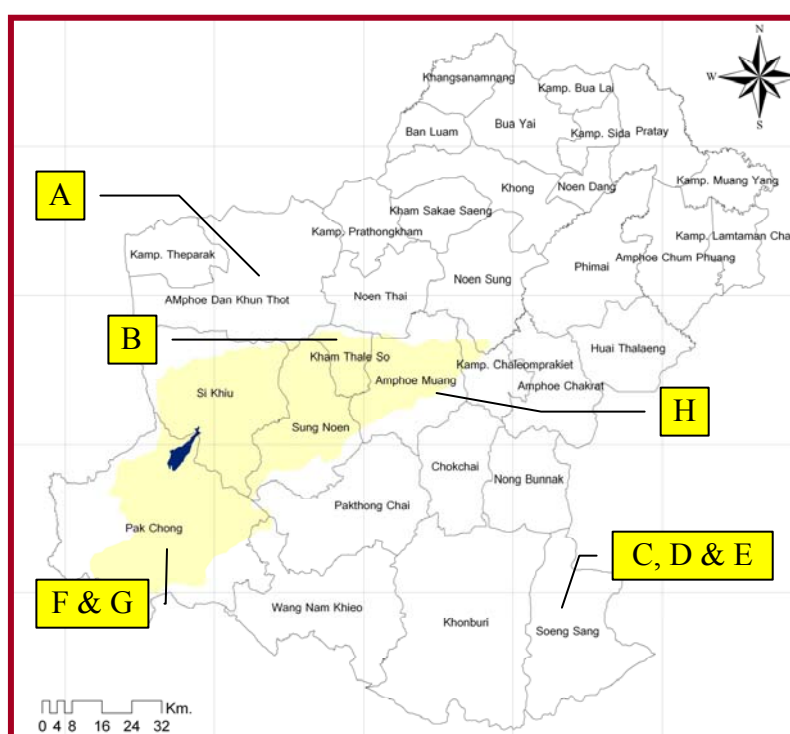


**Figure 7.1** Location of study sites in Nakhon Ratchasima, Thailand.

#### 7.4.2 Climate description

During 1977 - 2007, the mean annual temperature ranged between 21.9 and 32.8°C and the average annual precipitation was about 89 mm per month (Nakhon Ratchasima Meteorology Station; Appendix A).

### 7.4.3 Method of soil sampling

Soil were collected on May, 2008, by randomly sampling about 10 - 15 holes per each. Each soil depth, 0 - 10, 10 - 60 and 60 - 120 cm, was bulked into a composite sample. Soils were air-dried and sieved to 2 mm.

### 7.4.4 Methods of soil physical and chemical property measurement

Soils were analyzed for soil particle size distribution by the hydrometer method (Bouyoucos, 1962), bulk density (Blake, 1965), pH<sub>(H<sub>2</sub>O)</sub> (1:5 soil water ratio), electric conductivity (1:5 soil water suspension), cation, exchangeable cations (CEC), base saturation, and total C and total N by dry combustion method using LECO analyzer (CNS 2000). The mean C storage in soil at 1.2 m depth was calculated as following Eq. (7.1).

$$\text{C Storage (gC m}^{-2}\text{)} = \text{Bulk density} \times \text{SOC} \times \text{Soil depth} \quad (7.1)$$

### 7.4.5 Method of microbial biomass measurement

A pool size of microbial biomass was measured by chloroform fumigation extraction (CFE-MBC) (Voroney et al., 1993) and chloroform fumigation incubation (CFI-MBC) method (Jenkinson, 1988).

Briefly for CFE-MBC, one portion of soil was fumed with free alcohol CHCl<sub>3</sub> in the dark for 24 h. After, added 0.5 M K<sub>2</sub>SO<sub>4</sub> to the bottles containing the unfumigated control and fumigated subsamples, using the equivalent oven-dry soil weight (g): extractant volume (mL) ratio of 1:5. Shaked two subsamples for 1 h and passed the soil suspension through filter papers. The filtrates were store at 4°C for organic C measurement by the Walkley-Black wet oxidation method (Walkley and Black, 1934). The CFE-MBC values were calculated from the differences between the fumigated and unfumigated soil as shown in Eq. (7.2) (more details in chapter III).

$$\text{CFE} - \text{MBC} \left( \mu\text{gCg}^{-1}\text{soil} \right) = \frac{\text{OC}_F - \text{OC}_{UF}}{k_{EC}} \quad (7.2)$$

where  $k_{EC} = 0.35$

Briefly for CFI-MBC, soils were fumigated with chloroform, inoculated with 1% unfumigated soils, and then incubated at 25°C for 10 days in the presence of NaOH to absorb CO<sub>2</sub> released from soil. Unfumigated soils were also incubated in the same manner as control. The CFI-MBC was calculated by dividing the difference in CO<sub>2</sub>-C evolution between fumigated and unfumigated soils with 0.45 as shown in Eq. (7.3).

$$\text{CFI} - \text{MBC} \left( \text{mgCg}^{-1}\text{soil} \right) = \frac{\text{CO}_2(F) - \text{CO}_2(UF)}{0.45} \quad (7.3)$$

#### 7.4.6 Carbon availability index

Similarly, 0.5 M K<sub>2</sub>SO<sub>4</sub>-extractable C (K<sub>2</sub>SO<sub>4</sub>-C) was obtained at the same time as CFE-MBC was determined the unfumigated soils.

#### 7.4.7 Flush of CO<sub>2</sub> following rewetting of dried soils

Flush of CO<sub>2</sub> following rewetting of dried soils was determined using the incubation method as described by Chen et al. (2000). In brief, 30 g of air-dried soil were moistured in a polystyrene jar and incubated aerobically in a 1L sealed glass jar at 35°C for 10 days (the jars were flushed with air every 1 - 2 days to ensure aerobic conditions). After the incubation, excess 1.5 M BaCl<sub>2</sub> was added to the NaOH solution to precipitate CO<sub>3</sub><sup>2-</sup> and the remaining NaOH was titrated with HCl using phenolphthalein as an indicator. CO<sub>2</sub> production was calculated by following Eq. (7.4).

$$\text{CO}_2 - \text{C} \text{ (mg g}^{-1}\text{soil)} = \frac{(A_1 - A_2) \times N \times E}{w} \quad (7.4)$$

where  $A_1$  is the volume (mL) of acid used to titrate the blanks,  $A_2$  is the volume (mL) of acid used to titrate the treatments,  $N$  is the normality of titrating acid,  $E$  is the equivalent weight of C, and  $w$  is the soil weights.

#### 7.4.8 Statistical analysis

Analysis of variance and non-linear regression were performed using SPSS 10.0 for Windows and  $p < 0.05$  and  $p < 0.01$  were used for significance tests. Stepwise multiple regressions were carried out and explanatory variables with incremental  $F$  values above 4.0 were added into the model. If two explanatory variables in a model were highly correlated, the “ $F$  to enter” and “ $F$  to remove” values were increased to 4.5 and 4.4, respectively, so as to obtain a concise model.

## 7.5 Results

### 7.5.1 Pool sizes and CO<sub>2</sub> evolution rates

Table 7.1 showed averages of some soil properties of different vetiver soils and Table 7.2 presented their substrate availability index, MBC and CO<sub>2</sub> flush during 10 days (more details in Appendix C). Relationship among C fractions and soil properties showed in the correlation matrix ( $r$  - values), by Table 7.3 was of whole soils while Table 7.4 to 7.6 were toward to soil depths.

Across depth (0 - 10, 10 - 60 and 60 - 120 cm, same below), total C (TC) in the air dried soils ranged from 0.78 to 5.49%, 0.64 to 4.23% and 0.49 to 4.13% and as for TN were from 0.07 to 0.4%, 0.07 to 0.36% and 0.06 to 0.45%, respectively. The mean C

storage in soils at 1.2 m depth was calculated ranging from 102 to 450 tC ha<sup>-1</sup> by the lowest and the highest were of site no. 15 and no. 5.

The amounts of C availability index (K<sub>2</sub>SO<sub>4</sub>-C) were ranged from 2.33 to 3.69 mg g<sup>-1</sup>soil, 1.22 to 3.83 mg g<sup>-1</sup>soil and 1.54 to 3.05 mg g<sup>-1</sup>soil, accounting for 9.87 ± 14.71%, 10.24 ± 15.22% and 9.95 ± 17.17% (mean ± SD%, same below) of TC.

CFE-MBC across depth contained in different soils ranged from 0 to 1.82 mg g<sup>-1</sup>soil, 0.03 to 3.19 mg g<sup>-1</sup>soil, and 0 to 3.83 mg g<sup>-1</sup>soil. Rather than CFE-MBC, microbial biomass determined by CFI technique (CFI-MBC) was accounted across depth ranging from 3.22 to 8.53 mg g<sup>-1</sup>soil, 3.56 to 9.44 mg g<sup>-1</sup>soil and 2.95 to 9.82 mg g<sup>-1</sup>soil. However, a pool size of microbial biomass was significantly correlated with soil textures rather than soil layers. CFE-MBC corresponded to soil textural groups (fine, medium and coarse) for 11.87, 5.30 and 3.21% of TC and CFI-MBC accounted for 40.32 ± 74.81, 24.52 ± 52.37, 26.15 ± 51.95% of TC.

During 10 day incubation, CO<sub>2</sub> production across depth ranged from 1.94 to 4.81 mg g<sup>-1</sup>soil, 1.07 to 5.67 mg g<sup>-1</sup>soil and 1 to 5.14 mgCO<sub>2</sub>-C g<sup>-1</sup>soil with an average value of 2.82 ± 0.95 mgCO<sub>2</sub>-C g<sup>-1</sup>soil. The specific respiratory activity of MBC across depth ranged from 1.07 to 104.21 mgCO<sub>2</sub>-C g<sup>-1</sup>MBC 10d<sup>-1</sup>, 0.48 to 143.71 mgCO<sub>2</sub>-C g<sup>-1</sup>MBC 10d<sup>-1</sup> and 0.31 to 12.04 mgCO<sub>2</sub>-C g<sup>-1</sup>MBC 10d<sup>-1</sup> with the average values of 14.11, 25.07 and 2.93 mgCO<sub>2</sub>-C g<sup>-1</sup>MBC 10d<sup>-1</sup>, respectively.

There were moderate correlations between K<sub>2</sub>SO<sub>4</sub>-C and CFE-MBC ( $r = -0.55^{**}$ ,  $n = 54$ ) and between TC and CFI-MBC ( $r = -0.61^{**}$ ,  $n = 54$ ), as shown in Figure 7.2.

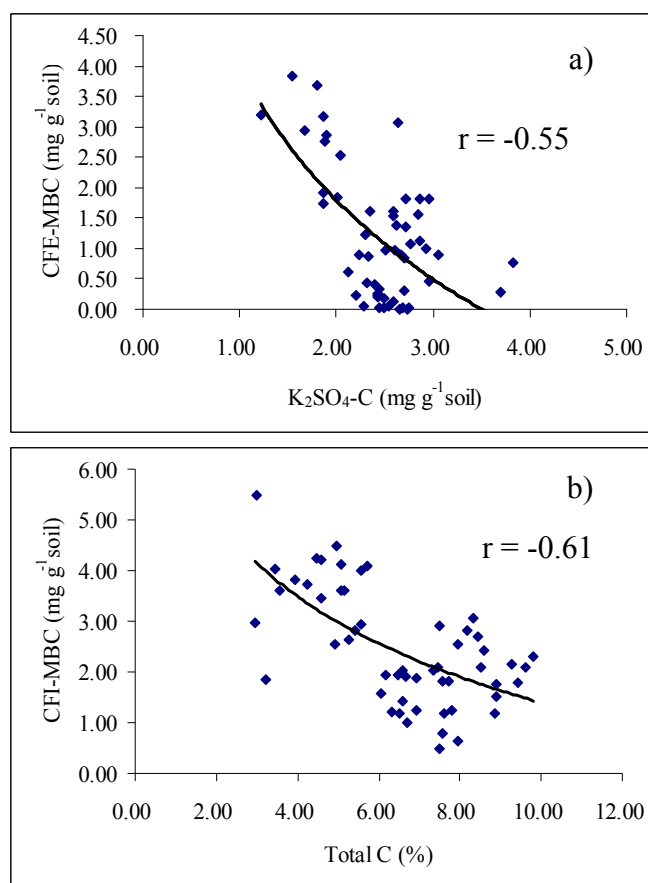


**Figure 7.2** Relationship between substrate availability index, total C and MBC.

### 7.5.2 Interactive effects of microbial biomass, substrate supply and other soil properties to soil respiration

The relationships of soil respiration rate to TC,  $K_2SO_4$ -C, MBC (CFE-MBC and CFI-MBC), TN, clay content, pH, EC, BD and their linear combinations were explored using stepwise multiple regressions.

The results showed that prediction of  $CO_2$ -C flush could be improved by combining TC and clay content into a linear equation ( $r = 0.84^*$ ,  $n = 54$ ), as shown in Eq. (7.5). However, the incremental  $F$  values for TC and clay content were 13 and 23, respectively, indicating that the increase in predicting  $CO_2$  emission gained by adding clay content to the equation is larger than by adding TC.

$$\text{CO}_2 - \text{C} (\text{mg g}^{-1}\text{soil}10\text{d}^{-1}) = 1.91 + 0.84 \text{TC} - 0.055\text{clay} \quad (7.5)$$

A stepwise multiple regression of soil C storages to MBC, substrate availability index and soil properties showed that TC from different vetiver soils could be accounted by a linear combination of electrical conductivity (EC), bulk density (BD) and years of continuous vetiver ( $r = 0.87^*$ ,  $n = 54$ ), as shown in Eq. (7.6). The incremental  $F$  values for EC, BD and years of continuous vetiver were 19, 9 and 22, respectively, which suggested that adding years of continuous vetiver into the equation had the largest effect on the prediction of soil C storages.

$$\text{TC} (\%) = 1.26 + 0.0066\text{EC} - 0.51\text{BD} + 0.33\text{year} \quad (7.6)$$

The ratio of  $\text{CO}_2\text{-C}/\text{TC}$  was negatively correlated with clay content ( $r = -0.64^{**}$ ,  $n = 54$ ) and had no or very slightly correlation with MBC and other soil properties. The predicting equation obtained from the stepwise regression was shown in Eq. (7.7).

$$\text{CO}_2 - \text{C}/\text{TC} (\text{mg g}^{-1}\text{soil}10\text{d}^{-1}) = 0.212 - 0.0039\text{clay} \quad (7.7)$$

Incorporating an organic C availability index ( $\text{K}_2\text{SO}_4\text{-C}$ ) and soil properties into the prediction of microbial biomass (CFE-MBC), the regression equation was shown in Eq. (7.8) ( $r = 0.65^*$ ,  $n = 54$ ), which CFE-MBC was negatively correlated with  $\text{K}_2\text{SO}_4\text{-C}$  and bulk density.

$$\text{CFE} - \text{MBC} (\text{mg g}^{-1}\text{soil}) = 4.94 - 1.23(\text{K}_2\text{SO}_4 - \text{C}) - 0.8\text{BD} \quad (7.8)$$

The microbial biomass determined by CFI method (CFI-MBC) was negatively correlated with the amount of TC and positively correlated with clay content ( $r = 0.78^*$ ,  $n = 54$ ), as shown in Eq. (7.9).

$$\text{CFI-MBC (mg g}^{-1}\text{soil)} = 7.73 - 1.14 \text{ TC} + 0.078 \text{ clay} \quad (7.9)$$

## 7.6 Discussion

### 7.6.1 Clay interactions with C storage

Clay content is known to play a role in determining microbial biomass and activities as well as influencing the composition of microbial community (McCulley and Burke, 2004). Soils with high clay content lead to more stabilization of SOC and higher MBC (Schimel et al., 1994). Consistent with this study that the clay content was positively correlated with microbial biomass (CFE-MBC) at subsoils ( $r = 0.56^*$  for 10 - 60 cm layer and  $r = 0.60^{**}$  for 60 - 120 cm layer; Table 7.5 and 7.6, respectively), but did not at the surface soils. Significant protective effect of clay on organic C decomposition was shown in the stepwise regression (Eq. (7.5) and (7.7)). Labile organic C was presumably unprotected by soil minerals, so the clay content played an important role in limiting the rate of  $\text{CO}_2$  production flush and  $\text{CO}_2\text{-C/TC}$ . Consequently, more clay contained low labile organic C, indicating by negative correlations between clay and  $\text{K}_2\text{SO}_4\text{-C}$  at subsoils ( $r = -0.68^{**}$  for 10 - 60 cm layer and  $r = -0.58^*$  for 60 - 120 cm layer; Table 7.5 and 7.6, respectively). The negative correlation between clay content and soil respiration rate per unit of TC ( $\text{CO}_2\text{-C/TC}$ ) in Eq. (7.7) was a common practice in the modeling of the C mineralisation rate reduced with increasing clay content (Jensen et al., 1994). At subsoils, this study found fine-textured soils had a more relative microbial population (CFE-MBC) than coarse-textured soils ( $r = -0.63^{**}$  for 10 - 60 cm layer and  $r = -0.52^*$  for 60 - 120 cm

layer; data did not show), but was opposite with Franzluebbbers et al. (1996). Investigations on structural diversity of microbial community using the phospholipids fatty acids pattern and 16S rRNA gene fragments gave strong evidence that microbes within the clay fraction was mostly due to bacteria; on the other hand, a high abundance of linoleic acid (18:2 $\omega$ 6c) in the coarse sand is attributed to a fungal-specific membrane component (Poll et al., 2003). This document could be used to explain a retention of plant lignin in more clay content because completely lignin degradation must need bacterial and fungal cooperation.

Under the study, CEC ranged between 0.4 and 10.7 cmol kg<sup>-1</sup>, which was not surprising for the kaolinitic soils (Hatphadon and Wiriyakitnathikun, 2002) (CEC of kaolinite ranging between 2 and 10 cmol kg<sup>-1</sup>; Velde, 1992). Due to the property of kaolinite, the soil has low activity of swelling, shrinking, CEC and base exchange capacity because the structure has no internal surface areas; therefore, ionic exchange or other reactions depend on the specific outer surface areas (Tan, 2000). Soils with higher clay contents, especially clays with higher CEC, could retain more C in the humus fractions and certain organic substances decomposed more slowly when in intimate contact with clays (Wattel-Koekkoek et al., 2003), but for kaolinite it was found a little effect on the stabilization of amino acid-C (Huang, 1990). Non-expanding layer silicates with the exception of kaolinite sorb little dissolved organic C (Kaiser and Zech, 2000). Compared to goethite, kaolinite is far less effective in the sorption of dissolved organic matter (Meier et al., 1999).

However, the considerable SOC retention in kaolinitic soils is partly due to significant contents of Fe and Al oxides, hydroxides and oxyhydroxides in the clay fraction, as demonstrated in studies using synthetic oxides (e.g. Kaiser and Zech, 1997; Varadachari et al., 1997) and oxide-bearing soils (e.g. Kahle et al., 2004). Study of Zinn et al. (2007) in kaolinitic soils showed that quantitative clay mineralogy showed that bulk SOC and clay-sized SOC pools were well correlated with Fe oxides in topsoil and

amorphous Al oxides in subsoil, but this mineralogical control is secondary to the textural control, since it depends on clay content.

Under slightly alkaline and high amounts of Ca and/or Na ions, the ions could be a bridge for amino acids and clays by the negatively charged amino acids (carboxyl group) could react with Ca and/or Na ions and function as a bridge connecting amino acids to the clay surfaces (Tan, 2000). Likewise, water or any of the metal ions, such as Ca, Al, Fe, or Mn, can serve as a bridge between the organic ligand (humic acid) and the clay micelle (Cheshire et al., 2000; D'Acqui et al., 1998), which is the way to avoid repulsion between negative charges of humic acid and clays (by most negative charges of humic acid receiving from dissociation of carboxylic groups and phenolic OH groups) (Spark et al., 1997). In the study, iron oxide in soils of site 1 to 7, referring red color (data did not show), assumed as a significant bridge between clay and organic C to sequester C.

Moreover, Schmitt et al. (2002) found that natural organic matter (NOM) adsorbed more strongly onto kaolinite compared to montmorillonite. This was due to the higher negative surface charge of montmorillonite and subsequent higher repulsive forces between montmorillonite and anionic NOM. Furthermore, adsorption onto kaolinite was strongly dependent on the pH value, increasing pH led to decreasing adsorption. Under Al, Fe and Zn present, about 50% of the DOC was adsorbed on kaolinite at pH 5, while at pH 7 about 25% was adsorbed. For montmorillonite, adsorption of NOM was about 10%. For pure polycarboxylic aromatic acids, Evanko and Dzombak (1998) reported no adsorption onto iron oxide surfaces at pH value exceeds the point of zero net surface charge ( $pH_{zpc}$ ). However, polyhydroxybenzenes particularly with hydroxyl groups in ortho-position could still attack electrophilic central metal ions of oxide surfaces at  $pH > pH_{zpc}$ . The authors addressed this effect to the formation of chelate surface complexes supported by hydroxyl groups in ortho-position.

### 7.6.2 Bulk density on total C accumulation

Bulk density (BD) is defined as the mass (weight) of a unit volume of dry soil, which for topsoils a value of 1.1 - 1.3 g cm<sup>-3</sup> is about normal whereas for subsoils values are usually greater than those for topsoils ranging from 1.3 - 1.7 g cm<sup>-3</sup> (Chesworth, 2008). High BD at deep soils limited microbe type and size community as caused by less oxygen supply. Likewise, a negative correlation between BD and CFE-MBC exhibited only the deep soils ( $r = -0.64^{**}$ ; Table 7.6) and corresponded the stepwise regression (Eq. (7.6)) with a slightly effect of BD on TC.

## 7.7 Conclusions

7.7.1 The rate of vetiver soil respiration under favorable temperature and moisture condition of different vetiver soils was restricted by clay content rather than by amount of total C, whereas the supply of biologically available substrate and microbial biomass had no significant effect on the soil respiration.

7.7.2 Due to the soil samples composed of more kaolinite, most reactions of SOC preservation such as adsorption and chelation depended on outer clay surfaces, bridges (such as metal ions or water), and pH condition.

7.7.3 Soil C storage assumed the preservation strongly by soil ions and by continuous vetiver.

## 7.8 References

- Blake, G.R. (1965). Bulk density. In American Society of Agronomy. **Methods of Soil Analysis** (ed. C.A.Black). Wisconsin: 374-390.
- Bouyoucos, G.J. (1962). Hydrometer method improved for making particle size analyses of soils. **Agronomy Journal** 54: 464-465.

- Broos, K., Macdonald, L.M., Warne, M.S.J., Heemsbergen, D.A., Barnes, M.B., Bell, M. and McLaughlin, M.J. (2007). Limitation of soil microbial biomass carbon as an indicator of soil pollution in the field. **Soil Biology and Biochemistry** 39: 2693-2695.
- Buscot, F and Varma, A. (eds.). (2005). **Microorganisms in Soils: Roles in Genesis and Functions**. Berlin: Springer.
- Chen, C.R., Condron, L.M., Davis, M.R. and Sherlock, R.R. (2000). Effects of afforestation on phosphorus and biological properties in a New Zealand grassland soil. **Plant and Soil** 220: 151-163.
- Cheshire, M.V., Dumat, C., Fraser, A.R., Hillier, S. and Staunton, S. (2000). The interaction between soil organic matter and soil clay minerals by selective removal and controlled addition of organic matter. **European Journal of Soil Science** 51: 497-509.
- Chesworth, W. (ed.). (2008). **Encyclopedia of Soil Science**. Dordrecht: Springer.
- D'Acqui, L.P., Daniele, E., Fornasier, F., Radaelli, L. and Ristorri, G.G. (1998). Interaction between clay microstructure, decomposition of plant residues and humification. **European Journal of Soil Science** 49: 579-587.
- Evanko, C.R. and Dzombak, D.A. (1998). Influence of structural features on sorption of NOM-analogue organic acids to goethite. **Environmental Science and Technology** 32: 2846-2855.
- Franzluebbers, A.J., Haney, R.L., Hons, F.M. and Zuberer, D.A. (1996). Determination of microbial biomass and nitrogen mineralization following rewetting of dried soil. **Soil Science Society of America Journal** 60: 1133-1139.
- Hargreaves, P.R., Brookes, P.C., Ross, G.J.S. and Poulton, P.R. (2003). Evaluating soil microbial biomass carbon as an indicator of long term environment change. **Soil Biology and Biochemistry** 35: 401-407.

- Hatphadon, A. and Wiriyaakitnathikun, W. (2002). Alfisols in Thailand. **Journal of Soils and Fertilizers** 24(1): 22-39.
- Huang, P.M. (1990). Role of soil minerals in transformations of natural organics and xenobiotics in soil. In J.-M. Bollage and G. Stotzky. (eds.). **Soil Biochemistry**. Vol. 6 (pp 29-116). New York: Mercel Dekker.
- Jenkinson, D.S. (1988). Determination of microbial biomass carbon and nitrogen in soil. In J.R. Wilson (ed.). **Advances in Nitrogen Cycling in Agricultural Ecosystems** (pp 368-386). Wallingford: CAB International.
- Jensen, C., Stougaard, B. and Ostergaard, H.S. (1994). Simulation of nitrogen dynamics in farm land areas of Denmark (1989 - 1993). **Soil Use and Management** 10: 111-118.
- Kahle, M., Kleber, M. and Jahn, R. (2004). Retention of dissolved organic matter by phyllosilicate and clay fractions in relation to mineral properties. **Organic Geochemistry** 35: 269-276.
- Kaiser, K. and Zech, W. (2000). Dissolved organic matter sorption by mineral constituents of subsoil clay fractions. **Journal of Plant Nutrition and Soil Science** 163: 531-535.
- Kaiser, K., and Zech, W. (1997). Competitive sorption of dissolved organic matter fractions to soils and related mineral phases. **Soil Science Society of America Journal** 61: 64-69.
- Kara, Ö. and Bolat, I. (2008). The effect of different land uses on soil microbial biomass carbon and nitrogen in Bartın Province. **Turkish Journal of Agriculture and Forestry** 32: 1-7.
- McCulley, R.L. and Burke, I.C. (2004). Microbial community composition across the Great Plains: Landscape versus regional variability. **Soil Science Society of America Journal** 68: 106-115.

- Meier, M., Namjesnik-Dejanovic, K., Maurice, P.A., Chin, Y.-P. and Aiken, G.R. (1999). Fractionation of aquatic natural organic matter upon sorption to goethite and kaolinite. **Chemical Geology** 157: 275-284.
- Poll, C., Thiede, A., Wermbter, N., Sessitsch, A. and Kandeler, E. (2003). Micro-scale distribution of microorganisms and microbial enzyme activities in a soil with long-term organic amendment. **European Journal of Soil Science** 54: 715-724.
- Schimel, D.S., Braswell, B.H., Holland, E.A., McKeown, R., Ojima, D.S., Painter, T.T., Parton, W.J. and Townsend, A.R. (1994). Climatic, edaphic, and biotic controls over storage and turnover of carbon in soils. **Global Biogeochemical Cycles** 8: 279-293.
- Schmitt, D., Taylor, H.E., Aiken, G.R., Roth, D.A. and Frimmel, F.H. (2002). Influence of natural organic matter on the adsorption of metal ions onto clay minerals. **Environmental Science and Technology** 36: 2932-2938.
- Spark, K.M., Wells, J.D. and Johnson, B.B. (1997). Characteristics of the sorption of humic acid by soil minerals. **Australian Journal of Soil Research** 35: 103-112.
- Tan, K.H. (2000). **Environmental Soil Science** (2nd ed.). New York: Marcel Dekker.
- Varadachari, C., Chattopadhyay, T. and Ghosh, K. (1997). Complexation of humic substances with oxides of iron and aluminum. **Soil Science** 162: 28-34.
- Velde, B. (1992). **Introduction to Clay Minerals: Chemistry, Origins, Uses, and Environmental Significance**. London; New York: Chapman & Hall.
- Voroney, R.P., Winter, J.P. and Beyaert, R.P. (1993). Soil microbial biomass C and N. In M.R. Carter. (ed.). **Soil Sampling and Methods of Analysis** (pp 277-286). Canadian Society of Soil Science, Boca Raton: Lewis Publishers.
- Walkley, A. and Black, A.I. (1934). An examination of the different method for determining soil organic matter, and proposed modification of the chromic acid titration method. **Soil Science** 37: 29-38.

- Wattel-Koekkoek, E.J.W., Buurman, P., Van der Plicht, J., Wattel, E. and Van Breemen, N. (2003). Mean residence time of kaolinite and smectite-associated soil organic matter. **European Journal of Soil Science** 54: 269-278.
- Zinn, Y.L., Lal, R., Bigham, J.M. and Resck, D.V.S. (2007). Edaphic controls on soil organic carbon retention in the Brazilian Cerrado: Texture and mineralogy. **Soil Science Society of America Journal** 71: 1204-1214.

**Table 7.1** Soil properties \*

Soil	Clay (%)	BD g cm <sup>-3</sup>	pH (H <sub>2</sub> O)	EC (μS cm <sup>-1</sup> )	Na	K	Mg	Ca	CEC	BS (%)
					(cmol kg <sup>-1</sup> soil)					
1/1	20.17	0.31	9.20	158.10	0.70	0.50	0.66	4.10	3.40	175.42
1/2	31.24	0.51	7.15	66.88	0.45	0.15	1.03	3.96	4.20	133.10
1/3	33.24	0.78	7.18	62.39	0.46	0.14	0.40	6.53	4.10	183.62
2/1	12.52	0.39	8.38	115.53	0.50	0.41	0.38	2.11	2.60	130.51
2/2	17.52	0.73	8.49	105.30	0.10	0.18	0.27	1.75	2.40	95.62
2/3	21.02	0.77	9.09	43.20	0.59	0.13	0.36	1.63	2.23	121.67
3/1	12.52	0.48	9.23	194.43	0.53	0.23	1.01	3.52	2.13	248.22
3/2	17.52	0.85	7.22	68.73	0.26	0.11	1.01	2.85	2.60	162.96
3/3	22.52	1.21	9.84	60.79	0.09	0.11	0.29	1.78	2.87	79.31
4/1	12.95	0.78	8.84	269.53	0.35	0.28	0.31	3.08	2.87	140.40
4/2	8.02	1.03	9.24	64.46	0.19	0.11	0.18	1.92	2.80	85.69
4/3	14.52	1.10	9.88	70.77	0.61	0.14	0.26	2.04	3.50	87.32
5/1	10.52	0.59	8.49	89.30	0.61	0.61	0.74	5.63	5.30	143.22
5/2	15.02	0.72	6.73	54.52	0.44	0.33	0.52	5.11	4.80	133.43
5/3	26.24	1.33	7.20	58.57	0.44	0.23	0.72	6.67	5.20	155.12
6/1	24.55	0.99	8.98	95.27	0.30	0.86	0.90	1.76	3.50	109.27
6/2	27.52	0.98	6.42	97.50	0.61	0.65	0.82	1.51	3.20	111.77
6/3	35.52	0.89	8.87	109.03	0.71	0.23	1.01	1.64	4.20	85.26
7/1	15.55	1.09	8.10	117.77	0.44	0.02	0.15	0.43	0.87	120.21
7/2	29.55	1.10	7.26	52.07	0.19	0.02	0.36	0.52	1.53	70.83
7/3	13.55	1.09	7.09	30.19	0.36	0.01	0.40	0.51	1.60	80.16
8/1	5.52	1.43	7.58	61.98	0.19	0.08	0.12	0.43	1.00	81.69
8/2	10.52	1.29	7.65	19.67	0.79	0.05	0.20	0.44	1.20	123.80
8/3	17.52	1.29	8.73	26.63	0.26	0.04	0.24	0.38	2.10	44.07
9/1	5.52	1.36	7.23	38.99	0.19	0.01	0.19	0.52	1.20	76.32
9/2	12.02	1.13	7.66	20.85	0.44	0.01	0.56	0.53	1.80	85.60
9/3	17.52	1.54	6.98	36.84	0.27	0.01	0.54	0.55	1.50	91.32
10/1	7.52	0.77	7.93	21.29	0.27	0.04	0.04	1.97	6.00	38.58
10/2	15.02	1.43	7.87	10.39	0.27	0.03	0.24	1.22	3.97	44.65
10/3	17.52	1.96	8.65	26.53	0.53	0.03	0.20	1.23	3.87	51.42
11/1	35.52	0.80	8.89	49.60	0.09	0.51	0.06	1.53	4.47	49.15
11/2	33.52	0.89	9.37	18.97	0.18	0.07	0.53	1.54	3.50	66.40
11/3	34.52	1.24	9.78	27.80	0.27	0.21	0.05	0.61	2.60	43.63
12/1	14.52	0.63	9.61	26.20	0.35	0.42	0.01	0.89	3.20	52.38
12/2	29.52	0.67	8.44	34.73	0.52	0.32	0.24	1.46	4.13	61.71
12/3	31.02	0.62	7.44	36.60	0.84	0.28	0.24	2.94	8.70	49.41
13/1	34.52	0.30	8.55	73.87	0.87	0.15	1.70	8.89	10.73	108.16
13/2	7.02	0.98	9.28	29.93	0.86	0.20	1.32	6.42	6.63	132.82
13/3	13.02	1.36	8.95	11.99	0.51	0.25	1.82	5.60	7.70	106.17

**Table 7.1** (Continued).

Soil	Clay (%)	BD g cm <sup>-3</sup>	pH (H <sub>2</sub> O)	EC (μS cm <sup>-1</sup> )	Na	K	Mg	Ca	CEC	BS (%)
						(cmol kg <sup>-1</sup> soil)				
14/1	25.52	0.45	11.61	99.88	0.54	0.03	0.13	0.56	0.60	210.07
14/2	35.23	0.48	9.70	148.67	0.18	0.03	0.10	0.54	0.53	160.42
14/3	38.8	1.95	8.22	97.07	1.14	0.01	0.20	0.53	0.60	312.54
15/1	4.52	1.47	9.21	17.17	0.34	0.14	0.64	3.14	6.27	68.13
15/2	6.8	1.54	8.22	19.90	0.77	0.15	0.50	3.04	5.03	88.57
15/3	13.3	1.41	8.60	44.57	0.65	0.03	1.31	2.53	5.60	80.86
16/1	30.52	0.51	6.85	57.50	0.41	1.13	1.32	7.53	4.40	236.26
16/2	26.02	0.62	6.95	36.47	0.40	0.98	1.17	7.48	4.40	227.70
16/3	39.52	1.18	6.81	44.57	0.33	0.69	1.33	7.71	4.60	218.70
17/1	28.52	0.74	6.68	50.00	0.52	0.09	0.22	3.95	0.80	597.87
17/2	44.52	1.14	7.03	38.27	0.35	0.01	0.06	3.52	0.60	657.69
17/3	45.52	1.20	6.46	51.70	0.52	0.09	0.18	3.13	0.60	654.21
18/1	4.67	1.06	8.59	31.50	0.41	0.08	0.22	3.03	0.40	932.62
18/2	5.67	1.27	8.29	11.29	0.62	0.07	0.24	3.75	0.47	1000.72
18/3	6.17	1.41	8.73	9.70	0.84	0.07	0.20	2.87	0.60	663.21

\*all values are the average by n = 3.

**Table 7.2** Substrate availability index, MBC and CO<sub>2</sub> production.

Soil	K <sub>2</sub> SO <sub>4</sub> -C <sup>a</sup>	CFE-MBC <sup>a</sup>	CFI-MBC <sup>a</sup>	CO <sub>2</sub> -C <sup>a</sup>	CO <sub>2</sub> -C/ CFE-MBC	TC <sup>b</sup>	TN <sup>b</sup>	TC/TN	C storage at 1.2 m (tC ha <sup>-1</sup> )
	(mg g <sup>-1</sup> soil)					(%)	(%)		
1/1	2.59	1.61	4.25	4.81	2.99	3.72	0.07	55.50	
1/2	1.87	1.73	5.06	3.60	2.08	3.60	0.07	52.92	290.96
1/3	1.54	3.83	5.55	3.11	0.81	4.01	0.06	72.47	
2/1	2.60	0.97	3.00	5.43	5.62	5.49	0.18	31.25	
2/2	2.28	0.06	4.45	4.39	71.46	4.23	0.09	45.01	364.20
2/3	2.65	0.00	5.71	2.85	NE <sup>c</sup>	4.08	0.08	50.33	
3/1	2.62	1.39	4.96	4.27	3.07	4.48	0.11	40.09	
3/2	2.92	1.00	4.94	4.67	4.67	2.55	0.09	28.58	321.91
3/3	1.90	2.86	5.28	4.12	1.44	2.64	0.11	23.81	
4/1	2.77	1.07	3.46	4.21	3.92	4.03	0.18	22.00	
4/2	2.35	1.61	5.41	5.67	3.52	2.83	0.19	14.81	372.96
4/3	2.96	1.81	2.95	5.14	2.85	2.96	0.21	13.96	
5/1	2.44	0.34	4.58	4.72	13.81	4.23	0.40	10.66	
5/2	2.44	0.03	3.95	4.32	143.71	3.82	0.32	12.07	450.12
5/3	1.87	2.76	5.16	4.12	1.49	3.60	0.29	12.43	
6/1	2.23	0.91	4.57	4.45	4.91	3.45	0.26	13.14	
6/2	2.51	0.96	3.56	3.67	3.83	3.59	0.28	13.07	430.70
6/3	1.86	1.91	5.08	3.94	2.06	4.13	0.21	19.97	
7/1	2.68	0.03	5.56	3.09	104.21	2.95	0.28	10.64	
7/2	2.21	0.24	8.45	2.01	8.28	2.71	0.24	11.12	371.87
7/3	2.32	0.45	7.48	2.70	6.06	2.92	0.20	14.34	
8/1	2.74	0.00	7.60	2.55	NE	1.19	0.13	9.02	
8/2	2.75	0.03	7.80	2.70	94.14	1.23	0.16	7.95	190.00
8/3	2.67	0.90	6.33	2.36	2.63	1.21	0.18	6.70	
9/1	2.72	1.36	3.22	3.05	2.25	1.84	0.22	8.56	
9/2	2.12	0.61	8.91	2.17	3.57	1.51	0.26	5.77	220.63
9/3	2.87	1.81	8.84	2.30	1.27	1.19	0.26	4.66	
10/1	2.54	0.06	6.19	3.29	56.96	1.93	0.26	7.46	
10/2	2.50	0.03	6.67	2.79	90.39	1.91	0.25	7.62	364.34
10/3	2.71	0.32	7.71	2.32	7.35	1.81	0.18	9.87	
11/1	2.70	0.85	8.33	1.97	2.33	3.07	0.35	8.83	
11/2	1.86	3.18	7.56	1.75	0.55	1.82	0.36	5.08	246.45
11/3	2.59	1.53	6.91	1.79	1.17	1.89	0.24	7.86	
12/1	2.32	0.88	8.17	2.52	2.88	2.81	0.28	9.90	
12/2	2.59	0.13	7.33	1.87	14.27	2.04	0.25	8.28	166.03
12/3	3.05	0.90	9.26	1.40	1.55	2.15	0.25	8.72	
13/1	2.96	0.46	7.46	2.62	5.68	2.10	0.28	7.55	
13/2	3.83	0.76	6.94	2.25	2.95	1.23	0.21	5.74	233.30
13/3	2.64	3.08	6.60	1.41	0.46	2.04	0.31	6.64	

**Table 7.2** (Continued).

Soil	K <sub>2</sub> SO <sub>4</sub> -C <sup>a</sup>	CFE-MBC <sup>a</sup>	CFI-MBC <sup>a</sup>	CO <sub>2</sub> -C <sup>a</sup>	CO <sub>2</sub> -C/ CFE-MBC	TC <sup>b</sup>	TN <sup>b</sup>	TC/TN	C storage at 1.2 m (tC ha <sup>-1</sup> )
			(mg g <sup>-1</sup> soil)			(%)	(%)		
14/1	3.69	0.27	6.57	2.01	7.37	1.42	0.30	4.65	
14/2	2.30	1.22	8.58	1.07	0.87	2.41	0.27	8.99	309.41
14/3	2.04	2.54	9.62	1.04	0.41	2.10	0.32	6.57	
15/1	2.43	0.20	7.56	2.43	12.39	0.78	0.31	2.50	
15/2	2.40	0.40	7.93	1.54	3.88	0.64	0.28	2.26	102.42
15/3	2.43	0.26	7.51	2.00	7.60	0.49	0.27	1.80	
16/1	2.71	1.82	8.53	1.94	1.07	2.09	0.28	7.46	
16/2	2.02	1.83	9.44	1.15	0.63	1.79	0.29	6.18	189.52
16/3	1.68	2.93	8.90	1.00	0.34	1.74	0.31	5.61	
17/1	2.43	0.24	6.49	2.06	8.76	1.93	0.26	7.34	
17/2	1.22	3.19	7.94	1.53	0.48	2.53	0.31	8.28	324.85
17/3	1.81	3.69	9.82	1.16	0.31	2.31	0.45	5.18	
18/1	2.85	1.56	6.49	2.64	1.69	1.17	0.35	3.31	
18/2	2.85	1.13	6.07	2.26	2.01	1.57	0.32	4.87	196.34
18/3	2.49	0.18	6.71	2.13	12.04	0.99	0.26	3.82	

<sup>a</sup>the values are the average with n = 10.

<sup>b</sup>the values are the average with n = 3.

<sup>c</sup>NE, Cannot be estimated.

**Table 7.3** Correlation matrix (*r* - values) for physical, chemical and microbiological characteristics in different vetiver soils (0 – 120 cm depth).

	CO <sub>2</sub> -C	CFE-MBC	CFI-MBC	K <sub>2</sub> SO <sub>4</sub> -C	TC	TN	Clay	BD	Ph	EC	Na	K	Mg	Ca	CEC	BS
CFE-MBC	-0.12															
CFI-MBC	-0.85**	0.10														
K <sub>2</sub> SO <sub>4</sub> -C	0.07	-0.55*	-0.14													
TC	0.67**	0.13	-0.61**	-0.24												
TN	-0.47**	0.12	0.42**	-0.06	-0.34*											
Clay	-0.36**	0.52**	0.35*	-0.48**	0.19	0.19										
BD	-0.01	-0.37**	0.06	0.03	-0.30*	-0.02	-0.41**									
Ph	0.14	-0.13	-0.17	0.37**	-0.02	-0.09	-0.19	-0.22								
EC	0.46**	0.03	-0.45**	0.05	0.62**	-0.29*	0.10	-0.02	0.21							
Na	-0.14	-0.07	0.09	0.23	-0.09	0.10	0.01	-0.10	0.01	0.02						
K	0.10	0.11	-0.05	-0.07	0.29*	0.15	0.20	-0.21	-0.15	0.17	-0.01					
Mg	0.01	0.19	-0.01	0.02	0.02	0.01	0.07	-0.20	-0.14	0.05	0.25	0.44**				
Ca	-0.02	0.33*	0.00	-0.10	0.10	0.13	0.16	-0.27*	-0.27*	0.00	0.26	0.50**	0.68**			
CEC	0.03	-0.02	0.02	0.13	0.01	0.07	0.03	-0.28*	0.02	-0.14	0.23	0.32*	0.61**	0.58**		
BS	-0.22	0.23	0.11	-0.09	-0.17	0.33*	0.03	0.12	-0.17	-0.10	0.22	-0.10	-0.15	0.21	-0.45**	
Year	0.83*	0.08	-0.74**	-0.19	0.82**	-0.35**	-0.02	-0.13	0.07	0.50**	-0.12	0.21	-0.02	0.02	-0.03	-0.09

\*. Correlation is significant at the 0.05 level (2 - tailed).

\*\* . Correlation is significant at the 0.01 level (2 - tailed).

**Table 7.4** Correlation matrix for physical, chemical and microbiological characteristics in different vetiver soils (0 - 10 cm depth).

	CO <sub>2</sub> -C	CFE-MBC	CFI-MBC	K <sub>2</sub> SO <sub>4</sub> -C	TC	TN	Clay	BD	Ph	EC	Na	K	Mg	Ca	CEC
CFE-MBC	0.23														
CFI-MBC	-0.83**	-0.23													
K <sub>2</sub> SO <sub>4</sub> -C	-0.35	-0.05	0.11												
TC	0.82**	0.29	-0.62**	-0.30											
TN	-0.43	-0.27	0.41	0.05	-0.31										
Clay	-0.31	0.07	0.36	0.21	0.08	0.17									
BD	0.03	-0.05	-0.11	-0.47	-0.31	-0.01	-0.65**								
Ph	0.09	-0.06	0.01	0.45	0.1	0.06	0.05	-0.59*							
EC	0.59**	0.26	-0.58*	0.14	0.65**	-0.55*	0.03	-0.19	0.25						
Na	0.27	0.04	-0.14	0.22	0.24	-0.09	0.29	-0.29	0.20	0.29					
K	0.22	0.49*	0.08	-0.36	0.39	0.09	0.42	-0.10	-0.10	0.08	0.01				
Mg	0.16	0.30	0.06	-0.05	0.15	-0.05	0.39	-0.09	-0.09	0.17	0.60**	0.47*			
Ca	0.02	0.25	0.18	-0.03	0.07	0.13	0.41	-0.01	-0.25	0.07	0.66**	0.40	0.85**		
CEC	0.02	-0.14	0.26	-0.16	0.01	0.24	0.30	-0.15	0.01	-0.16	0.34	0.23	0.63**	-0.66**	
BS	-0.19	0.29	0.05	0.13	-0.24	0.18	-0.05	0.23	-0.15	-0.10	0.19	-0.16	-0.06	0.16	-0.42

\*. Correlation is significant at the 0.05 level (2 - tailed).

\*\* . Correlation is significant at the 0.01 level (2 - tailed).

**Table 7.5** Correlation matrix for physical, chemical and microbiological characteristics in different vetiver soils (10 - 60 cm depth).

	CO <sub>2</sub> -C	CFE-MBC	CFI-MBC	K <sub>2</sub> SO <sub>4</sub> -C	TC	TN	Clay	BD	Ph	EC	Na	K	Mg	Ca	CEC
CFE-MBC	-0.22														
CFI-MBC	-0.83**	0.18													
K <sub>2</sub> SO <sub>4</sub> -C	0.19	-0.56*	-0.23												
TC	0.62**	-0.01	-0.70**	-0.29											
TN	-0.56*	0.29	0.36	-0.22	-0.34										
Clay	-0.36	0.56*	0.19	-0.68**	0.35	0.16									
BD	-0.10	-0.24	0.20	-0.05	-0.13	-0.03	-0.06								
Ph	-0.15	0.10	0.23	0.27	-0.33	0.05	-0.18	0.01							
EC	0.27	-0.02	-0.33	-0.09	0.66**	-0.32	0.36	0.37	0.10						
Na	-0.23	-0.26	0.05	0.52*	-0.52*	0.10	-0.44	0.00	-0.13	-0.44					
K	-0.04	0.03	-0.09	0.02	0.15	0.16	0.10	-0.31	-0.40	0.11	0.18				
Mg	0.07	0.09	-0.13	0.35	-0.03	-0.23	-0.10	-0.48*	-0.26	-0.05	0.32	0.53*			
Ca	-0.05	0.23	-0.07	0.17	-0.04	0.09	-0.12	-0.44	-0.20	-0.20	0.32	0.56*	0.65**		
CEC	0.10	-0.17	-0.19	0.37	-0.08	-0.04	-0.25	-0.59*	0.01	-0.24	0.35	0.43	0.65**	0.56*	
BS	-0.21	0.35	0.02	-0.09	-0.13	0.31	0.00	0.14	-0.09	-0.21	0.16	-0.10	-0.21	0.28	-0.48*

\*. Correlation is significant at the 0.05 level (2 - tailed).

\*\*. Correlation is significant at the 0.01 level (2 - tailed).

**Table 7.6** Correlation matrix for physical, chemical and microbiological characteristics in different vetiver soils (60 - 120 cm depth).

	CO <sub>2</sub> -C	CFE-MBC	CFI-MBC	K <sub>2</sub> SO <sub>4</sub> -C	TC	TN	Clay	BD	Ph	EC	Na	K	Mg	Ca	CEC
CFE-MBC	0.00														
CFI-MBC	-0.88**	0.03													
K <sub>2</sub> SO <sub>4</sub> -C	-0.04	-0.66**	-0.02												
TC	0.56*	0.30	-0.51*	-0.39											
TN	-0.54*	0.28	0.58*	-0.07	-0.43										
Clay	-0.29	0.60**	0.38	-0.58*	0.32	0.32									
BD	0.00	-0.64**	0.15	0.40	-0.47	-0.03	-0.53*								
Ph	0.39	-0.32	-0.60**	0.37	-0.01	-0.41	-0.38	-0.06							
EC	0.39	0.39	-0.20	-0.49*	0.54*	-0.04	0.54*	-0.29	0.02						
Na	-0.24	-0.19	0.22	0.11	0.00	0.27	0.10	0.00	-0.01	0.33					
K	-0.17	0.35	0.04	-0.29	0.13	0.18	0.43	-0.45	-0.19	0.03	-0.14				
Mg	-0.14	0.22	-0.03	-0.18	-0.08	0.24	-0.11	-0.09	-0.09	-0.03	-0.05	0.48*			
Ca	-0.06	0.57*	-0.07	-0.50*	0.21	0.16	0.23	-0.42	-0.41	-0.04	-0.07	0.69**	0.54*		
CEC	-0.01	0.08	-0.10	0.17	0.07	-0.02	-0.04	-0.22	0.01	-0.10	0.05	0.48*	0.57*	0.50*	
BS	-0.33	0.22	0.32	-0.34	-0.16	0.52*	0.19	-0.03	-0.32	-0.05	0.36	-0.06	-0.19	0.18	-0.49*

\*. Correlation is significant at the 0.05 level (2 - tailed).

\*\*.. Correlation is significant at the 0.01 level (2 - tailed).

# CHAPTER VIII

## CARBON FUNCTIONAL GROUPS IN VETIVER SOILS

### BY 1D <sup>1</sup>H NMR STUDY

#### 8.1 Abstract

This chapter used one-dimension proton nuclear magnetic resonance (1D <sup>1</sup>H NMR) spectroscopy to characterize C functional groups accumulated in different vetiver soils. Almost spectra illustrated similarly chemical shifts, but differed in resonance intensities. As a result, C functional groups in soils presented through 1D <sup>1</sup>H NMR spectra were attributed to alkyl of proteins/peptides and polysaccharides (e.g. amine, lignin, and aryl amine); however, aromatic compounds were negligently resonated. The <sup>1</sup>H intensities increased with an increasing of soil profiles, except site 6 of continuous vetiver for 7 years. Physically protected biodegradation such as spontaneous cross-linking and repacking polysaccharides at cell wall, rapidly water removal from intermediate surroundings of macromolecules, or encapsulation for labile proteins, were suggested the main reasons of low resonance signal at the deep soil of continuous vetiver for 7 years. Dominant alkyl group presentation in almost vetiver soils indicted to be during a processing of humification. The resonant signals ( $\delta$  3.8 ppm) which referring to lignin degradation could be found in most vetiver soils that mean lignin was rapidly and slowly decomposed. Consistently, a recently lignin model by isotope radio of Rasse et al. (2006) calling a two compartment model explained a large lignin pool was rapid turnover within 1 year and a smaller pool was substantially slower turnover.

In conclusion, chemicals releasing in vetiver soils under the study composed of more protective proteins/peptides and polysaccharides and derivatives of lignin degradation. Also, a humification process was progressive coupling with a biodegradation.

**Keywords:** 1D  $^1\text{H}$  NMR, lignin, alkyl, physically protected biodegradation

## 8.2 Introduction

In nature, soils comprise of many mixtures of decayed plant and animal biomass. Early characterization studies of soil substances employed classical structural chemistry, chemical degradation and, more recently, spectroscopic techniques.

One-dimensional proton (1D  $^1\text{H}$ ) NMR spectroscopy provides a fast, nondestructive, and quantitative analysis rich in molecular structure information in addition to its traditional application to elucidate chemical structures. 1D  $^1\text{H}$  NMR is especially well-suited for quantification based on the fact that all protons show an identical response factor in solution samples, regardless of the molecules to which they are attached (Simpson et al., 2001). The peak patterns for each molecule in a  $^1\text{H}$  NMR spectrum are often very distinctive and unique, and they are indicative of the chemical linkages between different atoms and chemical groups. All of these features attributed 1D  $^1\text{H}$  NMR very convenient for rapid identification and quantification using well-resolved peaks for a given analyze (Cardozaa et al., 2004).

As previous chapter, different vetiver soils were estimated C contents via total C, microbial biomass and  $\text{CO}_2$  evolution, but lack of a characterization of C functional groups, which the results could be consisted in consideration of C sequestration through vetiver plantation. Therefore, this chapter further used some vetiver soils from chapter VII to characterize C functional groups but the study scoped only surface soils, except site 1, 6

and 7 were done across soil profiles. The reason to select only surface soils was because NMR spectroscopy could not signal if the C concentration of the sample was too low.

### **8.3 Objectives of this chapter**

8.3.1 To characterize C functional groups of different vetiver soils.

8.3.2 To find relationships between C functional groups and vetiver soils.

### **8.4 Materials and methods**

#### **8.4.1 Soil property measurement**

Soils were sampling from 8 site followed to chapter VII, as seen the briefly of soil physical and chemical properties in Table 8.1 (more detail in Appendix C). The methods for identifying/quantifying soil types used hydrometer method; soil  $\text{pH}_{(\text{H}_2\text{O})}$  used ratio (1:5 soil water ratio); Cation Exchange Capacity used Büchner funnel filtration; and total C and total N used LECO analyzer (CNS 2000)



**Table 8.1** Some physical and chemical properties of soils collecting from the study sites in Nakhon Ratchasima (more details showing in Appendix C).

Sign	Location	Cont.vetiver (year)	depth (cm)	Soil type	BD g cm <sup>-3</sup>	pH (H <sub>2</sub> O)	CEC (cmol kg <sup>-1</sup> )	BS TC TN		
								(%)		
1/1	TTDI	5	0-10	sandy clay loam	0.31	9.20	3.40	175.42	3.72	0.07
1/2	TTDI	5	10-60	sandy clay loam	0.51	7.15	4.20	133.10	3.60	0.07
1/3	TTDI	5	60-120	sandy clay loam	0.78	7.18	4.10	183.62	4.01	0.06
6/1	TTDI	7	0-10	sandy clay loam	0.99	8.98	3.50	109.27	3.45	0.26
6/2	TTDI	7	10-60	sandy clay loam	0.98	6.42	3.20	111.77	3.59	0.28
6/3	TTDI	7	60-120	sandy clay loam	0.89	8.87	4.20	85.26	4.13	0.21
7/1	TTDI	3	0-10	sandy loam	1.09	8.10	0.87	120.21	2.95	0.28
7/2	TTDI	3	10-60	sandy clay loam	1.10	7.26	1.53	70.83	2.71	0.24
7/3	TTDI	3	60-120	loam	1.09	7.09	1.60	80.16	2.92	0.20

**Table 8.1** (Continued).

Sign	Location	Cont.vetiver (year)	depth (cm)	Soil type	BD g cm <sup>-3</sup>	pH (H <sub>2</sub> O)	CEC (cmol kg <sup>-1</sup> )	BS	TC	TN
								(% )		
10/1	Kam Tha Lae Soa	3	0-10	loamy sand	0.77	7.93	6.00	38.58	1.93	0.26
11/1	Soang Sang	3	0-10	sandy clay	0.77	8.89	4.47	49.15	3.07	0.35
16/1	Pak Chong	2	0-10	sandy clay loam	0.51	6.85	4.40	236.26	2.09	0.28
17/1	LDD, Pak Chong	3	0-10	clay loam	0.74	6.68	0.80	597.87	1.93	0.26
18/1	LDD, Jo Hor, Muang	3	0-10	loamy sand	1.06	8.59	0.40	932.62	1.17	0.35

#### 8.4.2 Soil preparation for NMR measurement

The procedure of soil preparation for NMR analysis showed in Figure 8.1 followed to the outline of Schnitzer (1982).

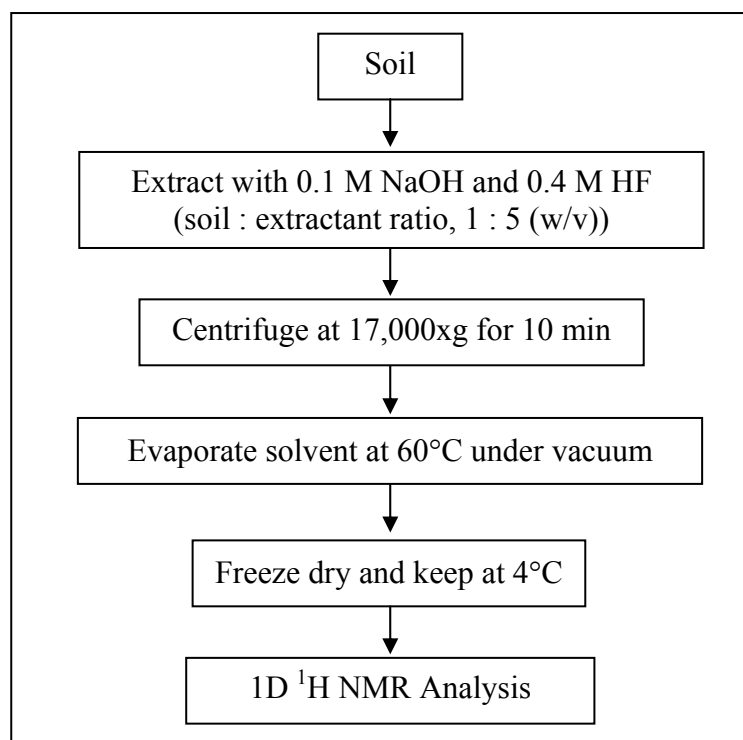


**Figure 8.1** The procedure of soil sample preparation for NMR analysis.

#### 8.4.3 Conditions for <sup>1</sup>H NMR study

Thirty milligrams of the freeze-dried material was dissolved in 600  $\mu$ L of D<sub>2</sub>O in a 5 mm NMR tube. Proton was obtained on a Varian Unity INOVA 300 MHz, a liquid-state NMR spectroscopy at a calibrated probe temperature of 30°C. A pulse of 90° was calibrated for each sample before data acquisition. The conditions used were: spectrometer frequency, 300 MHz; spectral width, 4801.9 Hz with an acquisition time of 3.742 s; inverse-gated decoupling; delay time, 1.67 s; and line broadening factor, 100 Hz. This factor was used to enhance the characteristic broad signals of extracted organic matter. Chemical shifts ( $\delta$ ) were given in parts per million relative to the resonance of an external standard of TSP (3-[trimethylsilyl] propionic acid). The signal areas were calculated by

electronic integration and signal assignments were made according to literature data (Kögel-Knabner et al., 1992). Both the lock and shimming were optimized automatically for each NMR sample.

#### 8.4.4 1D $^1\text{H}$ NMR analysis

According to substitution on tetrahedral C, it results to form  $\text{CH}_3\text{X}$ ,  $\text{XCH}_2\text{Y}$  and  $\text{XCH}(\text{Y})\text{Z}$ . By this, the remaining hydrogens in tetrahedral C reflect  $^1\text{H}$  NMR spectra. Base on literatures (Kanjanapoom, 2009; Macomber, 1998), the formula used to preliminarily characterize C functional groups from 1D  $^1\text{H}$  NMR spectra was expressed in Eq. (8.1), which  $^1\text{H}$  substituent parameters could be checked from Table 8.2 (for substituents on tetrahedral C), Table 8.3 (for substituents on vinyl C), and Table 8.4 (for substituents on aromatic C). Eq. (8.2) was specific to two substituents on tetrahedral C.

$$\delta_{\text{cal}} = \text{base value} + \sum(\Delta\delta_x) \quad \dots(8.1)$$

$$\Delta\delta(\text{XCH}_2\text{Y}) = 0.23 + \Delta\delta_{\alpha\text{-X}} + \Delta\delta_{\alpha\text{-Y}} \quad \dots(8.2)$$

where the base value is the chemical shift of the appropriate unsubstituted molecule (e.g.  $\delta$  0.23 for methane,  $\delta$  5.28 for ethylene and  $\delta$  7.27 for benzene) and  $\sum(\Delta\delta_x)$  is the sum of  $\Delta\delta_x$  values for all contributing substituents.

**Table 8.2**  $^1\text{H}$  Substituent parameters ( $\Delta\delta_x$ , ppm) for substituents on tetrahedral carbons<sup>a</sup>.

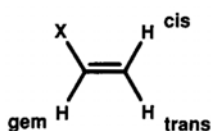
Group $X^b$	$\Delta\delta_{\alpha-x}$	$\Delta\delta_{\beta-x}^c$	Group $X^b$	$\Delta\delta_{\alpha-x}$	$\Delta\delta_{\beta-x}^c$
-R	0.62	0.01	-SPh	2.27	
-CF <sub>3</sub>	1.20		-S(=O) <sub>1,2</sub> R	2.37	
-CH=C(R/H) <sub>2</sub>	1.37	0.15	-Br	2.47	0.95
-C≡C(R/H)	1.50	0.35	-SC≡N	2.47	
-C(=O)OR	1.77	0.33	-N=CR <sub>2</sub>	2.67	
-C(=O)N(R/H) <sub>2</sub>	1.77	0.25	-N <sup>+</sup> (R/H) <sub>3</sub>	2.72	0.55
-C(=O)OH	1.87	0.33	-NHC(=O)R	2.72	0.25
-S(R/H)	1.87	0.43	-SO <sub>3</sub> (R/H)	2.77	
-C(=O)R	1.87	0.20	-Cl	2.80	0.70
-C≡N	1.92	0.43	-O(R/H)	2.97	0.35
-I	1.94	0.90	-P <sup>+</sup> Cl <sub>3</sub>	3.07	
-C(=O)H	1.97	0.25	-N=C=S	3.17	
-NR <sub>2</sub>	2.00	0.20	-OC(=O)(R/H)	3.40	0.45
-Ph	2.00	0.33	-OSO <sub>2</sub> R	3.47	
PR <sub>2</sub> , -P(=O)R <sub>2</sub>	2.00		-OPh	3.60	0.45
-C(=O)Ph	2.17	0.33	-OC(=O)Ph	3.60	0.80
-SSR	2.17		-NO <sub>2</sub>	3.82	0.75
-NH <sub>2</sub>	2.27		-F	4.00	0.70

<sup>a</sup>Compiled from Silverstein et al. (1991 quoted in Macomber, 1998). All numeric data present in ppm. When calculating the chemical shift of a methylene group (X-CH<sub>2</sub>-Y), decrease by 10% the value calculated from Eq. (8.1) [See Eq. (8.2)].

<sup>b</sup>R represents any alkyl group; R/H represents either alkyl or hydrogen; Ph represent phenyl.

<sup>c</sup>When using these values to calculate the methyl chemical shift of CH<sub>3</sub>CH<sub>2</sub>X, be sure to add 0.62 ppm for the effect of the CH<sub>2</sub> group.

**Table 8.3** Substituent parameters ( $\Delta\delta_x$ , ppm) for vinyl hydrogen chemical shift<sup>a</sup>.



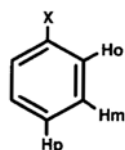
-X	$\Delta\delta_{\text{gem}}$	$\Delta\delta_{\text{cis}}$	$\Delta\delta_{\text{tran}}$
-C≡N	0.23	0.78	0.58
-R(alkyl)	0.44	-0.26	-0.29
-C≡CR	0.50	0.35	0.10
-CH <sub>2</sub> SR	0.53	-0.15	-0.15
-CH <sub>2</sub> NR <sub>2</sub>	0.66	-0.05	-0.23
-CH <sub>2</sub> OR	0.67	-0.02	-0.07
-CH <sub>2</sub> I	0.67	-0.02	-0.07
-NR <sub>2</sub>	0.69(2.30)	-1.19(-0.73)	-1.31(-0.81)
-Cycloalkenyl <sup>b</sup>	0.71	-0.33	-0.30
-CH <sub>2</sub> Cl	0.72	0.12	0.07
-CH <sub>2</sub> Br	0.72	0.12	0.07
-C(=O)OR	0.84(0.68)	1.15(1.02)	0.56(0.33)
-CH=CH <sub>2</sub>	0.98(1.26)	-0.04(0.08)	-0.21(-0.01)

**Table 8.3** (Continued).

-X	$\Delta\delta_{\text{gem}}$	$\Delta\delta_{\text{cis}}$	$\Delta\delta_{\text{tran}}$
-C(=O)OH	1.00(0.69)	1.35(0.97)	0.74(0.39)
-Cl	1.00	0.19	0.03
-SR	1.00	-0.24	-0.04
-C(=O)H	1.03	0.97	1.21
-Br	1.04	0.40	0.55
-C(=O)R	1.10(1.06)	1.13(1.01)	0.81(0.95)
-C(=O)Cl	1.10	1.41	0.99
-OR	1.18(1.14)	-1.06(-0.65)	-1.28(-1.05)
-Ph	1.35	0.37	-0.10
-C(=O)NR <sub>2</sub>	1.37	0.93	0.35
-SO <sub>2</sub> R	1.58	1.15	0.95
-OC(=O)R	2.09	-0.40	-0.67

<sup>a</sup>Data (in ppm) from Silverstein et al. (1991 quoted in Macomber, 1998). Recall that a negative value of  $\Delta\delta$  corresponds to an upfield shift. The data in parentheses are to be used if either the X group or the C=C is further conjugated.

<sup>b</sup>The double bond is endocyclic to a ring.

**Table 8.4** Aromatic substituent parameters ( $\Delta\delta_x$ , ppm)<sup>a</sup>.

X	H <sub>ortho</sub>	H <sub>meta</sub>	H <sub>para</sub>	X	H <sub>ortho</sub>	H <sub>meta</sub>	H <sub>para</sub>
-CH <sub>3</sub>	-0.17	-0.09	-0.18	-I	0.40	-0.26	-0.03
-CH <sub>2</sub> CH <sub>3</sub>	-0.15	-0.06	-0.18	-OH	-0.50	-0.14	-0.4
-CH(CH <sub>3</sub> ) <sub>2</sub>	-0.14	-0.09	-0.18	-OR	-0.27	-0.08	-0.27
-C(CH <sub>3</sub> ) <sub>3</sub>	0.01	-0.10	-0.24	-OC(=O)R	-0.22	0	0
-CH=CH <sub>2</sub>	0	0	0	-OSO <sub>2</sub> Ar	-0.26	-0.05	0
-C≡CH	0.20	0	0	-C(=O)H	0.58	0.21	0.27
-Ph	0.18	0	0.08	-C(=O)R	0.64	0.09	0.3
-CF <sub>3</sub>	0.25	0.25	0.25	-C(=O)OH	0.80	0.14	0.20
-CH <sub>2</sub> Cl	0	0.01	0	-C(=O)OR	0.74	0.07	0.20
-CHCl <sub>2</sub>	0.10	0.06	0.10	-C(=O)Cl	0.83	0.16	0.30
-CCl <sub>3</sub>	0.80	0.20	0.20	-C≡N	0.27	0.11	0.30
-CH <sub>2</sub> OH	-0.10	-0.10	-0.10	-NH <sub>2</sub>	-0.75	-0.24	-0.63
-CH <sub>2</sub> OR	0	0	0	-NR <sub>2</sub>	-0.60	-0.10	-0.62
-CH <sub>2</sub> NH <sub>2</sub>	0.0	0.0	0.0	-NHC(=O)R	0.23		
-SR	-0.03	0	0	-N <sup>+</sup> H <sub>3</sub>	0.63	0.25	0.25
-F	-0.30	-0.02	-0.22	-NO <sub>2</sub>	0.95	0.17	0.33
-Cl	0.02	-0.06	-0.04	-N=C=O	-0.20	-0.20	-0.20
-Br	0.22	-0.13	-0.03				

<sup>a</sup>Data abstracted from Gunther (1973) and Silverstein et al. (1991) both were quoted in Macomber (1998).

### 8.4.5 $^1\text{H}$ NMR information

$^1\text{H}$  NMR chemical shifts associated C functional groups could be also investigated from Figure 8.2. However, this summary showed only the mainly C groups, it still needs more information e.g.  $^1\text{H}$  integration and spectral features.

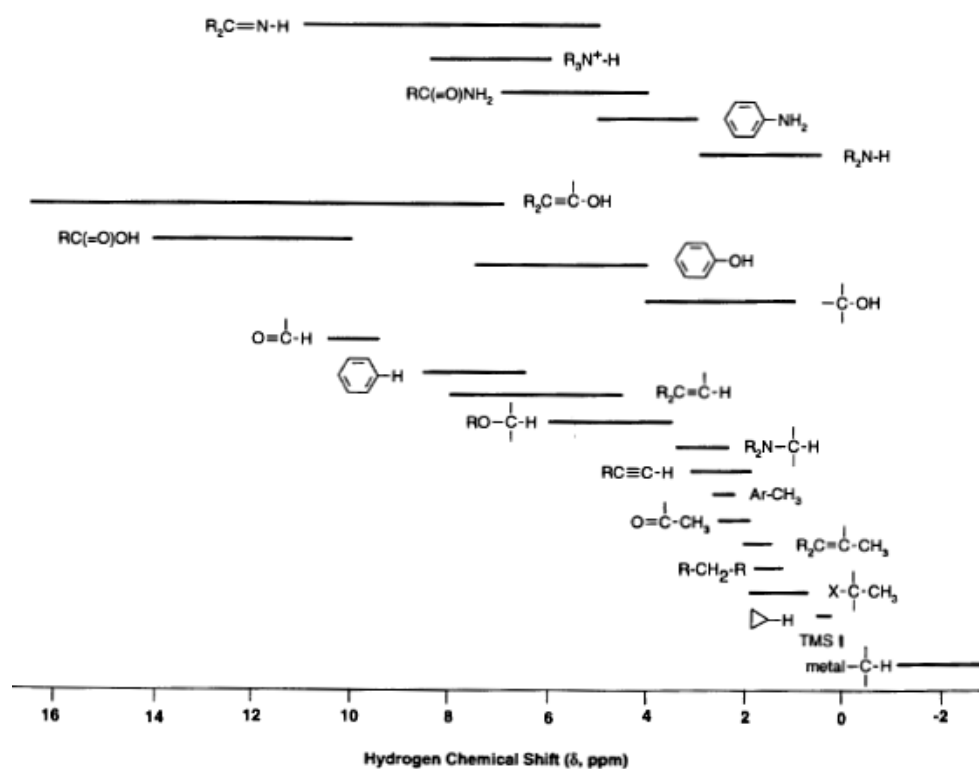


**Figure 8.2**  $^1\text{H}$  NMR chemical shift information (Macomber, 1998).

## 8.5 Results

Chemical components in soil samples could be characterized by 1D  $^1\text{H}$  NMR spectroscopy and expressed on  $^1\text{H}$  chemical shift. As a result, the spectra were mixtures of broad and singlet signals. Comparative C functional groups on soil profiles and soil types could be seen in Figure 8.3 to Figure 8.8. Although most spectra signals were similarly, they differed in hydrogen intensities (see Appendix D). According to results of hydrogen information and data literatures (Adani et al., 2006; Kanjanapoom, 2009; Macomber, 1998), signals resonated into regions of aliphatic ( $\delta$  0.5 - 2.5 ppm), carbohydrate/peptide/other moieties such as esters, methoxyl and hydroxyl ( $\delta$  3.0 - 5.5 ppm) and formyl hydrogen ( $\delta$  8 - 10.5 ppm), while aromatic ( $\delta$  6.5 - 8.0 ppm) were negligible or absent in the soil samples.

### 8.5.1 Spectra lower than $\delta$ 2.5 ppm

In particular, unclear of small broad spectra located lower than  $\delta$  2.5 ppm attributed to protons of alkyl groups ( $-\text{CH}_3$ ,  $-\text{CH}_2$ ). And, the spin-spin coupling between quartet signal at  $\delta$   $\sim$ 1.1 ppm and the triplet signals at  $\delta$   $\sim$ 1.8 ppm referred to the interaction of methyl and methylene group bonded substituent groups ( $\text{CH}_3\text{CH}_2\text{X}$ ). As from the  $^1\text{H}$  substituent parameter calculation, the "X" under  $\Delta\delta_{\beta\text{-X}}$  related to carbonyl [ $-\text{C}(=\text{O})\text{R}$ ,  $-\text{C}(=\text{O})\text{H}$ ], N-alkyl [ $-\text{NHC}(=\text{O})\text{R}$ ] or  $-\text{NR}_2$  groups. Small peak at  $\delta$   $\sim$ 2.3 ppm was contributed protons of methyl, with the substituents of carbonyl [ $-\text{C}(=\text{O})\text{Ph}$ ] or phenyl groups [ $-\text{Ph}$ ]. Short peak at  $\delta$   $\sim$ 1.0 ppm could link to sugar in plant species like L-rhamnose. L-rhamnose can be found in common plant and its methyl group at  $\text{C}_6$  presents specific chemical shift at  $\sim$   $\delta$  1.0 ppm (Kanjanapoom, 2009).

### 8.5.2 Spectra $\delta$ 3.0 - 5.5 ppm

As the previous saying, signals covered  $\delta$  3.0 - 5.5 ppm influencing several compounds, mainly carbohydrate and/or peptide. Many studies on C sequestration are expected to find recalcitrant C like lignin or lignin components, which helps to preserve C in surface or subsoils. Lignin of graminoids contains sinapyl and coniferyl alcohol, up to 30% p-coumaryl alcohol and small amount of cinnamic acid (Lin and Dence, 1992 quoted in Larcher, 2001). As a result of the  $^1\text{H}$  calculation, protons in methylene group ( $\text{RCH}_2\text{-OH}$ ) and methyl group ( $\text{PhO-CH}_3$ ) in lignin structure contributed the expected chemical shifts at  $\delta$  ( $\Delta\delta_{\alpha-x}$ ) 3.4 ppm [ $0.9$  ( $0.23 + 0.62 + 2.97$ )] and  $\delta$  ( $\Delta\delta_{\alpha-x}$ ) 3.8 ppm [ $0.23 + 3.60$ ], respectively. This study, spectra of lignin (or its derivatives) were found in all experiments, except soil 6/3 (the deep soil of 7 years of continuous vetiver) (Figure 8.3).

### 8.5.3 Spectra $\delta$ ~8.3 ppm

The small peak at  $\delta$  ~8.3 ppm was estimated to formic acid which the formyl hydrogen ( $\text{H}(\text{C}=\text{O})\text{OH/OR/NR}_2$ ) resonated at  $\delta$  8 - 10.5 ppm because the carbonyl group has a strong deshielding effect by virtue of the highly electronegative oxygen. Almost soil samples demonstrated resonance at this position, except soil 11/1 and 17/1 (both were the surface soils of 3 years of continuous vetiver).

### 8.5.4 Effects of soil profiles and soil types

Comparative soil layers, C components of 3 and 5 years of continuous vetiver (site 7 and 1, respectively) exhibited higher contents with deeper soil, while those signals of 7 years (site 6) were too low resonance. When comparing soil types, physical soil was significant differences between sand and clay particles of surface soils of site 15 and 16,

respectively. The sand soil of site 15 accumulated only alkyl groups and lost almost organic C. Unlikely, surface soils of site 11 and 17 disappeared of formic acid and lignin structure, even the two sites contained clay particles (sandy clay and clay loam, respectively)

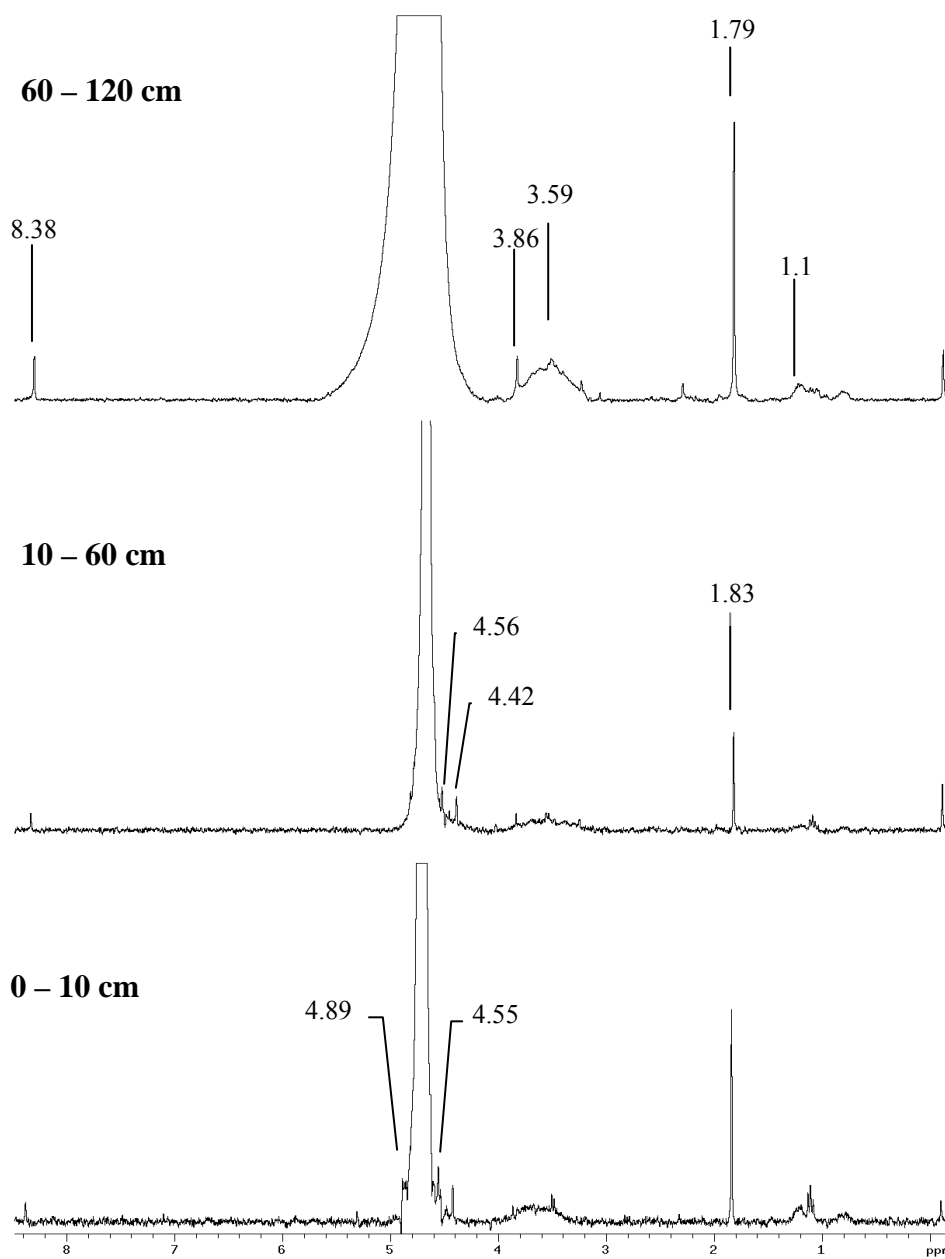


**Figure 8.3** 1D  $^1\text{H}$  NMR spectra of continuous vetiver for 3 year soils, samplings from TTDI. Spectra arranged across soil profiles.

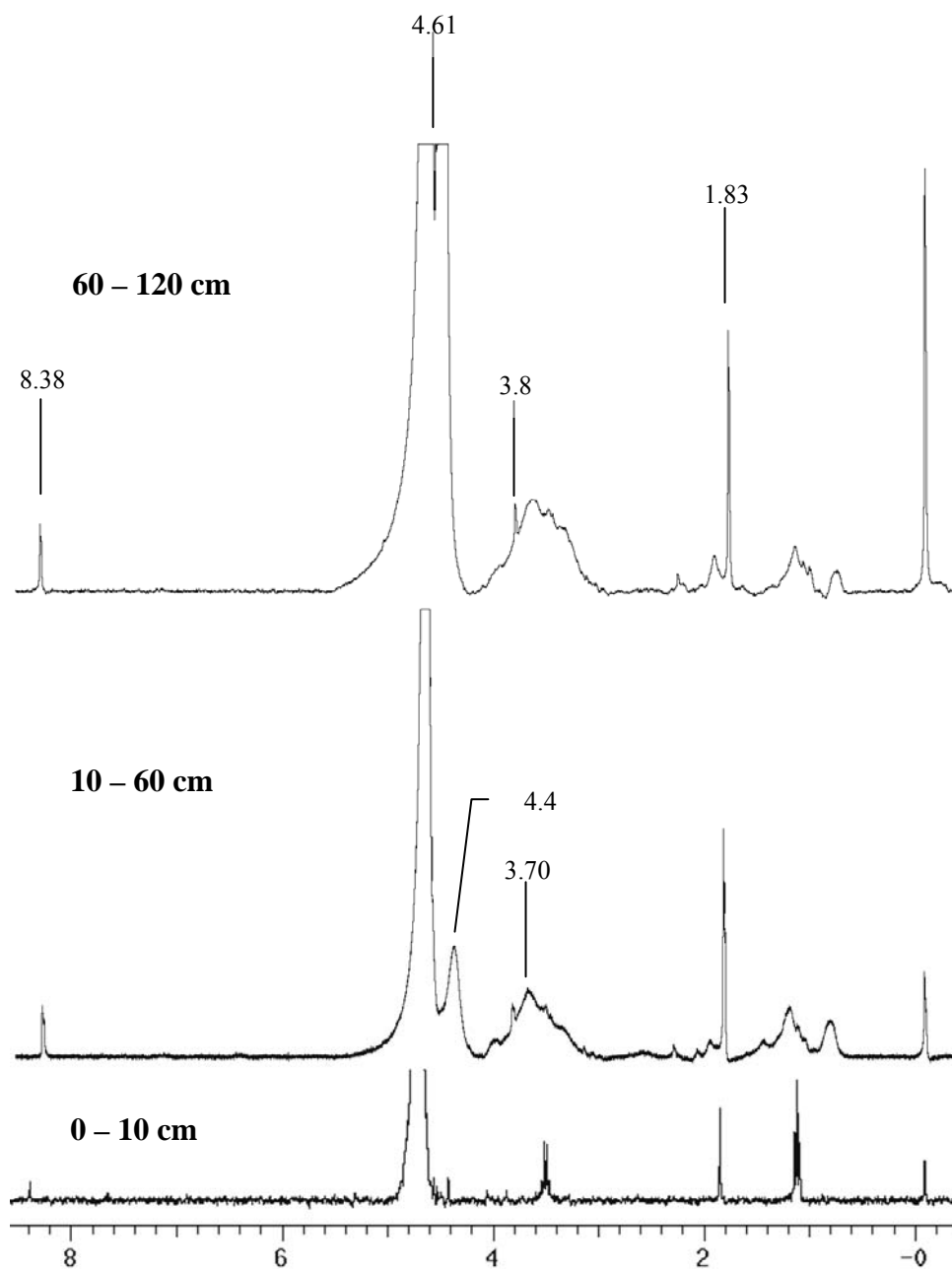


**Figure 8.4** 1D  $^1\text{H}$  NMR spectra of continuous vetiver for 5 year soils, samplings from TTDI. Spectra arranged across soil profiles.

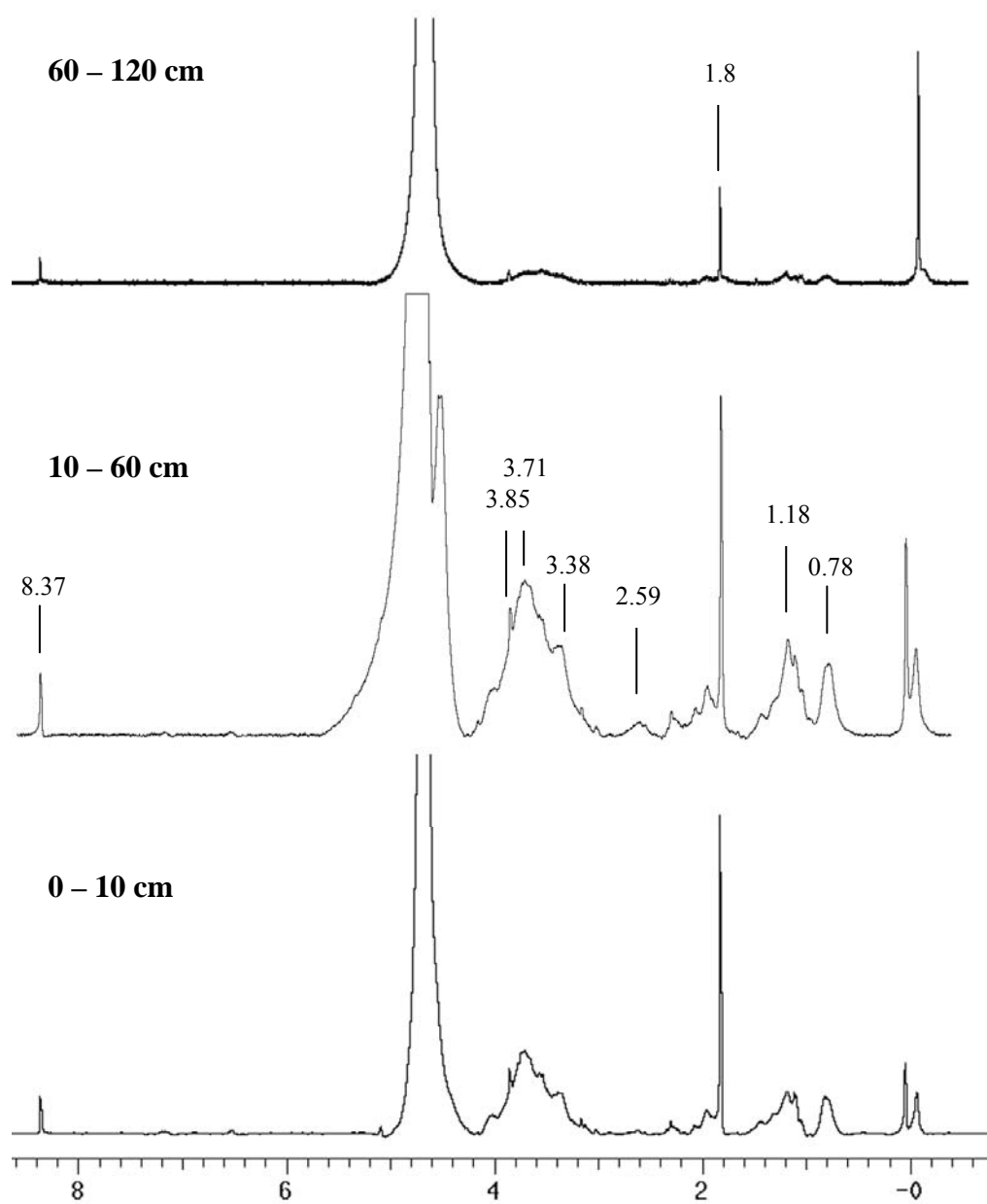


**Figure 8.5** 1D  $^1\text{H}$  NMR spectra of continuous vetiver for 7 year soils, samplings from TTDI. Spectra arranged across soil profiles.

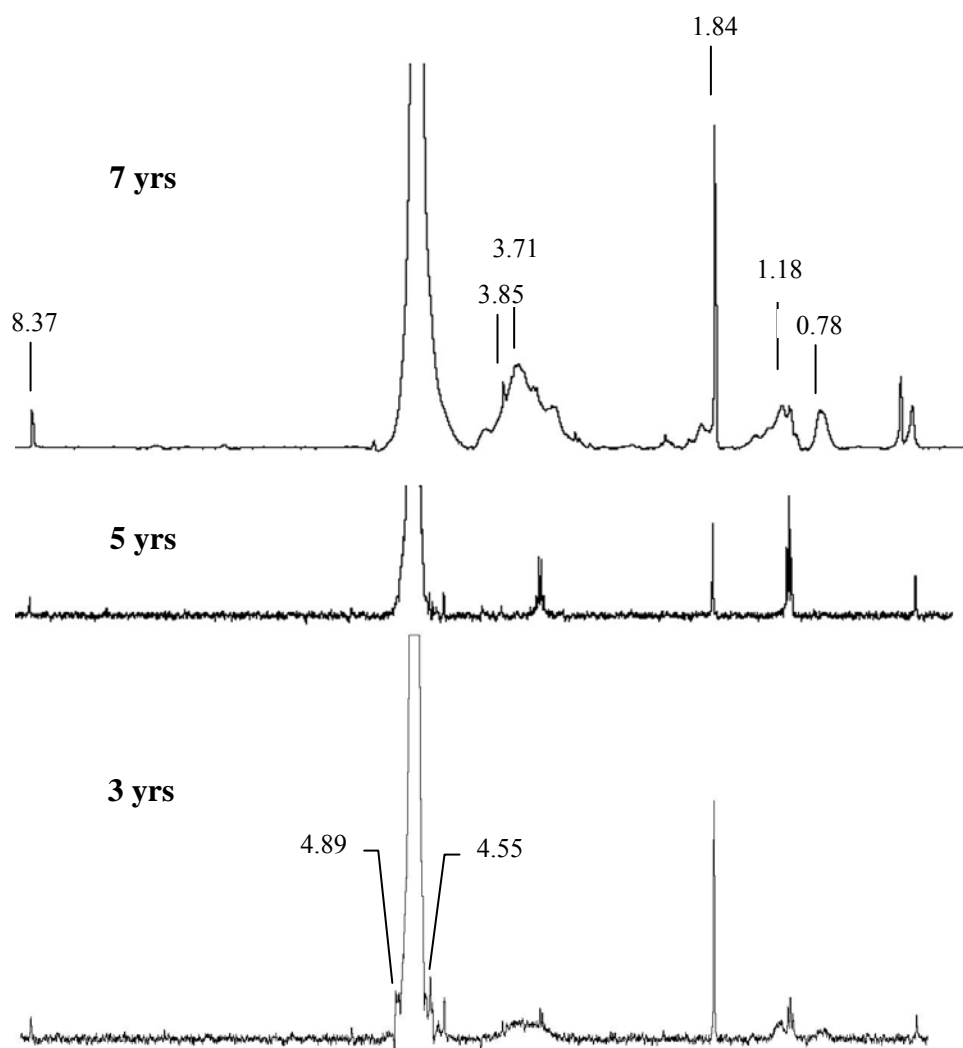


**Figure 8.6** 1D  $^1\text{H}$  NMR spectra of surface soils of continuous vetiver for 3, 5 and 7 years, samplings from soil 7/1, 1/1 and 6/1 at TTDI, respectively.

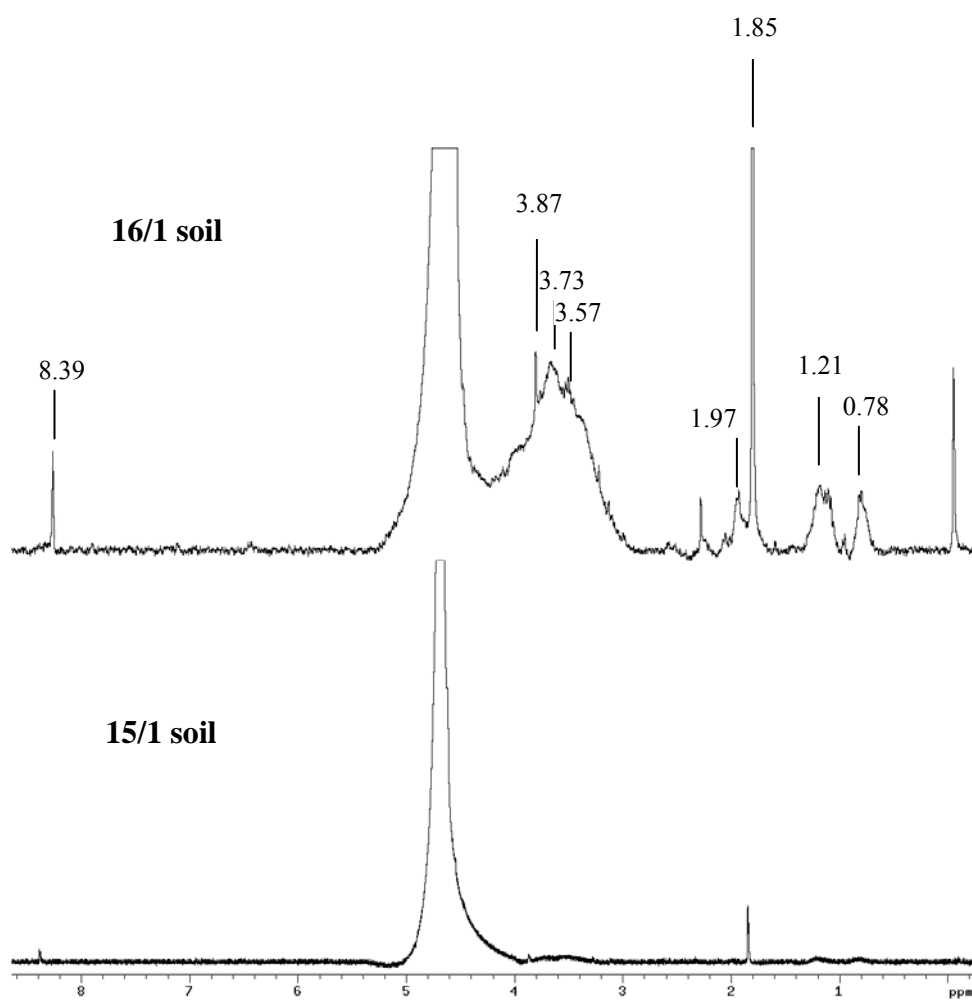


**Figure 8.7** 1D <sup>1</sup>H NMR spectra of surface soils of continuous vetiver for 2 years, samplings from soil 15/1 and 16/1.

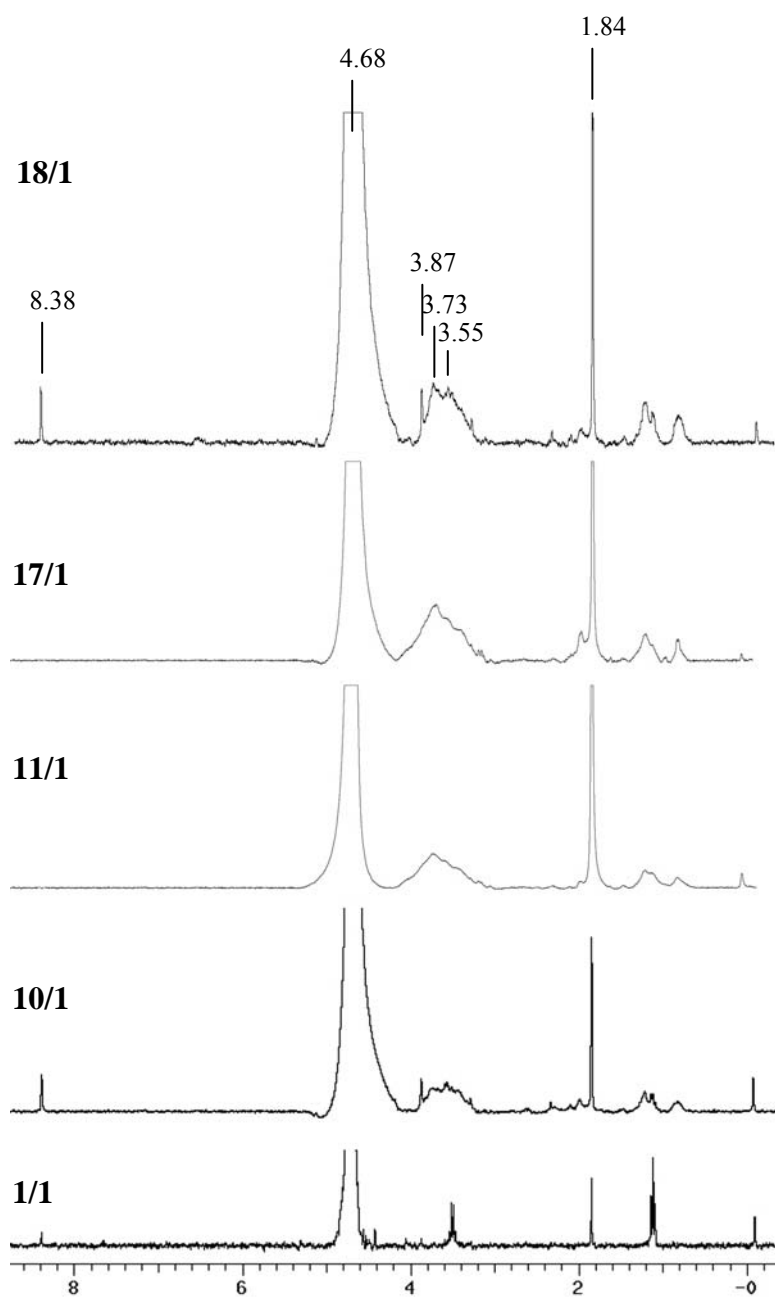


**Figure 8.8** 1D  $^1\text{H}$  NMR spectra of surface soils of continuous vetiver for 3 years, samplings from soil 1/1, 10/1, 11/1, 17/1 and 18/1.

## 8.6 Discussion

### 8.6.1 Spectra $\delta$ 3.8 ppm: the evidence of lignin existence

Confirmative soil samples under the study containing lignin and/or its derivative was the presence of sharp peak at  $\delta$  3.8 ppm as consistent to Adani et al. (2006). They mentioned that methoxyphenylpropyl (MeOPhPr), a repeating unit of lignin structure, yielded the signal at  $\delta$  3.8 ppm.

Simpson et al. (2006) concluded lignin lose from the intermediate stage containing partially decomposed residues to produce the highly alkyl. Similar, vetiver soils found lignin degradation since 2 year cultivation (but no evidence for the first year). However, a recent study by Rasse et al. (2006) using isotope radio found large proportion of lignin was decomposed within the 1 year and small remainder slowly decomposed in the longer years, which they called “A two compartment model”. The model assumed an unprotected lignin pool and a stabilized pool. The former contained about 92% of the lignin and had a turnover time of less than 1 year, while the latter contained only 8% of the soil lignin pool, but contained lignin with a longer mean residence time in the soil (18 years). Consequently, all lignin detected in soil samples represents this slow pool as lignin in the fast pool turns over too fast to significantly accumulate in the soil. Such a two-compartment model could also explain the observation at Rotthalmünster (Ludwig et al. 2005). At this site, the annual input of lignin is estimated to be about 89% of the lignin stock in the Ap horizon, resulting in a mean residence time for lignin in the Ap horizon of only 1.1 year. On the other hand, the isotope data indicated that, after 23 year of continuous maize cropping, 27% of the lignin still derives from the previous C3 vegetation. The existence of a large pool (about 95% of the annual lignin input) with a rapid turnover (residence time less than 1 year) and a smaller pool (about 5% of the annual lignin input)

with substantially slower turnover (residence time of 20 year) explains both the low current lignin stock in the soil ( $111 \text{ g m}^{-2}$  (30 cm)). As a conclusion, if more than 90% of lignin input into soil is rapidly degraded, there is obviously no inherent recalcitrance of the lignin molecule itself. The processes stabilizing the remaining lignin fraction and being responsible for its accumulation, however, there should be some factors play as a potential protection mechanism.

The degradation of lignin needs fungal degraders and oxygen in the oxidative turnover of lignin peroxidase and manganese peroxidase enzyme (Buscot and Varma, 2005; Hofmann et al., 2009); this condition can inhibit lignin degradation in fields which was seen in the 6/3 soil (low resonant signal at  $\delta$  3.8 ppm).

Lignin degradation in soils occurs by mechanisms including free radicals leading to cleavage reactions in both the side chains and rings. The resulting partly degraded lignin has more hydroxyl and carboxyl groups than the mother polymer. The formation compact structure becomes gradually more dispersed and more hydrophilic. Large cleavage products of lignin with hydroxyl and carboxyl groups that are sometimes in vicinal positions can complex with surfaces of metal oxides or with metal ions in solutions. Therefore, partly degraded lignin becomes stabilized against further decay, but still contain large fragments with typical structural features of lignin (Huang et al., 2002; Hofmann et al., 2009).

### **8.6.2 Physically protected biodegradation**

As a result of the  $^1\text{H}$  NMR spectra, C functional groups in different vetiver soils mostly composed of polysaccharides, proteins or peptides, but had less or no aromatic compounds. The latter could be explained in form of less contents or large molecules in detection; however, the disappearance of aromatic resonances prominent the appearance of

methyl groups (Hertkorn et al., 2001). Guggenberger (2005) illustrated the ideas of physically protected biodegradation for organic compounds in humic substances that maybe the answer for the spectra present in this study. Spontaneous cross-linking and repacking polysaccharides at cell wall e.g. cuticans and suberans was a selective key to against microbial activities. Another, a trick to reduce accessibility of the organic substrate enzymes was by rapidly water removal from intermediate surroundings of macromolecules. As a result, hydrophobic condition did not support microbial enzymatic activities which could slowly down decomposition processes. The 3D structure of some peptides like amide anticipated attributing water draining. Moreover, more labile proteins and peptides found in humic substances can be preserved by the encapsulation (Figure 8.9).

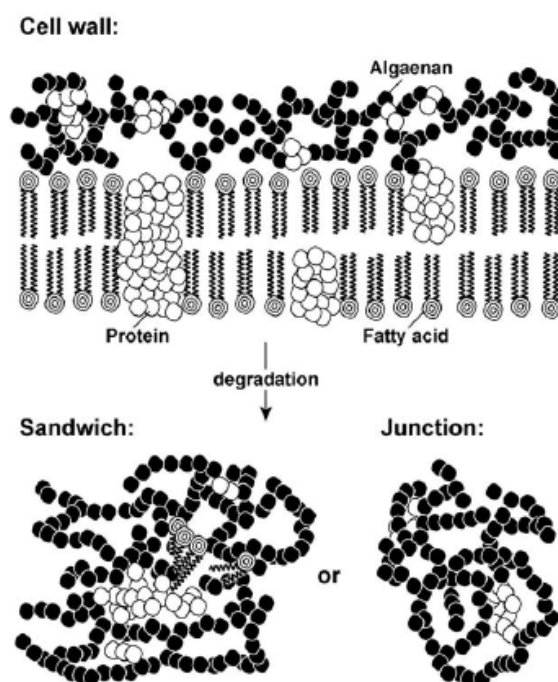


**Figure 8.9** Schematic illustration of the structure of an algaenan-containing algae cell wall (above) and proteinaceous organic matter encapsulated within degraded algal cell wall material (below). By capsulation instinctively labile proteins and peptides might be physically protected from biodegradation (Knicker and Hatcher, 2001).

### 8.6.3 Alkyl: referring humification process

Alkyl groups were also dominantly in this study. In principle, polysaccharides decompose rapidly while the alkyl, aromatic and carbonyl materials decompose more slowly. Many studies attributed high alkyl contents in highly decomposed materials to selective preservation (Theng et al., 1992). However, Kögel-Knabner et al. (1992) suggested that selective preservation is not the dominant process leading to the high alkyl content in forest soil organic matter but rather an increasing of cross linking of long chain alkyl during humification. Similar trends are also evident between soils and in soil profiles

with the most decomposed materials containing significantly higher levels of alkyl and aryl materials (Fox et al., 1994).

## 8.7 Conclusions

8.7.1 Resonant signals of lignin and its derivatives (spectra  $\delta$  3.8 ppm) presented in almost vetiver soils that means lignin starting decomposed at an early stage, which was consistent to a two compartment model of Rasse et al. (2006) explaining a large unprotected lignin pool and a few stabilized pool.

8.7.2 Due to the resonances presented the signals of polysaccharide, peptide or protein compounds even under longer continuous vetiver, it could be assumed that because caused by physically protective mechanisms such as spontaneous cross-linking and repacking polysaccharides at cell wall, rapidly water removal from intermediate surroundings of macromolecules, or encapsulation for labile proteins.

8.7.3 The present of alkyl groups in vetiver soils could refer to humification processing.

## 8.8 References

- Adani, F., Genevini, P., Tambone, F. and Montoneri, E. (2006). Compost effect on soil humic acid: A NMR study. **Chemosphere** 65: 1414-1418.
- Buscot, F and Varma, A. (eds.). (2005). **Microorganisms in Soils: Roles in Genesis and Functions**. Berlin: Springer.
- Cardozaa, L.A., Korira, A.K., Ottob, W.H., Wurreyc, C.J. and Larive, C.K. (2004). Applications of NMR spectroscopy in environmental science. **Progress in Nuclear Magnetic Resonance Spectroscopy** 45: 209-238.

- Fox, C.A., Preston, C.M. and Fyfe, C.A. (1994). Micromorphological and  $^{13}\text{C}$  NMR characterization of a humic, lignic and histic folisol from British Columbia. **Canadian Journal of Soil Science** 74: 1-15.
- Guggenberger, G. (2005) Humidification and mineralization in soils. In F. Buscot and A. Varma. (eds.). **Microorganisms in Soils: Roles in Genesis and Functions** (pp 107-125). Berlin: Springer.
- Gunther, H. (1973). **NMR Spectroscopy: An Introduction**. New York: Wiley. Quoted in R.S. Macomber. (1998). **A Complete Introduction to Modern NMR Spectroscopy**. New York: Wiley.
- Hertkorn, N., Schmitt-Kopplin, Ph., Perminova, I. V., Kovalevski, D. and Kettrup, A. (2001). Two dimensional NMR spectroscopy of humic substances. In R.S. Swift and K.M. Spark. (eds.). **Understanding and Managing Organic Matter in Soils, Sediments, and Waters**. IHSS.
- Hofmann, A., Heim, B.T., Christensen, A., Miltner, M. Gehre, M. and Schmidt, M.W.I. (2009). Lignin dynamics in two  $^{13}\text{C}$ -labelled arable soils during 18 years. **European Journal of Soil Science** 60: 250-257.
- Huang, P.M., Bollag, J.-M. and Senesi, N. (eds.). (2002). **Interactions between Soil Particles and Microorganisms: Impact on the Terrestrial Ecosystem**. New York: John Wiley and Sons.
- Kanjanapoom, T. (2009). **Structure Elucidation of Aromatic Glycosides by Nuclear Magnetic Resonance Spectroscopy**. Bangkok: Julalongkhorn University Publisher.
- Knicker, H. and Hatcher, P.G. (2001). Sequestration of organic nitrogen in the sapropel from mangrove lake, Bermuda. **Organic Geochemistry** 32: 733-744.

- Kögel-Knabner, I., de Leeuw, J.W. and Hatcher, P.G. (1992). Nature and distribution of alkyl carbon in forest soil profiles: Implications for the origin and humification of aliphatic biomacromolecules. **The Science of the Total Environment** 117/118: 175-185.
- Lin, S.Y. and Dence, C.W. (1992). **Methods in Lignin Chemistry**. Berlin: Springer. Quoted in W. Larcher. (2001). **Physiological Plant Ecology: Ecophysiology and Stress Physiology of Functional Groups** (4th ed.). Berlin: Springer.
- Ludwig, B., Helfrich, M. and Flessa, H. (2005). Modelling the long-term stabilization of carbon from maize in a silty soil. **Plant and Soil** 278: 315-325.
- Macomber, R.S. (1998). **A Complete Introduction to Modern NMR Spectroscopy**. New York: Wiley.
- Rasse, D.P., Dignac, M.F., Bahri, H., Rumpel, C., Mariotti, A. and Chenu, C. (2006). Lignin turnover in an agricultural field: from plant residues to soil-protected fractions. **European Journal of Soil Science** 57: 530-538.
- Schnitzer, M. (1982). Organic matter characterization. In A.L. Page (ed.) **Methods of Soil Analysis** (pp 581–594). Part 2. 2nd ed. ASA, Madison, WI.
- Silverstein, R.M., Bassler, G.C. and Morrill, T.C. (1991) **Spectrometric Identification of Organic Compounds** (5th ed.). New York: Wiley. Quoted in R.S. Macomber. (1998). **A Complete Introduction to Modern NMR Spectroscopy**. New York: Wiley.
- Simpson, A.J., Kingery, W.L., Shaw, D.R., Spraul, M., Humpfer, E. and Dvortsak, P. (2001). The application of  $^1\text{H}$  HR-MAS NMR spectroscopy for the study of structures and associations of organic components at the solid-aqueous interface of a whole soil. **Environmental Science and Technology** 35: 3321-3325.

- Simpson, A.J., Simpson, M.J., Kingery, W.L., Lefebvre, B.A., Moser, A., Williams, A.J., Kvasha, M. and Kelleher, B.P. (2006). The application of  $^1\text{H}$  high-resolution magic-angle spinning NMR for the study of clay-organic associations in natural and synthetic complexes. **Langmuir** 22: 4498-4503.
- Theng, B.K.G., Tate, K.R. and Becker-Heidmann, P. (1992). Towards establishing the age, location and identity of the inert soil organic matter of a Spodosol. **Zeitschrift für Pflanzenernährung und Bodenkunde** 155:181-184.

# CHAPTER IX

## SOIL LABILE ORGANIC CARBON AND CARBON TURNOVER TIMES

### 9.1 Abstract

Vetiver was grown in the Thai Tapioca Development Institute, Nakhon Ratchasima, northeast Thailand, along contours for soil erosion reduction in tapioca fields. Soils after continually cultivating vetiver for 1, 2, 3, 5 and 7 years were measured for SOC and organic N using a sequential fumigation incubation procedure for microbial biomass C ( $C_{\text{microbial}}$ ), labile organic C ( $C_{\text{labile}}$ ) and potential turnover rate ( $k$ ). This study found SOC and organic N levels increased significantly due to continuous vetiver cover. The mean C storages in soil at 120 cm depth were 23.63, 28.62, 66.30, 28.68 and 228.90 tC ha<sup>-1</sup> for the 1, 2, 3, 5, to 7 year site, respectively. The  $C_{\text{microbial}}$  content enriched maximally at 0-10 cm (0.15 mg g<sup>-1</sup>soil) and for the  $C_{\text{labile}}$  content the maximum was at 60 - 120 cm (0.744 mg g<sup>-1</sup>soil). The potentially labile organic C turnover was the fastest at 18 days from 0 - 10 cm layer of the 3 year site and for the slowest was 108 days at 60 - 120 cm layer of the 7 year site.

**Keywords:** vetiver, soil microbial biomass C, soil labile organic C, C turnover time

## 9.2 Introduction

Soil organic C is one type of C pools in the pedosphere, which the current SOC pool in the world soils is estimated at 1500 Pg (Eswaran et al., 1995). The SOC pool is about 2.1 times that of the atmosphere pool and about 2.7 times that of the biotic pool comprising land plants. Processes that enhance SOC content are plant biomass production, humification, aggregation, and sediment deposition, while processes that degrade SOC content are soil erosion, leaching, and soil organic matter (SOM) decomposition.

SOC is important for improving soil quality and regulating global C cycling. SOC contains fractions with a rapid turnover rate as well as fractions with a slower turnover rate (Schimel et al., 1985). Microbial biomass C and labile organic C, the rapidly responding fractions in C turnover, suggested as an early indicator of the effects of land use on SOC pools (Gregorich et al., 1994) and as an important indicator of soil quality. The majority of studies on SOC and its different labile fractions have used only topsoil samples; however, few studied have focused on a connection with soil profile and plant species.

Vetiver is a tropical plant which grows naturally. In Thailand, vetiver can be found growing in a wide range of areas from highlands to lowlands in various soil conditions. Two ecotypes commonly found in Thailand are *Vetiveria zizanioides* Nash and *Vetiveria nemoralis* A. Camus (Pothinam, 2006). The grass has a deep thick root system which spreads vertically rather than horizontally. The roots densely bind together like an underground curtain or wall enabling it to store water and moisture. His Majesty King Bhumibhol Adulyadej of Thailand has long expressed his ideas about vetiver, the wonder grass with proven potential in preventing erosion and conserving soil moisture, and its multifold applications such as prevention and treatment of polluted water and contaminated land.

The objective of this study was to evaluate C sequestration efficiency of vetiver by investigating the distribution of SOC and its active fractions through soil profile.

### **9.3 Objectives of this chapter**

9.3.1 To estimate soil properties of continuous vetiver soils

9.3.2 To estimate labile organic C of continuous vetiver soils

9.3.3 To estimate labile organic C turnover times of continuous vetiver soils

### **9.4 Materials and methods**

#### **9.4.1 Site description**

The research was conducted at the Thai Tapioca Development Institute (TTDI), Nakhon Ratchasima Province, northeast Thailand (15°16' N, 101°51' E; 312 m a.s.l.). This land, approximately 320 ha, mainly cultivates tapioca since last 10 years. Vetiver was planted along contours across the slope to protect soil erosion. The organic C input into soil was through manure, plant root system, stubble and crop residues remaining on the field. The soils in the study area are sandy loam and sandy clay loam. During 1977 - 2007, the mean annual temperature ranged between 21.9 and 32.8°C with average monthly precipitation of about 89 mm (Nakhon Ratchasima Meteorology Station; Appendix A).

#### **9.4.2 Soil sampling**

Soil samples were collected on January 2008, from the contours of continuous vetiver for 1, 2, 3, 5 and 7 years. Soils were bulked into a composite sample with three depth layers at 0 - 10, 10 - 60 and 60 - 120 cm. Soil samples were separated into two parts: first, fresh-moist soils were kept at 4°C for investigating for  $C_{\text{microbial}}$  and  $C_{\text{labile}}$ ; and second, soils were air-dried for physical and chemical analysis.

### 9.4.3 Physical and chemical properties of soils

Dried soils were sieved to 2 mm and analyzed for soil particle size distribution by the hydrometer method (Bouyoucos, 1962), bulk density (Blake, 1965), pH<sub>(H2O)</sub> (1:5 soil water ratio), EC in 1:5 soil water suspension, cation, exchangeable cations, SOC by the Walkley-Black wet oxidation method (Walkley and Black, 1934) and organic N by the Kjeldahl method (Bremner and Mulvaney, 1982). The mean C storage in soil at 120 cm depth was calculated as following Eq. (9.1):

$$\text{C Storage (gC m}^{-2}\text{)} = \text{Bulk density} \times \text{SOC} \times \text{Soil depth} \quad (9.1)$$

### 9.4.4 Soil microbial biomass C

$C_{\text{microbial}}$  was measured with a chloroform fumigation incubation technique (Jenkinson and Powlson, 1976). Two 30 g subsamples of field-moist soils were placed in 100 mL containers. One subsample was fumigated with free alcohol  $\text{CHCl}_3$  in the dark for 24 h, while the another subsample was kept in the dark at 4°C for 24 h. Both fumigated and nonfumigated soils were incubated at 25°C for 10 d. The  $\text{CO}_2$  evolved from the soils was absorbed in 1 M NaOH and determined titrimetrically with 1 M HCl using phenolphthalein as an indicator. Microbial biomass C was calculated from Eq. (9.2).

$$B = \frac{F}{K} \quad (9.2)$$

$B$  is soil biomass C in  $\text{mgC g}^{-1}\text{soil}$ ;  $F$  is the  $\text{CO}_2\text{-C}$  evolved during the 10 ds' incubation from the fumigated, minus the nonfumigated soil; and  $K$  is 0.45.

#### 9.4.5 Soil labile organic C

$C_{\text{labile}}$  was determined by a sequential fumigation-incubation procedure (Zou et al., 2005). The fumigated soil was incubated 50 - 80 days (5 - 8 cycles). The  $\text{CO}_2\text{-C}$  evolution was measured every 10 d, after adding 0.5 mL supernatant of 1 g inoculated soil. The amount of  $\text{CO}_2\text{-C}$  ( $C_t$ ) was calculated from Eq. (9.3) (Carter, 1993).

$$C_t = \frac{[(A_t - V_t)N_tE - Q_t]}{w} \quad (9.3)$$

$A_t$  is the volume (mL) of acid used to titrate the blank;  $V_t$  is the volume (mL) of acid used to titrate the treatment;  $N_t$  is the normality of titrating acid;  $E = 6$  is equivalent weight;  $w$  is the initial weight of soil.  $Q_t$  is a correction factor for the inoculated soil after each fumigation as shown in Eq. (9.4).

$$Q_t = \frac{C'}{(r+1)} + \sum \left[ \frac{C_{t-1}}{(r+1)} \right], t = 1, \dots, n, \quad (9.4)$$

$C'$  is the amount of  $\text{CO}_2\text{-C}$  from the nonfumigated soil during the first 10 days incubation;  $r$  is the weight ratio of fumigated soil to inoculation soil. The accumulated  $\text{CO}_2\text{-C}$  ( $M_t$ ,  $t = 1, \dots, n$ ) from the fumigated soil is calculated following to Eq. (9.5) (Stanford and Smith, 1972).

$$M_t = C_{\text{labile}} (1 - e^{-kt}) \quad (9.5)$$

$C_{labile}$  is estimated from pool size of soil labile organic C and  $k$  is the potential turnover rate. Eq. (9.5) can be transformed to linear regression in Eq. (9.6).

$$\ln(C_t) = \ln(k C_{labile}) - kt, \quad (t = 1, 2, \dots, n) \quad (9.6)$$

$k$  is the slope,  $\ln(kC_{labile})$  is the intercept (a), and  $C_{labile}$  equals to  $e^a/k$ .

#### 9.4.6 Statistical analysis

Statistical analysis of the data was carried out on the replicates by one-way ANOVA. If the main effects were significant at  $p < 0.05$ , a post hoc separation of means was done by univariate least significant difference (LSD) test. Statistical analysis was conducted with SPSS and Microsoft Excel for Window 2000.

### 9.5 Results

#### 9.5.1 Soil organic C and nitrogen

The physical and chemical soil properties for each site and soil layer are shown in Table 9.1. The SOC and organic N concentrations at 0 - 10 and 10 - 60 cm layer were greater than that of 60 - 120 cm, except at the 7 year site which SOC at 60 - 120 cm layer increased steeply to 53.96 g kg<sup>-1</sup>soil (Figure 9.1). The SOC and organic N concentrations varied significantly with year of continuous vetiver ( $p < 0.05$ ) by the SOC increase being maximum in the 7 year site and the organic N content being maximum in the 5 year site. Both SOC and organic N contents increased distinctly after continuous vetiver for 3 years.

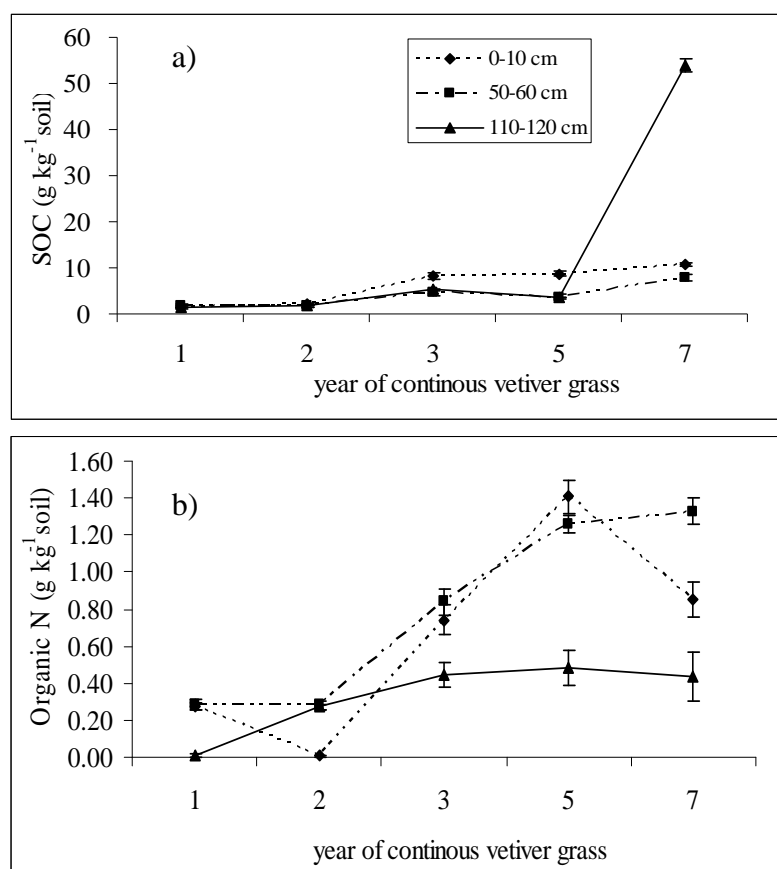


**Figure 9.1** Levels of (a) SOC and (b) organic N in a chronosequence of soils under continuous vetiver. Error bars indicate standard deviation ( $n = 3$ ).

The mean C storages in soil at 120 cm depth were 23.63, 28.62, 66.30, 28.68 and 228.90 tC ha<sup>-1</sup> for the 1, 2, 3, 5 and 7 year site, respectively (Figure 9.2). Carbon sequestration under a field experiment was significantly relative with the year of continuous vetiver as shown in Eq. (9.7). The mean C storage at 120 cm increased with a decreasing rate, which the storage was 9.69 times larger in the 7 year site compared to the 1 year site.

$$Y = 107.72 \ln(x) - 13.788 \quad (9.7)$$

where  $Y$  is C storage at 120 cm depth (tC ha<sup>-1</sup>) and  $x$  is the year of vetiver grown.

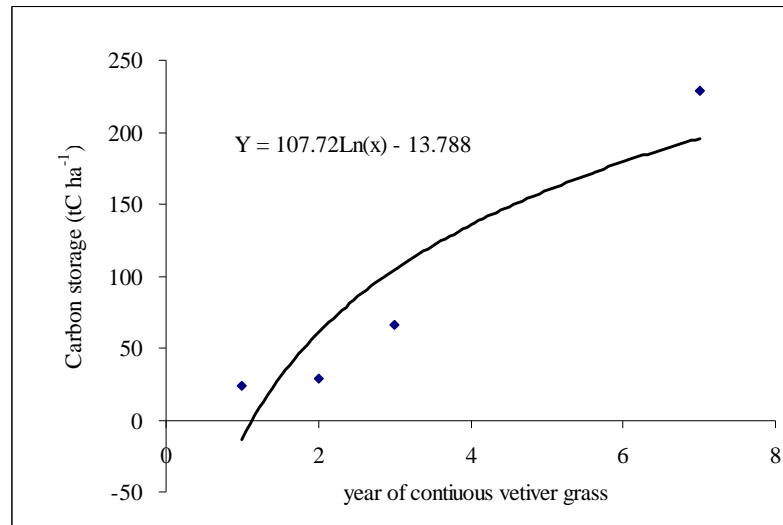


**Figure 9.2** Changes in the mean C storage in soil at 120 cm depth under continuous vetiver (the equation excluded the 5 year site by data validation).



**Table 9.1** Selected characteristic of the study soils from the sites at TTDI, Nakhon Ratchasima, Thailand.

site	Soil	Bulk	Particle size distribution			pH	EC	Exchangeable Cation				CEC	SOC	Organic N
	depth	Density	Sand	Silt	clay	(H <sub>2</sub> O)	( $\mu\text{S cm}^{-1}$ )	Ca	K	Mg	Na	( $\text{cmol kg}^{-1}$ soil)	(g $\text{kg}^{-1}$ soil)	
	(cm)	( $\text{mg m}^{-3}$ )	(g $\text{kg}^{-1}$ soil)					(cmol $\text{kg}^{-1}$ soil)						
1 year	0-10	1.37	82.48	12	5.52	8.68 <sup>B</sup> (0.18)	15.10 <sup>Da</sup> (0.82)	0.108 <sup>Da</sup> (0.001)	0.035 <sup>Da</sup> (0.001)	0.023 <sup>Cb</sup> (0.001)	0.033 <sup>Ba</sup> (0.006)	0.43 <sup>Cb</sup> (0.08)	1.37 <sup>Cb</sup> (0.13)	0.27 <sup>Ca</sup> (0.02)
	10-60	1.15	79.98	9.5	10.52	8.33 <sup>B</sup> (0.21)	10.90 <sup>Db</sup> (1.04)	0.094 <sup>Eb</sup> (0.001)	0.027 <sup>Cb</sup> (0.006)	0.024 <sup>Eb</sup> (0.001)	0.027 <sup>Aa</sup> (0.006)	0.56 <sup>Db</sup> (0.16)	1.95 <sup>Da</sup> (0.25)	0.28 <sup>Ca</sup> (0.03)
	60-120	1.19	76.48	6	17.52	8.64 <sup>C</sup> (0.38)	8.45 <sup>Dc</sup> (0.25)	0.034 <sup>Ec</sup> (0.001)	0.025 <sup>Db</sup> (0.001)	0.038 <sup>Da</sup> (0.001)	0.013 <sup>Cb</sup> (0.006)	1.42 <sup>Da</sup> (0.10)	1.49 <sup>Db</sup> (0.12)	0.01 <sup>Cb</sup> (0.01)
2 years	0-10	1.37	86.48	8	5.52	9.59 <sup>A</sup> (0.43)	7.53 <sup>Eb</sup> (0.68)	0.088 <sup>Ec</sup> (0.001)	0.013 <sup>E</sup> (0.006)	0.015 <sup>Db</sup> (0.001)	0.005 <sup>Ec</sup> (0.001)	0.46 <sup>Cb</sup> (0.03)	1.97 <sup>C</sup> (0.21)	0.01 <sup>Db</sup> (0.01)
	10-60	1.08	81.98	6	12.02	9.47 <sup>A</sup> (0.23)	6.96 <sup>Eb</sup> (0.64)	0.133 <sup>Da</sup> (0.006)	0.010 <sup>E</sup> (0.000)	0.076 <sup>Aa</sup> (0.001)	0.015 <sup>Bb</sup> (0.001)	0.73 <sup>Da</sup> (0.13)	1.85 <sup>D</sup> (0.36)	0.28 <sup>Ca</sup> (0.02)
	60-120	1.54	70.98	11.5	17.52	9.96 <sup>A</sup> (0.25)	9.68 <sup>Da</sup> (0.58)	0.122 <sup>Db</sup> (0.001)	0.013 <sup>E</sup> (0.006)	0.076 <sup>Ba</sup> (0.001)	0.023 <sup>Ba</sup> (0.006)	0.07 <sup>Ec</sup> (0.12)	1.72 <sup>D</sup> (0.15)	0.27 <sup>Ba</sup> (0.01)

**Table 9.1** (Continued).

site	Soil	Bulk	Particle size distribution			pH	EC	Exchangeable Cation				CEC	SOC	Organic N
	depth	Density	Sand	Silt	clay	( <sub>H2O</sub> )	( $\mu\text{S cm}^{-1}$ )	Ca	K	Mg	Na	( $\text{cmol kg}^{-1}$ soil)	(g $\text{kg}^{-1}$ soil)	
	(cm)	( $\text{mg m}^{-3}$ )	(g $\text{kg}^{-1}$ soil)					(cmol $\text{kg}^{-1}$ soil)						
3 years	0-10	1.04	75.88	8.57	15.55	8.47 <sup>Ba</sup> (0.35)	114.89 <sup>Ca</sup> (1.04)	0.413 <sup>Cc</sup> (0.001)	0.313 <sup>Aa</sup> (0.015)	0.064 <sup>Ab</sup> (0.001)	0.023 <sup>Cb</sup> (0.006)	2.77 <sup>A</sup> (0.75)	8.37 <sup>Ba</sup> (0.70)	0.74 <sup>Ba</sup> (0.08)
	10-60	1.00	66.88	3.57	29.55	7.69 <sup>Cb</sup> (0.43)	48.72 <sup>Cb</sup> (1.13)	0.553 <sup>Ca</sup> (0.001)	0.226 <sup>Ab</sup> (0.001)	0.053 <sup>Cc</sup> (0.001)	0.015 <sup>Bb</sup> (0.001)	2.70 <sup>A</sup> (0.35)	4.60 <sup>Bb</sup> (0.56)	0.84 <sup>Ba</sup> (0.07)
	60-120	1.09	50.45	36.00	13.55	7.56 <sup>Db</sup> (0.15)	25.26 <sup>Cc</sup> (0.63)	0.498 <sup>Cb</sup> (0.001)	0.135 <sup>Ac</sup> (0.001)	0.083 <sup>Aa</sup> (0.006)	0.033 <sup>Aa</sup> (0.006)	3.47 <sup>B</sup> (0.19)	5.29 <sup>Bb</sup> (0.10)	0.44 <sup>Ab</sup> (0.07)
5 years	0-10	0.92	60.76	19.07	20.17	9.18 <sup>Aa</sup> (0.16)	145.98 <sup>Aa</sup> (1.78)	0.987 <sup>Bb</sup> (0.001)	0.195 <sup>Ca</sup> (0.001)	0.045 <sup>Bc</sup> (0.001)	0.043 <sup>Aa</sup> (0.006)	1.92 <sup>B</sup> (0.34)	8.70 <sup>Ba</sup> (0.45)	1.41 <sup>Aa</sup> (0.09)
	10-60	0.64	51.76	17.00	31.24	7.19 <sup>Dc</sup> (0.08)	72.21 <sup>Bb</sup> (1.06)	0.945 <sup>Bc</sup> (0.001)	0.195 <sup>Ba</sup> (0.001)	0.063 <sup>Bb</sup> (0.001)	0.025 <sup>Ab</sup> (0.001)	1.80 <sup>C</sup> (0.05)	3.72 <sup>Cb</sup> (0.48)	1.26 <sup>Aa</sup> (0.05)
	60-120	0.40	49.76	17.00	33.24	7.68 <sup>Db</sup> (0.18)	58.91 <sup>Bc</sup> (0.64)	1.777 <sup>Ba</sup> (0.001)	0.077 <sup>Cb</sup> (0.006)	0.076 <sup>Ba</sup> (0.001)	0.025 <sup>Bb</sup> (0.001)	2.28 <sup>C</sup> (0.25)	3.64 <sup>Cb</sup> (0.08)	0.48 <sup>Ab</sup> (0.09)

**Table 9.1** (Continued).

site	Soil	Bulk	Particle size distribution			pH	EC	Exchangeable Cation				CEC	SOC	Organic N
	depth	Density	Sand	Silt	clay	( <sub>H2O</sub> )	( $\mu\text{S cm}^{-1}$ )	Ca	K	Mg	Na	( $\text{cmol kg}^{-1}$ soil)	(g $\text{kg}^{-1}$ soil)	
	(cm)	( $\text{mg m}^{-3}$ )	(g $\text{kg}^{-1}$ soil)					(cmol $\text{kg}^{-1}$ soil)						
7 years	0-10	1.07	50.31	25.14	24.55	8.71 <sup>Bb</sup> (0.21)	118.61 <sup>Ba</sup> (1.88)	1.632 <sup>Ab</sup> (0.001)	0.213 <sup>Ba</sup> (0.006)	0.045 <sup>Bb</sup> (0.001)	0.014 <sup>D</sup> (0.001)	2.95 <sup>Ab</sup> (0.13)	10.74 <sup>Ab</sup> (0.39)	0.85 <sup>Bb</sup> (0.10)
	10-60	0.97	51.98	20.50	27.52	6.77 <sup>Dc</sup> (0.24)	83.40 <sup>Ac</sup> (1.55)	1.615 <sup>Ac</sup> (0.001)	0.015 <sup>Dc</sup> (0.001)	0.045 <sup>Db</sup> (0.001)	0.014 <sup>B</sup> (0.002)	2.33 <sup>Bc</sup> (0.08)	7.87 <sup>Ac</sup> (0.55)	1.33 <sup>Aa</sup> (0.07)
	60-120	0.55	48.98	15.50	35.52	9.30 <sup>Ba</sup> (0.27)	92.85 <sup>Ab</sup> (1.20)	2.219 <sup>Aa</sup> (0.001)	0.127 <sup>Bb</sup> (0.006)	0.064 <sup>Ca</sup> (0.001)	0.015 <sup>C</sup> (0.001)	3.90 <sup>Aa</sup> (0.05)	53.96 <sup>Aa</sup> (1.44)	0.44 <sup>Ac</sup> (0.14)

Data are means with the standard deviation in parentheses (n = 3). Different higher and lower case letters represent significant differences

(p < 0.05) of the treatment among sites and among treatment within the same site, respectively.

### 9.5.2 Soil microbial biomass C and soil labile organic C

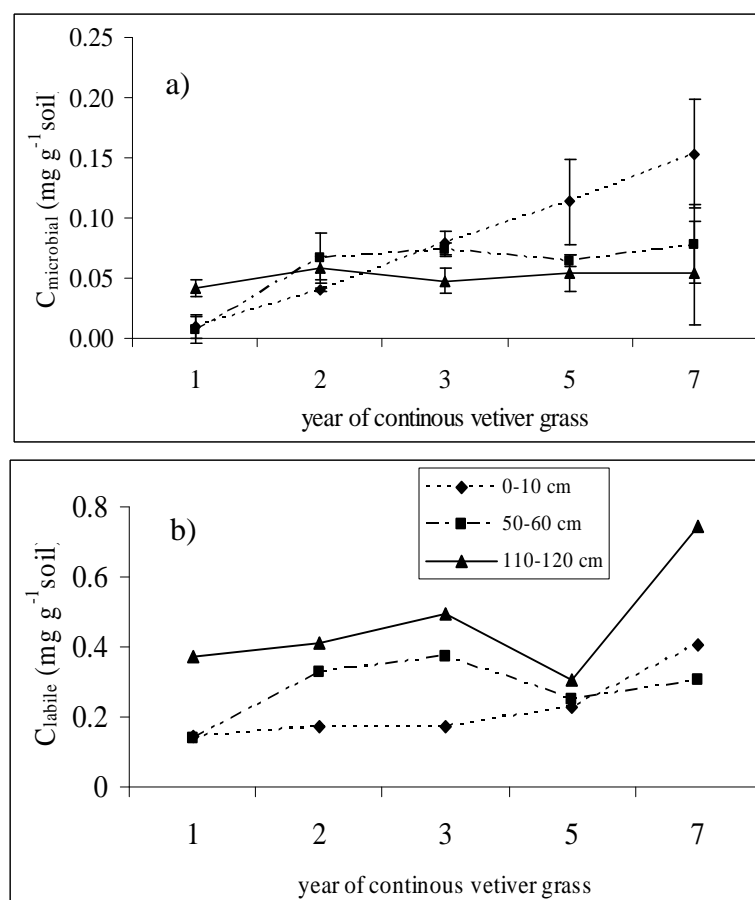


**Figure 9.3** Effect of continuous vetiver on (a) soil microbial biomass C and (b) soil labile organic C. Error bars indicate standard deviation (n = 3).

The levels of  $C_{\text{microbial}}$  and  $C_{\text{labile}}$  are given in Figure 9.3 and Table 9.2. The  $C_{\text{microbial}}$  and  $C_{\text{labile}}$  contents were greatest at the 7 year site in 0 - 10 and 60 - 120 cm layer, respectively. Averaged across the sites, the  $C_{\text{microbial}}$  content in 0 - 10 cm layer ranged between 0.01 and 0.15 mg g<sup>-1</sup>soil, in 10 - 60 cm layer was between 0.01 and 0.08 mg g<sup>-1</sup>soil, and in 60 - 120 cm layer was between 0.04 and 0.06 mg g<sup>-1</sup>soil. The  $C_{\text{labile}}$  content in the 0-10 cm layer varied between 0.144 and 0.404 mg g<sup>-1</sup>soil, the 10 - 60 cm layer ranged between 0.137 and 0.372 mg g<sup>-1</sup>soil, and the  $C_{\text{labile}}$  content in the 60 - 120 cm layer was between 0.308 and 0.744 mg g<sup>-1</sup>soil. The effect of continuous vetiver on  $C_{\text{microbial}}$  was

significant, reflecting the steep increment in the surface layers ( $0.15 \text{ mg g}^{-1}\text{soil}$ ). Also, the growth of vetiver affected the deeper soils, with a  $C_{\text{labile}}$  of  $0.744 \text{ mg g}^{-1}\text{soil}$ . The potential C turnover rates for each site and soil layer are shown in Table 9.2. The fastest labile organic C turnover was found at the 0 - 10 cm layer of the 3 year site (18 d) and the slowest was at 60 - 120 cm layer of the 7 year site (108 d). The proportion of  $C_{\text{microbial}}$  to  $C_{\text{labile}}$  was found to decrease from soil surface to deep layers in all sites, except the 1 year site, by the highly found in 0 - 10 cm layer of the 5 year site (47.90%). The  $C_{\text{microbial}}$  to SOC ranged between 0.09% and 3.60%, with the maximum at the 10 - 60 cm level of the 2 year site.

**Table 9.2** Soil microbial biomass C and pool sizes of soil labile organic C.

Site	Soil	$C_{\text{microbial}}$	$C_{\text{labile}}$	k (cycle <sup>-1</sup> )	10/k	$C_{\text{microbial/}}$	$C_{\text{microbial/}}$
	depth					$C_{\text{labile}}$	SOC
	(cm)	(mg g <sup>-1</sup> )	(mg g <sup>-1</sup> )		(day)	(%)	(%)
1 year	0-10	0.01 <sup>Cb</sup>	0.144	0.543	18.4	6.94	0.73
	10-60	0.01 <sup>Bb</sup>	0.137	0.348	28.7	7.28	0.51
	60-120	0.04 <sup>a</sup>	0.370	0.424	23.6	10.82	2.71
2 year	0-10	0.04 <sup>Cc</sup>	0.174	0.196	51.1	23.22	2.05
	10-60	0.07 <sup>Aa</sup>	0.327	0.146	68.4	20.41	3.60
	60-120	0.06 <sup>b</sup>	0.413	0.156	64.1	14.13	3.39
3 year	0-10	0.08 <sup>Ba</sup>	0.171	0.564	17.7	46.70	0.96
	10-60	0.07 <sup>Aa</sup>	0.372	0.228	43.8	18.82	1.52
	60-120	0.05 <sup>b</sup>	0.494	0.481	20.8	10.11	0.95
5 year	0-10	0.11 <sup>Aa</sup>	0.230	0.240	41.7	47.90	1.26
	10-60	0.06 <sup>Ab</sup>	0.249	0.359	27.8	24.07	1.61
	60-120	0.05 <sup>b</sup>	0.308	0.332	30.2	16.24	1.37
7 year	0-10	0.15 <sup>A</sup>	0.404	0.214	46.7	37.17	1.40
	10-60	0.08 <sup>A</sup>	0.304	0.285	35.1	26.31	1.02
	60-120	0.05	0.744	0.093	107.5	6.72	0.09

Different higher and lower case letters represent significant differences ( $p < 0.05$ ) of the treatment among sites and among treatment within the same site, respectively.

## 9.6 Discussion

Some environmental factors such as soil characteristics, soil profile, vegetation cover and geography have been attributed to SOC and organic N accumulation. Solomon et al. (2002) showed that most of SOM (stable soil C) was bound to the clay-size separates (40 to 63% of SOC and 56 to 71% of organic N), while only 4 to 13% of SOC and 2 to 9% of organic N were found in the sand-size separates, and 29 to 52% of SOC and 25 to 40% of organic N was contained in the silt. As in this study, the 7 year site enriched with SOC and organic N contained more clay particles than other sites. Plant decomposition leads to the selective preservation of some resistant plant constituents, such as lignin. In addition, the turnover of microorganisms produces compounds, which are precursors of SOM (Chesworth, 2008). High lignin, tannin and polyphenol contents of leaves and roots may have inhibited mineralization through phytotoxic interactions and chemical interactions with both organic and inorganic N sources (Reyes-Reyes et al., 2007), which means more C and nitrogen is retained in subsoils. However, the labile cytoplasm components are readily leached from plant residues and provide the initial energy and nutrients to start the decomposition process (Chesworth, 2008). Sediment deposition from soil erosion may be another possible reason for the SOC and organic N measurements at the 7 year site.

$C_{\text{microbial}}$  and other active fractions suggest regulated by soil textures. This study found that the  $C_{\text{labile}}$  content enriched in the deep soil of the 7 year site ( $0.744 \text{ mg g}^{-1}\text{soil}$ ), comprising high clay particles (Table 9.2). O-alkyl-C structures (mainly carbohydrate-derived), is known to be the moiety preferentially used by soil microorganisms, found enriched in clay-size separates rather than silt-size (Solomon et al., 2002). Moreover, SOM from Scanning Electron Microscope study associated with the clay-size separates was

composed of completely decomposed organic structures, while SOM associated with the sand-size separates was composed of undecomposed and macromorphologically identifiable particulate plant residues (Solomon et al., 2002).

A particular proportion of the SOM input is readily utilized by the organisms, such that the biomass C generally comprises only 1 - 5% of SOC in 0 - 10 cm layer (Jeckinson and Ladd, 1981; Smith and Paul, 1990). In this study, the proportions of  $C_{\text{microbial}}$  to SOC in the topsoil were in the range (between 0.73 and 2.05%) and similar to that of *Acacia nilotica* (1.84%), *Eucalyptus tereticornis* (1.81%) and *Populus deltoids* (1.88%) (Kaur et al., 2000). The SOC values in this study of 3, 5 and 7 years were 8.37, 8.7 and 10.74 mg g<sup>-1</sup>soil, respectively, which all are greater than that of 6 years of *A. nilotica*, *E. tereticornis* and *P. deltoids* (6.8, 4.8 and 5 mg g<sup>-1</sup> soil, respectively). Anderson (2003) considered the  $C_{\text{microbial}}:C_{\text{org}}$  ratio < 2.0 for neutral arable soils. The  $C_{\text{microbial}}:C_{\text{org}}$  ratio could be used as an indicator of stability to recognize environmental changes, gives an “Eco-physiological profile” of a site (Anderson, 2003). Ross et al. (1994) stated that higher values of  $C_{\text{microbial}}$  could be found in soil samples with a pH above 6.0. The level of  $C_{\text{microbial}}$  was significant larger in soil sampled under the canopy of shrubs, such as “huisache” (*Acacia tortuosa*; 0.32 mg g<sup>-1</sup>soil) and “mesquite” (*Prosopis laevigata*; 0.373 mg g<sup>-1</sup>soil), compared to the soil cultivated with “maize” (*Zea mays*) for > 19 years (0.122 mg g<sup>-1</sup>soil).

## 9.7 Conclusions

Continuous vetiver in clay particles could increase large amounts of soil organic C, soil microbial biomass C and labile organic C. Vetiver can also enhance general soil quality, as well as sequestration of C.

## 9.8 References

- Anderson, T.H. (2003). Microbial eco-physiological indicators to assess soil quality. **Agriculture Ecosystems Environment** 98: 285-293.
- Blake, G.R. (1965). Bulk density. In American Society of Agronomy. **Methods of Soil Analysis** (ed. C.A.Black). Wisconsin: 374-390.
- Bouyoucos, G.J. (1962). Hydrometer method improved for making particle size analyses of soils. **Agronomy Journal** 54: 464-465.
- Bremner, J.M. and Mulvaney, C.S. (1982). Nitrogen-Total. In A.L. Page (ed.). **Methods of Soil Analysis, Part 2 Chemical and Microbiological Properties**. SSSA Book series No. 9. (pp 595-622). Madison.
- Carter, M.R. (1993). **Soil Sampling and Methods of Analysis**. Toronto: Lewis Publishers.
- Chesworth, W. (ed.). (2008). **Encyclopedia of Soil Science**. Dordrecht: Springer.
- Eswaran, H., Van den Berg, E., Reich, P. and Kimble, J. (1995). Global soil carbon resources. In R. Lal, J. Kimble, E. Levine and B.A. Steward. (eds.). **Soils and Global Change** (pp 27-43). Boca Raton: CRC/Lewis Publisher.
- Gregorich, E.G., Carter, M.R., Angers, D.A., Monreal, C.M. and Ellert, B.H. (1994). Towards a minimum data set to assess soil organic matter quality in agricultural soils. **Canadian Journal of Soil Science** 74: 367-385.
- Jeckinson, D.S. and Ladd, J.M. (1981). Microbial biomass in soil: Measurement and turnover. In E.D. Paul and J.M. Ladd. (eds.). **Soil Biochemistry**, Vol. 5. (pp 415-471). New York: Dekker.

- Jenkinson, D.S. and Powlson, D.S. (1976). The effects of biocidal treatments on metabolism in soil. V: a method for measuring soil biomass. **Soil Biology and Biochemistry** 8: 209-213.
- Kaur, B., Gupta, S.R. and Singh, G. (2000). Soil carbon, microbial activity and nitrogen availability in agroforestry systems on moderately alkaline soils in northern India. **Applied Soil Ecology** 15: 283-294.
- Pothinam, A. (2006). Vetiver root and soil moisture conservation from vetiver grass establishment on degraded soils. In **the Proceeding of International Workshop on Sustained Management of the Soil-Rhizosphere System for Efficient Crop Production and Fertilizer Use**, 16 - 20 October.
- Reyes-Reyes, B.G., Alcántara-Hernández, R.A., Rodríguez, V., Olalde-Portugal, V. and Dendooven, L. (2007). Microbial biomass in a semi arid soil of the central highlands of Mexico cultivated with maize or under natural vegetation. **European Journal of Soil Biology** 43: 180-188.
- Ross, D.J., McQueen, D.J. and Kettles, H.A. (1994). Land rehabilitation under pasture on volcanic pattern materials: Changes in soil microbial biomass and C and N metabolism. **Australian Journal of Soil Research** 32: 1321-1337.
- Schimel, D.C., Coleman, D.C. and Horton, K.A. (1985). Soil organic matter dynamics in paired rangeland and crop toposequences in North Dakota. **Geoderma** 36: 201-214.
- Smith, L.J. and Paul, E.A. (1990). The significance of soil microbial biomass estimations. In J.-M. Bollage and G. Stotzky. (eds.). **Soil Biochemistry**. Vol. 6 (pp 29-116). New York: Mercel Dekker.
- Solomon, D., Fritzsche, F., Tekalign, M., Lehmann, J. and Zech, W. (2002). Soil organic matter composition in the subhumid Ethiopian highlands as influenced by

deforestation and agricultural management. **Soil Science Society of America Journal** 66: 68-82.

Stanford, G. and Smith, S.J. (1972). Nitrogen mineralization potentials of soils. **Soil Science Society of America Journal** 36: 465-472.

Walkley, A. and Black, A.I. (1934). An examination of the different method for determining soil organic matter, and proposed modification of the chromic acid titration method. **Soil Science** 37: 29-38.

Zou, X.M., Ruan, H.H., Fu, Y., Yang, X.D. and Sha, L.Q. (2005). Estimating soil labile organic carbon and potential turnover rates using a sequential fumigation-incubation procedure. **Soil Biology and Biochemistry** 3: 1923-1928.

## **CHAPTER X**

### **CONCLUSIONS**

Based on the studies of internal leaf structure, phytolith abundance and chemical components in plant residues (chapter IV to VI), it could be concluded that LI provenance had the greatest potential of C sequestration by comparing among 11 provenances (Table 10.1). Results of the study showed all 11 vetiver provenances, in basically, could gain high photosynthetic capacity and great gas circulation through confirmations of Kranz structure and large lysigenous intercellular spaces, respectively; however, exceptional LI provenance seems special greater than the other ten. Bundle caps of LI leaves consisted of many fiber cells, which supported a dual function of mechanic and hydraulic. As a result, it could be anticipated in gaining more leaf humid and consequently retaining stomata open and gas exchange. Although the potentially water absorption of LI provenance was not great as well as RB, SK and ST provenance (confirming through phytolith abundance), it could yield the highest belowground biomass (about  $535 \text{ kg ha}^{-1}\text{yr}^{-1}$ ). Phytolith, by a structure, can stabilize C, but by chemical composition, it assumed to enhance thermal emissivity in the mid-infrared. Moreover, litter of LI provenance was proved as a great quality by attributing of large amounts of total C, total N, lignin and lignin/fibrous C ratio, while C/N ratio asserting the rate of N release from substrates contained the lowest. That all, LI provenance could be considerable tropical grass with high sequestration of C.

**Table 10.1** Conclusion of the potentially C sequestration of 11 vetiver provenances.

Potential	KP1	LI	NS	PK	RB	RE	KP2	PT	SK	SL	ST
1. Gas circulation	*	*	*	*	*	*	*	*	*	*	*
2. Photosynthetic capacity (Kranz)	*	*	*	*	*	*	*	*	*	*	*
3. Leaf hydraulic		*									
4. Leaf mechanic		*									
5. Phytolith abundance	*	**	*	**	***	*	**	*	***	**	***
6. Belowground biomass and litter quality	**	***				*			*		
Total	5	9	3	4	5	4	4	3	6	4	5

\*Fairly/present/low frequency, \*\*Good/medium frequency, \*\*\*Very good/more frequency.

The interaction among MBC, C substrate availability and soil properties to soil respiration (chapter VII) demonstrated that clay content was a key role in controlling microbial biomass, soil respiration, C mineralization and C storage. Labile organic C such as polysaccharide, peptide or protein compounds were selectively preserved in vetiver soils, whereas recalcitrant C such lignin was continually degraded since an early stage (chapter VIII). After continuous vetiver plantation for 7 years, the C storage at 1.2 m raised about 10 times (from 24 to 229 tC ha<sup>-1</sup>), and labile organic C could turnover the fastest within 18 days and the slowest within 108 days (chapter IX).

Finally, some partial C stocks had been schemed as shown in Figure 10.1.

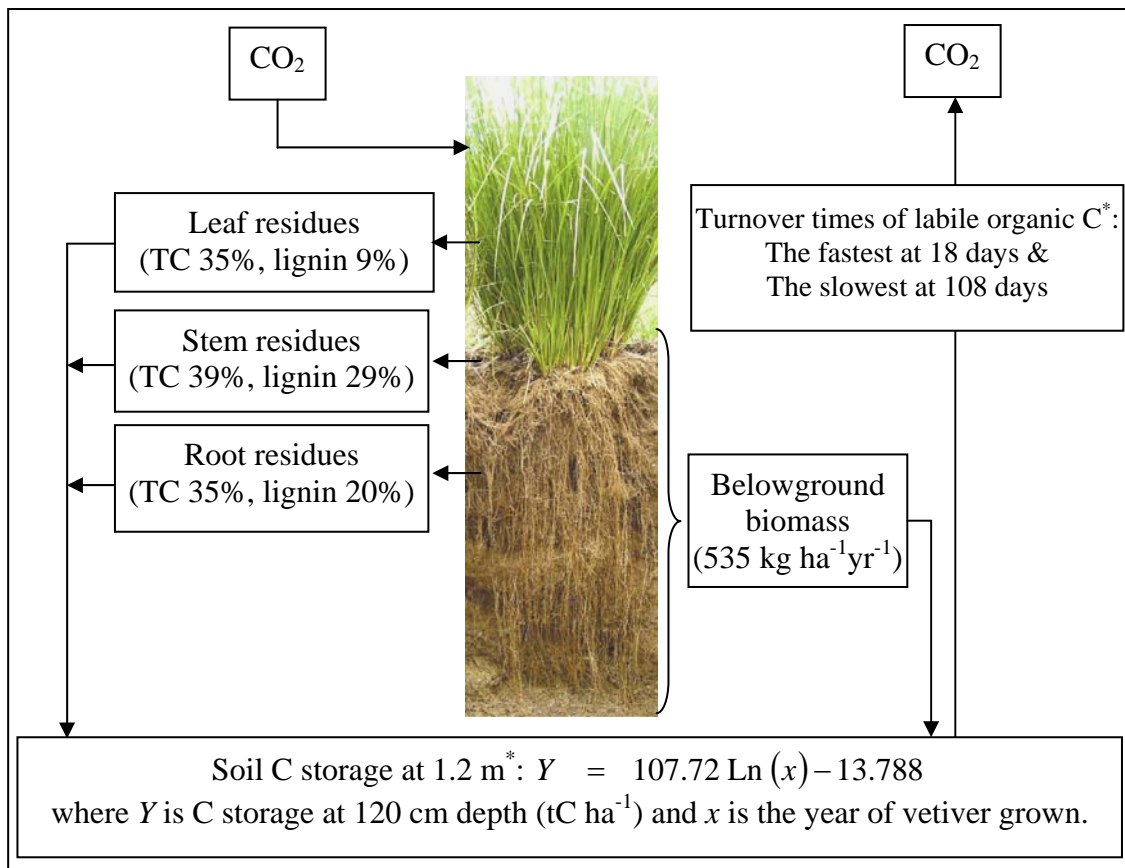


**Figure 10.1** Schematic of partial C storage during vetiver grown, representing by LI provenance (\* = the value did not specify in provenance).

**APPENDIX A**  
**CLIMATE DATA OF NAKHON RATCHASIMA**  
**DURING 2000 - 2008**

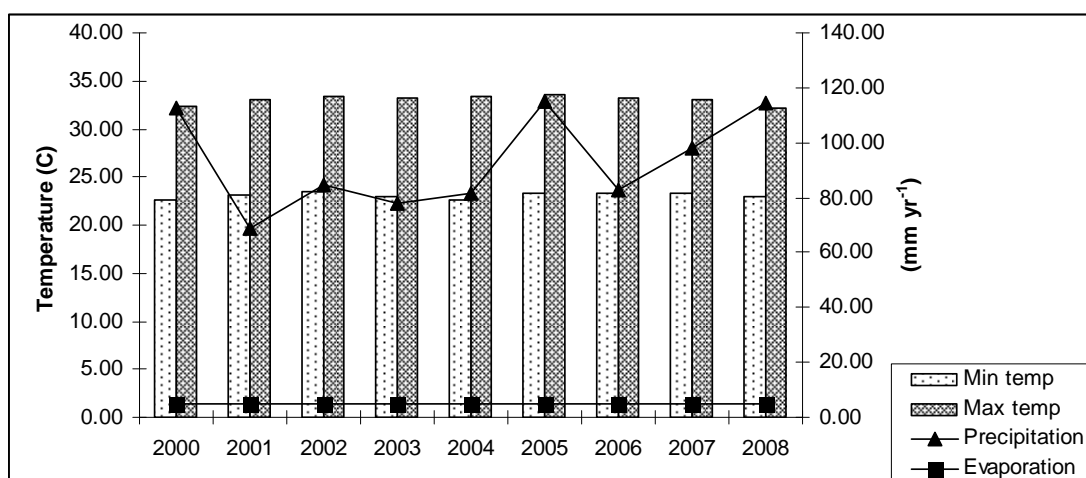


**Figure A.1** Averages of maximum and minimum temperature, precipitation and evaporation of Nakhon Ratchasima during 2000 - 2008 (data from Meteorological station of Nakhon Ratchasima).

**Table A.1** Averages of maximum temperature per month during 2000 - 2008.

Year	Maximum temperature (°C)												
	Jan	Feb	Mar	Apr	May	Jun	Jul	Aug	Sep	Oct	Nov	Dec	Aver.
2000	31	31.8	35.2	34.1	33.7	33.2	32.7	33.1	31.6	31.5	29.8	30.3	32.33
2001	32.5	33.8	33.1	38.3	34.5	34	34.5	33	33.1	31.6	29	29.7	33.09
2002	30.8	33.6	35.3	37.3	34.8	35.4	34.6	33	31.9	31.8	30.4	31.1	33.33
2003	30.2	33.6	34	36.8	35.8	34.9	33.7	33.6	32.2	31.7	32.5	29.7	33.23
2004	31.1	31.5	37	37.6	35.3	33.6	33.8	33.7	32.6	32	32.3	30.4	33.41
2005	31.7	36.6	35.3	37	36.7	35.1	33.7	34.4	32.3	31.2	30.5	28.2	33.56
2006	31.7	33.4	35.5	35.5	34.6	34.6	34.1	33.7	32	31.6	32.8	29.6	33.26
2007	29.9	34.4	36.3	36.3	33.1	35.8	34.7	33.2	32.3	30.1	28.7	31.2	33.00
2008	31.1	30	35.3	35.3	33.3	34	33.8	33	32	31.7	29.3	28.2	32.25

Data from Meteorological station of Nakhon Ratchasima.

**Table A.2** Averages of minimum temperature per month during 2000 - 2008.

Year	Minimum temperature (°C)												Aver.
	Jan	Feb	Mar	Apr	May	Jun	Jul	Aug	Sep	Oct	Nov	Dec	
2000	19.6	19.3	22.7	24.3	24.6	24.6	24.4	24.4	23.6	23.9	19.9	20	22.61
2001	21.4	21.5	23.1	25.7	24.8	24.8	24.9	24.8	24.3	24	19.3	19.3	23.16
2002	18.3	21.9	23.8	24.8	24.9	25.4	25.2	24.6	24.2	23.4	22.4	21.8	23.39
2003	17.7	21.7	23.3	25.3	25.4	25.1	24.7	25	24.2	23.6	21.2	17.9	22.93
2004	18.9	19	23.4	24.8	25	24.7	24.7	25	24.3	22.5	21.4	17.2	22.58
2005	18.7	22.6	22.7	25.2	25.8	25.8	25	25	24.2	23.8	22.4	19.3	23.38
2006	18.7	22.1	23.7	24.9	25	25.3	25.3	25	24.2	23.9	22.7	19.3	23.34
2007	19	21	24.8	25	25.1	25.8	25.1	24.9	24.6	23.5	19.9	20.5	23.27
2008	19	19.6	23.3	24.7	25	25.1	24.9	24.5	24.1	24.3	21.8	18.2	22.88

Data from Meteorological station of Nakhon Ratchasima.

**Table A.3** Averages of evaporation per month during 2000 - 2008.

Year	Evaporation (mm yr <sup>-1</sup> )												Aver.
	Jan	Feb	Mar	Apr	May	Jun	Jul	Aug	Sep	Oct	Nov	Dec	
2000	4.38	4.24	5.61	4.73	4.56	4.7	4.62	5.05	4.13	3.94	4.59	4.9	4.62
2001	4.28	4.93	4.94	6.72	5	5.53	5.7	4.62	4.41	4.28	4.37	4.64	4.95
2002	4.72	4.93	5.18	6.19	4.83	5.51	5.3	4.54	3.62	4.07	4.25	4.25	4.78
2003	4.51	4.97	5.31	5.43	5.65	5.13	4.8	5.04	3.57	4.58	5.05	4.88	4.91
2004	4.12	4.51	6.06	5.36	4.93	4.23	4.9	5.05	4.4	5.25	5.37	4.56	4.90
2005	4.23	5.4	5.7	5.78	5.66	5.18	5.12	4.42	3.71	4.35	3.75	4.58	4.82
2006	5.83	5.34	5.29	5.5	4.92	5.2	5.01	4.96	3.71	3.91	4.56	4.07	4.86
2007	4.87	5.2	5.54	5.66	4.15	5.04	5.66	4.41	3.67	3.72	4.56	4.55	4.75
2008	4.5	4.98	6.05	5.24	4.97	4.67	4.69	4.42	4.07	3.78	4.17	4.39	4.66

Data from Meteorological station of Nakhon Ratchasima.

**Table A.4** Averages of precipitation per month during 2000 - 2008.

Year	Precipitation (mm yr <sup>-1</sup> )												
	Jan	Feb	Mar	Apr	May	Jun	Jul	Aug	Sep	Oct	Nov	Dec	Aver.
2000	1	41.8	11	128.7	194.9	243.9	70	325.3	180.6	146.7	4.5	0	112.37
2001	0.1	0.9	78.8	6.5	212.4	107.5	47.4	123.4	110.3	127	10.1	0	68.70
2002	0.2	9.1	22.8	40	117.9	62.9	129.9	235.9	288.9	51.8	27.3	26.8	84.46
2003	0	32.3	84.3	61.1	50.7	179.9	128	140	142	114.7	0	0	77.75
2004	24.3	34.1	1.2	56.6	207.5	176.3	161.2	104.6	202.8	0	11.4	0	81.67
2005	0	5.7	20.5	49.7	193.3	74.6	176.9	111.5	546.1	98.3	103.1	0.7	115.03
2006	0	4.3	42	145.6	109.9	60.6	66.4	61.4	241.3	255.4	3.5	1.4	82.65
2007	0	0	94.3	53.3	254.3	106.3	132.2	157	147.9	231.2	1.3	0	98.15
2008	5.9	1.5	31	255.2	164.7	90.4	97.5	187.3	349.8	143	49.1	0.3	114.64

Data from Meteorological station of Nakhon Ratchasima.

**APPENDIX B**

**PHYTOLITHIC DISTRIBUTION**

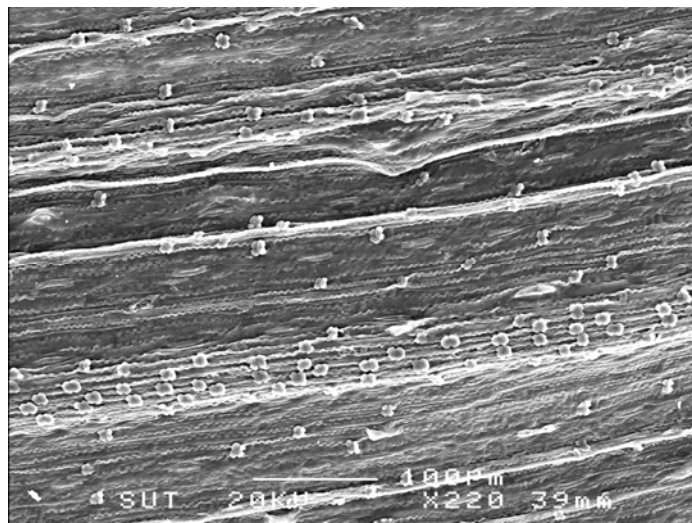


**Figure B.1** Phytolith distribution of leaf of Kamphaeng Phet 1 provenance.

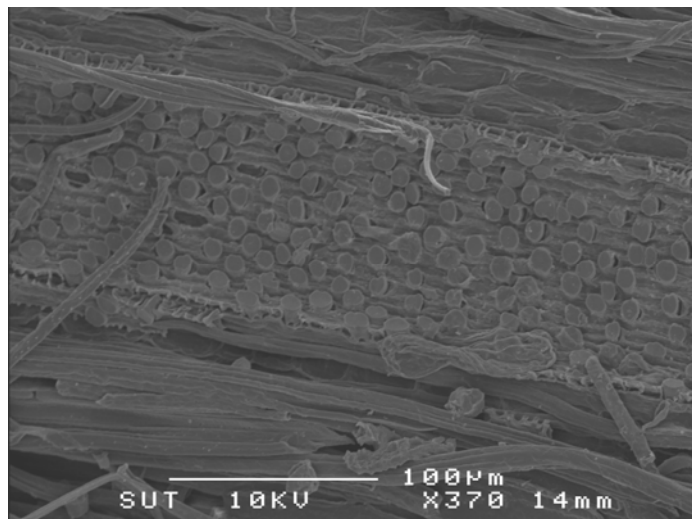


**Figure B.2** Phytolith distribution of leaf of Loei provenance.

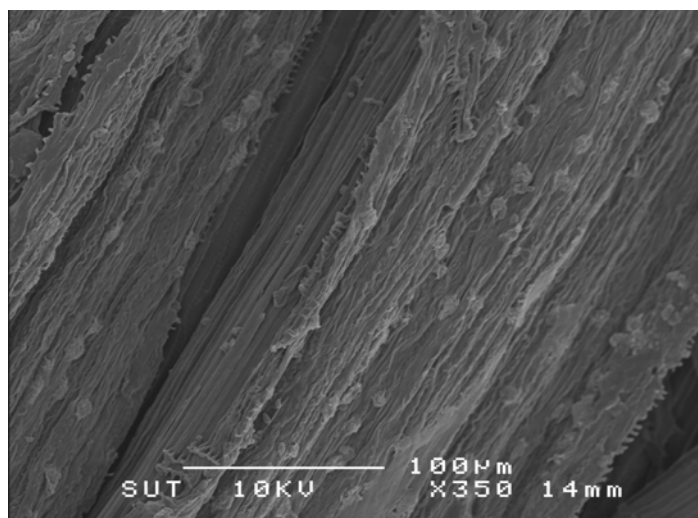


**Figure B.3** Phytolith distribution of leaf of Nakhon Sawan provenance.

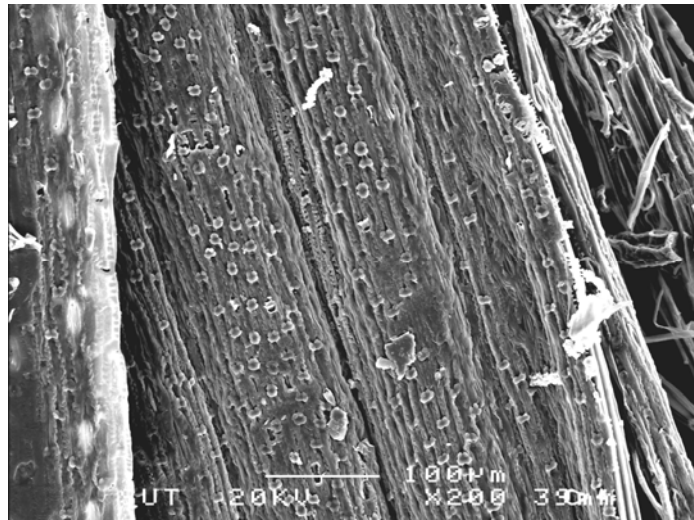


**Figure B.4** Phytolithic distribution of leaf of Prachuabkhirikhan provenance.

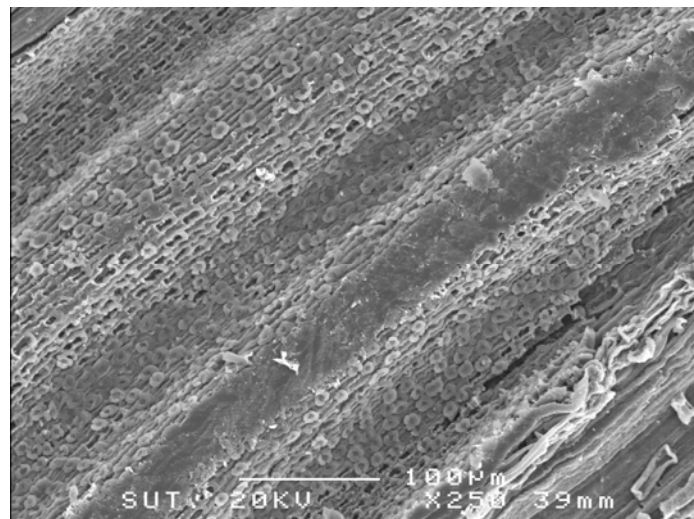


**Figure B.5** Phytolithic distribution of leaf of Ratchaburi provenance.

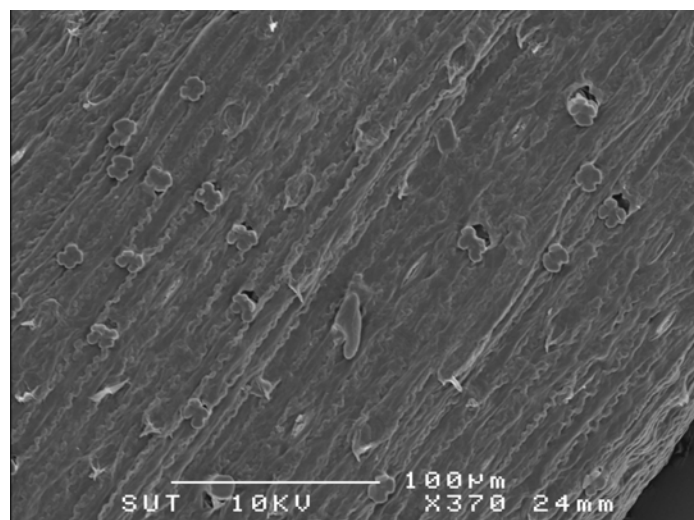


**Figure B.6** Phytolithic distribution of leaf of Roi Et provenance.

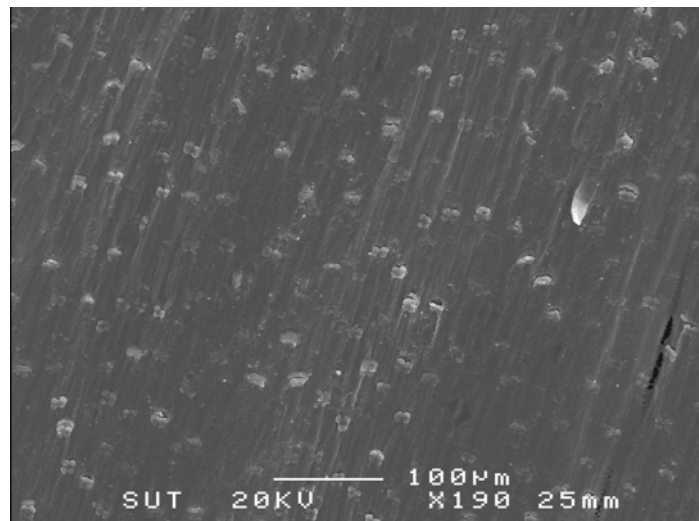


**Figure B.7** Phytolith distribution of leaf of Kamphaeng Phet 2 provenance.

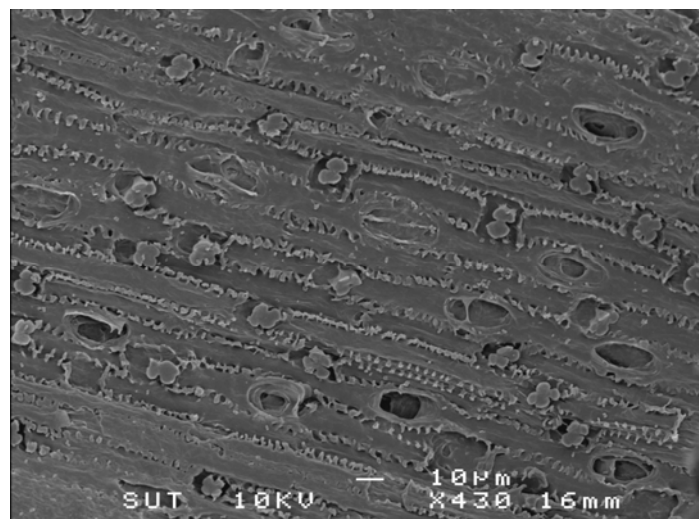


**Figure B.8** Phytolith distribution of leaf of Phraratchathan provenance.

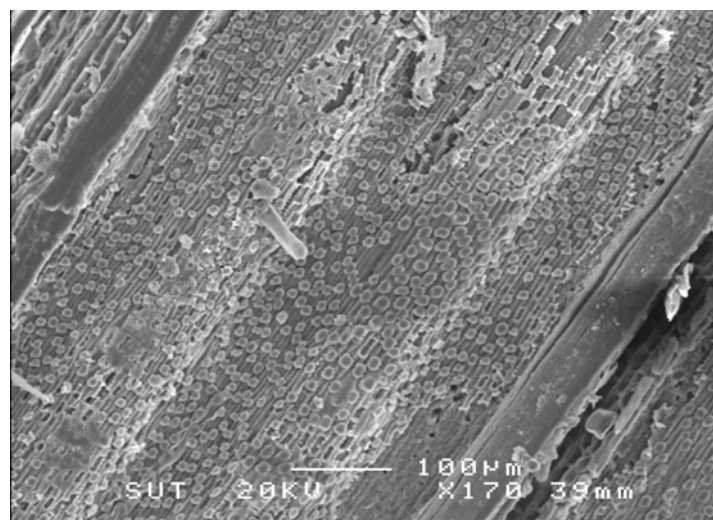


**Figure B.9** Phytolith distribution of leaf of Songkhla 3 provenance.

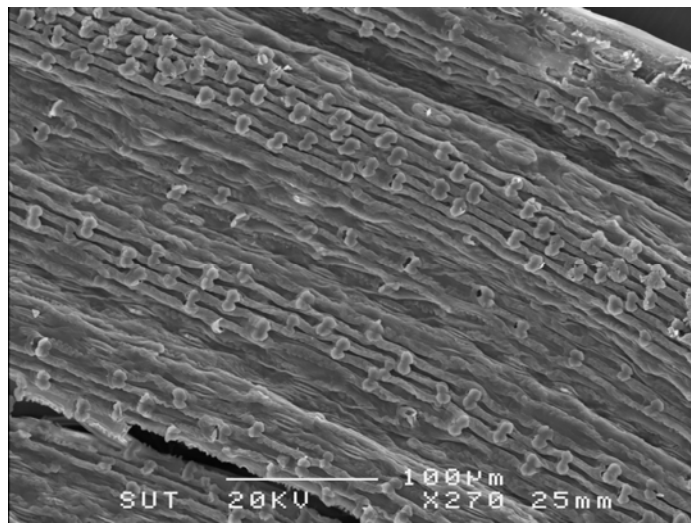


**Figure B.10** Phytolith distribution of leaf of Sri Lanka provenance.

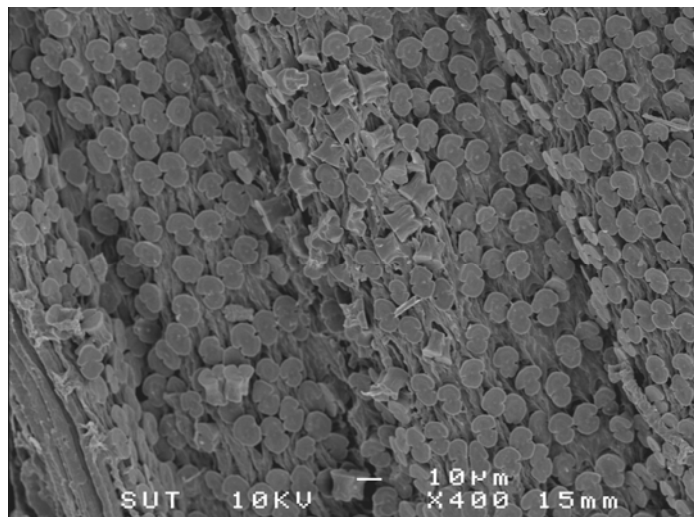


**Figure B.11** Phytolith distribution of leaf of Surat Thani provenance.

## **APPENDIX C**

### **SOIL PROPERTIES AND SOIL CARBON FRACTIONS**

**Table C.1** Location of study sites.

Location	Site	Coordinates			Cont.vetiver (year)
		Latitude	Longitude	Elevation (m)	
the Thai Tapioca Development Institute (TTDI), Huai Bong Subdistrict, Dan Kun Tod District,	1	N 15.09426	E 101.30426	315	5
	2	N 15.16104	E 101.51102	312	7
	3	N 15.16156	E 101.51250	308	7
	4	N 15.16129	E 101.51244	306	7
	5	N 15.15642	E 101.51389	324	7
	6	N 15.14275	E 101.50403	320	7
	7	N 15.14531	E 101.50527	316	3
Ban Nong Kradon, Bueng O Subdistrict, Kham Thale So District	8	N 15.04706	E 101.89987	210	1
	9	N 15.04707	E 101.90006	204	2
	10	N 15.04697	E 101.90022	202	3
Suk Pai Bun Subdistrict, Soeng Sang District,	11	N 14.52763	E 102.49441	236	3
	12	N 14.52743	E 102.49487	233	3
the Iam Seng factory (tapioca mill), Non Sombun Subdistrict, Soeng Sang District	13	N 14.43569	E 102.50488	220	1
	14	N 14.43746	E 102.50546	229	2
Tambol Noon Sumboon, Amphur Soang Sang	15	N 14.36168	E 102.43224	273	2
Ban Thai Charoen, Pak Chong District	16	N 14.76065	E 101.31931	423	2
Land Development Department, Pak Chong District	17	N 14.67203	E 101.41845	312	3
the Regional Office 3, Land Development Department, Mueang District	18	N 15.05923	E 102.13380	167	3

**Table C.2** Mean  $\pm$  SD of soil property\*.

Soil	Depth (cm)	Soil type		Sand		Silt		Clay		Bulk density		pH			
				aver.	SD.	aver.	SD.	aver.	SD.	aver.	SD.	aver.	SD.		
				(%)								(g cm <sup>-3</sup> )		(H <sub>2</sub> O)	
		Texture	Textural group	aver.	SD.	aver.	SD.	aver.	SD.	aver.	SD.	aver.	SD.		
1/1	0-10	sandy clay loam	medium	61.5	1.2	18.8	0.3	19.7	0.9	0.31	0.12	9.20	0.11		
1/2	10-60	sandy clay loam	medium	51.1	0.6	17.3	0.3	31.6	0.3	0.51	0.10	7.15	0.14		
1/3	60-120	sandy clay loam	medium	49.6	1.3	17.7	2.5	32.7	1.3	0.78	0.10	7.18	0.95		
2/1	0-10	sandy loam	coarse	74.6	0.8	12.7	0.6	12.7	0.2	0.39	0.11	8.38	0.39		
2/2	10-60	sandy loam	coarse	72.0	0.5	10.4	0.5	17.7	0.2	0.73	0.19	8.49	0.42		
2/3	60-120	sandy clay loam	medium	71.6	1.0	7.2	1.1	21.2	0.2	0.77	0.08	9.09	0.15		
3/1	0-10	loamy sand	coarse	81.1	1.4	6.2	1.5	12.7	0.2	0.48	0.10	9.23	0.47		
3/2	10-60	sandy loam	coarse	71.6	0.5	10.7	0.7	17.7	0.2	0.85	0.07	7.22	0.22		
3/3	60-120	sandy clay loam	medium	69.3	0.5	8.0	0.8	22.7	0.2	1.21	0.13	9.84	0.29		
4/1	0-10	loamy sand	coarse	80.3	0.6	6.7	0.6	13.0	0.0	0.78	0.13	8.84	0.48		
4/2	10-60	sand	coarse	89.5	1.3	2.5	1.3	8.0	0.0	1.03	0.10	9.24	0.33		
4/3	60-120	loamy sand	coarse	79.6	0.5	5.7	0.2	14.7	0.3	1.10	0.05	9.88	0.34		
5/1	0-10	sandy loam	coarse	77.5	0.1	12.0	0.1	10.5	0.0	0.59	0.16	8.49	1.46		
5/2	10-60	sandy loam	coarse	70.8	0.7	14.2	0.7	15.0	0.0	0.72	0.18	6.73	0.71		
5/3	60-120	sandy clay loam	medium	60.1	0.6	13.7	0.6	26.2	0.0	1.33	0.10	7.20	0.43		
6/1	0-10	sandy clay loam	medium	49.6	0.6	25.8	0.6	24.6	0.0	0.99	0.08	8.98	0.53		
6/2	10-60	sandy clay loam	medium	51.6	0.3	20.7	0.3	27.7	0.2	0.98	0.05	6.42	0.38		
6/3	60-120	sandy clay loam	medium	48.8	0.3	15.5	0.0	35.7	0.2	0.89	0.05	8.87	0.51		
7/1	0-10	sandy loam	coarse	75.5	0.3	8.8	0.3	15.7	0.2	1.09	0.16	8.10	0.42		
7/2	10-60	sandy clay loam	medium	66.5	0.3	3.8	0.3	29.7	0.2	1.10	0.10	7.26	0.59		
7/3	60-120	loam	medium	50.1	0.6	36.2	0.4	13.7	0.2	1.09	0.11	7.09	0.49		

**Table C.2 (Continued).**

Soil	Depth (cm)	Soil type		Sand		Silt		Clay		Bulk density		pH			
				aver.	SD.	aver.	SD.	aver.	SD.	aver.	SD.	aver.	SD.		
				(%)								(g cm <sup>-3</sup> )		(H <sub>2</sub> O)	
		Texture	Textural group	aver.	SD.	aver.	SD.	aver.	SD.	aver.	SD.	aver.	SD.		
8/1	0-10	loamy sand	coarse	82.0	0.5	12.4	0.5	5.7	0.2	1.43	0.07	7.58	0.59		
8/2	10-60	loamy sand	coarse	79.8	0.3	9.5	0.4	10.7	0.2	1.29	0.17	7.65	0.39		
8/3	60-120	sand	coarse	76.5	0.0	5.9	0.2	17.7	0.2	1.29	0.10	8.73	0.29		
9/1	0-10	sand	coarse	85.6	1.4	8.7	1.6	5.7	0.2	1.36	0.05	7.23	0.49		
9/2	10-60	loamy sand	coarse	82.0	0.5	5.9	0.7	12.2	0.2	1.13	0.06	7.66	0.57		
9/3	60-120	sandy clay loam	medium	70.8	0.3	11.5	0.4	17.7	0.2	1.54	0.05	6.98	0.17		
10/1	0-10	loamy sand	coarse	80.5	1.3	11.9	1.4	7.7	0.2	0.77	0.08	7.93	0.15		
10/2	10-60	sandy loam	coarse	75.3	0.3	9.5	0.1	15.2	0.2	1.43	1.39	7.87	0.16		
10/3	60-120	sandy loam	coarse	71.8	0.8	10.5	0.8	17.7	0.2	1.96	0.23	8.65	0.15		
11/1	0-10	sandy clay	coarse	56.6	1.6	7.7	1.5	35.7	0.2	0.80	0.10	8.89	0.54		
11/2	10-60	sandy clay loam	medium	56.1	0.3	10.3	0.3	33.7	0.2	0.89	0.03	9.37	0.30		
11/3	60-120	sandy clay loam	medium	57.6	0.3	7.7	0.0	34.7	0.2	1.24	0.21	9.78	0.39		
12/1	0-10	sandy loam	coarse	71.6	0.8	13.7	0.8	14.7	0.2	0.63	0.08	9.61	0.51		
12/2	10-60	sandy clay loam	medium	57.4	0.5	12.9	0.3	29.7	0.2	0.67	0.16	8.44	0.50		
12/3	60-120	sandy clay loam	medium	57.6	0.3	11.3	0.3	31.2	0.2	0.62	0.05	7.44	0.42		
13/1	0-10	sandy clay loam	medium	55.0	0.5	10.4	0.6	34.7	0.2	0.30	0.21	8.55	1.10		
13/2	10-60	loamy sand	coarse	83.9	1.0	8.9	0.8	7.2	0.2	0.98	0.17	9.28	0.25		
13/3	60-120	sandy loam	coarse	78.7	1.0	8.1	0.9	13.2	0.2	1.36	0.28	8.95	0.44		
14/1	0-10	sandy clay loam	medium	69.0	0.5	5.4	0.3	25.7	0.2	0.45	0.00	11.61	0.40		
14/2	10-60	sandy clay loam	medium	50.3	0.0	14.5	0.0	35.2	0.0	0.48	2.85	9.70	0.35		
14/3	60-120	sandy clay	fine	47.7	0.0	13.4	0.1	38.9	0.1	1.95	0.12	8.22	0.11		

**Table C.2 (Continued).**

Soil	Depth (cm)	Soil type		Sand		Silt		Clay		Bulk density		pH			
				aver.	SD.	aver.	SD.	aver.	SD.	aver.	SD.	aver.	SD.		
				(%)								(g cm <sup>-3</sup> )		(H <sub>2</sub> O)	
		Texture	Textural group	aver.	SD.	aver.	SD.	aver.	SD.	aver.	SD.	aver.	SD.		
15/1	0-10	sand	coarse	90.1	0.8	5.3	0.8	4.5	0.0	1.47	0.10	9.21	0.26		
15/2	10-60	loamy sand	coarse	86.7	0.0	6.5	0.0	6.8	0.0	1.54	0.11	8.22	0.29		
15/3	60-120	sandy loam	coarse	77.7	0.0	9.0	0.0	13.3	0.0	1.41	0.14	8.60	0.43		
16/1	0-10	sandy clay loam	medium	50.0	1.8	19.4	1.9	30.7	0.2	0.51	0.11	6.85	0.36		
16/2	10-60	sandy clay loam	medium	60.6	2.5	13.2	2.3	26.2	0.2	0.62	0.06	6.95	0.20		
16/3	60-120	sandy clay	fine	52.7	1.0	7.6	0.9	39.7	0.2	1.18	0.08	6.81	0.37		
17/1	0-10	clay loam	fine	41.5	0.5	29.8	0.3	28.7	0.2	0.74	0.11	6.68	0.34		
17/2	10-60	clay	fine	45.2	0.8	10.2	0.8	44.7	0.2	1.14	0.06	7.03	0.14		
17/3	60-120	sandy clay	fine	47.8	0.3	6.5	0.5	45.7	0.2	1.20	0.08	6.46	0.60		
18/1	0-10	loamy sand	coarse	84.8	0.5	10.7	0.7	4.5	0.2	1.06	0.09	8.59	0.41		
18/2	10-60	loamy sand	coarse	83.4	0.3	11.0	0.5	5.5	0.2	1.27	0.12	8.29	0.19		
18/3	60-120	loamy sand	coarse	84.6	1.2	9.3	1.4	6.0	0.2	1.41	0.16	8.73	1.09		

**Table C.3** Mean  $\pm$  SD of soil property\*.

Soil	Depth (cm)	EC		Na		K		Mg		Ca		CEC		BS
		(uS cm <sup>-1</sup> )				(cmol kg <sup>-1</sup> )						(cmol kg <sup>-1</sup> )		(%)
		aver.	SD.	aver.	SD.	aver.	SD.	aver.	SD.	aver.	SD.	aver.	SD.	aver.
1/1	0-10	158.1	10.7	0.70	0.01	0.50	0.00	0.66	0.01	4.10	0.10	3.40	0.20	175
1/2	10-60	66.9	11.4	0.45	0.00	0.15	0.00	1.03	0.05	3.96	0.15	4.20	0.20	133
1/3	60-120	62.4	17.7	0.46	0.00	0.14	0.01	0.40	0.01	6.53	0.05	4.10	0.10	184
2/1	0-10	115.5	21.5	0.50	0.02	0.41	0.00	0.38	0.02	2.11	0.11	2.60	0.00	131
2/2	10-60	105.3	30.2	0.10	0.01	0.18	0.00	0.27	0.01	1.75	0.04	2.40	0.00	96
2/3	60-120	43.2	3.4	0.59	0.03	0.13	0.01	0.36	0.01	1.63	0.03	2.23	0.06	122
3/1	0-10	194.4	35.0	0.53	0.01	0.23	0.01	1.01	0.03	3.52	0.03	2.13	0.12	248
3/2	10-60	68.7	21.1	0.26	0.01	0.11	0.00	1.01	0.02	2.85	0.05	2.60	0.00	163
3/3	60-120	60.8	20.5	0.09	0.01	0.11	0.00	0.29	0.02	1.78	0.03	2.87	0.12	79
4/1	0-10	269.5	112.1	0.35	0.01	0.28	0.01	0.31	0.04	3.08	0.07	2.87	0.12	140
4/2	10-60	64.5	6.2	0.19	0.01	0.11	0.00	0.18	0.01	1.92	0.01	2.80	0.00	86
4/3	60-120	70.8	29.5	0.61	0.01	0.14	0.02	0.26	0.01	2.04	0.06	3.50	0.30	87
5/1	0-10	89.3	18.1	0.61	0.00	0.61	0.01	0.74	0.00	5.63	0.05	5.30	0.26	143
5/2	10-60	54.5	16.5	0.44	0.01	0.33	0.01	0.52	0.04	5.11	0.07	4.80	0.00	133
5/3	60-120	58.6	8.3	0.44	0.01	0.23	0.00	0.72	0.02	6.67	0.02	5.20	0.69	155
6/1	0-10	95.3	41.8	0.30	0.22	0.86	0.01	0.90	0.01	1.76	0.03	3.50	0.10	109
6/2	10-60	97.5	10.5	0.61	0.00	0.65	0.03	0.82	0.01	1.51	0.02	3.20	0.36	112
6/3	60-120	109.0	12.4	0.71	0.01	0.23	0.01	1.01	0.12	1.64	0.01	4.20	0.20	85
7/1	0-10	117.8	13.1	0.44	0.01	0.02	0.00	0.15	0.00	0.43	0.03	0.87	0.12	120
7/2	10-60	52.1	7.6	0.19	0.01	0.02	0.00	0.36	0.03	0.52	0.03	1.53	0.12	71
7/3	60-120	30.2	4.4	0.36	0.01	0.01	0.00	0.40	0.06	0.51	0.01	1.60	0.00	80

**Table C.3 (Continued).**

Soil	Depth (cm)	EC ( $\mu\text{S cm}^{-1}$ )		Na		K		Mg		Ca		CEC ( $\text{cmol kg}^{-1}$ )		BS (%)
		aver.	SD.	aver.	SD.	aver.	SD.	aver.	SD.	aver.	SD.	aver.	SD.	aver.
8/1	0-10	62.0	17.7	0.19	0.01	0.08	0.00	0.12	0.01	0.43	0.01	1.00	0.00	82
8/2	10-60	19.7	6.4	0.79	0.01	0.05	0.00	0.20	0.01	0.44	0.01	1.20	0.00	124
8/3	60-120	26.6	5.0	0.26	0.01	0.04	0.00	0.24	0.00	0.38	0.03	2.10	0.10	44
9/1	0-10	39.0	14.6	0.19	0.01	0.01	0.00	0.19	0.00	0.52	0.03	1.20	0.20	76
9/2	10-60	20.9	8.3	0.44	0.01	0.01	0.00	0.56	0.02	0.53	0.04	1.80	0.00	86
9/3	60-120	36.8	22.7	0.27	0.01	0.01	0.00	0.54	0.01	0.55	0.04	1.50	0.10	91
10/1	0-10	21.3	1.7	0.27	0.02	0.04	0.05	0.04	0.01	1.97	0.03	6.00	0.35	39
10/2	10-60	10.4	0.6	0.27	0.01	0.03	0.00	0.24	0.00	1.22	0.02	3.97	0.32	45
10/3	60-120	26.5	14.5	0.53	0.01	0.03	0.00	0.20	0.01	1.23	0.01	3.87	0.12	51
11/1	0-10	49.6	8.3	0.09	0.01	0.51	0.04	0.06	0.00	1.53	0.02	4.47	0.12	49
11/2	10-60	19.0	5.9	0.18	0.01	0.07	0.01	0.53	0.06	1.54	0.04	3.50	0.26	66
11/3	60-120	27.8	2.9	0.27	0.01	0.21	0.00	0.05	0.00	0.61	0.02	2.60	0.35	44
12/1	0-10	26.2	17.9	0.35	0.01	0.42	0.02	0.01	0.00	0.89	0.01	3.20	0.20	52
12/2	10-60	34.7	13.7	0.52	0.01	0.32	0.02	0.24	0.02	1.46	0.03	4.13	0.12	62
12/3	60-120	36.6	20.4	0.84	0.01	0.28	0.01	0.24	0.02	2.94	0.05	8.70	0.56	49
13/1	0-10	73.9	18.5	0.87	0.02	0.15	0.00	1.70	0.07	8.89	0.08	10.73	0.12	108
13/2	10-60	29.9	2.0	0.86	0.01	0.20	0.01	1.32	0.03	6.42	0.19	6.63	0.21	133
13/3	60-120	12.0	3.1	0.51	0.02	0.25	0.02	1.82	0.13	5.60	0.01	7.70	0.30	106
14/1	0-10	99.9	10.5	0.54	0.02	0.03	0.00	0.13	0.00	0.56	0.04	0.60	0.00	210
14/2	10-60	148.7	15.6	0.18	0.01	0.03	0.00	0.10	0.00	0.54	0.01	0.53	0.12	160
14/3	60-120	97.1	6.2	1.14	0.01	0.01	0.00	0.20	0.01	0.53	0.02	0.60	0.00	313

**Table C.3** (Continued).

Soil	Depth (cm)	EC		Na		K		Mg		Ca		CEC		BS
		(uS cm <sup>-1</sup> )		(cmol kg <sup>-1</sup> )						(cmol kg <sup>-1</sup> )		(%)		
		aver.	SD.	aver.	SD.	aver.	SD.	aver.	SD.	aver.	SD.	aver.	SD.	aver.
15/1	0-10	17.2	3.7	0.34	0.01	0.14	0.18	0.64	0.08	3.14	0.22	6.27	0.50	68
15/2	10-60	19.9	7.6	0.77	0.02	0.15	0.02	0.50	0.02	3.04	0.06	5.03	0.60	89
15/3	60-120	44.6	12.0	0.65	0.00	0.03	0.00	1.31	0.02	2.53	0.03	5.60	0.20	81
16/1	0-10	57.5	2.1	0.41	0.02	1.13	0.01	1.32	0.03	7.53	0.20	4.40	0.35	236
16/2	10-60	36.5	3.9	0.40	0.00	0.98	0.04	1.17	0.05	7.48	0.05	4.40	0.00	228
16/3	60-120	44.6	1.3	0.33	0.00	0.69	0.01	1.33	0.06	7.71	0.04	4.60	0.40	219
17/1	0-10	50.0	4.6	0.52	0.01	0.09	0.02	0.22	0.01	3.95	0.05	0.80	0.00	598
17/2	10-60	38.3	1.8	0.35	0.00	0.01	0.00	0.06	0.02	3.52	0.03	0.60	0.00	658
17/3	60-120	51.7	6.5	0.52	0.01	0.09	0.02	0.18	0.01	3.13	0.03	0.60	0.00	654
18/1	0-10	31.5	13.0	0.41	0.00	0.08	0.00	0.22	0.03	3.03	0.02	0.40	0.00	933
18/2	10-60	11.3	1.5	0.62	0.01	0.07	0.00	0.24	0.07	3.75	0.04	0.47	0.12	1001
18/3	60-120	9.7	3.1	0.84	0.02	0.07	0.00	0.20	0.01	2.87	0.03	0.60	0.00	663

**Table C.4** Mean  $\pm$  SD of total C, total N and C/N ratio.

Soil	%Total C*					%Total N*					C/N ratio	TC at 1.2 m	
	n1	n2	n3	Aver.	SD.	n1	n2	n3	Aver.	SD.		(tC ha <sup>-1</sup> )	
1/1	3.64	3.75	3.77	3.72	0.07	0.07	0.08	0.05	0.07	0.01	55.50	28.83	
1/2	3.65	3.55	3.60	3.60	0.05	0.08	0.07	0.06	0.07	0.01	52.92	91.03	290.96
1/3	5.66	3.82	2.55	4.01	1.56	0.07	0.08	0.01	0.06	0.04	72.47	75.47	
2/1	5.66	4.96	5.85	5.49	0.47	0.13	0.22	0.18	0.18	0.05	31.25	21.36	
2/2	2.08	5.94	4.67	4.23	1.97	0.09	0.12	0.07	0.09	0.03	45.01	153.61	364.20
2/3	3.12	4.22	4.89	4.08	0.89	0.04	0.11	0.09	0.08	0.03	50.33	189.11	
3/1	5.63	3.25	4.55	4.48	1.19	0.12	0.13	0.09	0.11	0.02	40.09	37.94	
3/2	3.66	2.55	1.45	2.55	1.11	0.08	0.10	0.09	0.09	0.01	28.58	154.10	321.91
3/3	4.00	2.05	1.88	2.64	1.18	0.14	0.10	0.09	0.11	0.03	23.81	76.60	
4/1	3.11	4.59	4.40	4.03	0.81	0.18	0.22	0.15	0.18	0.04	22.00	44.27	
4/2	3.04	2.45	3.01	2.83	0.33	0.15	0.20	0.22	0.19	0.03	14.81	145.71	372.96
4/3	2.89	2.55	3.45	2.96	0.45	0.19	0.23	0.22	0.21	0.02	13.96	138.07	
5/1	4.87	3.15	4.66	4.23	0.94	0.49	0.33	0.37	0.40	0.08	10.66	56.11	
5/2	3.22	4.00	4.25	3.82	0.54	0.34	0.31	0.30	0.32	0.02	12.07	137.01	450.12
5/3	3.22	3.47	4.12	3.60	0.46	0.31	0.22	0.34	0.29	0.06	12.43	127.55	
6/1	2.90	4.01	3.45	3.45	0.56	0.26	0.25	0.28	0.26	0.02	13.14	34.30	
6/2	2.42	4.58	3.78	3.59	1.09	0.28	0.30	0.25	0.28	0.03	13.07	176.06	430.70
6/3	2.87	4.96	4.55	4.13	1.11	0.25	0.12	0.25	0.21	0.08	19.97	219.56	
7/1	2.06	3.78	3.00	2.95	0.86	0.29	0.19	0.35	0.28	0.08	10.64	32.28	
7/2	1.64	3.02	3.47	2.71	0.95	0.25	0.22	0.26	0.24	0.02	11.12	149.35	371.87
7/3	1.63	3.14	3.98	2.92	1.19	0.19	0.20	0.22	0.20	0.02	14.34	191.47	

**Table C.4 (Continued).**

Soil	% Total C*					% Total N*					C/N ratio	TC at 1.2 m	
	n1	n2	n3	Aver.	SD.	n1	n2	n3	Aver.	SD.		(tC ha <sup>-1</sup> )	
8/1	0.50	1.47	1.59	1.19	0.60	0.11	0.15	0.14	0.13	0.02	9.02	17.02	
8/2	0.66	1.56	1.48	1.23	0.50	0.18	0.11	0.18	0.16	0.04	7.95	79.75	190.00
8/3	1.08	1.99	0.56	1.21	0.72	0.18	0.14	0.22	0.18	0.04	6.70	93.45	
9/1	1.52	2.05	1.95	1.84	0.28	0.25	0.22	0.18	0.22	0.03	8.56	25.01	
9/2	0.88	2.19	1.47	1.51	0.65	0.29	0.25	0.25	0.26	0.02	5.77	85.31	220.63
9/3	0.76	1.69	1.12	1.19	0.47	0.26	0.21	0.30	0.26	0.05	4.66	109.97	
10/1	1.98	2.02	1.80	1.93	0.12	0.23	0.29	0.26	0.26	0.03	7.46	27.71	
10/2	0.55	2.62	2.55	1.91	1.18	0.21	0.25	0.29	0.25	0.04	7.62	73.27	364.34
10/3	1.56	0.99	2.89	1.81	0.98	0.20	0.15	0.20	0.18	0.03	9.87	213.49	
11/1	2.55	3.66	3.01	3.07	0.56	0.32	0.33	0.40	0.35	0.05	8.83	3.49	
11/2	1.73	1.65	2.09	1.82	0.24	0.36	0.40	0.32	0.36	0.04	5.08	3.42	246.45
11/3	1.40	2.22	2.06	1.89	0.44	0.22	0.22	0.28	0.24	0.03	7.86	27.72	
12/1	2.86	2.59	2.99	2.81	0.20	0.28	0.30	0.27	0.28	0.02	9.90	17.65	
12/2	1.73	1.98	2.40	2.04	0.34	0.26	0.20	0.28	0.25	0.04	8.28	67.79	166.03
12/3	2.64	1.60	2.22	2.15	0.52	0.25	0.22	0.27	0.25	0.03	8.72	80.69	
13/1	1.91	2.09	2.30	2.10	0.20	0.30	0.22	0.31	0.28	0.05	7.55	6.34	
13/2	1.53	1.05	1.11	1.23	0.26	0.24	0.21	0.19	0.21	0.03	5.74	17.99	233.30
13/3	2.29	1.15	2.69	2.04	0.80	0.29	0.32	0.31	0.31	0.01	6.64	44.34	
14/1	1.08	1.40	1.77	1.42	0.34	0.30	0.33	0.28	0.30	0.03	4.65	0.27	
14/2	2.02	2.58	2.64	2.41	0.34	0.29	0.30	0.22	0.27	0.04	8.99	235.84	309.41
14/3	1.25	2.99	2.05	2.10	0.87	0.32	0.30	0.34	0.32	0.02	6.57	60.11	

**Table C.4 (Continued).**

Soil	%Total C*					%Total N*					C/N ratio	TC at 1.2 m (tC ha <sup>-1</sup> )	
	n1	n2	n3	Aver.	SD.	n1	n2	n3	Aver.	SD.			
15/1	0.75	1.02	0.56	0.78	0.23	0.25	0.31	0.37	0.31	0.06	2.50	11.42	
15/2	0.58	0.45	0.90	0.64	0.23	0.22	0.31	0.32	0.28	0.05	2.26	49.49	102.42
15/3	0.48	0.50	0.49	0.49	0.01	0.23	0.28	0.31	0.27	0.04	1.80	41.63	
16/1	1.92	2.02	2.33	2.09	0.22	0.30	0.26	0.28	0.28	0.02	7.46	24.60	
16/2	1.45	2.03	1.89	1.79	0.31	0.34	0.29	0.24	0.29	0.05	6.18	45.89	189.52
16/3	1.88	1.45	1.90	1.74	0.25	0.34	0.25	0.34	0.31	0.05	5.61	65.31	
17/1	1.50	2.09	2.20	1.93	0.38	0.30	0.24	0.25	0.26	0.03	7.34	23.21	
17/2	1.82	2.99	2.78	2.53	0.62	0.34	0.33	0.25	0.31	0.05	8.28	143.61	324.85
17/3	2.17	2.06	2.70	2.31	0.34	0.49	0.50	0.35	0.45	0.08	5.18	102.22	
18/1	1.36	1.20	0.95	1.17	0.21	0.32	0.40	0.34	0.35	0.04	3.31	16.50	
18/2	1.77	1.65	1.30	1.57	0.24	0.33	0.31	0.33	0.32	0.01	4.87	83.18	196.34
18/3	1.11	0.85	1.02	0.99	0.13	0.19	0.21	0.38	0.26	0.10	3.82	75.60	

\*all values are the average with n = 3

**Table C.5** Mean  $\pm$  SD of C availability index ( $K_2SO_4$ -C).

Soil	$K_2SO_4$ -C (mg g <sup>-1</sup> soil) <sup>a</sup>										Aver.	SD.
	n1	n2	n3	n4	n5	n6	n7	n8	n9	n10		
1/1	2.15	2.46	2.56	2.66	2.05	NE <sup>b</sup>	2.97	3.07	3.17	2.25	2.59	0.41
1/2	2.09	0.11	1.10	2.86	2.09	2.09	3.19	2.20	0.00	2.97	1.87	1.13
1/3	1.00	2.55	1.22	0.44	0.00	3.10	0.22	3.32	3.44	0.11	1.54	1.41
2/1	2.29	2.39	2.49	2.59	NE	2.99	2.89	2.59	3.09	2.09	2.60	0.33
2/2	2.26	3.12	2.69	0.86	0.97	3.01	1.61	0.97	3.33	3.98	2.28	1.12
2/3	2.35	2.25	2.67	2.78	2.89	2.99	3.10	0.75	3.31	3.42	2.65	0.77
3/1	2.18	2.48	2.48	2.58	2.68	2.58	2.88	NE	3.07	NE	2.62	0.27
3/2	2.44	3.08	2.65	2.76	2.87	2.65	NE	3.18	3.29	3.40	2.92	0.33
3/3	0.11	0.00	0.22	2.80	1.18	3.01	2.58	NE	4.09	3.12	1.90	1.54
4/1	2.44	2.94	1.93	3.65	3.15	1.93	2.94	NE	3.15	NE	2.77	0.62
4/2	2.19	2.40	2.82	2.72	2.82	1.98	2.40	NE	1.46	NE	2.35	0.47
4/3	2.44	2.11	4.10	2.88	2.11	3.10	3.10	3.33	3.44	NE	2.96	0.66
5/1	2.19	1.89	2.49	2.39	1.59	2.39	3.19	3.69	1.40	3.19	2.44	0.73
5/2	2.21	1.68	2.63	2.74	2.63	2.95	3.05	3.16	2.42	0.95	2.44	0.68
5/3	0.00	1.64	2.74	0.11	2.96	0.11	3.29	3.29	3.40	1.21	1.87	1.43
6/1	2.05	2.46	0.51	2.66	0.10	2.87	2.97	3.07	3.17	2.46	2.23	1.07
6/2	3.90	2.38	1.08	2.82	2.06	2.06	3.14	2.17	3.03	NE	2.51	0.81
6/3	0.00	0.11	2.79	1.67	1.67	2.23	3.01	3.35	0.22	3.57	1.86	1.36
7/1	1.97	2.49	2.59	2.70	2.80	3.11	3.01	2.70	3.22	2.18	2.68	0.39
7/2	1.81	3.08	2.65	0.85	0.96	2.97	1.59	0.96	3.29	3.93	2.21	1.12
7/3	0.45	2.34	2.79	2.90	3.01	3.12	3.23	0.78	3.45	1.11	2.32	1.11
8/1	2.12	2.53	2.53	2.63	2.73	2.63	2.93	NE	3.13	3.44	2.74	0.38
8/2	2.01	2.91	2.51	2.61	2.71	2.51	2.91	3.01	3.11	3.21	2.75	0.36
8/3	2.38	3.24	2.59	2.81	3.24	3.03	2.59	NE	4.11	0.00	2.67	1.12
9/1	2.12	2.93	1.92	3.64	3.13	1.92	2.93	NE	3.13	NE	2.72	0.64
9/2	2.23	2.33	2.73	2.63	2.73	1.92	2.33	0.81	1.42	NE	2.12	0.65
9/3	2.18	2.07	4.04	2.84	2.07	3.06	NE	3.28	3.38	NE	2.87	0.71
10/1	2.12	1.92	2.53	2.43	1.62	2.43	3.23	2.73	3.13	3.23	2.54	0.56
10/2	2.16	1.73	2.70	2.81	2.70	3.02	3.13	3.24	2.48	0.97	2.50	0.70
10/3	2.43	1.66	2.76	1.88	2.98	2.98	3.31	3.31	3.42	2.32	2.71	0.62
11/1	NE	2.32	1.06	2.75	2.01	2.01	3.06	4.97	3.27	2.85	2.70	1.09
11/2	0.11	2.64	NE	1.72	1.72	3.21	0.11	3.44	0.11	3.67	1.86	1.47
11/3	NE	0.12	3.03	3.16	3.28	1.46	3.52	0.24	2.67	5.83	2.59	1.78
12/1	3.06	3.06	2.64	0.85	0.95	2.96	1.58	0.95	3.27	3.91	2.32	1.13
12/2	2.64	2.41	2.87	2.98	3.10	3.21	3.33	0.80	3.56	1.03	2.59	0.94
12/3	2.31	3.03	3.03	3.16	3.28	NE	3.52	NE	3.76	2.31	3.05	0.52
13/1	5.31	3.34	2.88	3.00	1.15	2.88	3.34	3.46	0.58	3.69	2.96	1.31
13/2	5.21	3.81	3.05	3.30	3.81	3.56	3.05	NE	4.83	3.81	3.83	0.75
13/3	2.66	0.42	0.14	5.04	4.34	0.14	4.06	NE	4.34	NE	2.64	2.10

**Table C.5** (Continued).

Soil	K <sub>2</sub> SO <sub>4</sub> -C (mg g <sup>-1</sup> soil) <sup>a</sup>										Aver.	SD.
	n1	n2	n3	n4	n5	n6	n7	n8	n9	n10		
14/1	3.18	3.66	4.29	4.13	4.29	3.02	3.66	4.77	2.23	NE	3.69	0.79
14/2	NE	0.11	4.17	2.93	0.23	3.15	0.90	3.38	3.49	NE	2.30	1.61
14/3	NE	2.20	2.89	2.77	1.85	2.77	0.23	0.12	0.46	5.08	2.04	1.60
15/1	2.06	2.35	2.45	2.55	1.96	2.74	2.84	2.94	2.25	2.16	2.43	0.34
15/2	2.28	2.18	0.99	2.58	1.88	1.88	2.88	1.98	4.66	2.68	2.40	0.95
15/3	2.25	2.25	1.02	2.66	1.94	1.94	2.97	2.05	4.40	2.76	2.43	0.88
16/1	NE	2.48	2.70	1.62	1.62	3.02	2.91	3.24	3.34	3.45	2.71	0.69
16/2	0.35	2.80	2.91	3.03	3.15	3.50	1.05	3.03	0.23	0.12	2.02	1.39
16/3	3.02	0.24	3.02	0.12	1.09	3.38	0.12	1.09	0.24	4.47	1.68	1.63
17/1	3.19	2.16	2.57	2.68	2.78	2.88	2.98	0.72	1.03	3.29	2.43	0.88
17/2	0.00	0.11	0.21	2.76	2.87	3.61	0.00	NE	NE	0.21	1.22	1.56
17/3	2.52	0.00	2.74	2.84	0.11	2.74	3.17	0.55	3.39	0.00	1.81	1.44
18/1	NE	2.98	2.38	2.58	2.98	2.78	2.38	NE	3.77	2.98	2.85	0.45
18/2	NE	2.93	1.92	3.64	3.13	1.92	2.93	NE	3.13	3.23	2.85	0.62
18/3	2.68	NE	2.79	2.68	2.79	1.96	NE	3.10	1.44	NE	2.49	0.58

<sup>a</sup>all values are the average with n = 10.

<sup>b</sup>NE = Can not be estimated.

**Table C.6** Mean  $\pm$  SD of microbial biomass measuring by chloroform fumigation extraction (CFE-MBC).

Soil	FeSO <sub>4</sub> - blank (mL)		OC (ug mL <sup>-1</sup> )		VS	MS	OC <sub>F</sub>	OC <sub>UF</sub>	MBC (mg g <sup>-1</sup> soil)
	Fume*	Unfume*	Fume	Unfume					
1/1	2.58	2.03	503.1	395.9	151.2	28.8	2640.7	2077.8	1.61
1/2	2.25	1.70	438.8	331.5	153.2	27.1	2477.2	1871.6	1.73
1/3	2.60	1.39	507.0	271.1	153.4	27.0	2881.4	1540.5	3.83
2/1	2.63	2.29	512.9	446.6	150.5	29.5	2617.9	2279.5	0.97
2/2	2.14	2.12	417.3	413.4	152.5	27.7	2299.8	2278.3	0.06
2/3	2.48	2.48	483.6	483.6	152.4	27.8	2651.4	2651.4	0.00
3/1	2.43	1.94	473.9	378.3	150.4	29.6	2410.3	1924.3	1.39
3/2	2.80	2.47	546.0	481.7	152.2	28.0	2972.1	2621.8	1.00
3/3	2.42	1.49	471.9	290.6	152.5	27.7	2602.7	1602.5	2.86
4/1	2.35	1.98	458.3	386.1	151.0	29.0	2384.7	2009.2	1.07
4/2	2.01	1.47	392.0	286.7	151.8	28.3	2099.1	1535.2	1.61
4/3	2.85	2.28	555.8	444.6	153.4	27.0	3158.8	2527.1	1.81
5/1	2.57	2.45	501.2	477.8	150.6	29.5	2561.9	2442.2	0.34
5/2	2.33	2.32	454.4	452.4	152.0	28.2	2451.4	2440.9	0.03
5/3	2.59	1.71	505.1	333.5	153.1	27.2	2839.6	1874.8	2.76
6/1	2.49	2.18	485.6	425.1	151.2	28.8	2548.0	2230.8	0.91
6/2	2.39	2.08	466.1	405.6	152.7	27.5	2588.0	2252.3	0.96
6/3	2.27	1.67	442.7	325.7	153.5	26.8	2532.5	1863.1	1.91
7/1	2.59	2.58	505.1	503.1	151.6	28.5	2687.9	2677.5	0.03
7/2	2.16	2.08	421.2	405.6	152.2	28.0	2293.5	2208.6	0.24
7/3	2.22	2.08	432.9	405.6	153.5	26.9	2473.2	2317.3	0.45
8/1	2.43	2.43	473.9	473.9	150.9	29.1	2456.4	2456.4	0.00
8/2	2.75	2.74	536.3	534.3	150.7	29.3	2760.4	2750.4	0.03
8/3	2.41	2.12	470.0	413.4	152.7	27.5	2605.6	2292.1	0.90
9/1	2.32	1.85	452.4	360.8	150.9	29.1	2345.2	1870.1	1.36
9/2	1.99	1.78	388.1	347.1	150.9	29.1	2013.5	1801.0	0.61
9/3	2.30	1.72	448.5	335.4	152.9	27.3	2511.1	1877.9	1.81
10/1	2.53	2.51	493.4	489.5	150.9	29.1	2557.5	2537.3	0.06
10/2	2.32	2.31	452.4	450.5	152.7	27.6	2506.3	2495.5	0.03
10/3	2.55	2.45	497.3	477.8	153.3	27.1	2816.7	2706.3	0.32
11/1	2.47	2.19	481.7	427.1	152.1	28.1	2609.4	2313.6	0.85
11/2	2.32	1.35	452.4	263.3	154.3	26.2	2660.5	1548.2	3.18
11/3	2.33	1.89	454.4	368.6	155.9	25.1	2828.2	2294.1	1.53
12/1	2.49	2.20	485.6	429.0	152.1	28.1	2630.5	2324.1	0.88
12/2	2.30	2.26	448.5	440.7	154.3	26.2	2637.6	2591.7	0.13
12/3	2.13	1.87	415.4	364.7	155.9	25.1	2585.4	2269.8	0.90
13/1	2.71	2.57	528.5	501.2	154.5	26.1	3125.8	2964.3	0.46

**Table C.6** (Continued).

Soil	FeSO <sub>4</sub> - blank (mL)		OC (ug mL <sup>-1</sup> )		VS	MS	OC <sub>F</sub>	OC <sub>UF</sub>	MBC (mg g <sup>-1</sup> soil)
	Fume*	Unfume*	Fume	Unfume					
13/2	2.82	2.61	549.9	509.0	157.3	24.1	3584.4	3317.5	0.76
13/3	1.90	1.13	370.5	220.4	160.3	22.3	2658.8	1581.3	3.08
14/1	2.04	1.98	397.8	386.1	164.6	20.2	3243.8	3148.4	0.27
14/2	1.83	1.45	356.9	282.8	153.8	26.6	2061.7	1633.6	1.22
14/3	2.25	1.48	438.8	288.6	154.5	26.1	2600.2	1710.3	2.54
15/1	2.55	2.48	497.3	483.6	150.1	29.9	2499.7	2431.1	0.20
15/2	2.56	2.42	499.2	471.9	150.4	29.6	2538.6	2399.8	0.40
15/3	2.46	2.37	479.7	462.2	151.2	28.8	2517.9	2425.8	0.26
16/1	2.64	2.05	514.8	399.8	152.6	27.6	2848.5	2211.9	1.82
16/2	2.28	1.73	444.6	337.4	154.8	25.9	2657.3	2016.3	1.83
16/3	2.24	1.39	436.8	271.1	155.8	25.1	2706.4	1679.4	2.93
17/1	2.44	2.36	475.8	460.2	151.4	28.7	2511.3	2429.0	0.24
17/2	1.95	0.90	380.3	175.5	152.2	27.9	2071.2	956.0	3.19
17/3	2.83	1.65	551.9	321.8	153.0	27.3	3096.6	1805.4	3.69
18/1	2.49	1.94	485.6	378.3	150.4	29.6	2470.7	1924.9	1.56
18/2	2.42	2.03	471.9	395.9	150.9	29.1	2444.9	2050.9	1.13
18/3	1.52	1.46	296.4	284.7	151.5	28.6	1568.8	1506.8	0.18

\*all values are the average with n = 10.

**Table C.7** Mean  $\pm$  SD of microbial biomass measuring by chloroform fumigation incubation (CFI-MBC).

Soil	CFI-MBC (mg g <sup>-1</sup> soil) <sup>a</sup>										Aver.	SD.
	n1	n2	n3	n4	n5	n6	n7	n8	n9	n10		
1/1	3.56	NE <sup>b</sup>	7.56	NE	5.56	1.11	0.22	8.22	NE	3.56	4.25	3.04
1/2	NE	8.44	0.22	5.33	4.89	4.00	NE	7.11	8.67	1.78	5.06	3.03
1/3	7.78	7.47	1.78	7.33	7.11	8.44	0.44	4.22	1.33	9.56	5.55	3.31
2/1	0.22	3.33	0.98	4.44	NE	3.78	4.00	4.22	NE	NE	3.00	1.69
2/2	NE	8.93	6.67	1.78	NE	0.89	NE	6.44	1.11	5.33	4.45	3.18
2/3	NE	8.22	4.00	NE	3.56	4.22	7.56	NE	11.33	1.11	5.71	3.47
3/1	NE	10.67	11.33	NE	6.00	0.00	NE	1.11	NE	0.67	4.96	5.14
3/2	0.22	NE	9.69	NE	4.89	2.89	NE	7.33	2.22	7.33	4.94	3.36
3/3	5.56	4.89	3.78	8.00	6.00	6.44	NE	0.44	NE	7.11	5.28	2.35
4/1	NE	10.22	2.67	3.33	NE	2.67	2.00	3.11	NE	0.22	3.46	3.16
4/2	NE	4.18	7.33	4.67	7.78	NE	NE	NE	3.11	NE	5.41	2.04
4/3	4.22	2.44	NE	8.00	0.89	0.22	NE	NE	2.67	2.22	2.95	2.57
5/1	NE	6.89	1.78	3.78	8.67	0.44	6.67	3.78	NE	4.67	4.58	2.74
5/2	0.22	3.33	6.89	5.56	-0.67	5.11	5.78	6.89	2.44	NE	3.95	2.79
5/3	7.11	NE	8.44	8.44	7.56	0.67	2.67	0.89	8.44	2.22	5.16	3.45
6/1	0.67	6.89	1.78	5.56	2.22	NE	NE	NE	7.33	7.56	4.57	2.93
6/2	6.44	1.56	6.89	0.22	0.89	0.00	1.11	5.11	8.44	4.89	3.56	3.13
6/3	3.78	0.67	5.33	5.78	4.00	2.89	NE	9.56	NE	8.67	5.08	2.94
7/1	0.22	8.67	2.67	NE	13.33	1.78	4.22	2.89	7.11	9.11	5.56	4.26
7/2	6.89	10.93	10.44	7.56	8.67	4.00	5.78	8.67	9.56	12.00	8.45	2.46
7/3	NE	10.89	7.33	11.56	8.00	9.33	0.89	9.11	0.22	10.00	7.48	4.14
8/1	5.33	3.11	14.89	7.78	7.56	8.00	NE	5.11	8.67	8.00	7.60	3.28
8/2	10.44	11.11	3.78	7.78	8.00	2.89	10.89	8.44	4.67	10.00	7.80	3.04
8/3	6.67	7.33	4.67	12.22	5.11	6.00	0.44	2.44	9.11	9.33	6.33	3.44
9/1	0.89	8.22	0.89	4.67	7.11	2.44	0.22	0.89	2.22	4.67	3.22	2.81
9/2	6.22	6.00	11.78	13.33	9.56	14.44	3.78	4.89	11.78	7.33	8.91	3.77
9/3	5.56	9.33	9.78	12.67	7.56	6.44	10.89	9.78	11.56	4.89	8.84	2.62
10/1	5.56	11.02	8.00	4.00	3.33	NE	6.22	6.89	7.56	3.11	6.19	2.55
10/2	12.22	4.22	8.44	8.22	NE	0.44	NE	1.33	7.78	10.67	6.67	4.26
10/3	3.56	4.44	4.22	11.33	5.11	14.44	11.33	6.22	9.56	6.89	7.71	3.72
11/1	9.78	7.78	9.11	5.33	7.78	8.44	6.00	9.33	10.44	9.33	8.33	1.64
11/2	3.11	4.67	10.67	9.11	6.89	8.44	8.89	8.22	8.00	NE	7.56	2.34
11/3	3.78	4.22	11.33	9.33	5.56	5.11	11.11	6.22	4.89	7.56	6.91	2.79
12/1	NE	NE	11.11	10.67	12.00	0.22	11.56	9.11	7.33	3.33	8.17	4.30
12/2	8.44	7.33	10.67	9.33	7.11	5.33	12.44	5.33	4.67	2.67	7.33	2.97
12/3	1.78	12.18	12.00	9.56	7.56	13.33	7.33	12.22	12.00	4.67	9.26	3.84
13/1	NE	6.22	9.11	3.33	11.11	NE	NE	12.89	5.11	4.44	7.46	3.62
13/2	NE	7.78	2.67	7.33	13.56	4.44	4.89	4.22	9.11	8.44	6.94	3.31

**Table C.7** (Continued).

Soil	CFI-MBC (mg g <sup>-1</sup> soil) <sup>a</sup>										Aver.	SD.
	n1	n2	n3	n4	n5	n6	n7	n8	n9	n10		
13/3	9.56	2.67	10.44	8.00	4.00	1.78	6.67	8.00	7.33	7.56	6.60	2.87
14/1	7.11	9.96	4.67	4.00	6.89	2.00	3.78	14.67	9.11	3.56	6.57	3.83
14/2	5.11	8.67	6.89	7.11	12.00	3.78	11.33	13.11	12.00	5.78	8.58	3.32
14/3	8.67	1.56	16.00	5.56	10.89	12.00	10.67	11.11	12.00	7.78	9.62	3.98
15/1	7.56	10.00	8.22	8.44	8.89	7.11	8.22	5.56	3.33	8.22	7.56	1.88
15/2	8.22	7.11	5.78	7.56	12.44	12.89	4.44	7.33	8.22	5.33	7.93	2.79
15/3	8.89	4.00	12.67	9.56	3.56	1.33	11.11	10.67	8.00	5.33	7.51	3.75
16/1	10.44	7.33	11.11	6.22	3.78	9.33	9.78	8.67	10.22	8.44	8.53	2.23
16/2	4.44	7.33	13.33	7.78	11.11	14.22	14.89	5.11	9.56	6.67	9.44	3.79
16/3	6.71	13.42	13.78	8.89	12.89	3.78	5.78	4.22	9.78	9.78	8.90	3.72
17/1	6.89	8.44	7.11	11.78	9.56	6.44	1.56	4.89	5.33	2.89	6.49	3.04
17/2	12.00	12.71	3.78	11.78	4.67	1.78	10.67	8.44	6.22	7.33	7.94	3.82
17/3	2.67	12.44	14.44	7.33	11.78	9.33	12.67	12.89	10.44	4.22	9.82	3.93
18/1	NE	8.22	4.22	8.89	8.00	8.44	5.78	3.33	6.00	5.56	6.49	1.99
18/2	4.22	7.11	3.78	12.44	2.44	5.56	3.11	10.00	7.33	4.67	6.07	3.19
18/3	8.67	9.33	6.44	8.44	6.67	4.89	1.33	6.00	10.00	5.33	6.71	2.57

<sup>a</sup>all values are the average with n = 10.

<sup>b</sup>NE = Can not be estimated.

**Table C.8** Mean  $\pm$  SD of CO<sub>2</sub> flush (CO<sub>2</sub>-C).

Soil	CO <sub>2</sub> -C (mg g <sup>-1</sup> soil)*										Aver.	SD.
	n1	n2	n3	n4	n5	n6	n7	n8	n9	n10		
1/1	3.60	8.3	2.8	4.1	2.9	5.8	5.5	3.6	7.1	4.4	4.81	1.83
1/2	4.20	3.6	4.8	2.2	4.3	2.6	6.9	2	2.2	3.2	3.60	1.52
1/3	1.90	3.5	4.6	3.4	1.2	1.8	6.7	2.9	2.6	2.5	3.11	1.59
2/1	4.50	5.9	6.8	5	5.9	3.3	3.4	4.8	6.5	8.2	5.43	1.54
2/2	4.08	3.1	2.9	4.6	7.6	3.6	5.2	4.1	5.1	3.6	4.39	1.37
2/3	3.30	2.3	2.2	4.2	3.7	2.9	2.6	3.8	1.4	2.1	2.85	0.89
3/1	3.10	2.6	2.4	7.5	2.1	3.2	5.8	3.4	7.7	4.9	4.27	2.09
3/2	5.50	4.8	3.1	4.5	5.2	5.5	7.1	4.1	3.6	3.3	4.67	1.22
3/3	3.50	3.4	5.6	3.3	3.7	3.6	6.9	4.8	3.6	2.8	4.12	1.27
4/1	3.70	2.8	5.5	4.9	3.6	4.2	3.7	1.8	6.1	5.8	4.21	1.37
4/2	5.50	5.4	3.3	4.5	3.9	8.2	7.9	4.4	5.8	7.8	5.67	1.76
4/3	4.10	3.9	5.5	3.8	5.5	3.7	6.8	7.9	4.8	5.4	5.14	1.39
5/1	6.30	3.1	5.1	5.2	3.3	4.9	3.6	5.1	7.7	2.9	4.72	1.53
5/2	5.50	2.9	3.9	4.1	6.9	4.3	4.2	2.1	3.9	5.4	4.32	1.36
5/3	3.60	4.8	3.3	2.8	2.9	6.1	4.4	4.5	3.2	5.6	4.12	1.15
6/1	4.70	4.3	4.6	3.1	3.4	4.2	6.1	6.9	3.3	3.9	4.45	1.22
6/2	3.30	4.1	3.7	2.5	3.6	2.8	4.9	3.9	3.3	4.6	3.67	0.75
6/3	4.30	4.3	5.1	3.7	2.9	3.7	4.2	2.8	4.8	3.6	3.94	0.75
7/1	3.90	3.5	4.2	3.9	1.4	3.8	2.9	3.6	1.8	1.9	3.09	1.02
7/2	2.10	2.2	1.9	1.3	1.7	2.2	2.4	3.1	1.1	2.1	2.01	0.56
7/3	3.90	2.5	3.6	1.8	1.7	2.6	2.8	3.3	3.9	0.9	2.70	1.01
8/1	2.60	2.8	0.8	1.1	3.4	2.4	4	3.6	0.9	3.9	2.55	1.23
8/2	1.10	2.4	3.9	3.6	3.8	1.9	0.7	3.6	3.9	2.1	2.70	1.22
8/3	2.20	2.1	1.9	0.9	2.8	4.1	3.8	2.9	1.1	1.8	2.36	1.05
9/1	3.80	2.5	4.2	1.8	1.2	3.9	3.7	2.2	3.3	3.9	3.05	1.04
9/2	2.00	2.3	1.2	1.1	3.1	0.9	3.1	2.8	1.9	3.3	2.17	0.90
9/3	3.10	2.1	2.2	0.8	3.3	3.4	1.7	2.2	2	2.2	2.30	0.79
10/1	4.10	2.5	3.1	2.1	4.1	3.9	3.2	2.4	3.9	3.6	3.29	0.75
10/2	1.30	2.1	3.2	2.7	4	2.6	4.1	3.8	1.9	2.2	2.79	0.96
10/3	3.60	2.8	2.1	1.8	3.3	0.9	1.1	1.2	2.9	3.5	2.32	1.03
11/1	1.20	3.9	1.1	1.6	0.9	3.3	2.3	1.8	2.5	1.1	1.97	1.02
11/2	2.20	0.7	2.5	1.3	0.9	0.8	3.2	1.2	1.9	2.8	1.75	0.90
11/3	0.90	3.1	1.2	2.6	0.3	3.1	2.4	1.9	1.8	0.6	1.79	1.01
12/1	1.70	2.6	2.2	2.6	1.8	3.9	1.8	2.9	2.1	3.6	2.52	0.76
12/2	1.60	1.5	2.2	1.2	1.3	2.6	1.7	2.2	2.6	1.8	1.87	0.51
12/3	2.60	1.8	1.5	0.8	1.7	1.3	2	0.6	1.2	0.5	1.40	0.66
13/1	3.30	3.1	1.9	1.9	2.4	3.3	3.7	1.2	2.9	2.5	2.62	0.78
13/2	2.20	2.9	3.2	2.9	1.4	2.8	1.8	2.7	1.3	1.3	2.25	0.74
13/3	1.30	1.8	1.5	0.9	1.4	2.6	1.8	0.8	1.5	0.5	1.41	0.60
14/1	2.20	2.8	2.5	1.4	1.7	2.1	1.3	0.8	3.1	2.2	2.01	0.71

**Table C.8** (Continued).

Soil	CO <sub>2</sub> -C (mg g <sup>-1</sup> soil)*										Aver.	SD.
	n1	n2	n3	n4	n5	n6	n7	n8	n9	n10		
14/2	0.90	0.7	1.3	1.5	1.6	0.9	0.9	0.9	1.2	0.8	1.07	0.31
14/3	1.10	2.1	0.5	1.1	0.6	1.1	1.1	0.7	0.8	1.3	1.04	0.46
15/1	2.80	2.9	1.8	3.6	3.3	3.2	2.1	1.9	0.9	1.8	2.43	0.86
15/2	2.90	1.8	1.1	1.1	1.6	1.2	1.2	1.3	1.1	2.1	1.54	0.59
15/3	2.40	2.2	1.6	1.8	2.1	2.8	1.6	2.4	1.6	1.5	2.00	0.44
16/1	1.30	1.3	1.4	1.6	3.1	2.4	1.7	2.9	2.8	0.9	1.94	0.79
16/2	1.40	0.7	1	1.1	1.2	0.9	0.6	1.1	2.1	1.4	1.15	0.42
16/3	0.80	0.8	1.4	0.9	1.6	1.1	1.2	0.7	0.8	0.7	1.00	0.31
17/1	2.10	1.6	1.5	2.3	2.2	1.9	1.7	2.6	2.3	2.4	2.06	0.37
17/2	1.00	1.1	1.5	1	1.3	2.4	1.9	2.2	1.6	1.3	1.53	0.49
17/3	1.60	1.8	0.5	1.1	1.3	0.8	0.8	1	1.3	1.4	1.16	0.40
18/1	3.30	3.6	1.1	2.6	2.2	2.4	2.8	3.4	2.7	2.3	2.64	0.72
18/2	2.90	1.9	3.1	1.2	2.9	2.3	2.6	2.3	1.5	1.9	2.26	0.63
18/3	2.10	2.6	1.1	1.3	1.6	3	3.1	1.9	2.1	2.5	2.13	0.68

## **APPENDIX D**

### **RESONANT SIGNALS FROM 1D <sup>1</sup>H NMR STUDY**

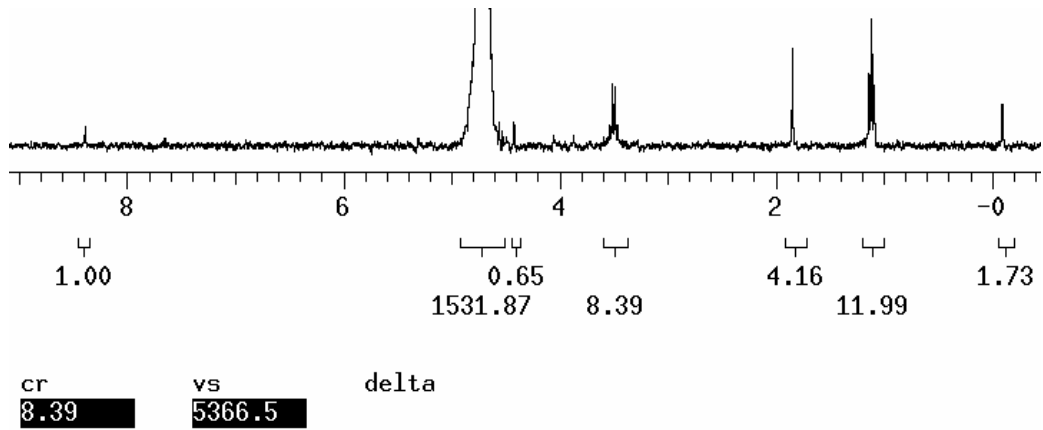


**Figure D.1** Soil 1/1: surface soil (0 - 10 cm), 5 years of continuous vetiver from TTDI.

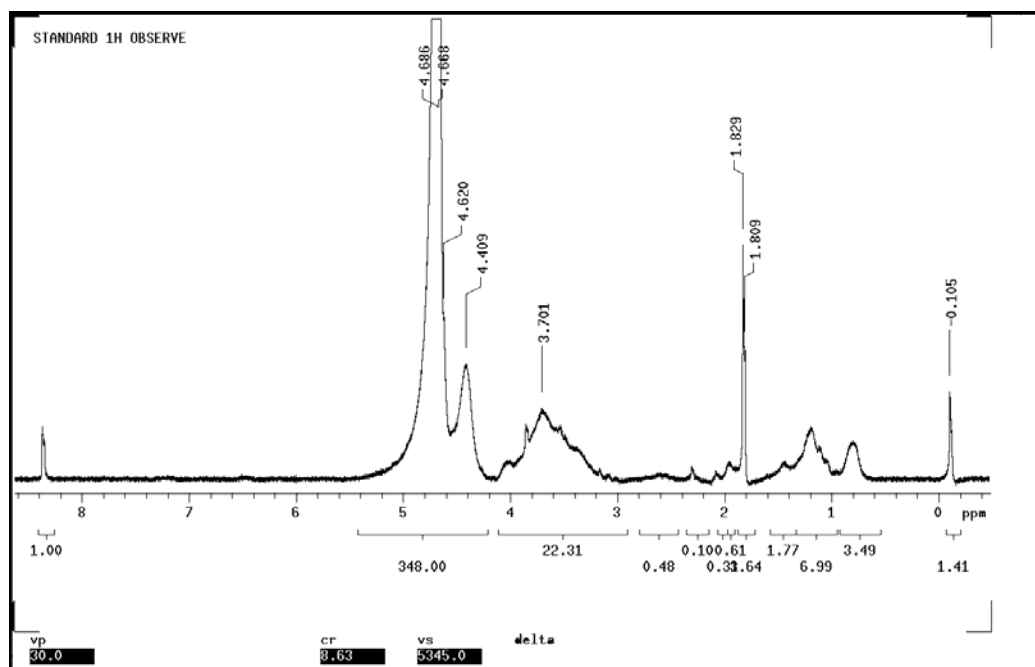


**Figure D.2** Soil 1/2: 10 - 60 cm depth, 5 years of continuous vetiver from TTDI.

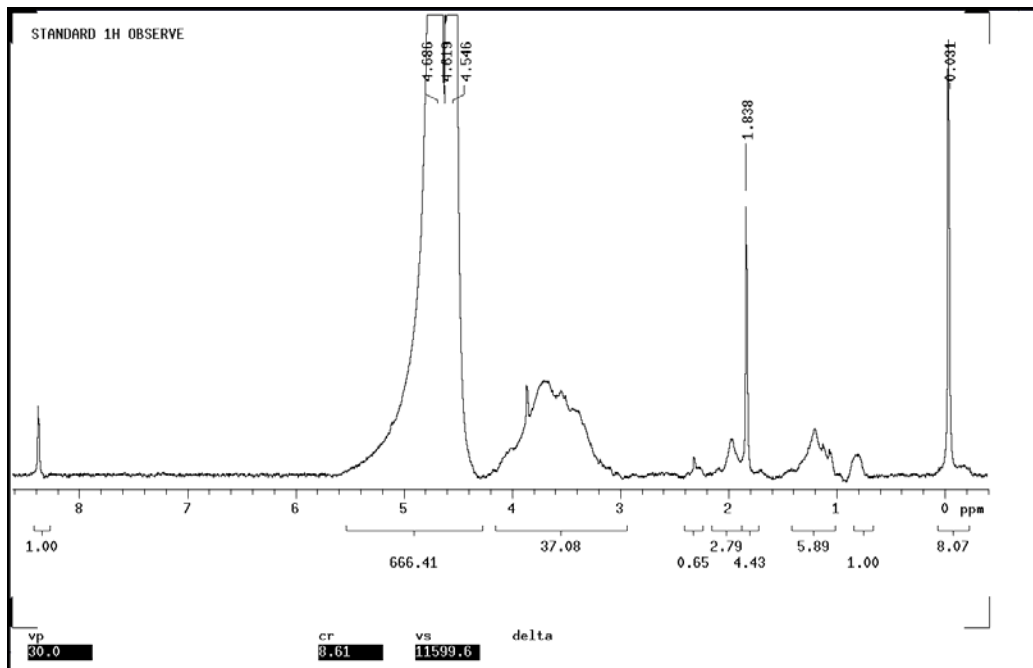


**Figure D3** Soil 1/3: 60 - 120 cm depth, 5 years of continuous vetiver from TTDI.

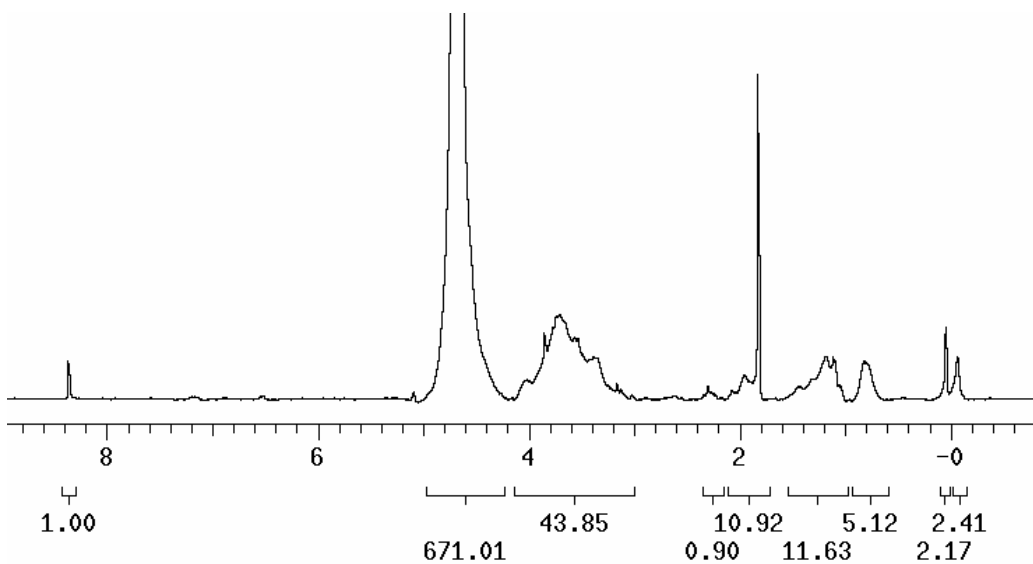


**Figure D.4** Soil 6/1: surface soil (0 - 10 cm), 7 years of continuous vetiver from TTDI.

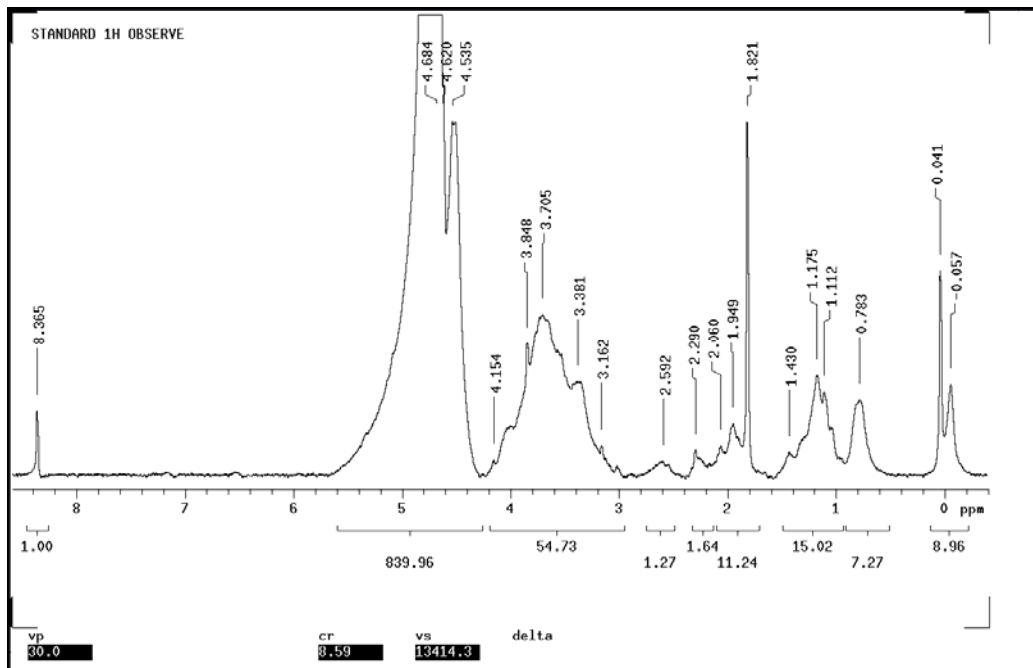


**Figure D.5** Soil 6/2: 10 - 60 cm depth, 7 years of continuous vetiver from TTDI.

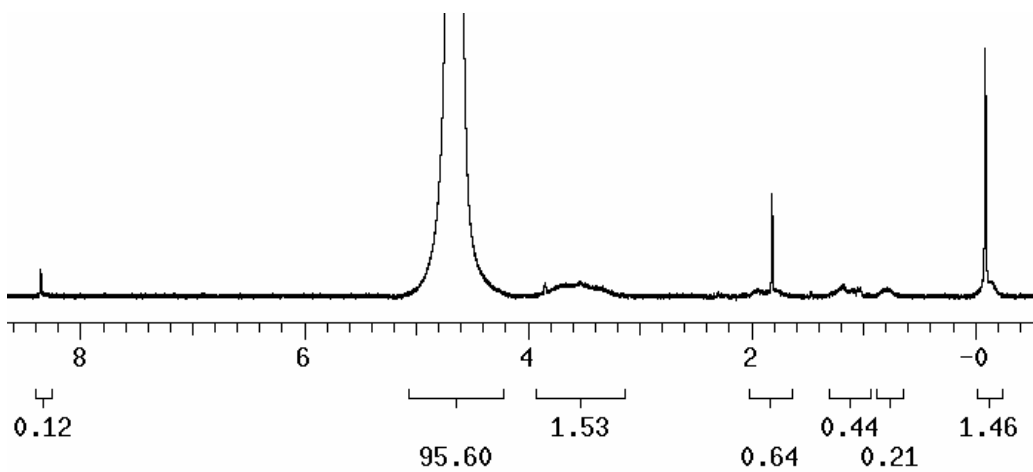


**Figure D.6** Soil 6/3: 60 - 120 cm depth, 7 years of continuous vetiver from TTDI.

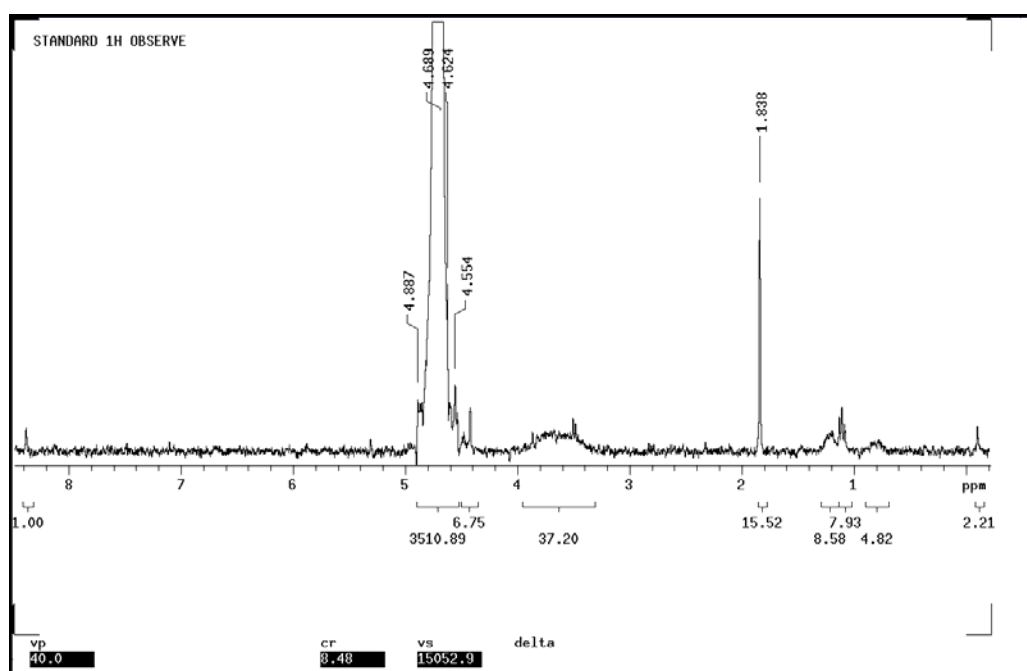


**Figure D.7** Soil 7/1: surface soil (0 - 10 cm), 3 years of continuous vetiver from TTDI, Huai Bong, Dan Kun Tod, Nakhon Ratchasima.

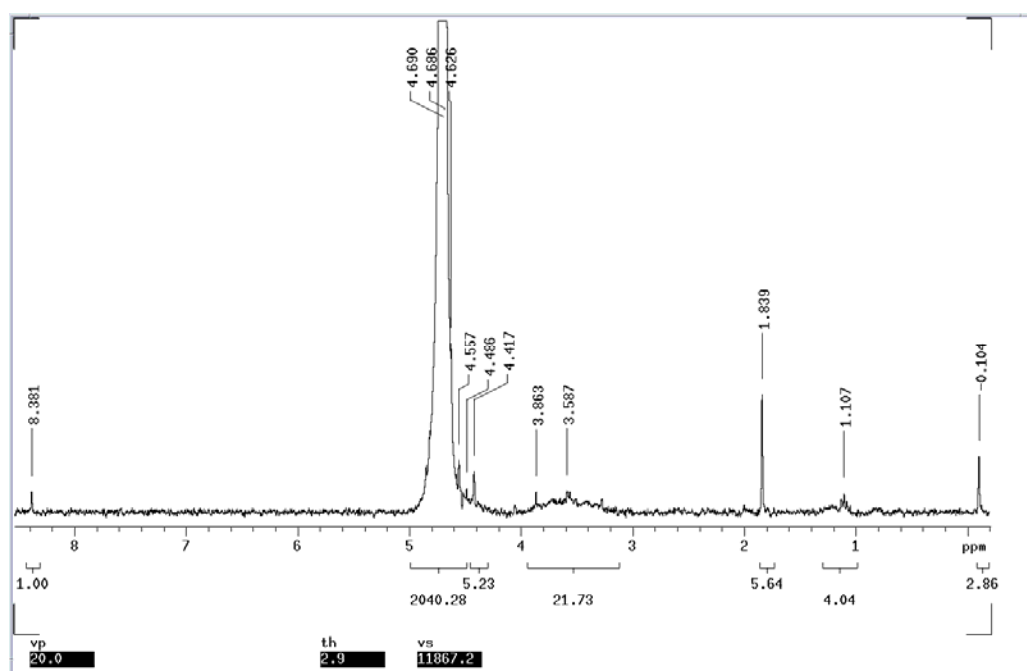


**Figure D.8** Soil 7/2: 10 - 60 cm depth, 3 years of continuous vetiver from TTDI.

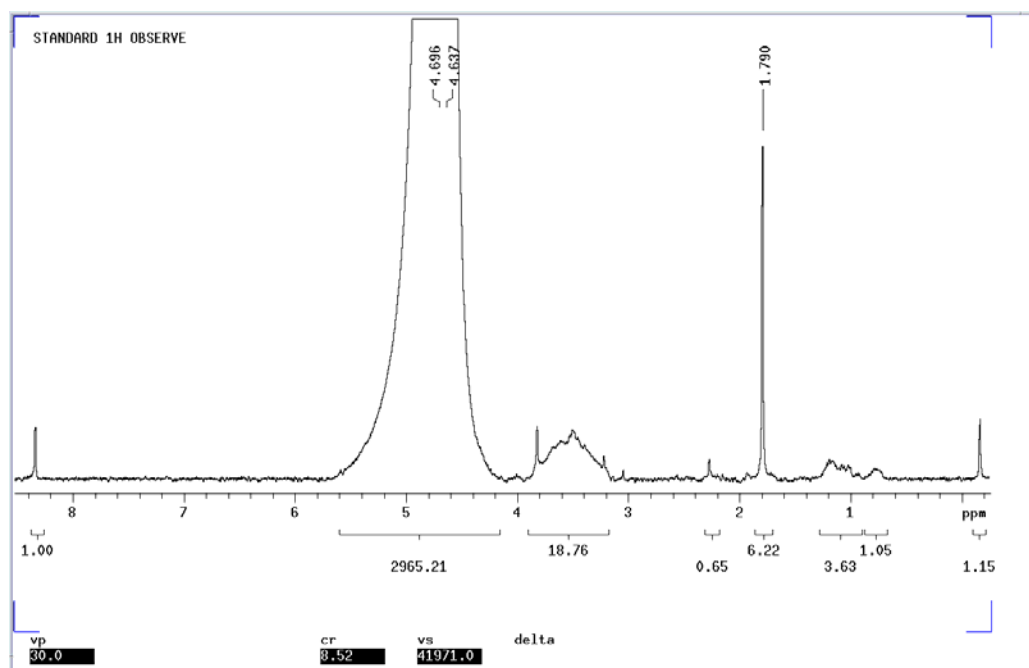


**Figure D.9** Soil 7/3: 60 - 120 cm depth, 3 years of continuous vetiver from TTDI.

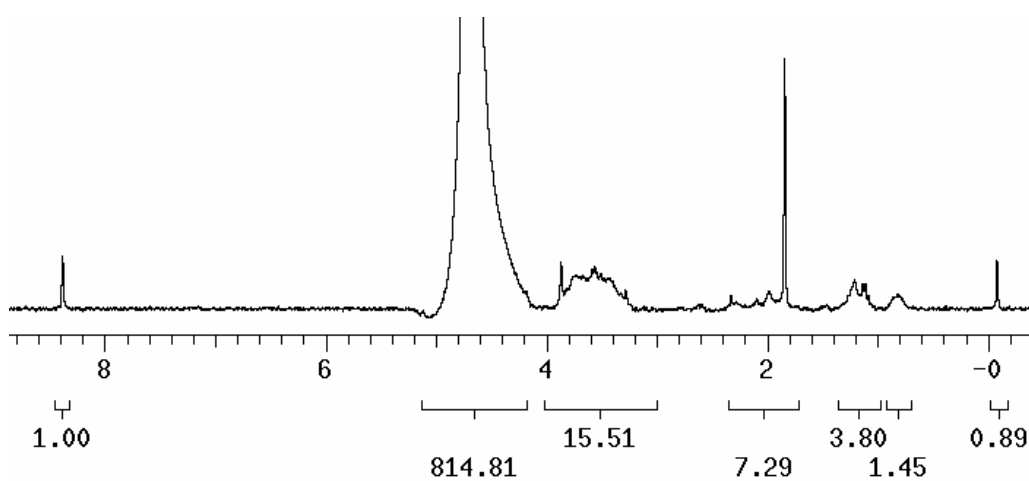


**Figure D.10** Soil 10/1: surface soil (0 - 10 cm), 3 years of continuous vetiver from Ban Nong Kra don, Bueng O Subdistrict, Kham Thale So, Nakhon Ratchasima.

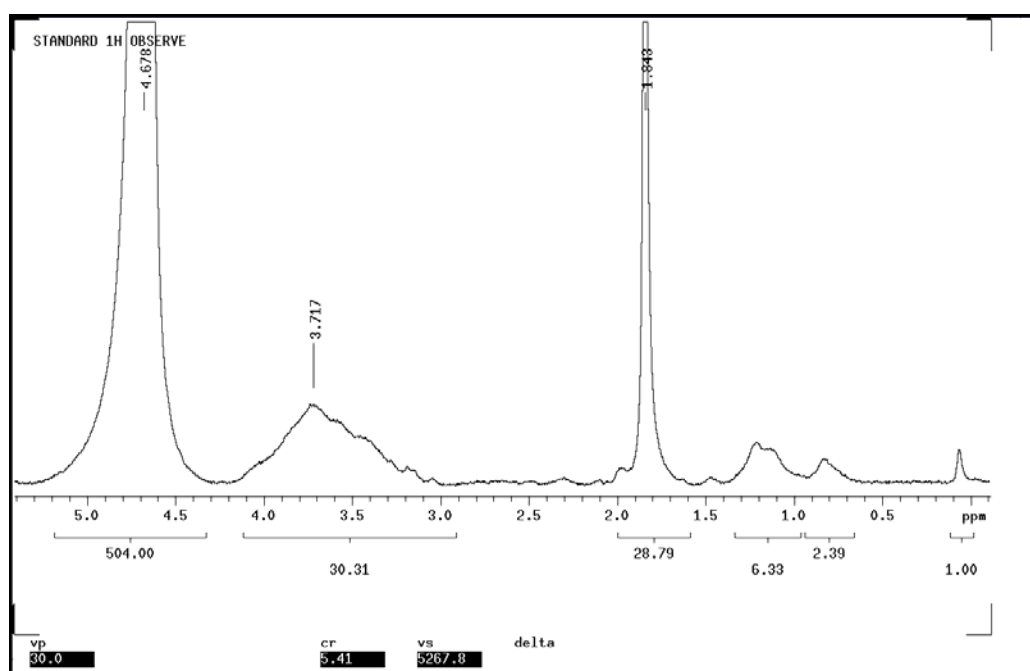


**Figure D.11** Soil 11/1: surface soil (0 - 10 cm), 3 years of continuous vetiver from Sukpaiboon Subdistrict, Soang Sang District, Nakhon Ratchasima.

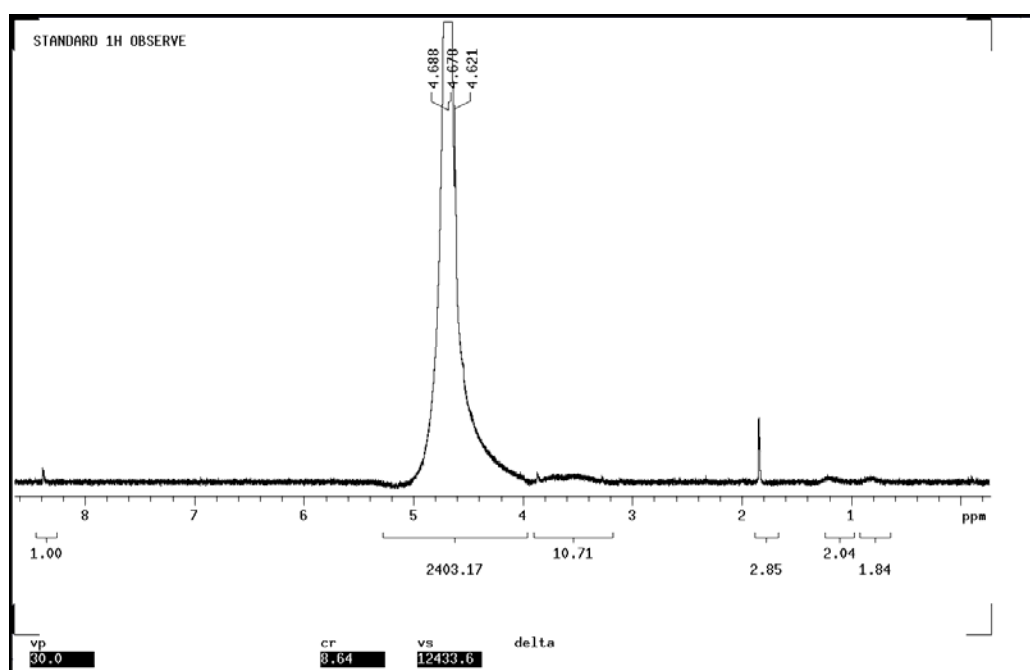


**Figure D.12** Soil 15/1: surface soil (0 - 10 cm), 2 years of continuous vetiver from Tambol Noon Sumboon, Amphur Soang Sang, Nakhon Ratchasima.

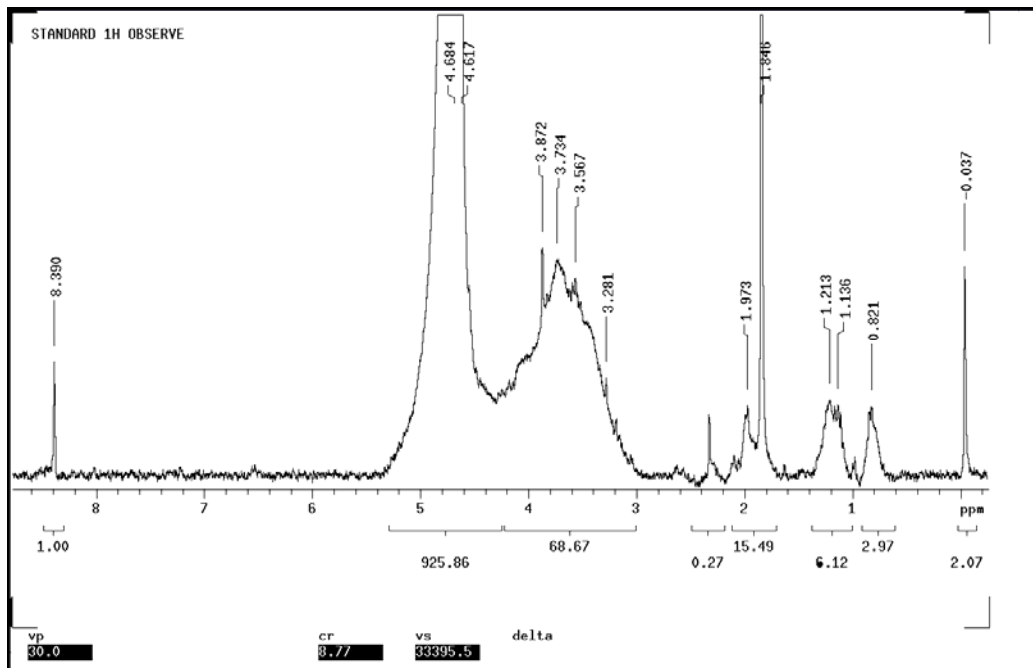


**Figure D.13** Soil 16/1: surface soil (0 - 10 cm), 2 years of continuous vetiver from Ban Thai Charoen, Pak Chong District, Nakhon Ratchasima.

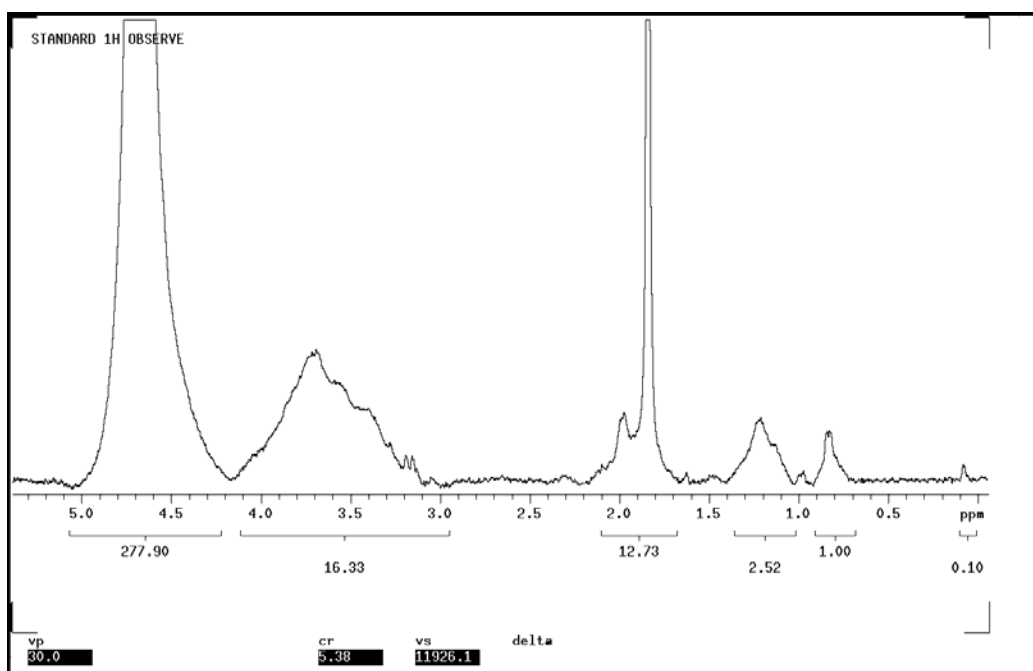


**Figure D.14** Soil 17/1: surface soil (0 - 10 cm), 3 years of continuous vetiver from Land Development Department, Pak Chong District, Nakhon Ratchasima.

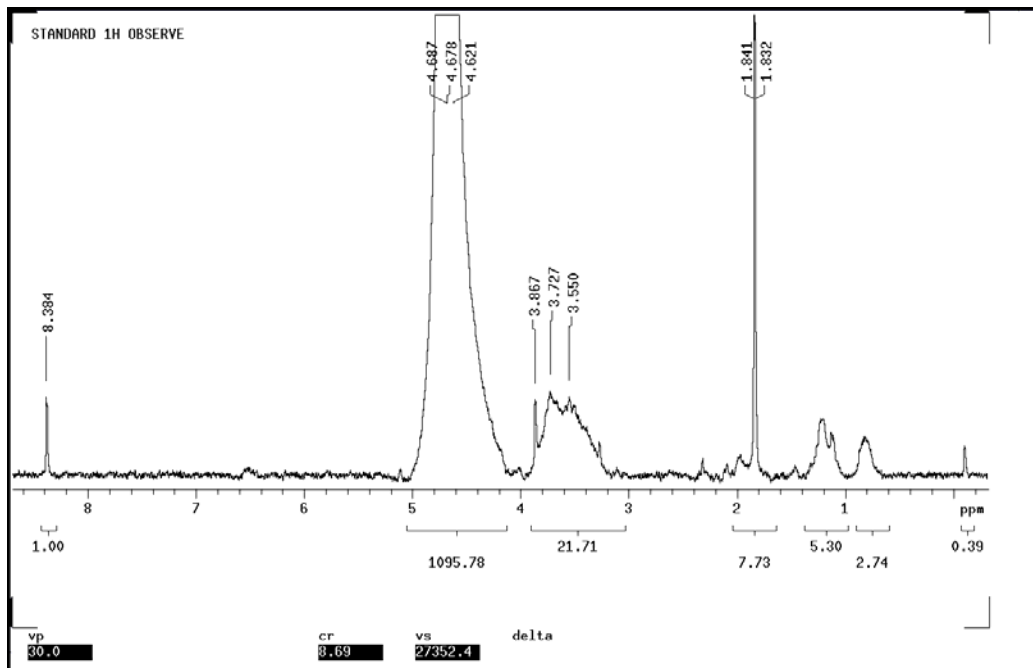


**Figure D.15** Soil 18/1: surface soil (0 - 10 cm), 3 years of continuous vetiver from the Regional Office 3, Land Development Department, Mueang District, Nakhon Ratchasima.

## **CURRICULUM VITAE**

**FIRST NAME:** PIYANUT

**LAST NAME:** KHANEMA

**GENDER:** Female

**NATIONALITY:** Thai

**DATE OF BIRTH:** October 19, 1975

**PLACE OF BIRTH:** Surin

### **EDUCATION BACKGROUND:**

1998 - 2001 M.Sc. (Environmental Biology), Suranaree University of  
Technology, Thailand

1994 - 1997 B.Sc. (Animal Production Technology), Suranaree University of  
Technology, Thailand

### **WORK EXPERIENCE:**

2002 - 2004 Lecturer, Department of Biology, Faculty of Science, Rajamangala  
University of Technology, Thanyaburi, Pathumtani Thailand